PB82-197153

Development of Criteria for Extension of Applicability of Low-Emission, High-Efficiency Coal Burners

Energy and Environmental Research Corp.
Santa Ana, CA

Prepared for

Industrial Environmental Research Lab.
Research Triangle Park, NC

Oct 81

U.S. Department of Commerce
National Technical Information Service
NTIS

United States
Environmental Protection
Agency

EPA-600/7-81-171c
October 1981

PB82-197153

Research and Development

DEVELOPMENT OF CRITERIA FOR EXTENSION OF APPLICABILITY OF LOW-EMISSION, HIGH-EFFICIENCY COAL BURNERS: THIRD ANNUAL REPORT

Prepared for

Office of Air Quality Planning and Standards

Prepared by

Industrial Environmental Research
Laboratory
Research Triangle Park NC 27711

REPRODUCED BY
NATIONAL TECHNICAL
INFORMATION SERVICE
U.S. DEPARTMENT OF COMMERCE
SPRINGFIELD, VA 22161

TECHNICAL REPORT DATA
(Please read Instructions on the reverse before completing)

1. REPORT NO. EPA-600/7-81-171c

2.

3. RECIPIENT'S ACCESSION NO. PB82 197153

4. TITLE AND SUBTITLE
Development of Criteria for Extension of Applicability of Low-emission, High-efficiency Coal Burners: Third Annual Report

5. REPORT DATE October 1981

6. PERFORMING ORGANIZATION CODE

7. AUTHOR(S) W. Nurick, R. Payne, J. Lee, P. Case, S. Chen, and D. Pershing

8. PERFORMING ORGANIZATION REPORT NO.

9. PERFORMING ORGANIZATION NAME AND ADDRESS
Energy and Environmental Research Corporation
8001 Irvine Boulevard
Santa Ana, California 92705

10. PROGRAM ELEMENT NO.

11. CONTRACT/GRANT NO. 68-02-2667

12. SPONSORING AGENCY NAME AND ADDRESS
EPA, Office of Research and Development
Industrial Environmental Research Laboratory
Research Triangle Park, NC 27711

13. TYPE OF REPORT AND PERIOD COVERED Annual; 10/79-10/80

14. SPONSORING AGENCY CODE EPA/600/13

15. SUPPLEMENTARY NOTES IERL-RTP project officer is Dennis C. Drehmel, Mail Drop 62, 919/541-7505. Reports of the same series, designated "a" and "b" cover the first two years of the program, respectively.

16. ABSTRACT The report describes the third year's efforts in a program to develop criteria for extending the applicability of low-emission, high-efficiency coal burners. For the small-scale fuel studies, 28 coals covering all ranks were tested under a wide variety of conditions to ascertain the impact of coal properties on the fate of fuel nitrogen (N). Significant accomplishments in this part of the program include: (1) bench-scale test results confirm the pilot-scale concept that decreasing the initial air/fuel ratio decreases fuel NOx formation; (2) detailed studies on optimizing a staged combustion system suggest that the stoichiometry producing minimum NOx emissions is a function of both fuel composition and primary-zone conditions; (3) distribution of the total fixed nitrogen (TFN) species--NO, NH3, and HCN--leaving the first stage is trongly dependent on coal composition; (4) distribution of the first-stage fuel N emissions has a significant impact on second-stage exhaust NO emissions (minimum second-stage NO emissions depend on competition between first-stage NO and increased gas- and solid-phase N species); and (5) during staged combustion, increasing the rate of heat extraction from the first stage (fuel-rich zone) decreases the decay of TFN species, but dramatically decreases TFN conversion in the second stage (first-stage extraction reduces exhaust NO emissions).

17. KEY WORDS AND DOCUMENT ANALYSIS

a. DESCRIPTORS	b. IDENTIFIERS/OPEN ENDED TERMS	c. COSATI Field/Group
Pollution	Pollution Control	13B
Coal	Stationary Sources	21D
Combustion	Staged Combustion	21B
Nitrogen	Fuel Nitrogen	07B
Stoichiometry		07D
Nitrogen Oxides		

18. DISTRIBUTION STATEMENT Release to Public	19. SECURITY CLASS *(This Report)* Unclassified	21. NO. OF PAGES 201
	20. SECURITY CLASS *(This page)* Unclassified	22. PRICE

EPA Form 2220-1 (9-73)

EPA-600/7-81-171c
October 1981

DEVELOPMENT OF CRITERIA FOR EXTENSION OF APPLICABILITY OF LOW-EMISSION, HIGH-EFFICIENCY COAL BURNERS

Third Annual Report
October 1, 1979 to October 1, 1980

Prepared for:

Industrial Environmental Research Laboratory
Combustion Research Branch
U.S. Environmental Protection Agency
Research Triangle Park, North Carolina 27711

Under Contract No. 68-02-2667

Prepared by:

W. Nurick
R. Payne
J. Lee
P. Case
S. Chen
D. Pershing

Energy and Environmental Research Corporation
8001 Irvine Boulevard
Santa Ana, California 92705

I-a

ABSTRACT

For the small-scale fuel studies, 28 coals covering all ranks were tested under a wide variety of conditions to ascertain the impact of coal properties on the fate of fuel nitrogen. Significant accomplishments in this part of the program include:

- The bench-scale test results confirm the pilot-scale concept that decreasing the initial air/fuel ratio decreases fuel NO_x formation.
- Detailed studies on the optimization of a staged combustion system suggest that the stoichiometry producing minimum NO_x emissions is a function of both fuel composition and primary-zone conditions.
- The distribution of the total fixed nitrogen (TFM) species (NO, NH_3, HCN) leaving the first stage is strongly dependent upon the coal composition.
- The distribution of the first-stage fuel nitrogen emissions had a significant impact on the second-stage exhaust NO emissions. The minimum second-stage NO emissions depend on competition between the first-stage NO and increased gas- and solid-phase nitrogen species.
- During staged combustion, increasing the rate of heat extraction from the first stage, or fuel-rich zone, decreases the decay of TFN species, but dramatically decreases TFN conversion in the second stage. Thus, first-stage heat extraction has the net effect of reducing exhaust NO emissions.

TABLE OF CONTENTS

Section Page

1.0 SUMMARY 1-1

2.0 INTRODUCTION 2-1

3.0 BENCH-SCALE STUDIES TO ASSESS THE IMPACT OF COAL TYPE ON NO_x FORMATION 3-1

3.1 Experimental 3-1

3.1.1 Furnace and Burner Systems 3-1
3.1.2 Oxidant Supply System 3-5
3.1.3 Measurement Systems and Analytical Methods . 3-5
3.1.4 Fuels Investigated 3-9

3.2 Fuel NO Formation During Pulverized Coal Combustion . 3-9

3.2.1 Hypothesis--The Fate of Coal Nitrogen . . . 3-14
3.2.2 Results From Unmodified Furnace 3-14
3.2.3 Questions to be Resolved 3-24

3.3 The Role of Char and Volatile Nitrogen 3-26

3.3.1 Conversion Characteristics 3-26
3.3.2 Char/Volatile Nitrogen Interaction 3-28
3.3.3 Impact of Flame Conditions 3-32

3.4 The Optimization of Staged Combustion 3-32

3.4.1 Mechanisms of Rich/Lean Process 3-32
3.4.2 Influence of Fuel Properties 3-35
3.4.3 First-Stage Combustion Parameters 3-41
3.4.4 Second-Stage Conversion 3-50

4.0 BENCH-SCALE STUDIES TO ASSESS THE IMPACT OF COAL TYPE ON SO_x EMISSIONS AND SORBENTS FOR SO_x EMISSIONS REDUCTION . 4-1

4.1 Gas-Phase Measurements--Analytical Methods/Instrumentation 4-1

4.2 Heterogeneous Systems--Sampling System/Analysis . . . 4-3

5.0 BOILER SIMULATOR FURNACE (BSF) OVERVIEW 5-1

5.1 Design 5-2

5.1.1 Furnace 5-2
5.1.2 Burner 5-4
5.1.3 Fuel System 5-12
5.1.4 Combustion Air System 5-15
5.1.5 Sorbent and Additive System 5-15
5.1.6 Sampling and Measurement 5-17
5.1.7 Cleanup System 5-17
5.1.8 Data Acquisition System 5-19

TABLE OF CONTENTS (Concluded)

Section | Page
5.2 Experimental Approach 5-21

6.0 GENERAL CONCLUSIONS 6-1

6.1 Bench-Scale Studies to Assess the Impact of Coal Type on NO_x Formation 6-1
  6.1.1 Excess Air 6-1
  6.1.2 Staged Combustion 6-2

6.2 Bench-Scale Studies to Assess the Impact of Coal Type on SO_x Emissions and Sorbents for SO_x Emissions Reduction 6-8

7.0 APPENDICES

Appendix A - Fuel and Thermal NO Emissions as a Function of Excess Air and Burner Type A-1

Appendix B - Fuel NO as a Function of Percent CO_2 in the Oxidant B-1

Appendix C - NO Produced Under Two-Stage Conditions C-1

Appendix D - NO Produced Under Three-Stage Conditions . . . D-1

Appendix E - TFN Species Distribution at the Exit of the First Stage and Exhaust NO Concentrations . . . E-1

LIST OF FIGURES

Figure		Page
1-1	Program Executive Summary of Key Results	1-2
2-1	EPA Low-NO_x Burner RD&D Programs	2-2
2-2	Program Structure for development of Criteria for Extension of Applicability of Low-Emission/High-Efficiency Coal Burners	2-4
3-1	Schematic of Furnaces	3-2
3-2	Schematic of Burners	3-4
3-3	Bench-Scale Reactor Oxidant Supply System	3-6
3-4	Schematic of Water-Spray Probe	3-7
3-5	Sample Train for In-Flame Measurements	3-8
3-6(a)	Nitrogen Content as a Function of Coal Rank	3-12
3-6(b)	Sulfur Content as a Function of Coal Rank	3-13
3-7	Fuel NO as a Function of Fuel Nitrogen Content	3-16
3-8	Influence of Thermal Environment at Two Mixing Conditions	3-18
3-9	Effects of Fuel Type/Mixing Characteristics on Staged NO Emissions	3-20
3-10	Effect of Mixing Characteristics on Minimum NO Emissions	3-21
3-11	Two- and Three-Stage Combustion of a Bituminous (Utah-II) Coal	3-22
3-12	Minimum Percent Conversion of Fuel Nitrogen in Two- and Three-Stage Combustion	3-23
3-13	Effect of Particle Size	3-25
3-14	Fuel Nitrogen Conversion in Low-Volatile Solids	3-27
3-15	Influence of Hydrocarbon Volatiles on Char Nitrogen Conversion	3-29
3-16	Importance of Volatile Fuel Nitrogen	3-30
3-17	Influence of Solid Phase in Volatile Nitrogen Conversion	3-31

LIST OF FIGURES (Continued)

Figure | Page

3-18 Effect of Mixing Conditions on Overall Fuel Nitrogen Conversion 3-33

3-19 Effects of Mixing Condition on Volatile and Char Nitrogen Conversion 3-34

3-20 Gaseous Species Concentrations, Solids Composition, and Temperature at the First-Stage Exit 3-36

3-21 Correlation of TFN Content at the Exit of the First Stage With NO Formed Under Excess Air Conditions 3-37

3-22 The Partition of TFN Species 3-38

3-23 Correlation of Char Nitrogen With Modified ASTM Analysis . . 3-40

3-24 Total Hydrocarbon as a Function of HCN 3-42

3-25 XN Species Distribution for Char and Char/Propane Flames at 1.17m From the Burner 3-43

3-26 Influence of Fuel Type and Primary Zone Stoichiometric Ratio on Exhaust NO Emissions Under Staged Conditions 3-44

3-27 Influence of Fuel/Air Contacting on TFN Concentrations . . . 3-45

3-28 Influence of Initial Fuel/Air Contacting on Solids Composition and Hydrocarbons 3-47

3-29 TFN Concentrations as a Function of First-Stage Residence Time 3-48

3-30 Effect of First-Stage Cooling on TFN Concentration With Coal 3-49

3-31 Effect of First-Stage Cooling on Solids Composition 3-51

3-32 Effect of Cooling in the First or Second Stage Upon NO Emissions 3-52

3-33 Impact of Second-Stage Air Addition Method on Exhaust Emissions 3-53

3-34 XN Species Distribution at Exit of First Stage 3-55

3-35 Second-Stage Conversion of TFN Species 3-56

3-36 Relationship Between Hydrocarbon Content of Gaseous Entering Second Stage and TFN Species 3-57

LIST OF FIGURES (Concluded)

Figure Page

3-37 XN Species Distribution--With and Without First-Stage Cooling . . . 3-59

3-38 Exhaust NO Emissions--With and Without First-Stage Cooling . . 3-60

3-39 Influence of Cooling on Second-Stage TFN Conversion--C_3H_8/NH_3 Flames . . . 3-61

3-40(a) Influence of Cooling on Gas Temperature at First-Stage Exit--Utah Coal Flames . . . 3-62

3-40(b) Influence of Cooling on Second-Stage TFN Conversion--Utah Coal Flames . . . 3-63

3-41 Influence of Cooling on Second-Stage TFN Conversion--NH_3 Additions to Char/C_3H_8 Flames . . . 3-64

3-42 Exhaust NO Emissions . . . 3-66

3-43 XN Species at First-Stage Exit . . . 3-67

3-44 Solid-Phase Nitrogen Conversion in the Second Stage . . . 3-68

4-1 H_2S Converter Test . . . 4-2

4-2 Schematic of Phase Discrimination Used for Sampling SO_2 in the Presence of Limestone . . . 4-4

4-3 Solid Sulfur Measurement Validation . . . 4-6

5-1 Boiler Simulator Concept . . . 5-3

5-2 Boiler Simulator Radiant Furnace . . . 5-5

5-3 Post-Flame Section . . . 5-6

5-4 Convective Section . . . 5-9

5-5 Test Burner Schematic . . . 5-13

5-6 Data Acquisition System . . . 5-20

6-1 Fuel NO Correlation . . . 6-3

6-2 Influence of Coal Rank on Gas-Phase Nitrogen Species Exiting First Stage . . . 6-4

6-3 Exhaust NO Can be Calculated by $NO_{ex} = 0.8(SR)(NO) + \frac{HCN + NH_3}{2 + 0.007\ (HCN+NH_3)} + 0.2\ (\text{Char N}) + 5$ . . . 6-7

LIST OF TABLES

Table		Page
3-1	Fuel Composition	3-10
5-1	Radiant Section Design Specifications	5-6
5-2	Post-Flame Section Design Specifications	5-8
5-3	Convective Sections Design Specifications	5-10
5-4	Air System	5-16
5-5	Gas-Phase Measurements	5-18

1.0 SUMMARY

A brief summary of progress on this program since its initiation in 1977 is provided in Figure 1-1 along with the experimental efforts proposed for fiscal year 1981. The major thrust of the program in 1980 has been in the small-scale efforts to define the impact of fuel properties and operating conditions on NO_x emissions. Initial studies have also been undertaken to assess the viability of using dry sorbents for SO_x control. The progress of the program's pilot-scale studies have been hindered because the large watertube simulator (LWS) and small watertube simulator (SWS) facilities have not been available since January 1980. Furnace deterioration necessitated complete rebuilding of these units before further testing could be accomplished. This rebuilding effort was completed in January 1981 and testing has now commenced.

For the small-scale fuel studies, 28 coals covering all ranks were tested under a wide variety of conditions to ascertain the impact of coal properties on the fate of fuel nitrogen. Significant accomplishments in this part of the program include:

- Potential sources of NO_x during coal combustion are: (1) fixation of nitrogen in the combustion air; (2) conversion of fuel NO in the volatiles; and (3) conversion of fuel NO in the solid phase. Under typical conditions, *oxidation of nitrogen chemically bound in the coal is the major source of NO_x emissions.* The conversion of nitrogen which remains in the solid phase during devolatilization is inherently low. Hydrocarbon volatiles do, however, appear to enhance this conversion. The conversion of nitrogen evolved with the volatiles appears to be higher than that of char nitrogen, but significantly less than suggested by gas- and liquid-phase results. The solid phase is believed to play a major role in suppressing volatile nitrogen conversion.
- The bench-scale test results confirm the pilot-scale concept that *decreasing the initial air/fuel ratio decreases fuel NO_x formation.* The initial fuel-oxidant contacting rate appears to have little influence on heterogeneous nitrogen oxidation; however, it has a strong effect on volatile nitrogen oxidation.

PROGRAM OBJECTIVES	AREAS OF STUDY CONCENTRATION OCT 1977 - OCT 1980	KEY RESULTS
1 — EXPAND FUEL CAPABILITY OF DISTRIBUTED MIXING BURNER (DMB)	• DEFINE IMPACT OF FUEL PROPERTIES AND RANK ON NO_x • MAJOR EFFORT IN SMALL-SCALE CONTROLLED EXPERIMENTS • LIMITED PILOT-SCALE EFFORTS	• SMALL SCALE • OPTIMUM STAGING CONDITION IS DEPENDENT ON FUEL PROPERTIES • NO EMISSIONS ARE RELATED TO TFN AS WELL AS OTHER FUEL AND PROCESS VARIABLES • SO_2 MEASUREMENT METHODS HAS BEEN DEFINED • PILOT SCALE • IMPACT OF FUEL PROPERTIES ON NO_x UNDER TYPICAL BURNER COMBUSTION CONDITIONS MORE COMPLEX THAN SIMPLY FUEL NITROGEN CONTENT RELATED
2 — EXPLORE ADDITIONAL CONCEPTS	• NO EFFORT EXPERIMENTALLY	• NEED FOR INBOARD TERTIARY AIR IDENTIFIED FOR RETROFIT BOILERS - AERODYNAMIC STAGING
3 — BURNER CONFIGURATIONS	• FRONT WALL FIRED • SINGLE BURNERS • BURNER SCALE • MULTI-BURNERS	• SINGLE BURNERS • DEVELOPED DESIGN DATA BASE FOR DMB (NO_x) • IDENTIFIED IN-SITU DRY SORBENT AS HAVING POTENTIAL FOR COMBINED NO_x/SO_x COMBUSTION MODIFICATION CONTROL • MULTIBURNERS • NO_x CHARACTERISTICS SIMILAR TO SINGLE BURNERS • EMISSIONS (NO_x) CORRELATE WITH TOTAL HEAT INPUT • TERTIARY AIR PORTS LOCATION CRITICAL TO CO LEVELS BUT INSENSITIVE TO NO_x • SCALE • SCALING BY VELOCITY RESULTS IN HIGHER NO EMISSIONS AT HIGHER HEAT INPUT (MIGHT BE RELATED TO FURNACE EFFECTS)
4 — COMPARE DMB WITH COMMERCIAL BURNERS	• EVALUATION OF COMMERCIAL BURNERS IN LWS	• GENERAL FLAME CHARACTERISTICS SIMILAR TO FIELD OPERATION • NO_x LEVELS 50-100 PPM LOWER THAN FIELD • CO LEVELS >> THAN FIELD • STABILITY AND PERFORMANCE SIMILAR TO FIELD
5 — INDUSTRY COORDINATION	• SETUP BROAD PARTICIPATION IN REVIEW PANELS	• HELD THREE TECHNICAL PANEL MEETINGS • HELD TWO TECHNOLOGY TRANSFER PANEL MEETINGS
6 — SUPPORT FIELD APPLICATION OF DMB TECHNOLOGY	• IDENTIFIED SEVERAL FIELD/COMMERCIAL PROBLEM AREAS AND LIMITS ON GENERAL ACCEPTABILITY OF RESULTS	• RETROFIT OF EXISTING BOILERS WITH TERTIARY AIR PORTS NOT ECONOMICAL • NEED FOR FLEXIBILITY IN LOCATION OF TERTIARY AIR PORTS • MORE DETAILED DESIGN CRITERIA REQUIRED SHOWING OPERATING LIMITS FOR DMB AND PERFORMANCE DATA • NEED FOR TESTING WITH WIDE RANGE OF FUELS

Figure 1-1. Program Executive Summary of Key Results.

With premixed or rapidly-mixed systems, fuel NO formation increases with increasing fuel nitrogen content; however, other fuel properties also significantly affect the fate of fuel-bound nitrogen during combustion. In particular, fuel nitrogen conversion is proportionally greater with coals containing a high fraction of volatile, reactive nitrogen.

- Detailed studies on the optimization of a staged combustion system suggest that the *stoichiometry producing minimum* NO_x *emissions is a function of both fuel composition and primary-zone conditions*. As first-stage stoichiometry is decreased, the NO formed in the first stage decreases, but other oxidizable gas nitrogen species increase as does nitrogen retention in the char.
- *The distribution of the total fixed nitrogen (TFM) species (NO,* NH_3*, HCN) leaving the first stage is strongly dependent upon the coal composition*. In general, the first stage NO percentage decreased significantly with decreasing coal rank from anthracite to lignite. However, the percentage of NH_3 grew with decreasing rank which may give greater NO emissions in the second stage. HCN was greater than NH_3 in all bituminous coals, but less than NH_3 with all subbituminous and lignite coals.
- The distribution of the first-stage fuel nitrogen emissions had a significant impact on the second-stage exhaust NO emissions. *The minimum second-stage NO emissions depends on competition between the first stage NO and increased gas and solid-phase nitrogen species.*
- During staged combustion, increasing the rate of heat extraction from the first stage, or fuel-rich zone, decreases the decay of TFN species, but dramatically decreases TFN conversion in the second stage. *Thus, first-stage heat extraction has the net effect of reducing exhaust NO emissions.*

This effort is now completed and future small-scale studies will concentrate on the dry sorbent for SO_x control efforts.

Previous effort suggested that careful control of the temperature/time/stoichiometry history in the burner zone was essential for effective utilization of a dry sorbent for removal of SO_2 in the furnace. Based on these results, a study was initiated to verify and develop the technical information to extend the results to an operating boiler system. The effort to date has concentrated on verifying the measurement techniques under both gas-phase and heterogeneous combustion conditions. The results suggest:

- Uniform dispersion of limestone in the combustion zone is critical to obtaining high sorbent utilization.
- That proper control of temperature/time/stoichiometry can produce significant SO_2 removal from combustion products.
- Experimental measurement methods can be designed which provide sufficient accuracy that reasonable sulfur balances can be obtained.

The major thrust of the experimental efforts during the next fiscal year is to provide critical data addressing those problems and concerns expressed by manufacturers and users which could limit their acceptability of the DMB demonstration results and burner concept. These areas are: (1) applying the distributed-mixing concept to a burner without outboard air to meet retrofit application; (2) determining the impact of a wide range in coal characteristics on boiler operation, maintenance, and performance; and lastly, (3) defining limits with respect to performance and flame stability. These efforts will be closely coordinated with the companion EPA demonstration programs 68-02-3130, 68-02-3127, and RFP DU-80-A162 (under negotiation) to ensure that the most relevant pilot-scale experiments are conducted.

---

*Specification of Contracts

1. 68-02-3130 "Application to Utility Boilers"
2. 68-02-3127 "Application to Industrial Boilers"
3. RFP DU-80-A162 " Large Utility Boilers"

2.0 INTRODUCTION

The Environmental Protection Agency's overall program in R/D and D of low-NO_x wall-fired burners is illustrated in Figure 2-1. Since initiation of this effort in the early 70's, EPA has recognized the importance of combustion modification through burner design as the most cost-effective NO_x control method. The Combustion Research Branch of IERL initiated the first study at the IFRF (68-02-0202) to better understand the influence of burner design on NO_x formation. The results of this study demonstrated that fuel/air contacting, which is largely controlled by burner design, is the key to controlling NO_x emissions. This result then led to the definition and demonstration of the first EPA distributed-mixing burner (DMB) in 1972. Under two separate contracts, the EPA then pursued the development of this concept. In the first study (68-02-1488), the basic burner design criteria were studied; units were scaled up to 100M Btu/hr and multiple-burner interaction investigated. The most significant result of this study was demonstration that under furnace-simulated conditions the system was capable of operating at less than 0.2 lbs $NO_x/10^6$ Btu. As a logical extension of this effort, EPA then undertook this contract (68-02-2667) to extend the burner criteria to cover a wider range of fuels as well as to study other burner configurations in addition to providing on-going support to the EPA demonstration programs (68-02-3127, 68-02-3130, and RFP DU-80-A162). Consequently, contract 68-02-2667, in addition to its prime R/D objective, must also act as the bridge between the R/D studies and resolution of practical field application problem areas.

The Development of Criteria for Extension of Applicability of Low-Emission, High-Efficiency Coal Burners program was initiated in October 1977. The overall program is structured to meet the following six objectives:

1. Expand fuel capability of DMB to include fuels proposed for use by utilities.
2. Explore additional burner concepts.
3. Determine effects of burner configurations on performance/emissions characteristics.
4. Provide direct comparison between DMB and commercial burners.
5. Ensure appropriate technology transfer to manufacturers and users.
6. Provide test support for field demonstrations.

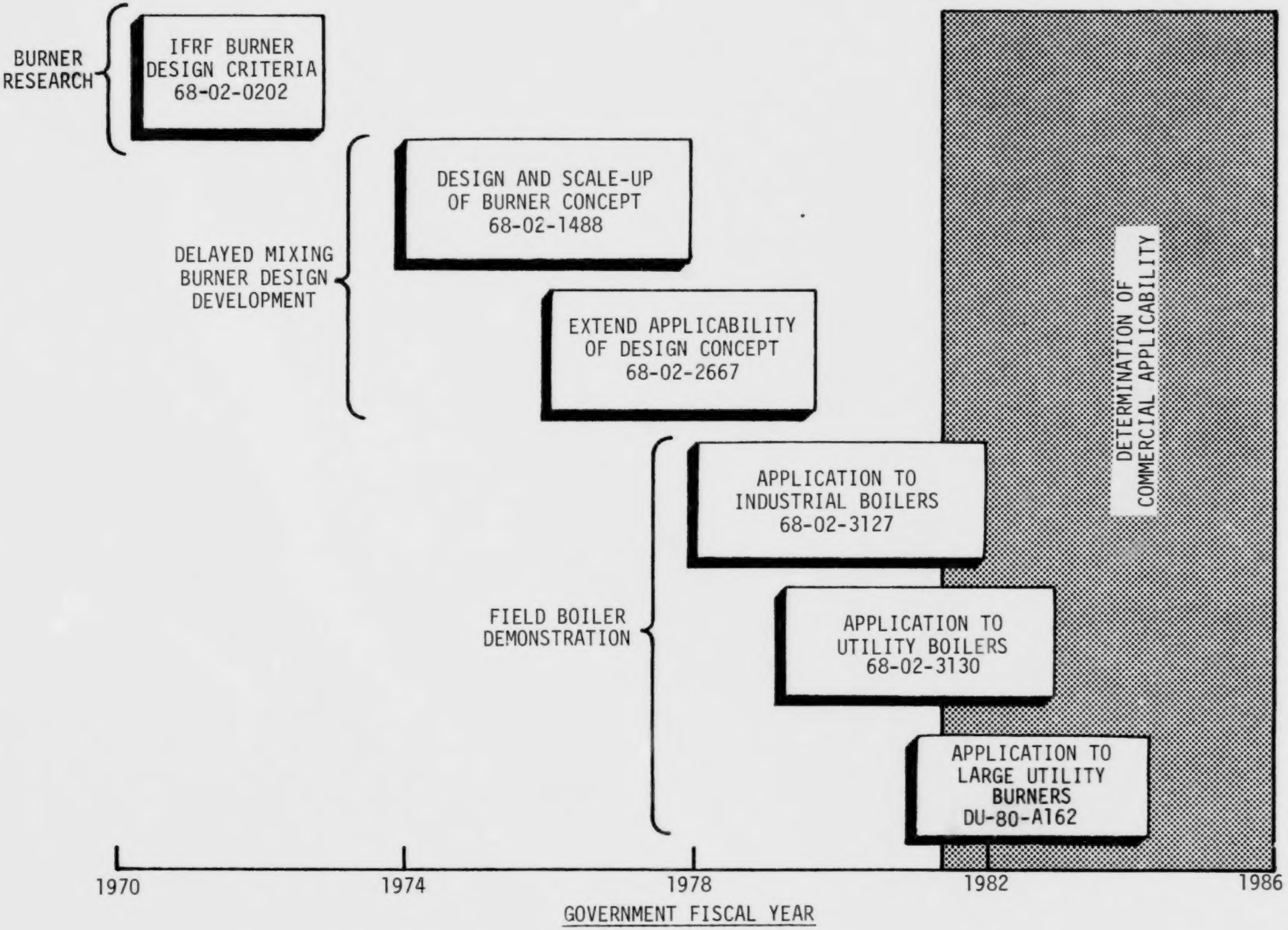

Figure 2-1. EPA Low-NO_x Burner RD&D Programs.

The program is divided into the seven tasks shown in Figure 2-2. Task 1--Program Definition--is designed to plan the three key elements of the program: (1) fuels selection; (2) experimental plan; and (3) measurements protocol. The remainder of the program is structured to carry out these efforts. Tasks 2 through 5 are experimental efforts designed to progressively move from bench-scale process studies (Task 2--Fuel Screening Experiments) to Single- (Task 3--Single-Burner Experiments) and multiple-burner configurations at pilot scale, which incorporate the distributed-mixing concept, and then to compare the operating and emissions characteristics of the DMB against commercial technology (Task 5--Comparison to Current Technology). Throughout the program, results are continually reviewed with the manufacturers and users to secure their advice and recommendations before finalization of the testing program as part of Task 6--Industry Coordination. All of the information is then analyzed in Task 7--Data Analysis and Criteria Development--and DMB design guidelines established.

The results of the initial three years of effort on the small scale experimental effort to define the impacts of fuel properties on NO_x emissions are presented in Section 3.0. The current status of the dry sorbent efforts is given in Section 4.0, and the design of the new Boiler Simulator Furnace (BSF) to be employed primarily in the sulfur efforts is detailed in Section 5.0. In Section 6.0 the general conclusions and plans for GFY1981 are presented.

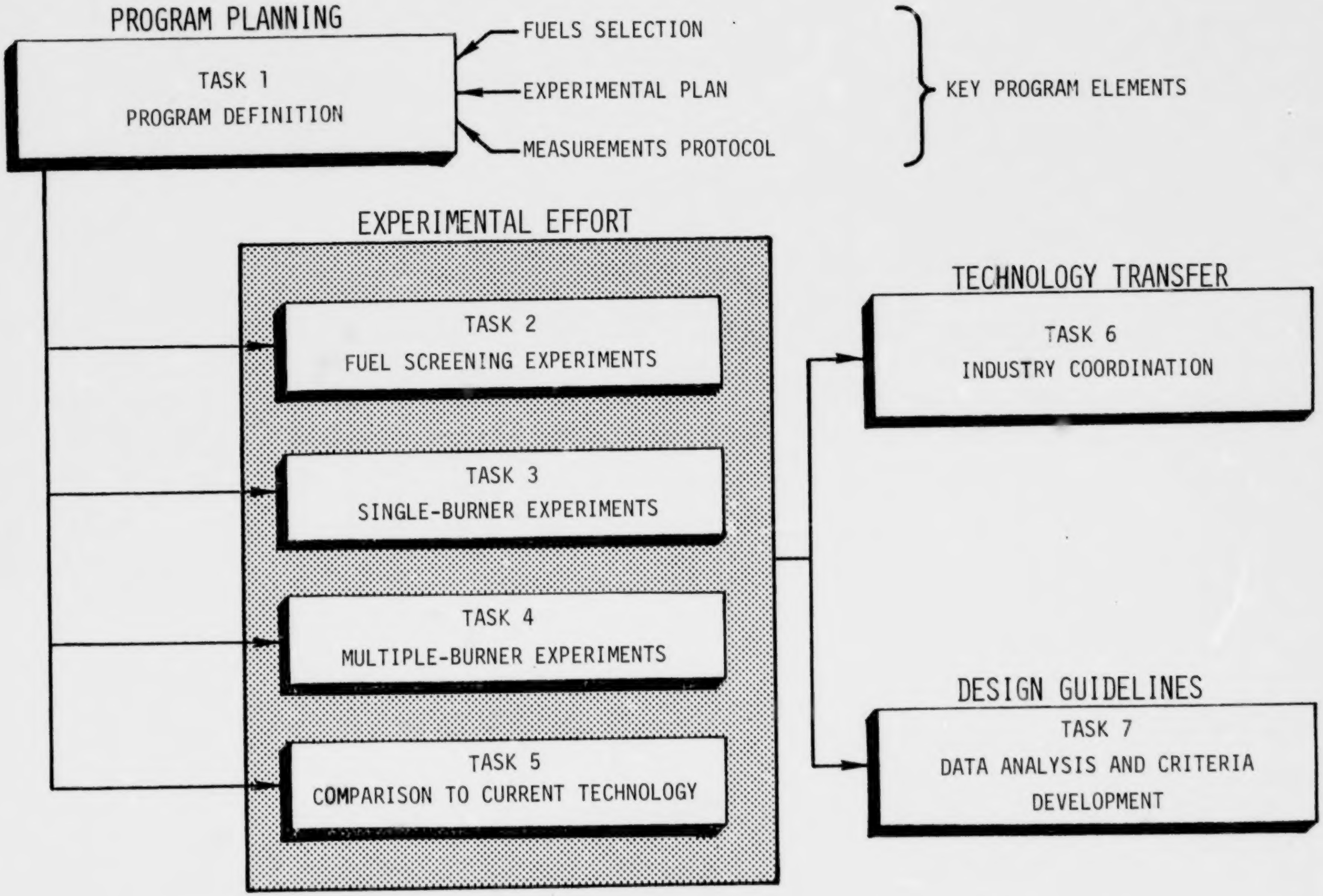

Figure 2-2. Program Structure for Development of Criteria for Extension of Applicability of Low-Emission/High-Efficiency Coal Burners.

3.0 BENCH-SCALE STUDIES TO ASSESS THE IMPACT OF COAL TYPE ON NO_x FORMATION

This section describes results from the bench-scale tunnel furnace. This study has been directed to assess the impact of coal type on NO_x formation. During the combustion of coal, nitrogen oxides (NO_x) are formed by at least two fundamentally different chemical mechanisms: high temperature fixation of atmospheric nitrogen (leading to thermal NO_x), and the oxidation of nitrogen chemically bound in the fuel (leading to fuel NO_x). The formation of thermal NO_x in gas systems has been studied extensively and is usually described using a modified Zeldovich mechanism. In turbulent, pulverized coal diffusion flames, approximately 80 percent of the NO results from coal nitrogen. Fuel NO has been subdivided into the fractions resulting from the volatile and char, and earlier pilot-scale studies have suggested that NO formed from nitrogen volatiles is both the most important and most controllable of the two fuel NO components.

Based on the above-described mechanistic approach, the bench-scale studies have been directed toward fulfilling the following two objectives:

1. Establish the influence of coal type on NO_x formation from pulverized coal and the impact of fuel properties on NO_x emission control strategy.
2. Identify optimum time/temperature/stoichiometry histories for minimum NO_x emissions from staged combustion systems.

The results of this effort are described below.

3.1 Experimental

Bench-scale reactors with 70 x 10^3 Btu/hr nominal firing rate were used in this program for fuel screening studies and concept development. This chapter describes the reactor facilities and the fuels investigated in this task.

3.1.1 Furnace and Burner Systems

The experimental furnace, illustrated in Figure 3-1(a), is a refractory-lined, down-fired tunnel which consists of five separate sections. Each section is made up of an outer steel shell and three layers of refractory insulation. The main combustion chamber is 15.2 cm in diameter. The furnace

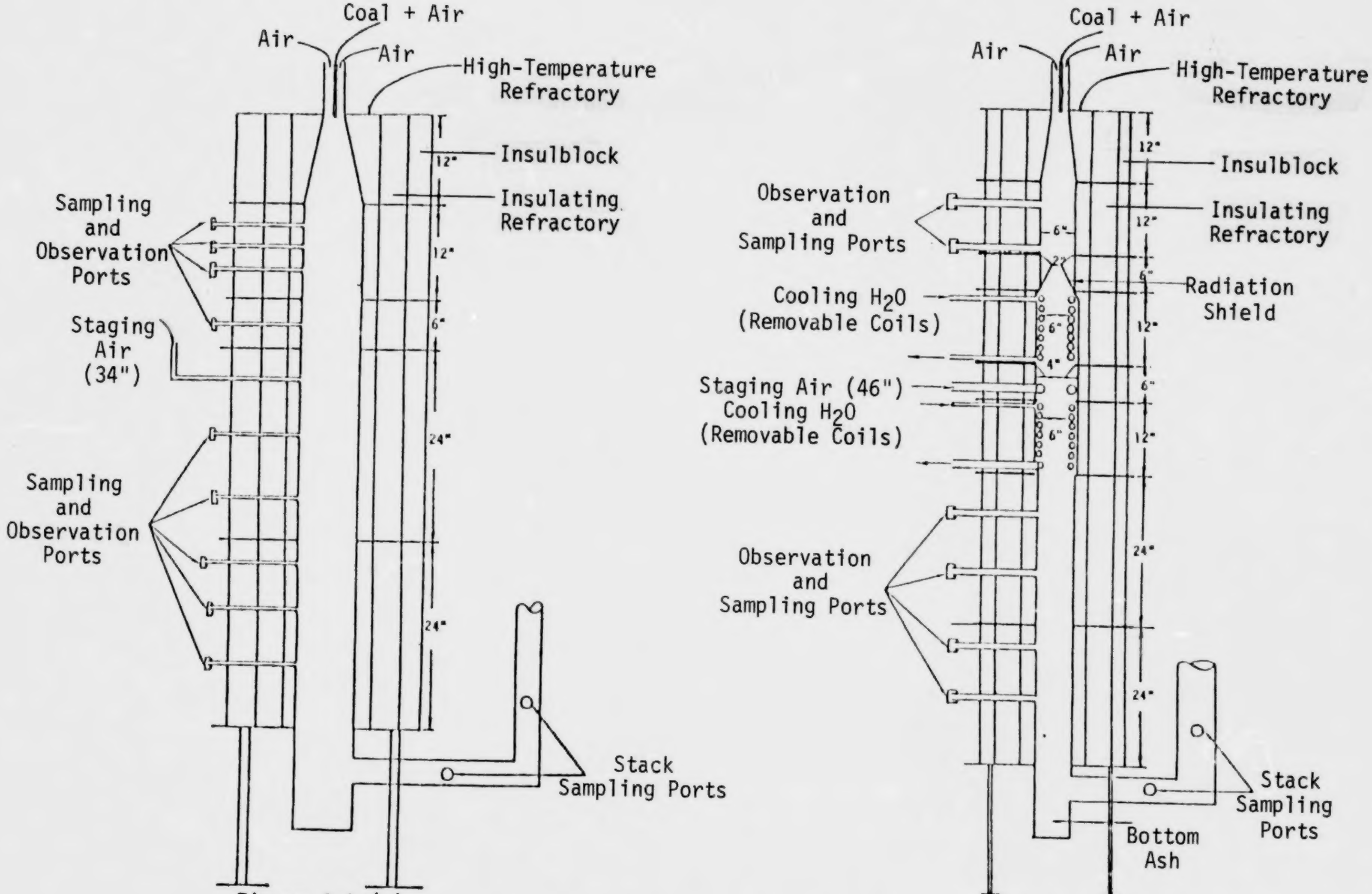

Figure 3-1 (a)

Figure 3-1 (b)

Figure 3-1. Schematic of Furnaces.

entry (top section) consists of a 30.5-cm-long refractory quarl that diverges gradually from 5.1 cm to the full 15.2 cm diameter. The long quarl helps to eliminate recirculation and improves the one-dimensionality of the flow field. Sampling or air/additive injection can be achieved through the access ports located at different axial positions.

All of the fuel screening studies were conducted with the straight tunnel configuration shown in Figure 3-1(a). However, during the latter phases of the program, the furnace was modified to facilitate the measurement of in-flame species concentrations, and to permit the investigation of temperature history effects. The modified furnace, as shown in Figure 3-1(b), includes:

1. A radiation shield upstream of the staging/cooling position to minimize the effects of downstream parameters upon upstream conditions.
2. Two new refractory sections with removable coils to allow cooling of first- and/or second-stage combustion products.
3. A refractory staging choke to insure isolation of the first stage.
4. A removable, radial air ring for second-stage air injection.

Pulverized coal supplied from a twin screw feeder is transported by primary air to the burner on top of the furnace. Figure 3-2 shows the burners used in this study. They are of three basic types: premixed, radial diffusion, and axial diffusion and are designed to simulate premixed, rapidly-mixed, and slowly-mixed systems, respectively. In the premixed burner, primary air and the pulverized coal are injected radially outward through six 0.32 cm holes (at a 30^0 Angle with the vertical) into a premixing chamber. The preheated main combustion air is injected radially inward into the chamber in six round jets opposing the coal jets. This burner produced predominately one-dimensional flow with negligible back-mixing. Ignition in the mixing chamber is prevented by a series of water-cooled tubes which separate the mixing chamber from the hot furnace.

The coal-plus-transport air can also be supplied to the diffusion burner where variable swirl is achieved by dividing the main combustion air into two streams; one which flows axially, parallel to the the injector, and the other which flows through swirl vanes (see Figure 3-2). Swirling all

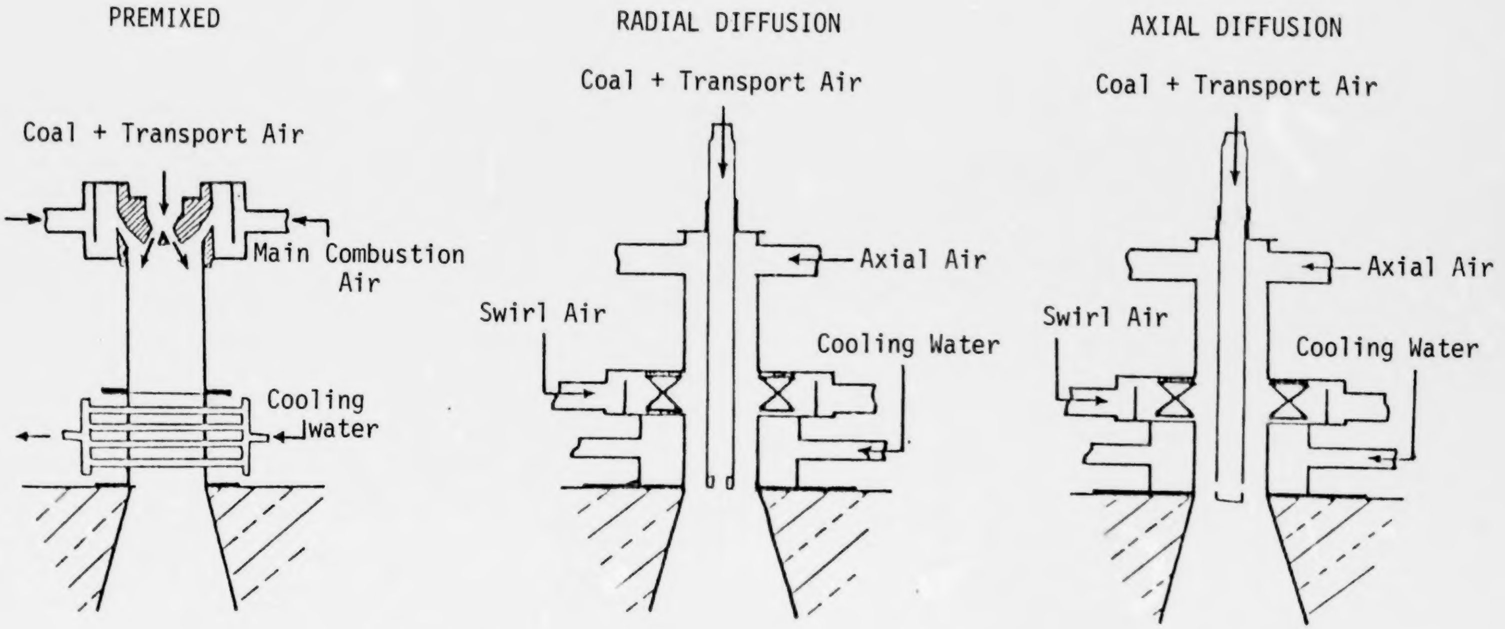

Figure 3-2. Schematic of Burners.

the combustion air and injecting the coal-plus-transport air through a 1.9-cm O.D. injector with six 0.48-cm-diameter holes spaced radially at the tip produces a short, intensely backmixed flame. Conversely, an axial diffusion flame is obtained with a single-hole, parallel injector (1.12-cm-diameter hole). In the axial mode, the combustion air is also added through swirl vanes to provide a stable ignition zone at the injector.

3.1.2 Oxidant Supply System

The oxidant supply system is shown schematically in Figure 3-3. Coal particles supplied from the screw feeder are transported to the burner/furnace either by air or a nitrogen-free oxidant consisting of a mixture of carbon dioxide, argon, and oxygen. Air is supplied from a compressor and artificial oxidant mixture is blended from high-pressure cylinders. Both the air and artificial oxidant are metered with 600 mm rotameters before electric heating to give the desired degree of preheat. The total oxidant stream can be subdivided to stage the heat-release process.

3.1.3 Measurement Systems and Analytical Methods

Fuel gas sampling was conducted with a stainless steel water-cooled probe (jacketed with cooling water) and the following gas species were measured continuously by the method indicated:

- NO - Chemiluminescence
- O_2 - Paramagnetism
- CO/CO_2 - Nondispersive Infrared.

This water-cooled probe when equipped with a heated sampling line was used to take samples for total hydrocarbon measurements with an FID analyzer.

In-flame gas samples were taken with a water-spray probe as shown in Figure 3-4. The probe is made of four concentric stainless steel tubes. The outside diameter of the probe is 3.2 cm and the sample flow passage is 1.26 cm in diameter. Water spray at the tip of the probe provides rapid quenching of the oncoming combustion products. The sample train for in-flame measurements is shown in Figure 3-5. Samples could be directed to either side of the system, i.e., dry measurements of NO, CO/CO_2 and O_2 species or wet measurements of NH_3 and HCN species. Gas-phase HCN and NH_3 species were collected in a gas

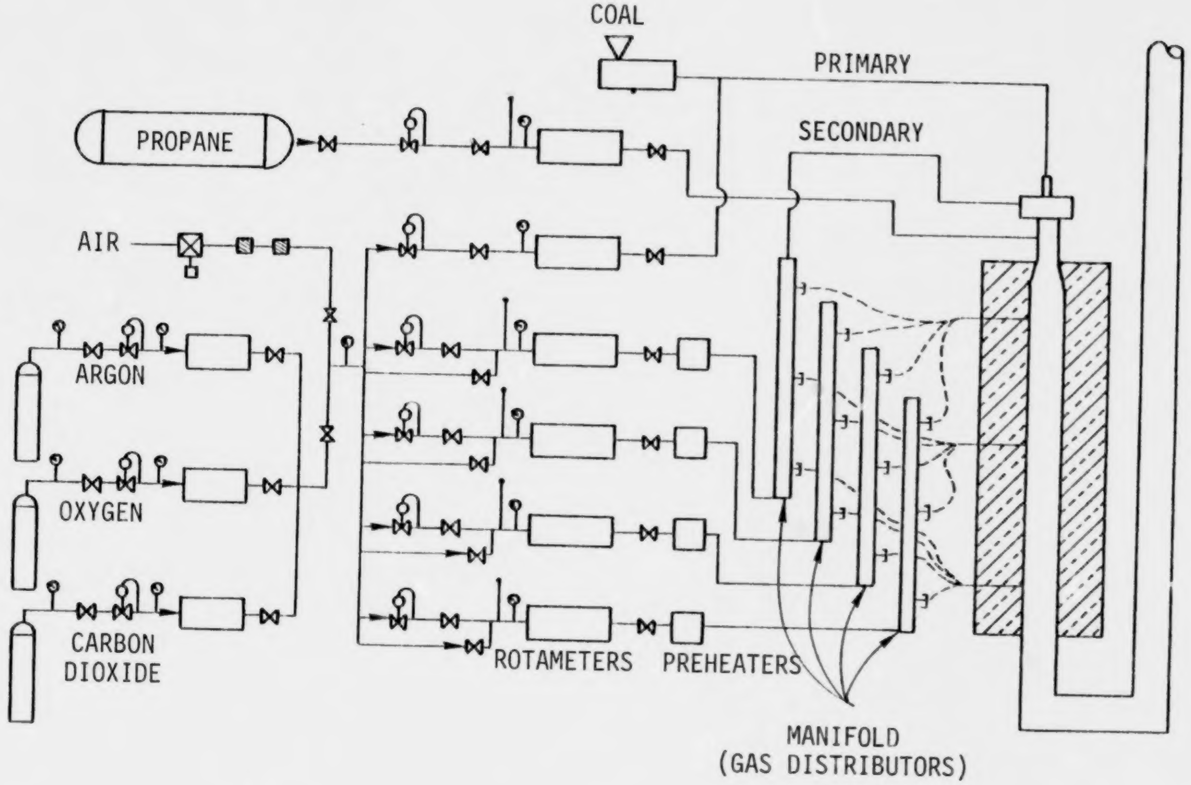

Figure 3-3. Bench-Scale Reactor Oxidant Supply System.

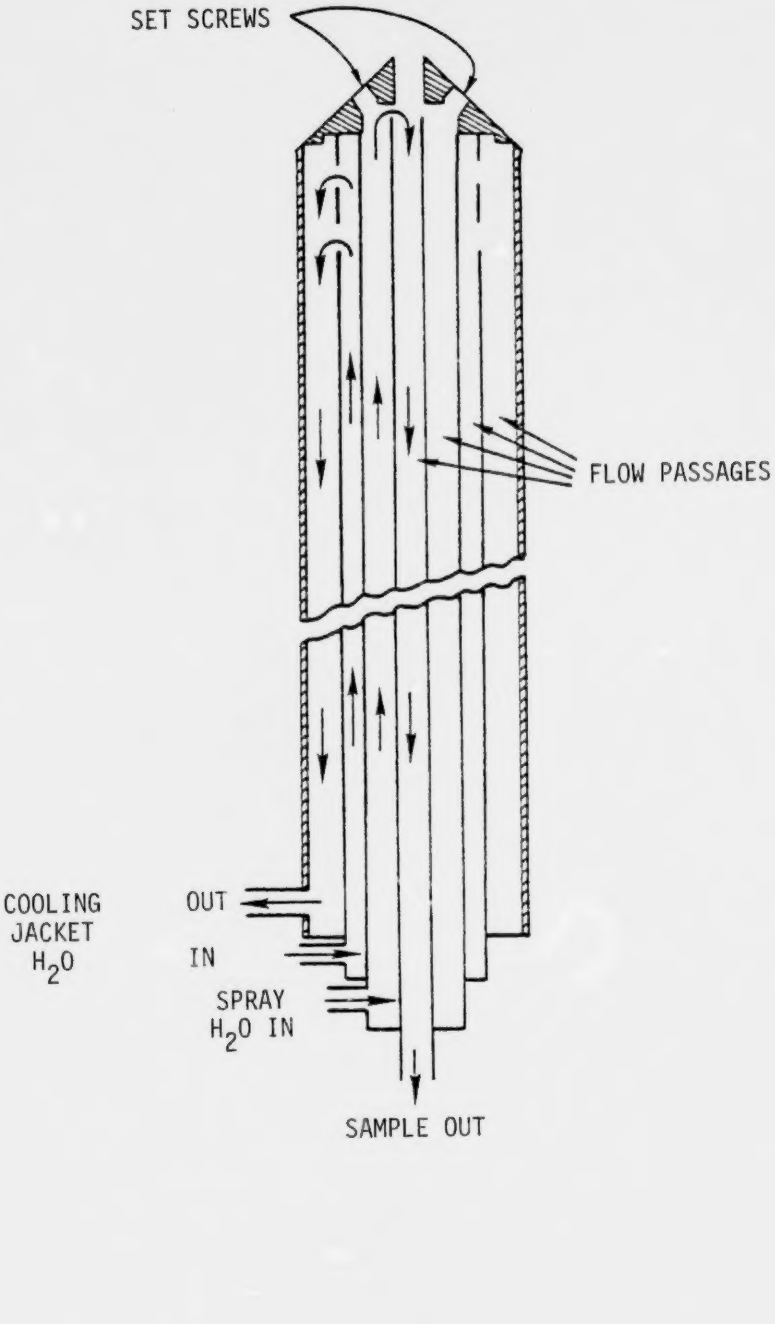

Figure 3-4. Schematic of Water-Spray Probe.

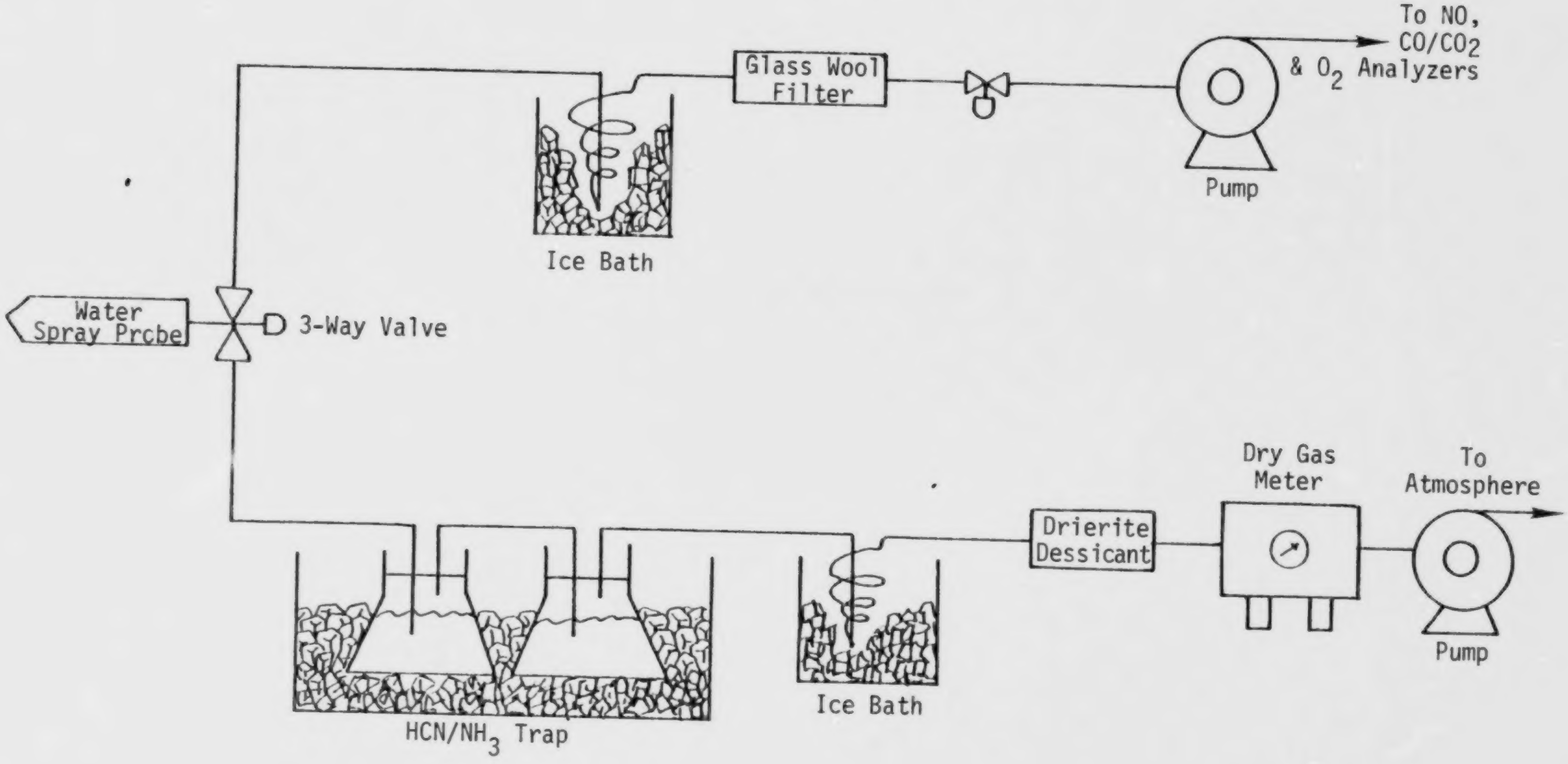

Figure 3-5. Sample Train for In-Flame Measurements.

washing unit which consists of an impinger in series with a bubbler containing a fritted glass cylinder. The sample solutions were subsequently analyzed for CN and dissolved ammonia using specific ion electrodes.

To remove sulfide interferences with the cyanide electrode, a scrubbing solution which contained lead carbonate and sodium carbonate was used in the gas washing unit. This solution was made basic by the sodium carbonate. Gas species, plus water and particulates, were withdrawn through the water-spray probe (see Figure 3-5) and directed to the gas washing unit. HCN and NH_3 were absorbed, and at the same time sulfide ions were removed as lead sulfide. The precipitate, along with the particulates, settled to the bottom of the solution. Only the top 100 ml of the sample solution was used for analysis.

An elbow-shaped water-quench probe was used for collecting in-flame solid samples isokinetically. This probe is similar to the one shown in Figure 3-4 except that the water-cooling jacket has been replaced with a layer of insulating ceramic fiber which minimizes thermal disturbances resulting from the cooling probe. The collected solid samples were analyzed for C, H, N and ash content with a Perkin-Elmer elemental analyzer.

3.1.4 Fuels Investigated

The compositions of the 28 coals studied are given in Table 3-1. A wide range of fuels was considered, including anthracite, bituminous, subbituminous, lignite, char, an Australian brown coal, and a German black coal. Figure 3-6 shows the nitrogen content and sulfur content of the coals studied as a function of coal rank. The majority of the coals investigated have high nitrogen and intermediate sulfur levels. The lignite coals have relatively low nitrogen and low sulfur levels. One coal, Cadiz (▣). has greater than nine percent sulfur on a dry ash-free (daf) basis. The predried Australian brown coal (◤), which contained 61 percent moisture originally, has the lowest nitrogen and the lowest sulfur content (daf).

3.2 Fuel NO Formation During Pulverized Coal Combustion

At least 80 percent of the nitrogen oxide formed during the combustion of pulverized coal are due to the oxidation of coal-bound nitrogen. Therefore, it is of major importance in the development of low-emission systems to understand the phenomena which control the fate of this fuel-bound nitrogen.

Table 3-1. Fuel Composition

Fuel Symbol	◗	✣	∩	⬡	◇	⌂	▽	⬭	○	◺	⊘	⊗	D
Fuel Source	Hazellon PA.	Upper Cliff Alabama	Rosa Alabama	Black Creek Alabama	W. KY.	W. VA.	Elkay W. VA.	Gauley Eagle W. VA.	Price Utah	Price Utah	Utah (Coal)	Utah (Char)	Cadiz Ohio
Proximate Analysis (% as received)													
Moisture	5.13	3.00	8.02	2.25	5.43	7.57	0.60	3.72	6.39	7.41	4.20	2.70	4.29
Ash	5.74	9.49	6.79	4.45	7.53	12.05	11.61	26.89	7.40	8.83	9.62	16.83	18.05
Volatile Matter	4.39	20.44	21.81	28.28	37.79	29.12	33.35	26.65	38.89	38.84	42.97	10.29	34.87
Fixed Carbon	84.74	67.07	63.38	65.02	49.25	51.26	54.44	42.74	47.32	44.92	43.21	70.18	42.79
Ultimate Analysis (% Dry)													
C	88.45	79.32	81.23	82.12	71.58	74.68	73.96	59.43	73.17	72.24	69.36	75.39	62.08
H	2.14	4.47	4.73	5.21	5.43	4.96	4.93	4.11	5.55	5.75	5.32	1.28	4.44
N	0.79	1.47	1.54	1.79	1.55	1.38	1.39	1.35	1.54	1.55	1.50	1.22	1.07
S	0.47	1.30	1.04	0.76	3.21	0.86	2.47	0.84	0.66	0.76	1.04	1.12	7.40
Ash	6.05	9.78	7.38	4.56	7.96	13.04	11.69	27.94	7.90	9.54	10.05	17.30	18.86
O	2.10	3.66	4.08	5.56	10.27	5.08	5.56	6.33	11.18	10.16	12.73	3.69	6.15
Heating Value (Btu/lb, Wet)	13,124	13,254	13,394	14,284	12,082	12,228	13,115	10,110	12,340	11,877	11,718	11,185	11,038
CLASSIFICATION (ASTM D388)	Anthracite	Medium Volatile Bituminous	Medium Volatile Bituminous	Medium Volatile Bituminous	High Volatile A Bituminous	High Volatile A Bituminous	High Volatile A Bituminous	High Volatile A Bituminous	High Volatile B Bituminous	High Volatile B Bituminous	High Volatile B Bituminous		High Volatile B Bituminous

Table 3-1. Fuel Composition (Concluded)

Fuel Symbol	◸	◑	⬠	▽	⬡	◹	⛉	◇	○	□	△	◤	●
Fuel Source	Farmington N. M.	Four Corners N. M.	Fruitland N. M.	Colstrip Montana	Hardin Montana	Hardin Montana	Shell Texas	Scranton N. D.	Beulah N. D.	Beulah N. D.	Savage Montana	Morwell Australia	Saar Germany
Proximate Analysis (% as received)													
Moisture	7.76	5.24	11.02	21.27	22.70	20.49	25.23	34.96	33.10	34.63	36.36	9.07	
Ash	17.96	24.06	20.72	9.58	11.26	8.62	10.28	7.50	7.12	4.97	4.61	3.38	
Volatile Matter	34.95	35.94	31.66	30.82	31.26	33.24	35.31	28.85	28.65	27.02	28.48	48.79	
Fixed Carbon	39.33	34.76	36.60	38.33	34.88	37.65	29.18	28.69	31.13	33.30	30.55	38.76	
Ultimate Analysis (% Dry)													
C	63.06	55.99	58.71	67.52	65.54	67.88	60.99	64.61	65.29	66.15	64.99	66.25	78.06
H	4.65	4.71	4.21	4.36	4.15	4.65	4.49	4.17	3.96	4.20	4.04	5.01	4.86
N	1.40	1.23	1.30	1.38	0.95	0.99	1.13	0.83	0.99	0.96	1.00	0.65	1.25
S	0.81	1.03	0.93	0.63	0.79	1.07	1.02	1.52	1.14	0.37	0.42	0.28	0.80
Ash	19.47	25.39	23.29	12.17	14.57	10.84	13.74	11.53	10.64	7.60	7.25	3.72	6.46
O	10.61	11.65	11.56	13.94	14.00	14.57	18.63	17.34	17.98	20.72	22.30	24.09	8.57
Heating Value (Btu/lb. Wet)	10,391	9,425	9,344	9,169	8,603	9,229	8,131	6,446	7,245	7,254	6,995	10,051	13,657 (dry)
CLASSIFICATION (ASTM D388)	High Volatile C Bituminous	High Volatile C Bituminous	High Volatile C Bituminous	Sub-Bituminous B	Sub-Bituminous B	Sub-Bituminous B	Sub-Bituminous C	Lignite A	Lignite A	Lignite A	Lignite A		

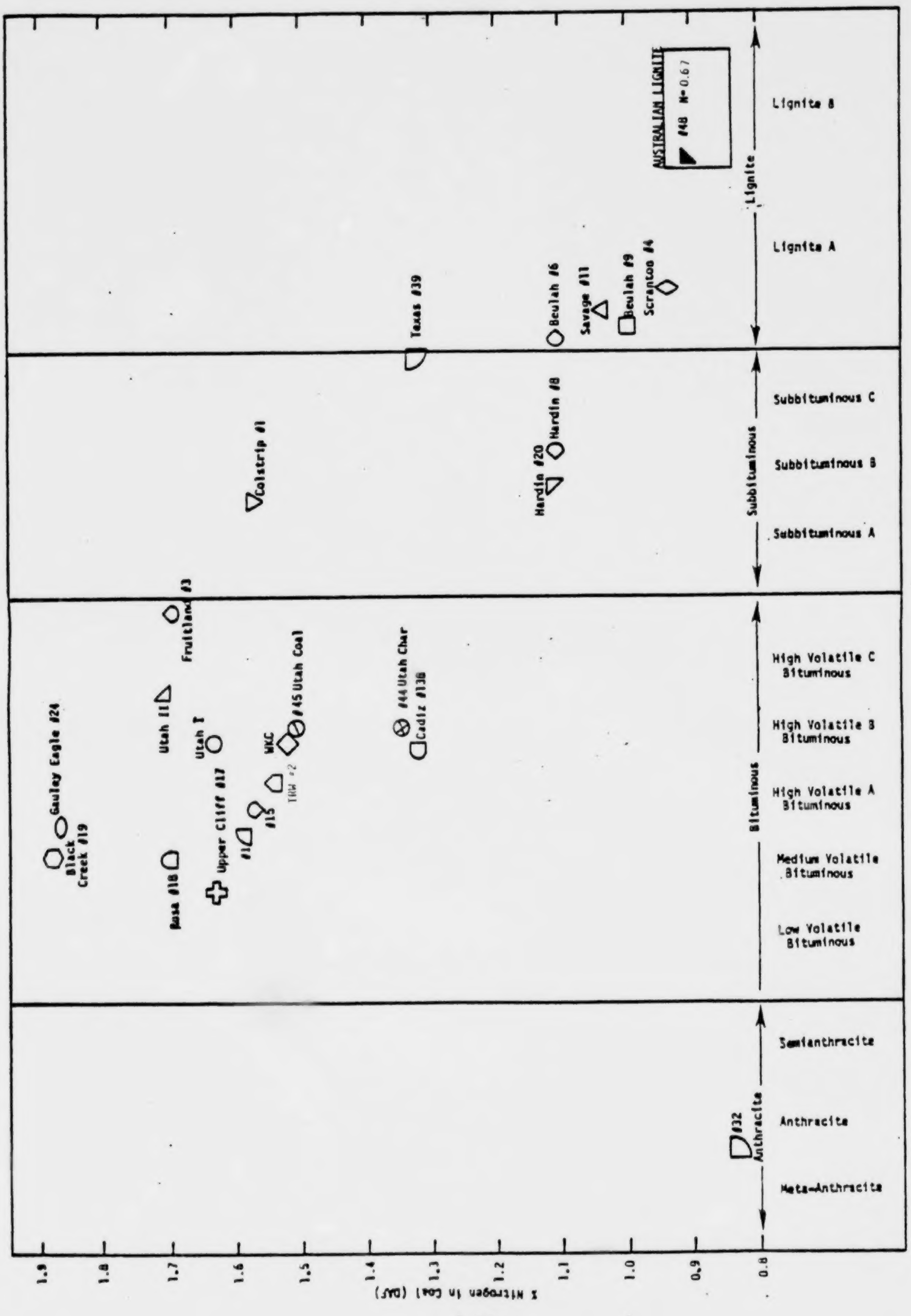

Figure 3-6(a). Nitrogen Content as a Function of Coal Rank.

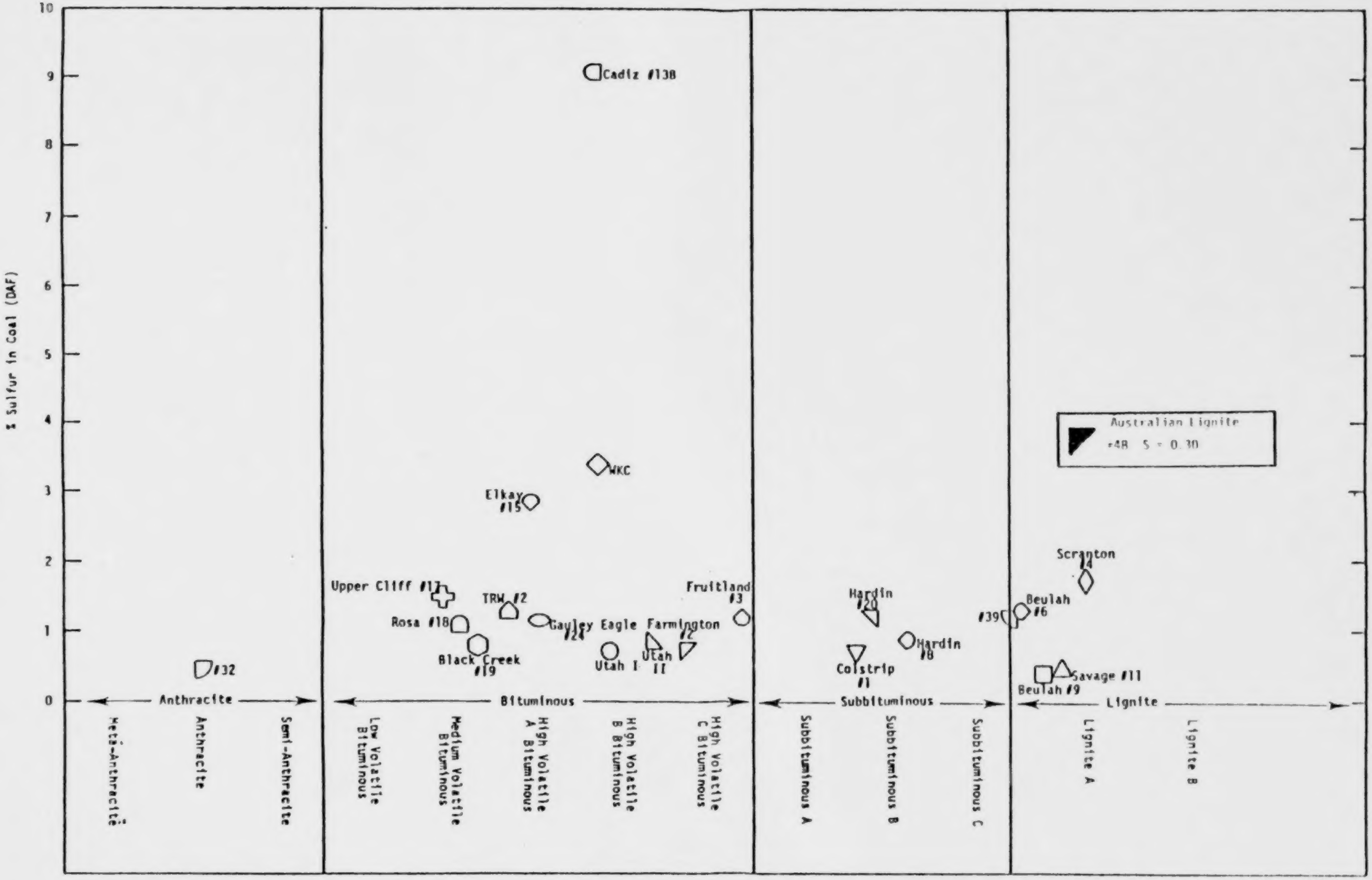

Figure 3-6(b). Sulfur Content as a Function of Coal Rank.

3.2.1 Hypothesis - The Fate of Coal Nitrogen

The current hypothesis concerning the fate of coal nitrogen during pulverized-coal combustion can be simplified to include the following three processes:

- Thermal Decomposition. As the coal particle is heated, it decomposes. Volatiles are evolved, and the nitrogen is split between the volatile and solid fractions. The nitrogen remaining in the solid, char nitrogen, is a function of the temperature attained by the particle and the time at that temperature.
- Gas-Phase Reactions. The gas-phase nitrogen which is produced from the volatile coal fractions can react to form NO, NH_3, NCH or N_2. The formation of NO is favored under fuel-lean conditions and the formation of N_2 is favored under fuel-rich conditions.
- Char Burnout. The char nitrogen which is associated with the solid, either as a pyrolysis product of tars or as the original coal char, can also be oxidized to form NO during char burnout.

This simplified hypothesis provides a basis to understand the potential fuel effects involved in NO formation during pulverized-coal combustion as well as recognizing the steps involved in the optimization of a staged-combustion system.

3.2.2 Results From Unmodified Furnace

The factors which determine the conversion of fuel nitrogen to NO are the fraction of the total nitrogen evolved with the volatiles and the fuel/air contacting process, and the conversion of char nitrogen associated with the remaining solid. The volatile nitrogen evolution will be dependent upon the particle size, the coal type, and the environment in which the particles find themselves since volatile nitrogen evaluation is largely temperature-dependent. This section discusses the effects of these parameters on fuel NO formation.

These data were obtained in the unmodified furnace at a nominal firing rate of 70 x 10^3 Btu/hr (21 kW) with 550^oK secondary air preheat. The particle size distribution, unless noted, was 65 percent through 200 mesh (distribution characteristics shown in a later section, Figure 3-13), and the unpreheated primary air was maintained at 15 percent of stoichiometric air. Fuel NO was defined as the emission when molecular nitrogen was excluded from the oxidant, and the fuel was burned in a mixture of argon, carbon dioxide, and oxygen.

Fuel/Mixing Characteristics. Of the 28 coals evaluated, a total of 25 were tested under excess air conditions in the unmodified furnace with both the premixed burner and the diffusion burners. Both total NO and fuel NO as a function of excess O_2 for all coals tested are presented in Appendix A. Figure 3-7 summarizes fuel NO emissions at 5 percent excess O_2 as a function of percent nitrogen in the original coal (dry, ash free).

The data obtained with the premixed burner (upper plot) indicate that, in general, fuel NO increases with increasing fuel nitrogen. However, a predried Australian lignite (◤), which has the lowest nitrogen content, gives uncharacteristically high emissions. As expected, the low-volatile anthracite (◸) produces significantly less fuel NO than the high-volatile bituminous coals. On the other hand, within any rank, there are other properties which have a significant impact on fuel nitrogen oxidation. For example, the Savage (▲) and Beulah (■) lignites both contain approximately 1.05 weight percent nitrogen, yet their emissions differ by more than 60 percent.

Radial swirling and axial diffusion flames were also used to investigate the coupling between fuel properties and fuel/air contacting. These data (lower plots, Figure 3-7) indicate that fuel effects are also significant in diffusion flames Fuel NO emissions produced with the radial diffusion burner also tend to increase with increasing fuel nitrogen content. The axial flame data show no obvious dependence on nitrogen content, but other composition parameters are obviously of major importance. The Australian lignite (◤) produced an extremely stable, well-attached axial flame and uncharacteristically low NO emissions.

Comparison of data for the three burner types indicates that initial premixing of the fuel and air leads to the highest conversion of the fuel nitrogen to fuel NO, particularly with high-volatile, bituminous coals. This can be attributed to the fact that as the coal/air mixing varies from the premixed to axial diffusion there is less oxygen in contact with the

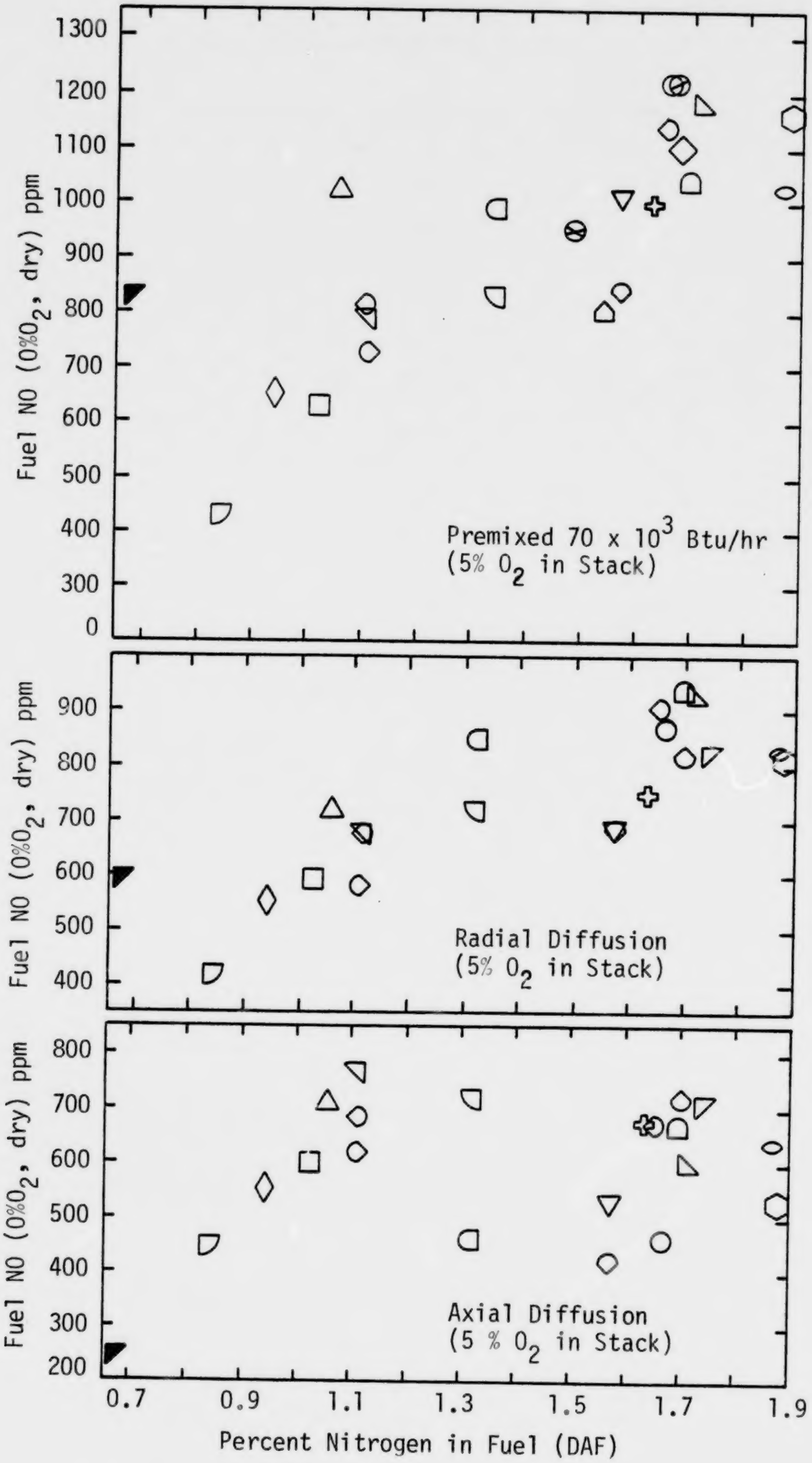

Figure 3-7. Fuel NO as a Function of Fuel Nitrogen Content.

volatile fuel nitrogen fractions, and, therefore, the formation of N_2 from the volatile nitrogen species is maximized. The anthracite data (▼) indicate that with a low volatile coal, initial fuel/air contacting has relatively little effect on the exhaust emissions.

Thermal Environment. If the formation of fuel NO under excess air conditions is dependent upon the availability of volatile fuel nitrogen compounds, then increasing the particle temperature should increase fuel NO formation since it will promote the evolution of volatile nitrogen species. The amount of carbon dioxide added to the artificial oxidant could be varied to obtain different flame temperatures, and thus, thermal environment. Appendix B presents all the fuel NO data obtained with different CO_2 concentrations in the oxidant under three different mixing conditions, i.e., premixed, radial diffusion and axial diffusion. The influence of thermal environment on fuel NO formation is summarized in Figure 3-8.

The theoretical flame temperature provides a measure of the final bulk temperature, and although the actual measured temperatures are not as high as those shown in Figure 3-8, they are indicative of changes in the particle environment. It can be seen that fuel NO formation from premixed coal flames increases with increasing particle temperature. This effect was not observed with axial diffusion flames. This is either because the particle temperatures are not significantly changed or because the increase of volatility is not converted to NO because of lack of oxygen in the core of the axial diffusion flame.

Staged Combustion. The production of NO or N_2 from the gas-phase fuel nitrogen species is believed to depend almost totally on reactant stoichiometry. The formation of N_2 is favored over the formation of NO under fuel-rich conditions. Consequently, modification of the combustion process to allow pulverized-coal to react initially under oxygen-deficient conditions (staged combustion) is the most effective method of controlling NO formation in pulverized-coal-fired combustors. Staged combustion can be accomplished by several different techniques. The combustion process can be staged, either by physically separating the fuel-rich zone from the burnout zone, or by using a burner which delays the mixing of the fuel with all the combustion air.

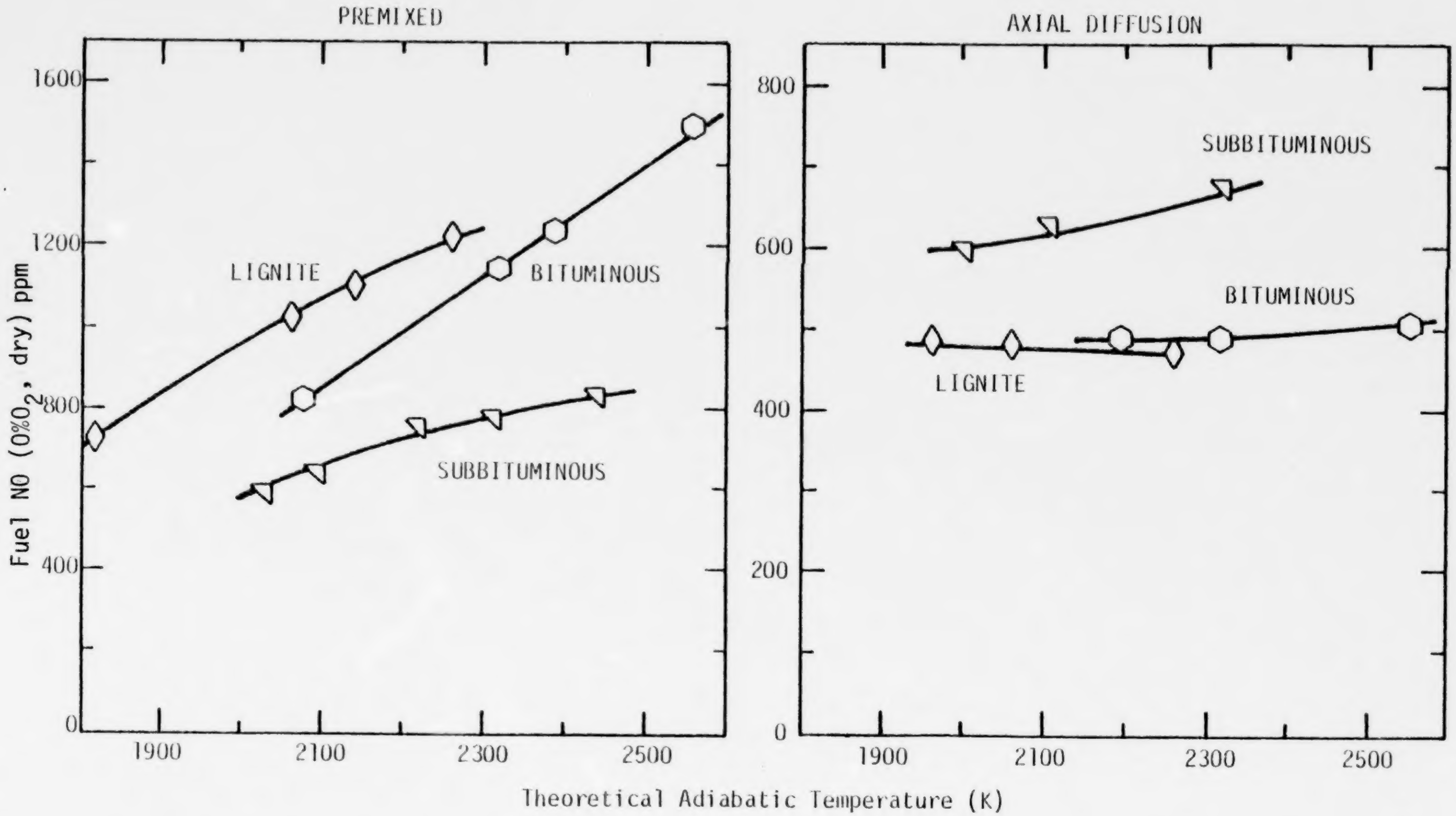

Figure 3-8. Influence of Thermal Environment at Two Mixing Conditions.

A series of experiments were carried out to assess the impacts of coal properties on NO formation under staged combustion conditions. Figure 3-9 shows typical staged combustion results for four coals of different rank with both the radial diffusion and premixed burners. Staged air was injected at 0.86m from the burner in these experiments and the overall stoichiometry was maintained at 1.25 with the first-stage stoichiometry varied from 0.9 to 0.4. Regardless of the initial fuel/air contacting conditions, for most of the coals tested, as the first-stage stoichiometry was reduced the exhaust NO decreased, reached a minimum, and then increased as the stoichiometry was further reduced. The anthracite tested with the diffusion burner did not exhibit this staging effect. Data for all the coals tested are presented in Appendix C. Figure 3-10 summarized these data in the form of minimum NO emissions as a function of the stoichiometric ratio at which the minimum occurs. Decreasing the initial fuel/air contacting rate not only lowered the minimum achievable NO levels but changed the optimum stoichiometric ratios.

Experiments were also conducted to determine whether the reduction of NO brought about by staging could be enhanced by more gradual addition of tertiary air (three-stage combustion). Figure 3-11 illustrates the furnace configuration and data obtained for the Utah-II bituminous coal for a typical three-stage combustion experiment. The first-stage stoichiometry (SR_1) was kept constant while the second-stage stoichiometry (SR_2) was varied by adding appropriate amounts of air at 0.53m and 0.86m to maintain the overall stoichiometric ratio at 1.25. Maintaining the SR_1 at 0.7, where the lowest NO emissions were obtained for two-stage combustion, produced lower emissions than when the first was maintained at 0.4. One possible explanation for this is that at the more fuel-lean condition the temperature in the first stage was increased. This could result in the production of more volatile nitrogen which was then converted to N_2 in later stages. A decrease of approximately 40 ppm was achieved in the three-stage configuration. Data for all the coals tested under three-stage conditions are presented in Appendix D. Figure 3-12 summarizes the minimum NO emissions under both two- and three-stage conditions. The differences between two- and three-stage operation are slight, and it appears that three-stage operation does not offer enough advantages to justify this additional complexity.

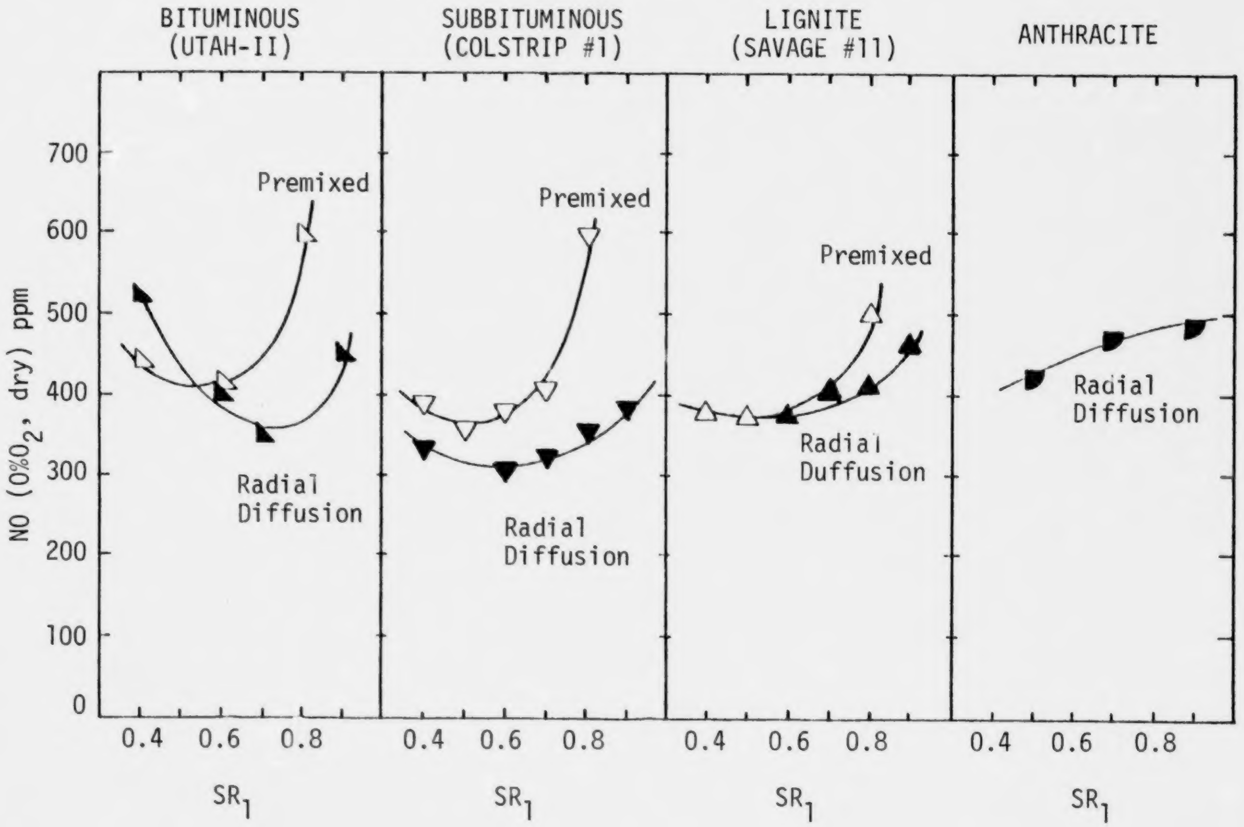

Figure 3-9. Effects of Fuel Type/Mixing Characteristics on Staged NO Emissions.

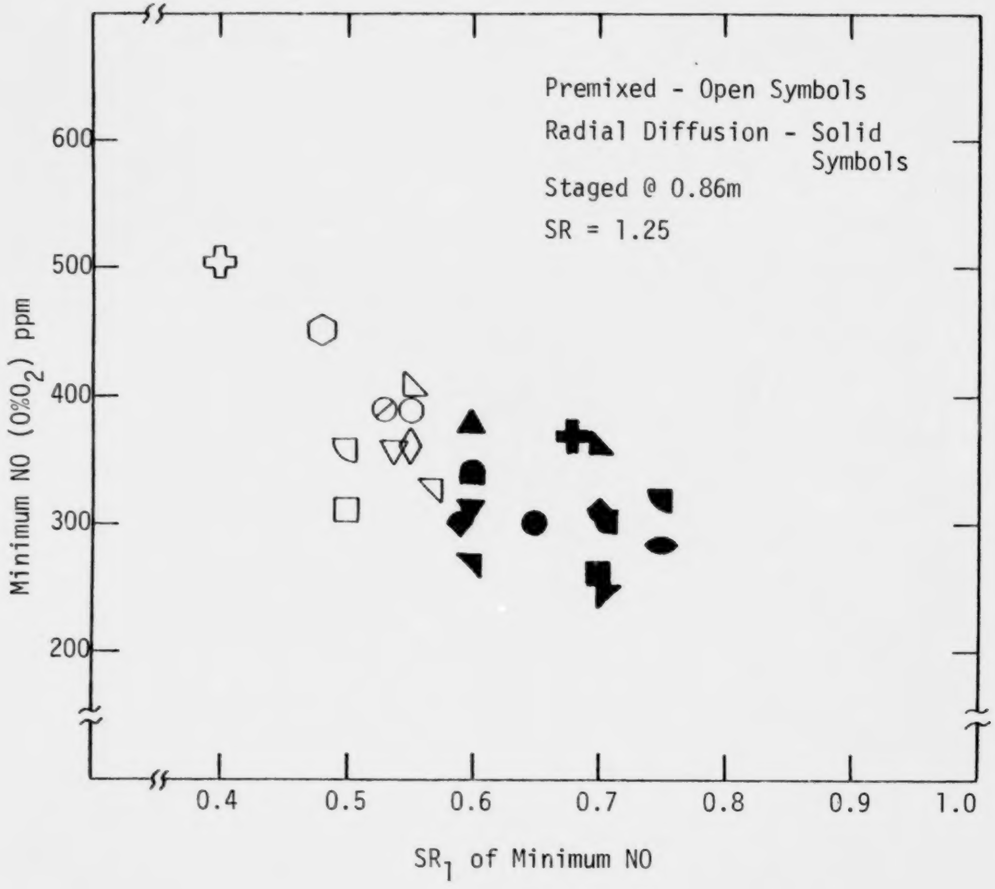

Figure 3-10. Effect of Mixing Characteristics on Minimum NO Emissions.

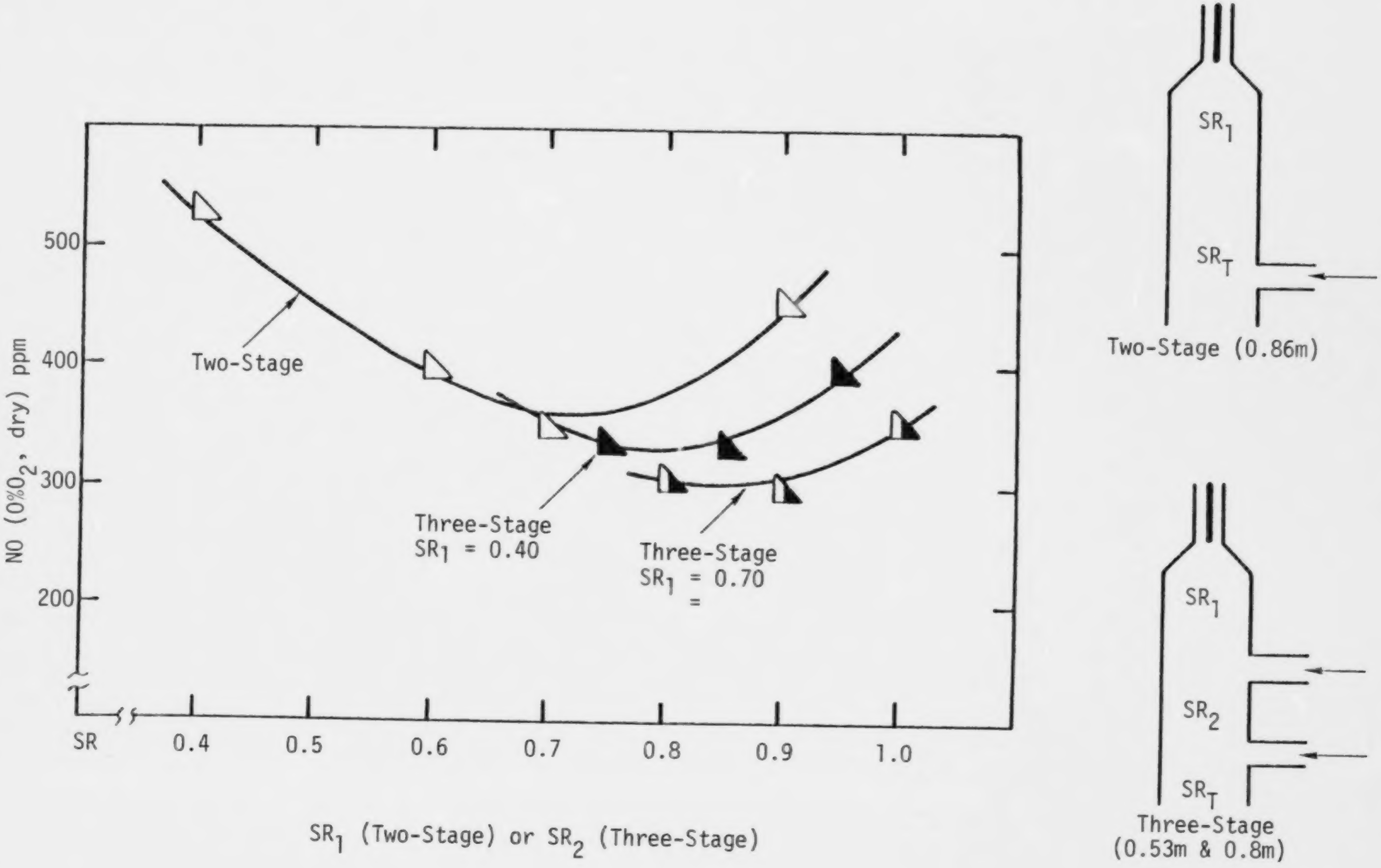

Figure 3-11. Two- and Three-Stage Combustion of a Bituminous (Utah-II) Coal.

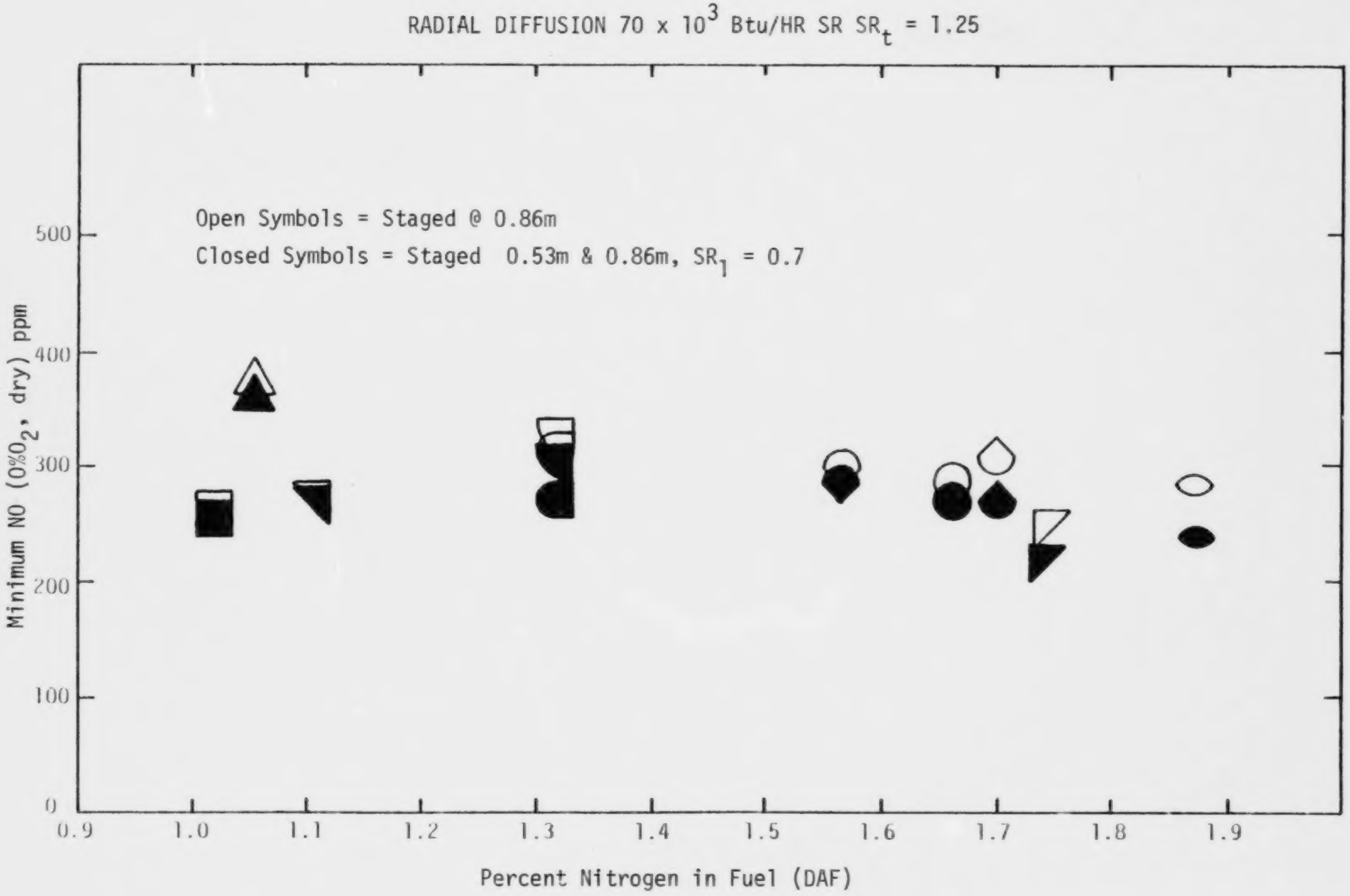

Figure 3-12. Minimum Percent Conversion of Fuel Nitrogen in Two- and Three-Stage Combustion.

Particle Size. The influence of particle size on the fate of fuel nitrogen was investigated by burning Utah bituminous coal mechanically sieved into narrow-size ranges. A cut of coal with a mean diameter of 165μ, and a cut smaller than 37μ was burned in the premixed mode. Figure 3-13 shows the size distribution of these cuts compared to the normal 65 percent through 200 mesh distribution. The results obtained in excess air experiments (i.e. unstaged) indicate that larger particles produce lower NO than the smaller particles. This is probably due to differences in volatile and char-nitrogen distribution resulting from different particle heating rates and subsequent volatile evolution.

Results obtained under staged-combustion studies indicate that the minimum NO is lower for smaller particles. Increasing particle size decreases the rate of volatile nitrogen evolution in the first stage, thereby reducing the time available for NO to N_2 conversion as well as increasing the quantity of nitrogen carried into the second stage with the char.

3.2.3 Questions to be Resolved

Results obtained with the original furnace have demonstrated that, under excess air conditions, fuel NO formation is dependent upon coal properties, mixing conditions, the thermal environment and the particle heating rate; and total fuel nitrogen content is not the only fuel property which controls the formation of NO. Under staged combustion conditions, NO emissions are dependent upon the fuel composition and initial fuel/air contacting.

However, these results did not provide information to answer the following questions which need to be resolved in order to understand the fate of coal nitrogen during combustion.

- What are the fuel characteristics that dominate fuel NO formation? Why did the two lignites, Beulah #9 and Savage #11 produce very different levels of fuel NO although both had very similar nitrogen contents (see Figure 3-7)?
- To what extent does fuel/air contacting interact with fuel characteristics in the formation of fuel NO? Why did the same differences in mixing not have as great an effect upon the lignite and subbituminous coals (see Figure 3-7)?

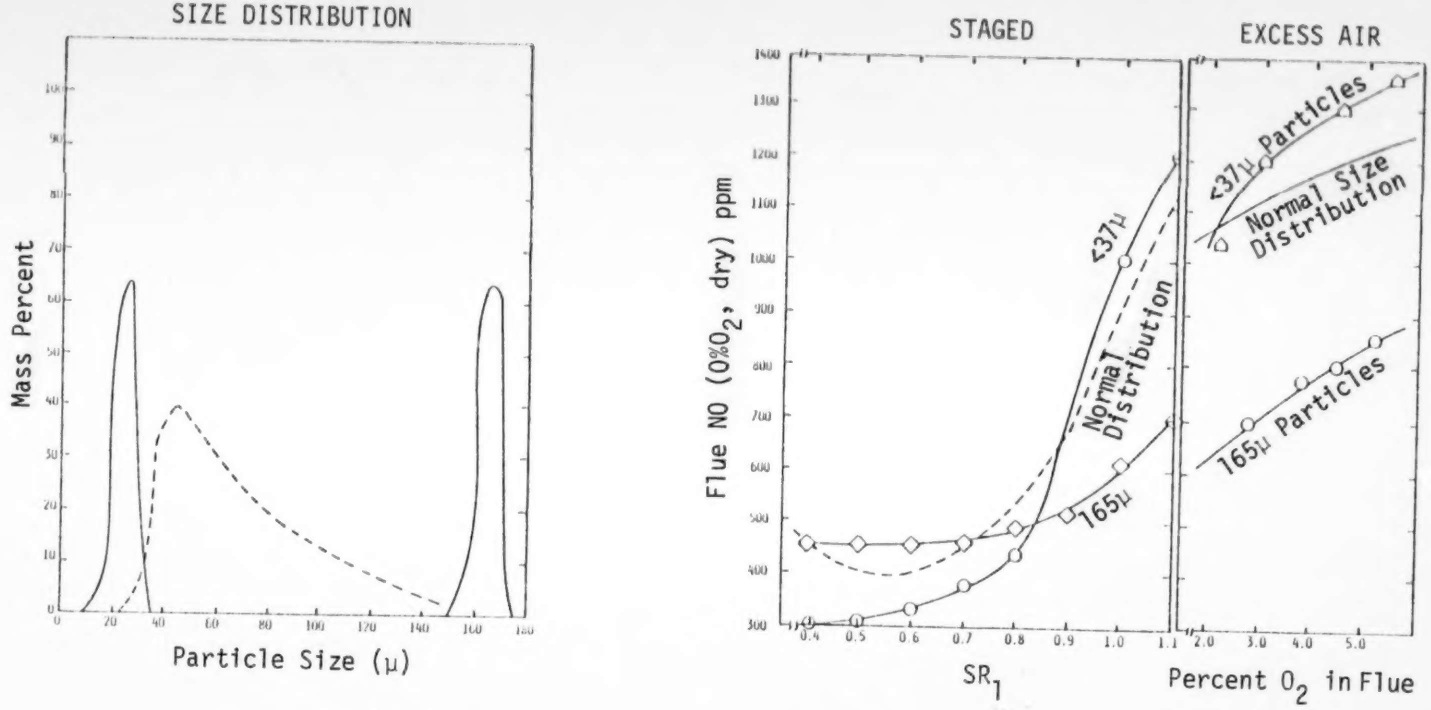

Figure 3-13. Effect of Particle Size.

- What are the coal properties that determine the exhaust NO emissions under staged combustion conditions? How do the coal properties affect the effluent composition of the first stage? Why did a minimum exist in exhaust NO concentrations?
- What are the optimum conditions for a staged combustion system? What are the impacts of these conditions on the distribution of the oxidizable nitrogen species in the first stage as well as the conversion of these nitrogen species in the second stage?

The original furnace was modified, as discussed previously, and a series of experiments was carried out in an effort to answer the above questions and advance the present knowledge of the fate of coal nitrogen. Results obtained from the modified furnace are discussed in the following two sections.

3.3 The Role of Char and Volatile Nitrogen

The combustion of pulverized coal can be considered as a combination of the combustion of volatile fuel fragments produced during thermal decomposition and the oxidation of char. If this conceptual picture is extended to explicitly include nitrogen species, then it is possible that the variations in the contribution of volatile nitrogen and char nitrogen may be one of the significant fuel parameters affecting overall fuel NO formation.

3.3.1 Conversion Characteristics

It has been suggested that the conversion of the volatile nitrogen in a coal flame is approximately the same as that observed in gas and liquid fuel flames, but significantly higher than char nitrogen conversion to NO. The percent conversion of fuel nitrogen to NO is shown in Figure 3-14 as a function of excess oxygen for these low-volatile solids. The conversion of fuel nitrogen from these low-volatile solids was significantly less than that obtained with bituminous coals.

The lower conversion of char nitrogen to NO may be due to the absence of volatile combustion which prevents the particles from attaining high temperatures and therefore reduces the quantity of volatile nitrogen. A series of experiments was carried out in which propane was added to the Utah char feed to raise the total hydrocarbon volatile content to 43 percent (equivalent to the parent Utah coal). The impact of the increased

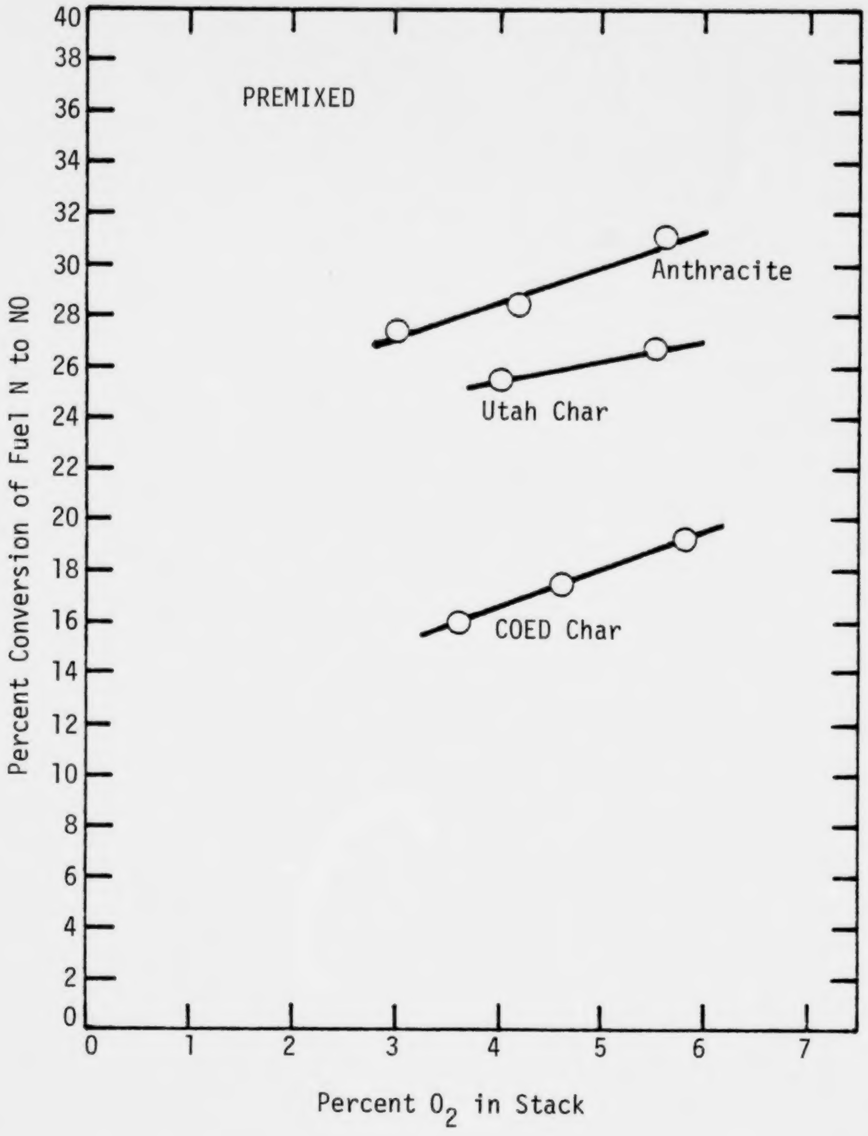

Figure 3-14. Fuel Nitrogen Conversion in Low-Volatile Solids.

volatile content on fuel nitrogen conversion is shown in Figure 3-15 for both the Utah and the COED char. The addition of propane results in a flame that visually appeared to be equivalent to pulverized coal, and the fuel nitrogen conversion was significantly increased in both cases. The addition of propane resulted in an increased burning rate, and an increased fraction of nitrogen released from the char which was then available for conversion in the gas phase.

The impact of volatile nitrogen on fuel NO formation is illustrated by the data presented in Figure 3-16 where the percentage of fuel nitrogen conversion for a Utah coal, the char derived from this coal, and a light liquid product derived from a bituminous coal (SRC-II) is shown as a function of excess oxygen content. The conversion of the fuel nitrogen in the char is significantly below that of the coal, and the conversion of the nitrogen in the SRC-II coal product is considerably higher than that obtained with any of the solid fuels. Thus, it appears that volatile nitrogen species are much more likely to produce NO than the nitrogen retained in the char. However, to further investigate this fact, several tests were carried out with a simulated coal composed of char, propane, and ammonia. The propane and ammonia were added in the quantities required to directly simulate the hydrocarbon volatile content and the total nitrogen content of the parent Utah coal. The results shown in Figure 3-16 indicate that the simulated coal produces emissions equivalent to the parent coal.

3.3.2 Char/Volatile Nitrogen Interaction

The percent conversion of the volatile nitrogen in the simulated coal, added as ammonia, can be calculated by assuming that the conversion of char nitrogen in the simulated coal is the same as that in the char/propane mixture. Figure 3-17 shows the ammonia conversion to NO in a series of experiments in which char was either present or absent. These experiments were conducted with identical propane and ammonia flow rates, the only difference being the presence of char. Without the char in the feed, the ammonia conversion was very similar to that obtained with the SRC-II coal liquid (see Figure 3-16). However, when the char was present the conversion was dramatically reduced, approximately to the level observed with pulverized coal. Experiments were also carried out by replacing ammonia with nitric oxide or

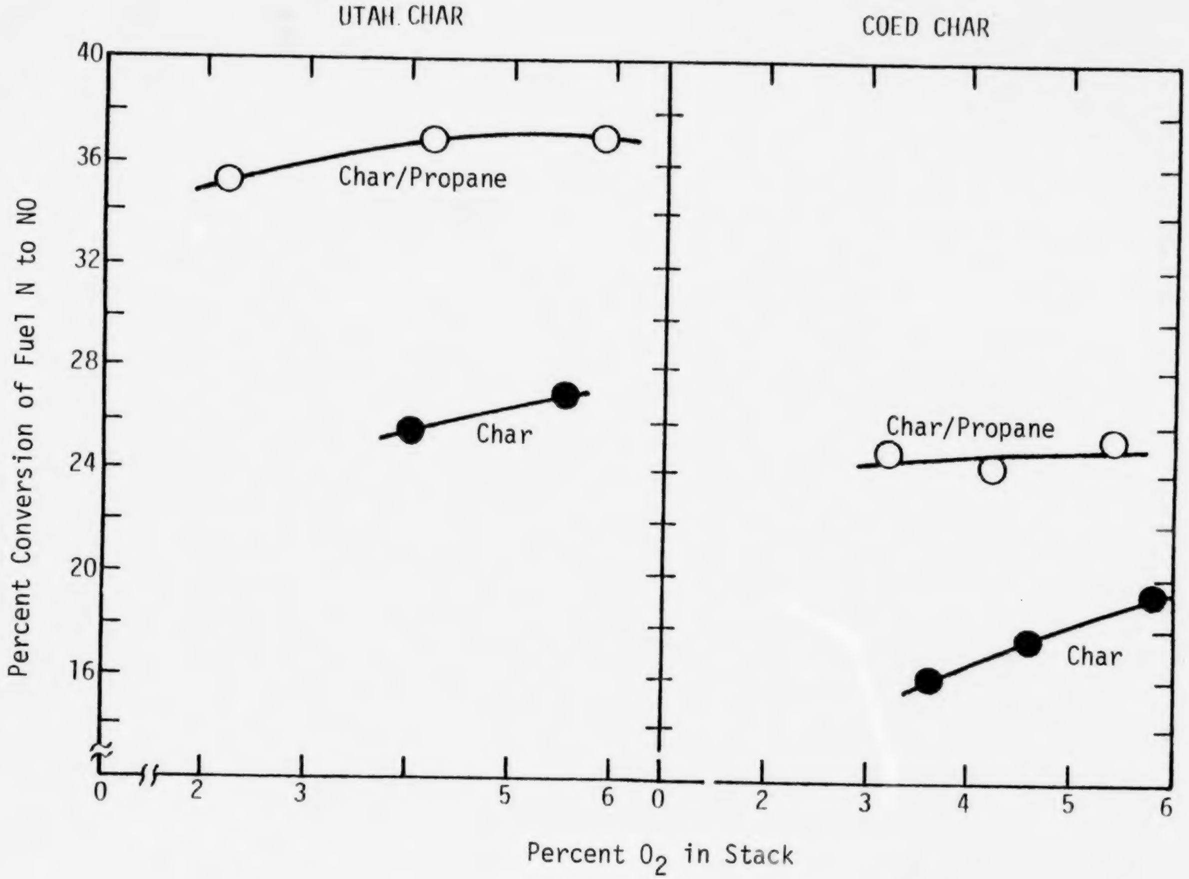

Figure 3-15. Influence of Hydrocarbon Volatiles on Char Nitrogen Conversion.

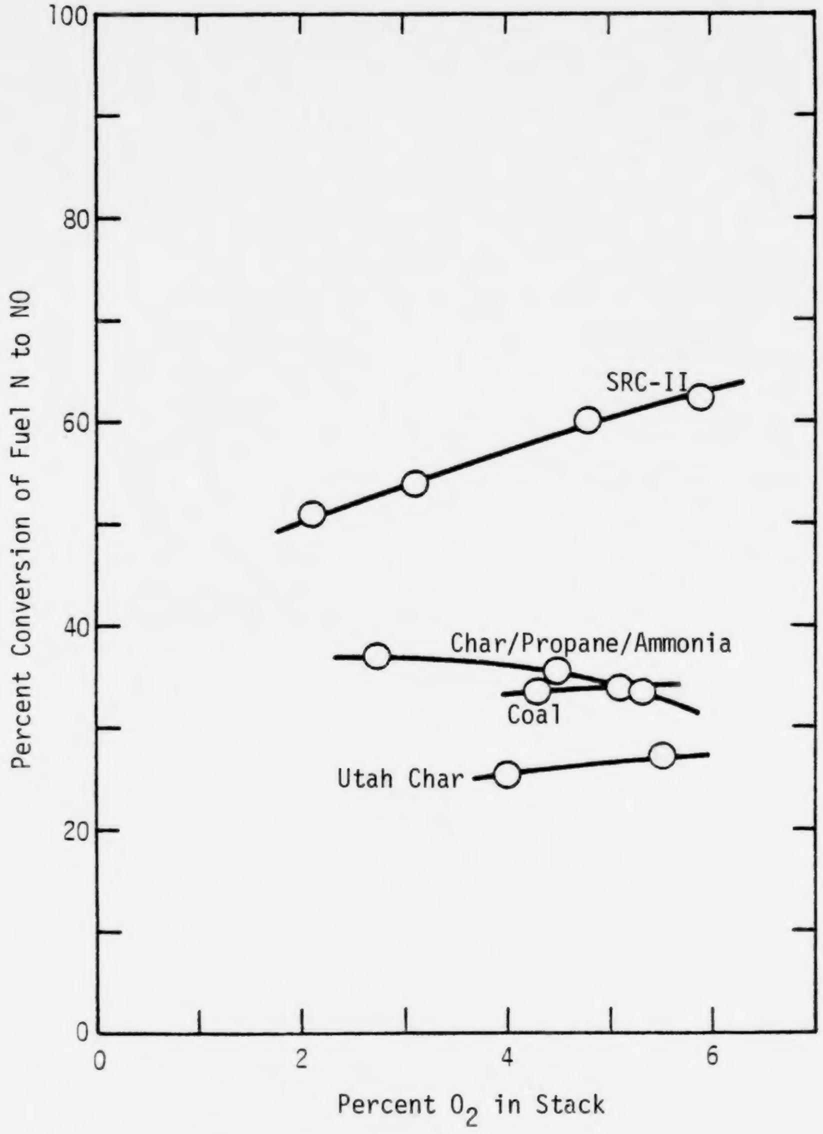

Figure 3-16. Importance of Volatile Fuel Nitrogen.

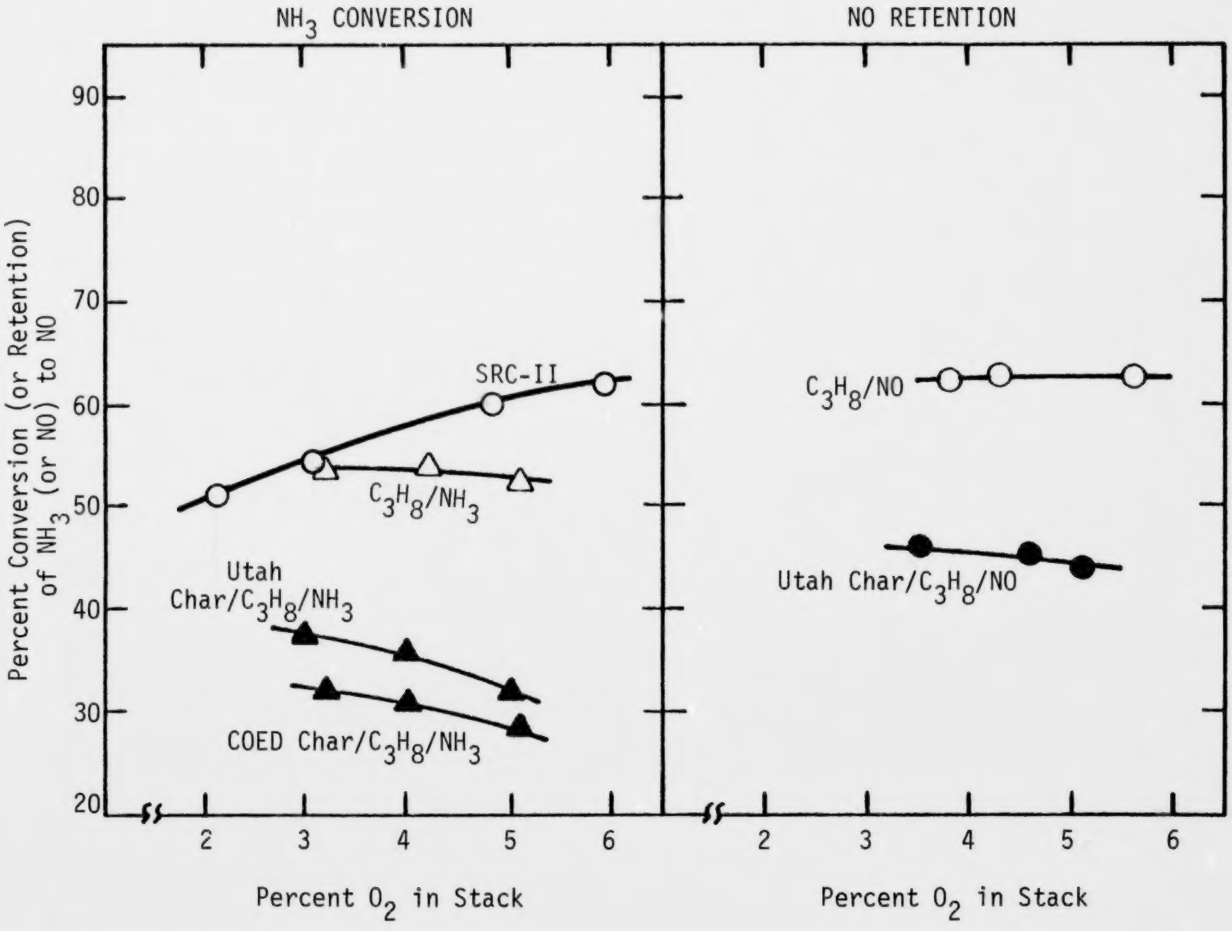

Figure 3-17. Influence of Solid Phase in Volatile Nitrogen Conversion.

replacing the Utah char with the COED char of lower volatile content. These results are also shown in Figure 3-17 and reveal that similar reduction of conversion efficiency was observed as with the NH_3 conversion.

3.3.3 Impact of Flame Conditions

The impact of oxygen availablity on fuel NO formation is illustrated by the data presented in Figure 3-18. Both the parent coal (Utah bituminous) and the simulated coal have the same hydrocarbon volatile content and the same total nitrogen content on a dry, ash-free basis. Conversion for both the coal and the simulated coal decreases with decreasing mixing rate.

Figure 3-19 shows similar results for the Utah char above and indicates that mixing rate appears to have relatively little effect on the conversion of char nitrogen. Also shown in Figure 3-19 is the conversion of the simulated nitrogen volatiles (based on data with and without ammonia) where it can be seen that the volatile nitrogen conversion decreases dramatically as the initial fuel/air contacting rate is reduced.

In conclusion, results obtained have demonstrated that char nitrogen conversion is much lower than the conversion of volatile nitrogen. Fuel/air contacting rate has little effect on the conversion of char nitrogen, a result which is consistent with the low-volatile anthracite data obtained in the unmodified furnace. Volatile nitrogen conversion is very sensitive to local oxygen availability.

3.4 The Optimization of Staged Combustion

This chapter will describe results obtained from the modified furnace to define the optimum conditions for staged combustion. The design parameters for any staged combustion system are:

- The primary zone stoichiometry.
- The residence time in the rich zone.
- The temperature history of the reactants.
- The conditions under which the second-stage air is added to the effluent of the first stage.

3.4.1 Mechanisms of Rich/Lean Process

Detailed in-flame measurements of gas species concentrations, solids composition and concentration, and temperature were made for 14 coals to

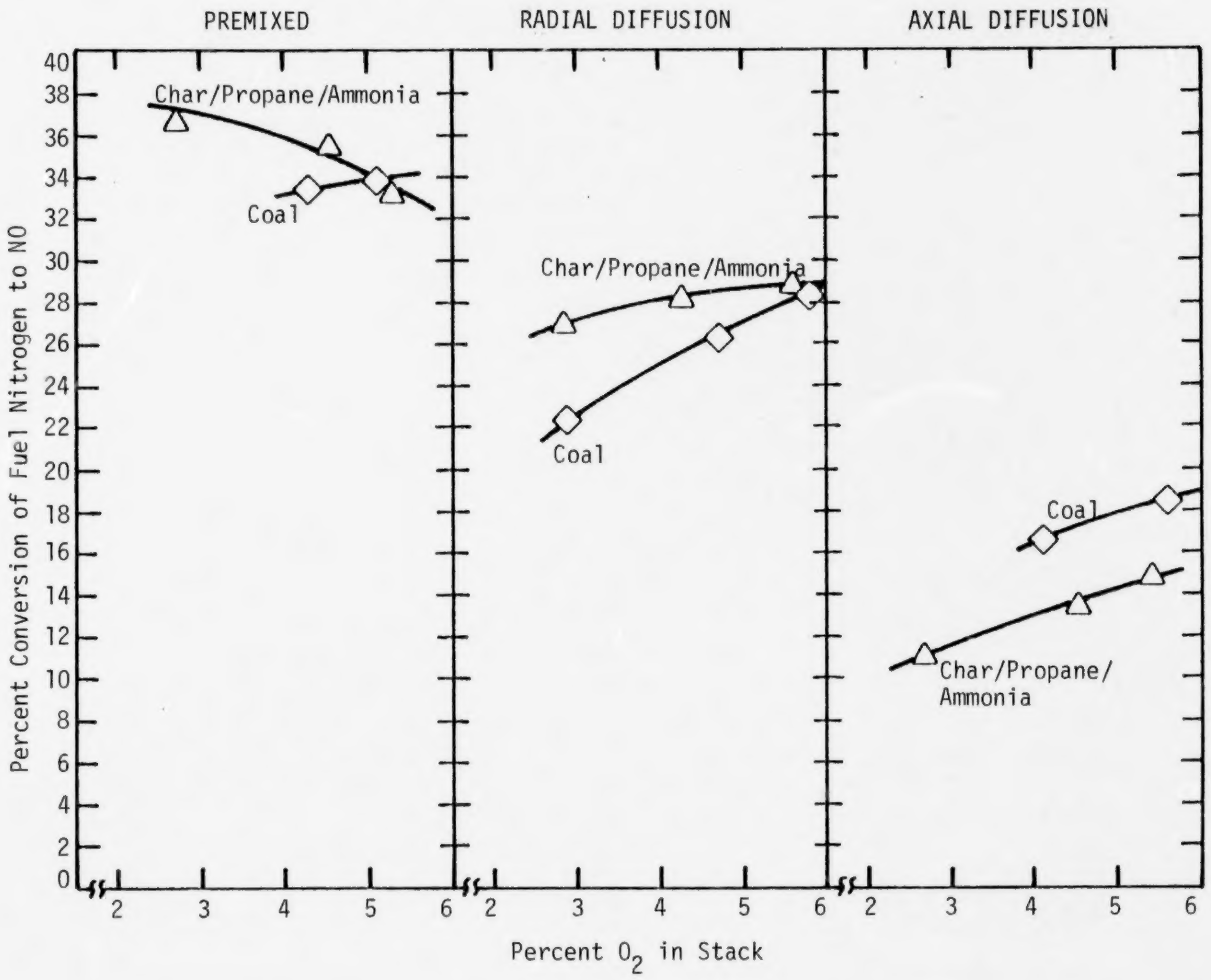

Figure 3-18. Effect of Mixing Conditions on Overall Fuel Nitrogen Conversion.

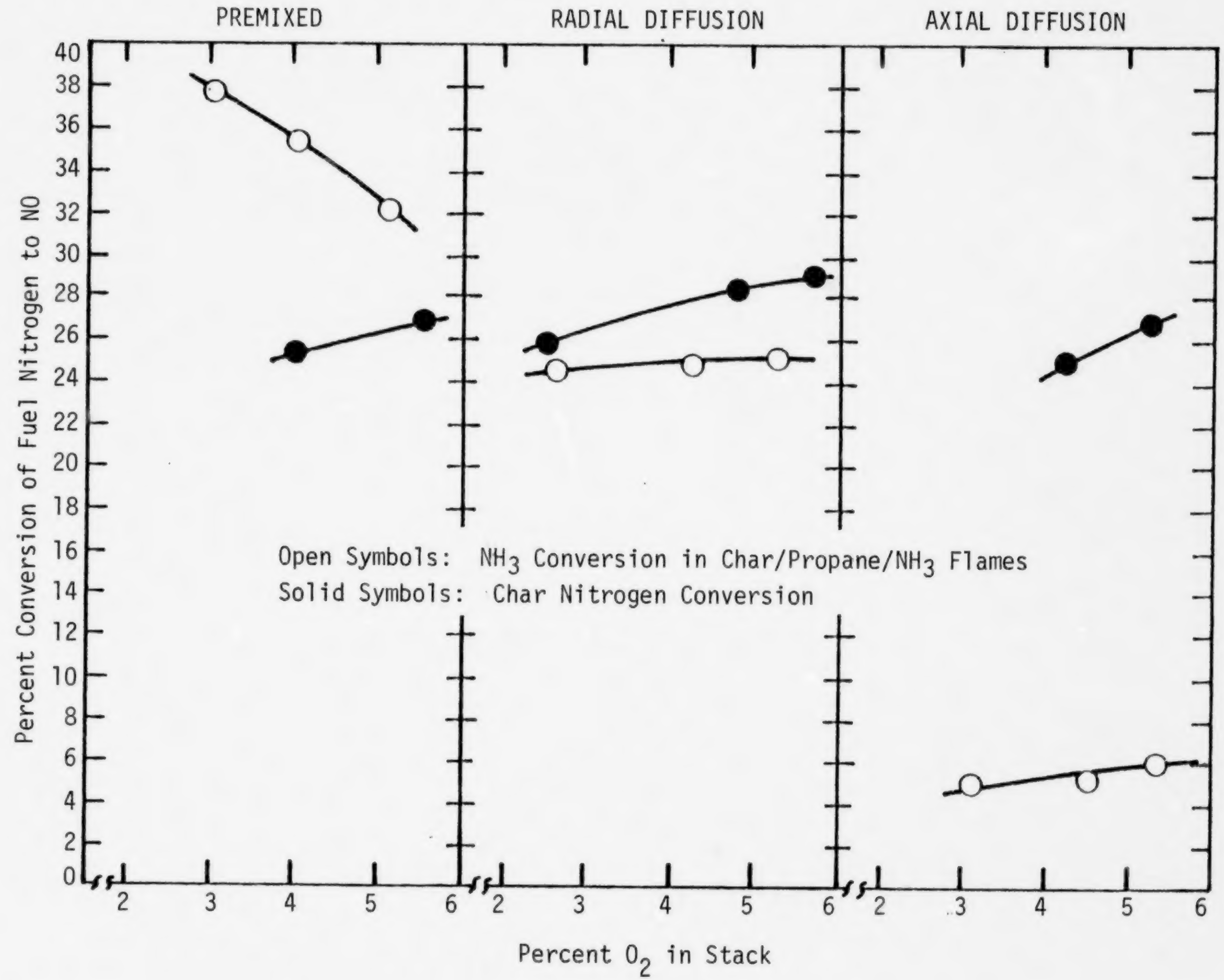

Figure 3-19. Effects of Mixing Condition on Volatile and Char Nitrogen Conversion.

define the relationship between coal composition and first-stage parameters. Figure 3-20 shows a set of typical results for the Beulah, North Dakota lignite with the premixed burner. All gas-phase concentration measurements are shown on an as-measured (dry) basis, except the exhaust NO concentrations which have been reduced to 0 percent O_2 (SR = 1.0). As the first-stage stoichiometry is reduced, the NO exiting the first stage decreases, but ultimately this is compensated for by an increase in other oxidizable nitrogen species (e.g., HCN and NH_3). The particle temperatures (measured at 0.53m using two-color pyrometry) also decrease, and a significant amount of both the nitrogen and carbon remain in the solid phase and are carried into the second-stage flame. Thus, there exists a minimum in exhaust NO concentrations because of the competition between decreased first-stage NO and increased oxidizable gas- and solid-phase nitrogen species.

Optimization of a staged system, consequently requires an appropriate minimization of the oxidizable gas- and solid-phase nitrogen species leaving stage. The next three sections of this chapter consider the influence of coal type and combustion parameters on the fate of gaseous and solid nitrogen in the first stage and their ultimate conversion in the second stage.

3.4.2 Influence of Fuel Properties

Total Gas-Phase Nitrogen. Figure 3-21 summarizes the total gas-phase fixed nitrogen (TFN = NO + NH_3 + HCN) measurements for the 14 coals tested. These data were obtained at a distance of 1.17m and a primary-zone stoichiometry of 0.75 with the premixed burner. In general, TFN increases with increasing fuel nitrogen content (Figure 3-21a) and correlates well with the exhaust NO emissions measured under unstaged (excess air) conditions (Figure 3-21b). Those coals which have high emissions under excess-air conditions, produce large amounts of gas-phase nitrogen species under fuel-rich conditions (e.g., the Utah, bituminous coal, ◍). The low-volatile anthracite (▼) gave very low emissions under excess-air operation and produced little TFN under fuel-rich conditions.

TFN Partition. Figure 3-22 shows the influence of coal composition on the partition of the gas-phase nitrogen species. The upper curves are for bituminous coals from the West (Utah), the South (Alabama), and Germany (Saar). The fraction of the TFN present as NH_3 was small for all of the

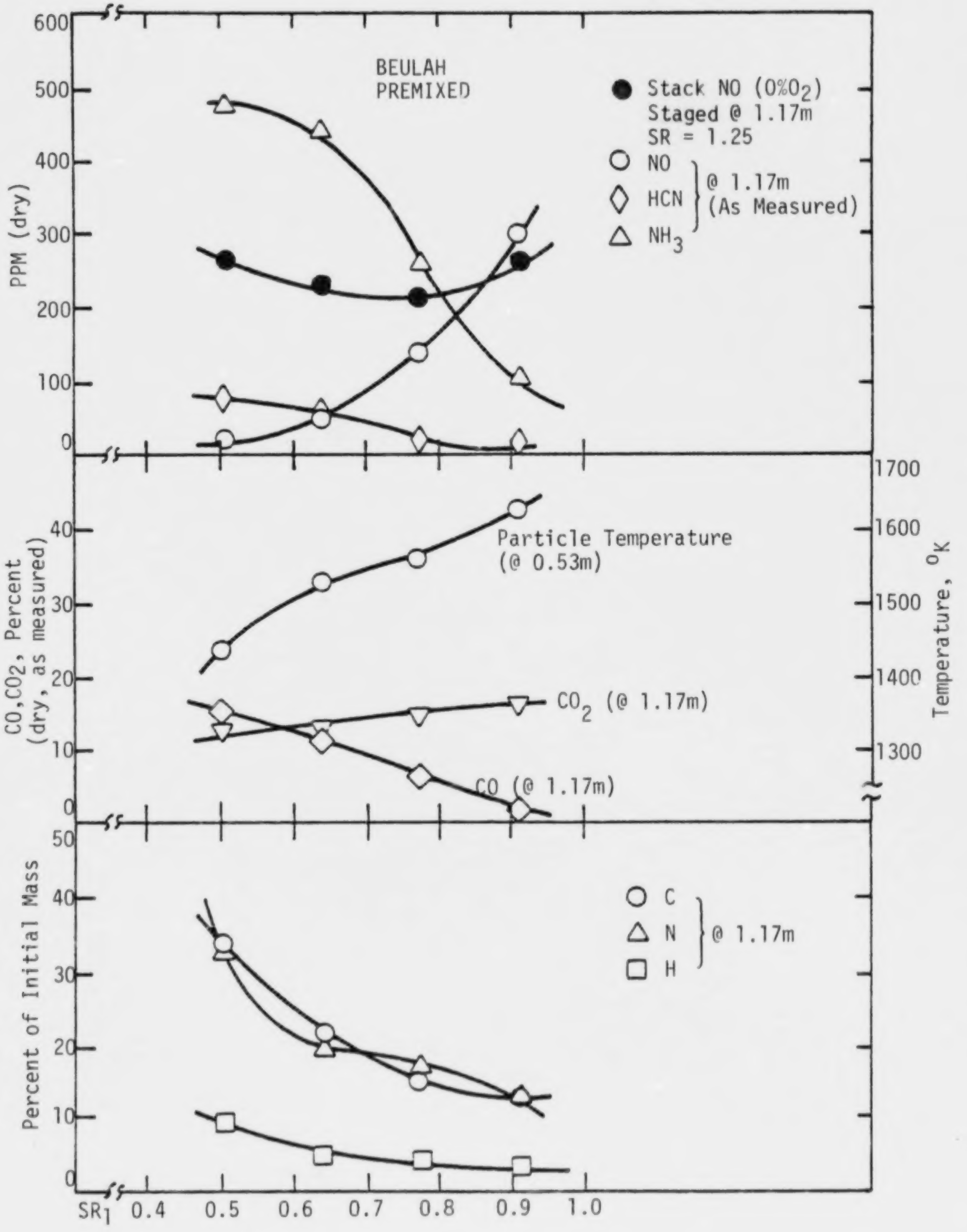

Figure 3-20. Gaseous Species Concentrations, Solids Composition and Temperature at the First-Stage Exit.

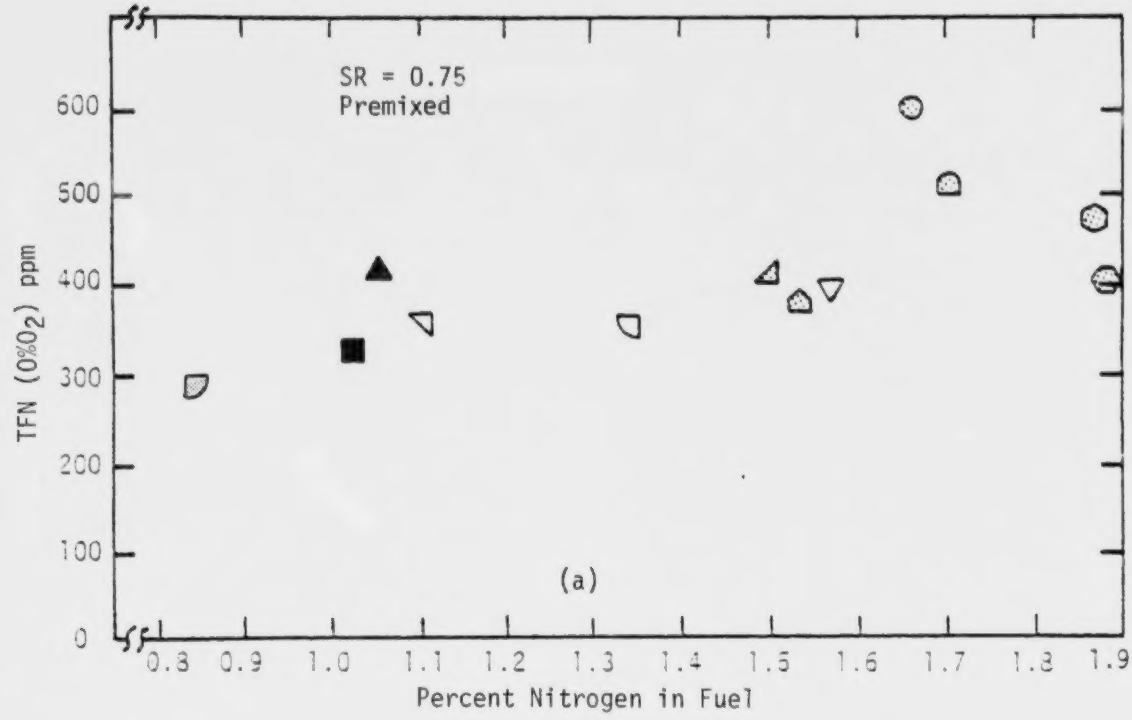

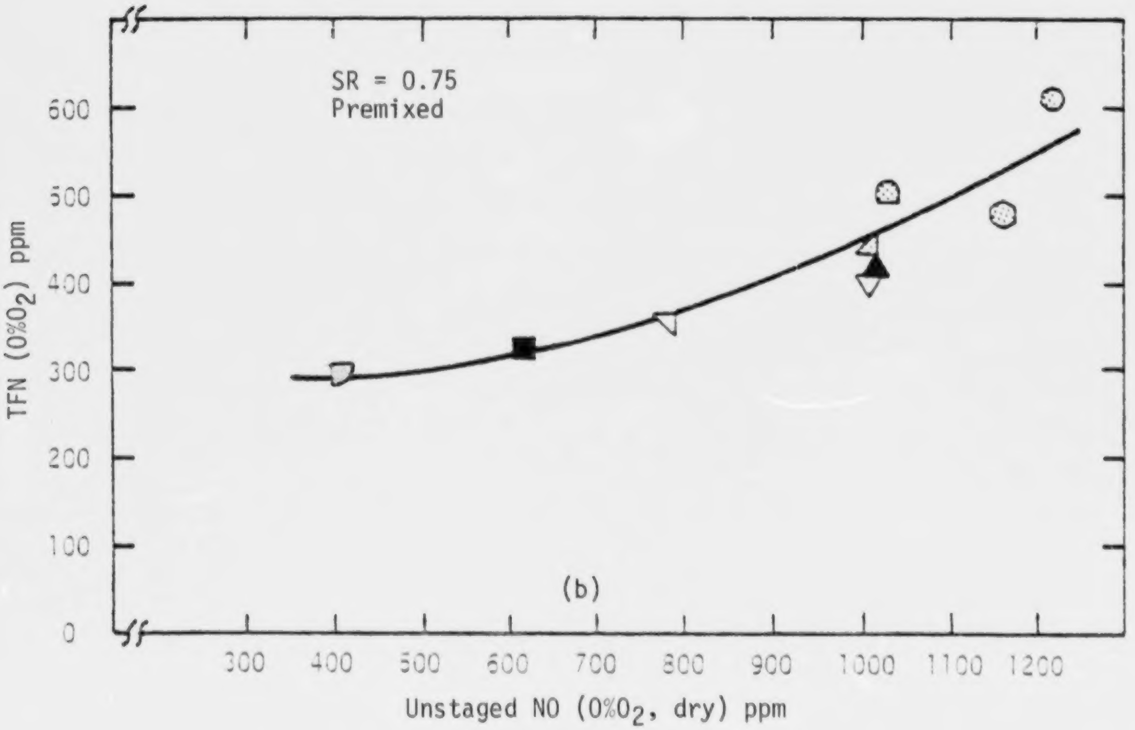

Figure 3-21. Correlation of TFN Content at the Exit of the First Stage With NO Formed Under Excess Air Conditions.

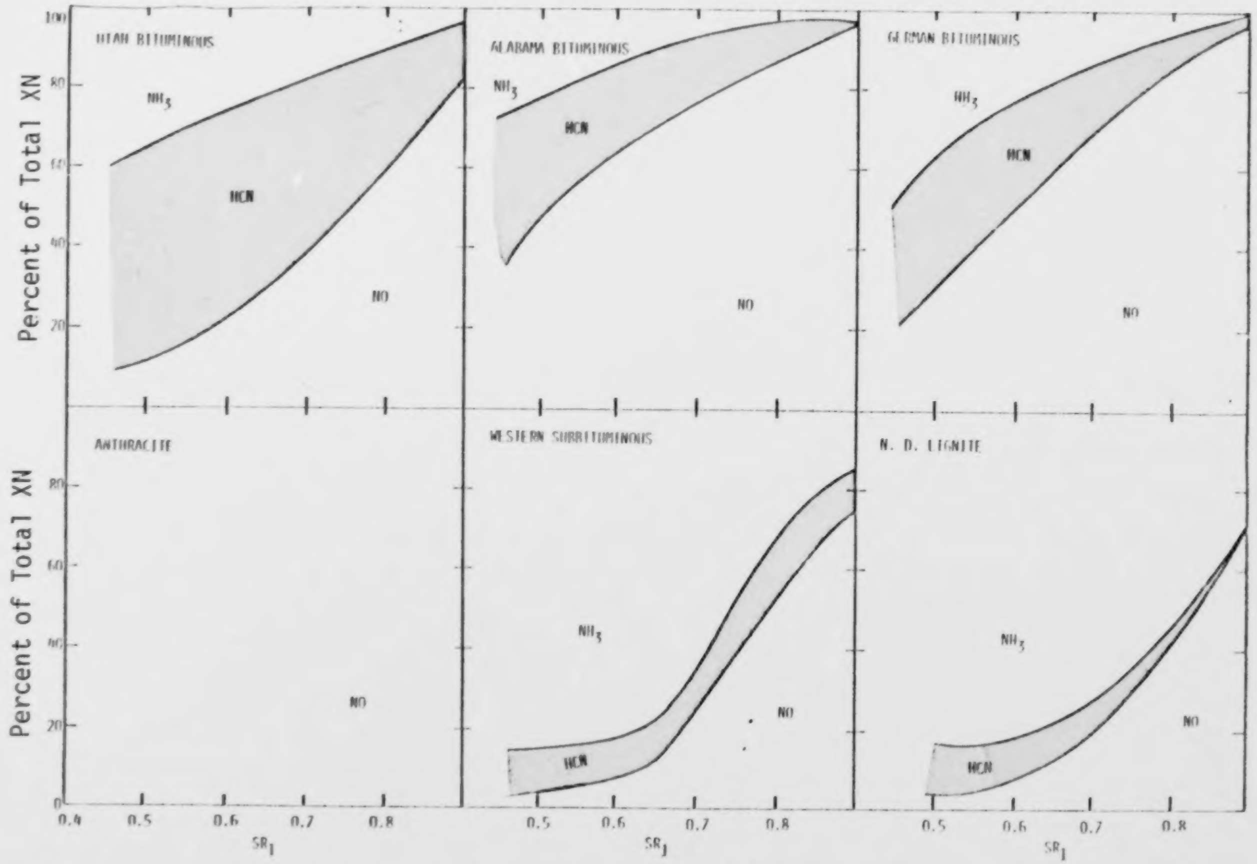

$(NH_3 + HCN + NO = 100$ Percent XN)

Figure 3-22. The Partition of TFN Species.

bituminous-coal studies (including the Rosa, Alabama coal, not shown). The Utah coal produced a significant amount of HCN compared to the other bitumnous coals.

The Pennsylvania anthracite (lower left) formed no HCN or ammonia; at all stoichiometries the only TFN species was NO. The Western subbituminous coals (Colstrip and Hardin,"not shown")exhibited much the same behavior as the Western lignite coals (Beulah and Savage,"not shown"). In each of these cases, the dominant TFN species was NH_3 below a stoichiometric ratio of approximately 0.7. HCN concentrations at 1.17m were small for all of the subbituminous and lignite coals. The fraction of the TFN leaving the first stage as NO was also substantially smaller than in the case of the bituminous and anthracite coals. Appendix E presents the TFN data for all the coals tested.

Solid Phase Nitrogen Retention. The relationship between fuel composition and the fraction of the fuel nitrogen retained in the solid phase under a given set of combustion conditions must be known if the optimum first-stage stoichiometry is to be predicted for a given fuel. Figure 3-23a shows the fraction of the initial nitrogen which remained in the char at 1.17m as a function of the initial nitrogen content for the premixed burner at a first-stage stoichiometry of 0.5. As expected, there is no obvious correlation with either total fuel nitrogen or rank. A standard ASTM proximate analysis of the original coal was made, and the resulting solid was analyzed for nitrogen to determine the fraction of the initial nitrogen volatilized under standard conditions. Figure 3-23b shows these results and indicates that there is at least qualitative agreement between the inflame solids sampling results and the modified ASTM coal analysis. The Savage, North Dakota lignite (■) retained only approximately 33 percent of its original nitrogen in the char after the ASTM volatile determination, and a similar, small fraction of the initial nitrogen was found in the solid material exiting the first stage of the experimental furnace. In contrast, the Alabama, bituminous coal (Rosa, ▨) retained over 60 percent of its nitrogen in the ASTM test, and also had a much higher fraction of its initial nitrogen still in the solid phase at the end of the first stage of the furnace.

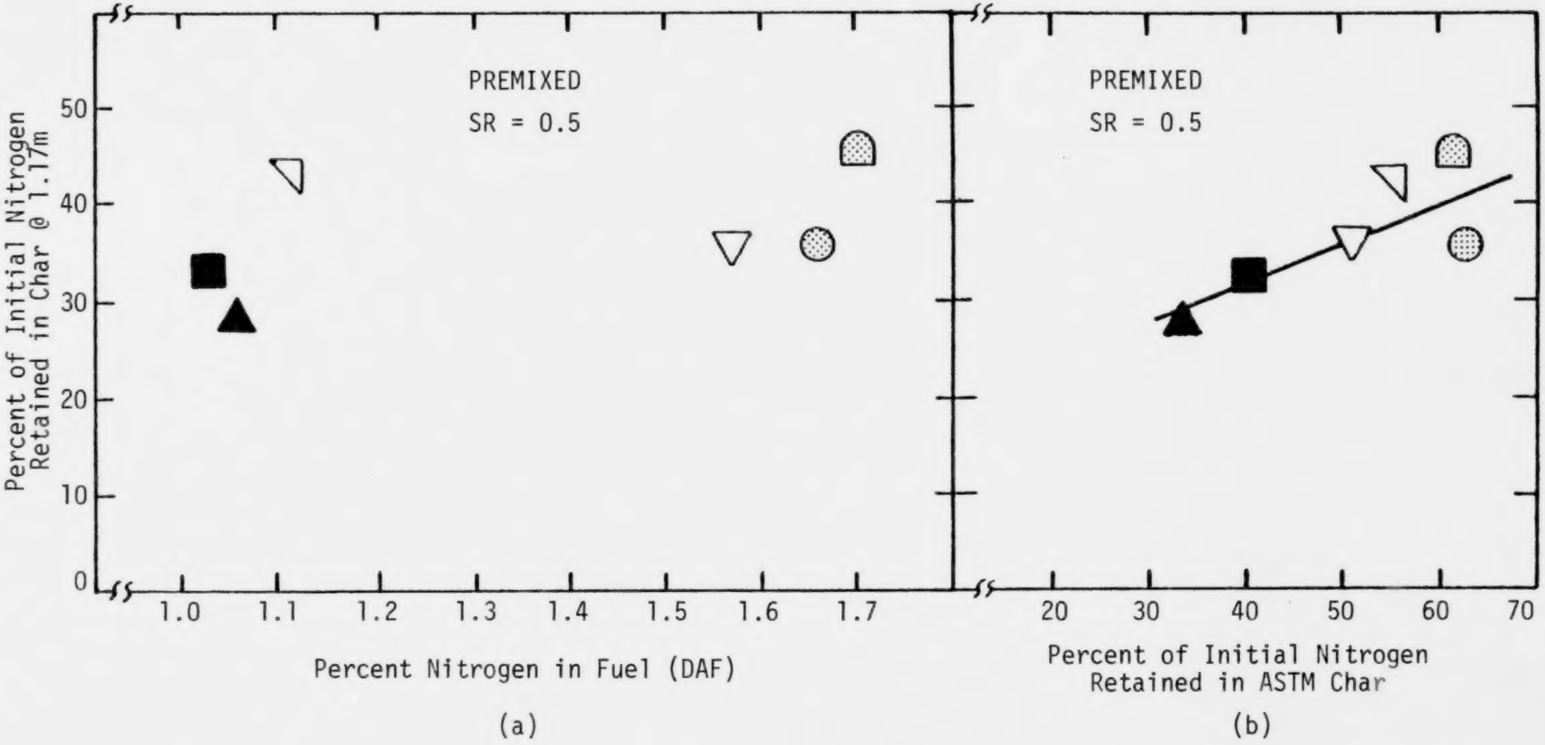

Figure 3-23. Correlation of Char Nitrogen With Modified ASTM Analysis.

Total Hydrocarbons. Figure 3-24 shows the total hydrocarbon content measured at the exit of the first stage for seven of the coals tested. The amounts of unburned hydrocarbon present in the three bituminous coal flames appeared to agree qualitatively with the HCN measured under fuel-rich conditions. Significant amounts of hydrocarbons were formed with the subbituminous and the lignite coals, although only small amounts of HCN were present in these flames. On the other hand, the low-volatile Utah char (⊗) produced little hydrocarbons, even under extremely fuel-rich conditions. To further investigate the role of hydrocarbons, experiments were conducted using the Utah char (Vm = 10.3 percent) with and without propane equivalent to a total volatile content of 43 percent. Figure 3-25 shows those results and indicates that hydrocarbons reduced first-stage NO by consuming a significant fraction of the total nitrogen available. Both HCN and NH_3 yields increased dramatically, resulting in a high TFN level.

3.4.3 First Stage Combustion Parameters

Primary Zone Stoichiometry. Figire 3-26 summarizes staged combustion results for a variety of fuels with the premixed burner in the modified furnace. The second-stage air was injected via the stainless steel air ring after the choke at a distance of 1.17m from the burner. All of the data were obtained at 5 percent overall excess O_2.

For all of the coals tested except the anthracite, the NO decreased, reached a minimum and then subsequently increased as the first-stage stoichiometry was progressively reduced. However, anthracite (and a Utah coal char, not shown) did not exhibit this minimum. Further, the optimum stoichiometric ratio was dependent on the fuel composition.

Fuel/Air Contacting. Measurements were also made to determine the input of initial fuel/air contacting rate. Figure 3-27 allows a comparison to be made between premixed and radial diffusion flames for two coals. The change in initial mixing had a greater effect on the bituminous coal than the lignite, as can be seen from either the exhaust emissions (top plot) or the internal XN concentrations (lower plots). In both cases, NO was the dominant species (middle plot) at high first-stage stoichiometries. The first-stage NO was decreased by decreasing the rate of fuel/air contacting (premixed to radial diffusion), resulting in lower exhaust emissions. When

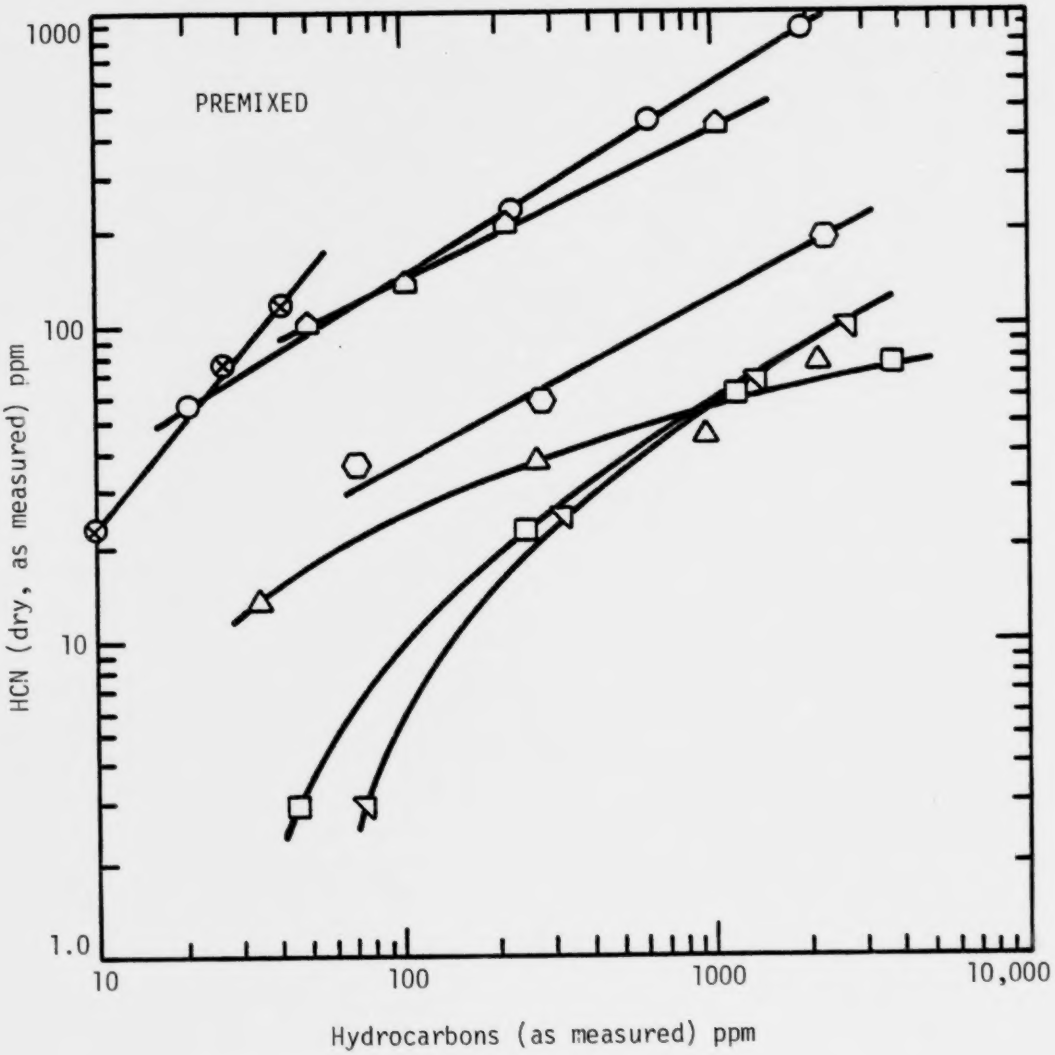

Figure 3-24. HCN as a Function of Total Hydrocarbons.

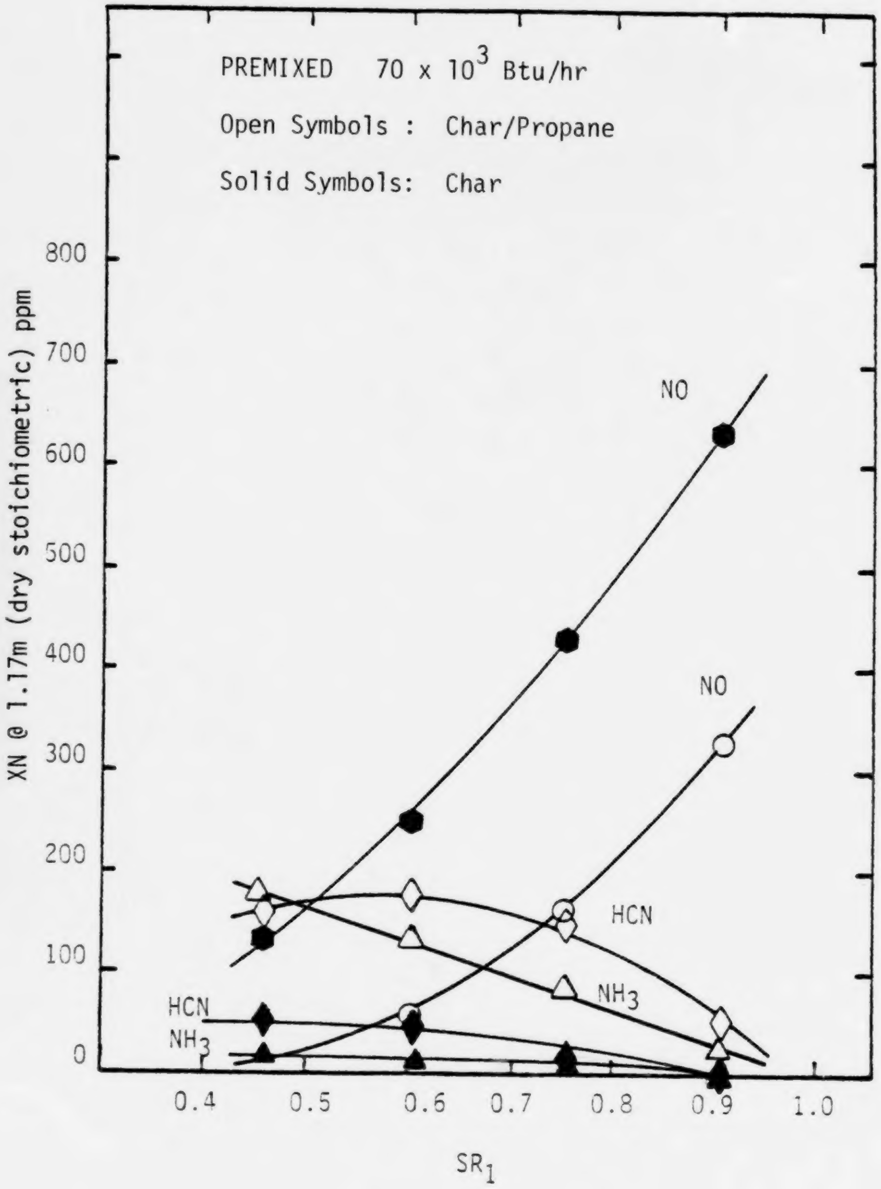

Figure 3-25. XN Species Distribution for Char and Char/Propane Flames at 1.17m From the Burner.

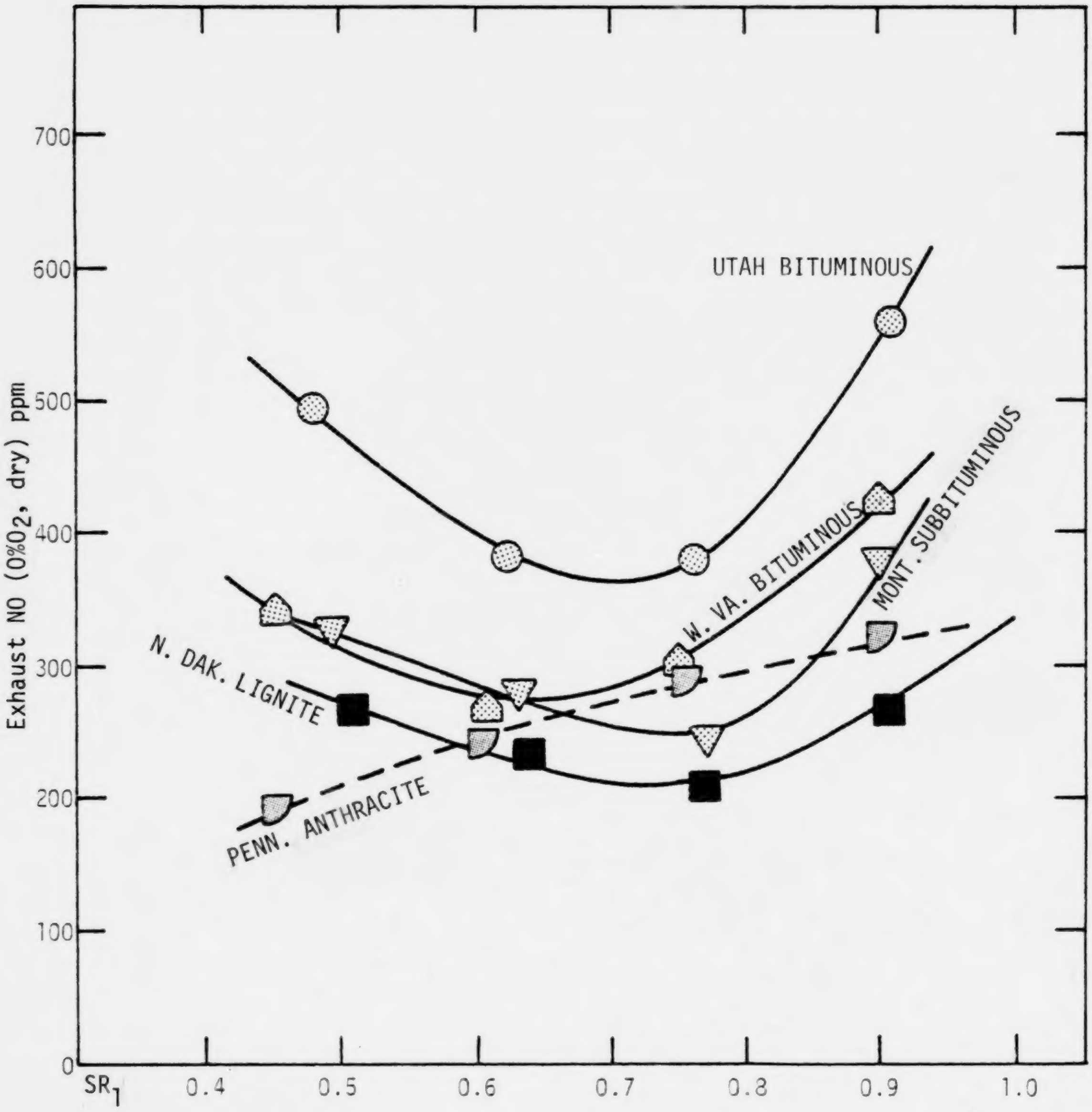

Figure 3-26. Influence of Fuel Type and Primary Zone Stoichiometric Ratio on Exhaust NO Emissions Under Staged Conditions.

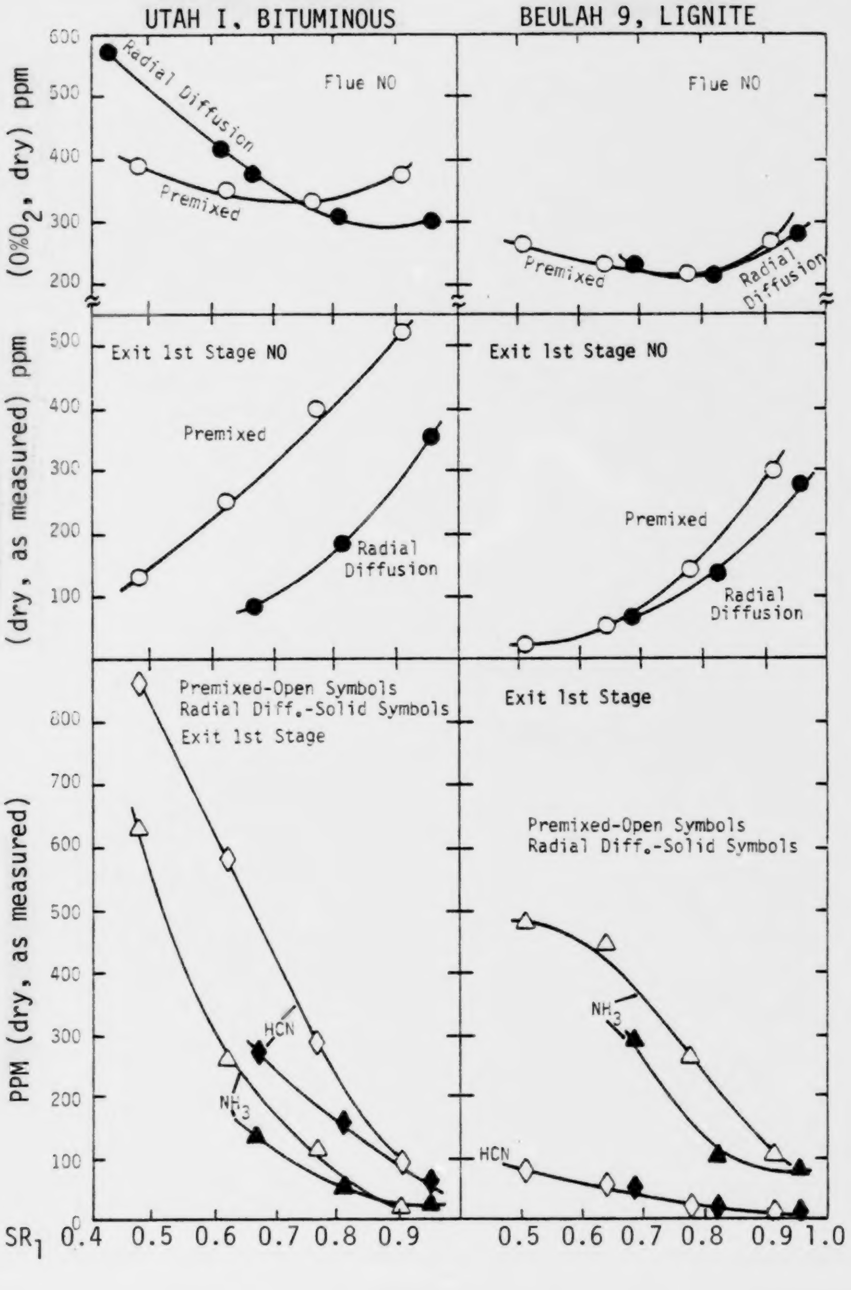

Figure 3-27. Influence of Fuel/Air Contacting on TFN Concentrations.

the first-stage stoichiometry became more fuel-rich, HCN was the primary contributor to the XN pool for the bituminous coal. In the case of the lignite coal, NH_3 was the major species, regardless of initial fuel/air contacting rate. Both HCN and NH_3 decreased with decreasing initial mixing rate. However, the radial diffusion flames produced higher exhaust NO than the premixed flames as the first-stage stoichiometry was reduced, although the nitrogen retained in the char was about the same for both flames, as shown in Figure 3-28 (lower plot). The carbon retention results (upper plot) indicate that the radial diffusion flames probably produced hotter first-stage effluent. Therefore, the higher NO emissions from the radial diffusion flames at lower stoichiometries are likely due to the higher conversion of TFN to NO at higher temperatures.

Residence Time. Figure 3-29 shows detailed axial profiles for three coals at a common stoichiometric ratio (SR_1 = 0.60) without the addition of second-stage air. The burnout results (based on the CO and the CO_2 measurements) indicate that the anthracite burns much slower initially than the bituminous and lignite coals. The first-stage NO from the anthracite forms slowly and then subsequently decays. Similar decays were observed with the Utah, bituminous and the North Dakota lignite; however, the initial NO formation was too rapid to be measured.

Significant amounts of HCN or ammonia were not observed with the Pennsylvania anthracite. Large quantities of HCN were formed and subsequently decayed with the Utah coal; small, relatively constant amounts of HCN were measured with the lignite coal. Significant amounts of NH_3 were measured at all axial positions with the lignite and to a lesser extent with the bituminous coals. From these data, it is clear that increasing the residence time in the first stage of a pulverized-coal combustor decreases the exhaust NO emissions because it allows time for the TFN concentrations to decrease from their early high values. It should be noted that although the input mixture is overall fuel rich, the gas-phase will be oxidizing in the early stages.

Temperature History. Figure 3-30 presents data on the impact of flame temperatures on gaseous nitrogen species within the fuel-rich first stage. These data compare conditions with and without the cooling coil immediately upstream of the staged air injection location (see Figure 3-1) for Utah coal

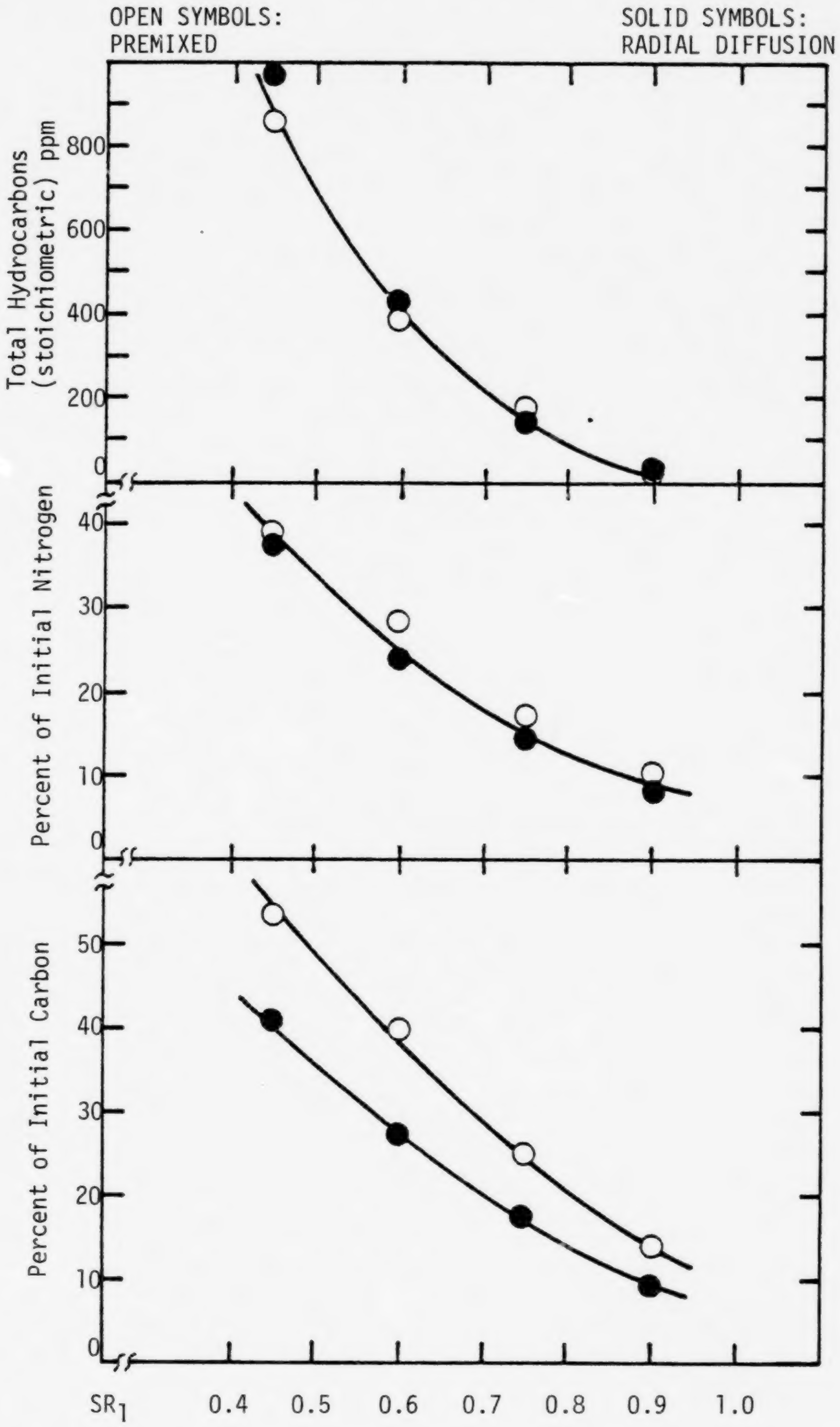

Figure 3-28. Influence of Initial Fuel/Air Contacting on Solids Composition and Hydrocarbons.

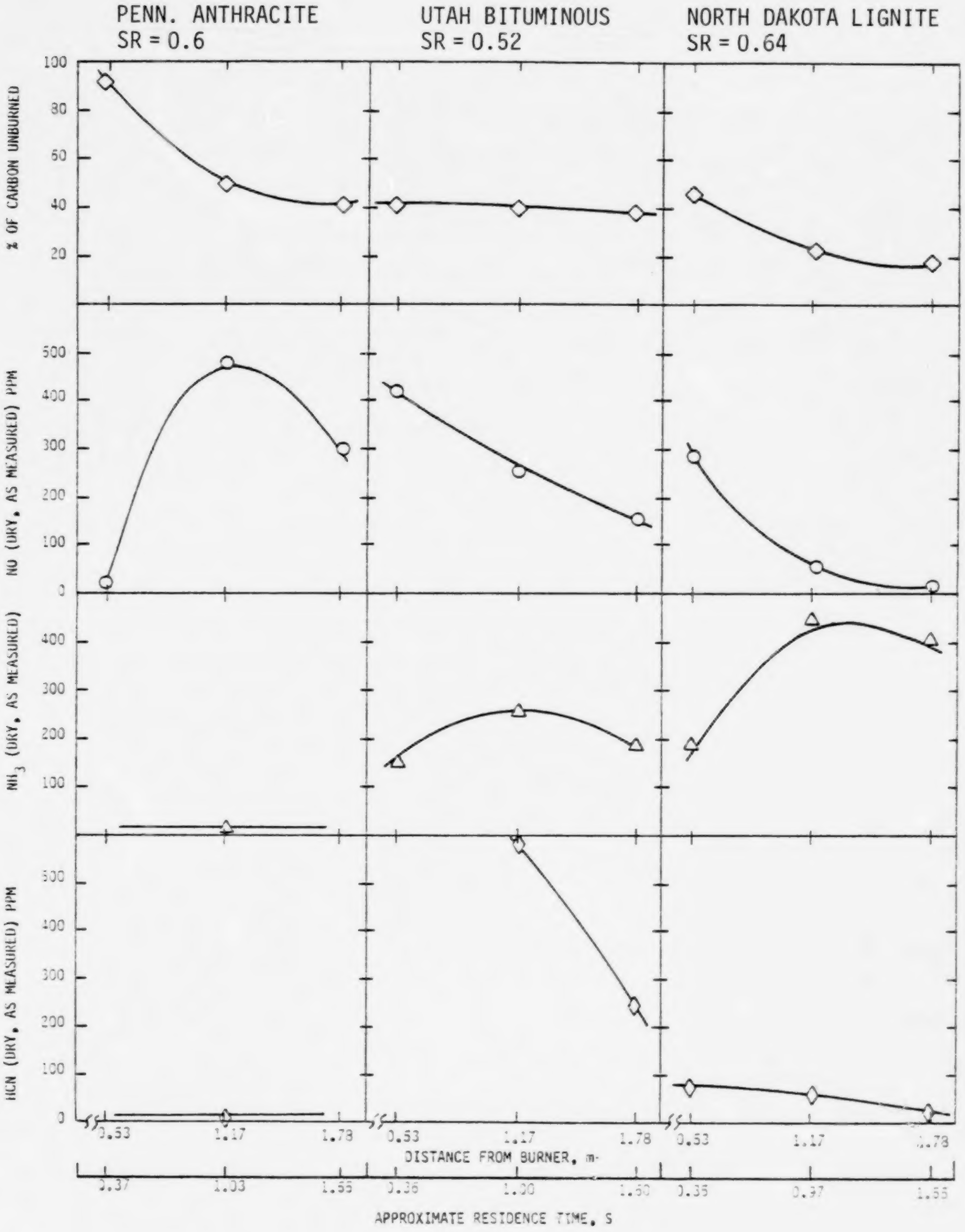

Figure 3-29. TFN Concentrations as a Function of First-Stage Residence Time.

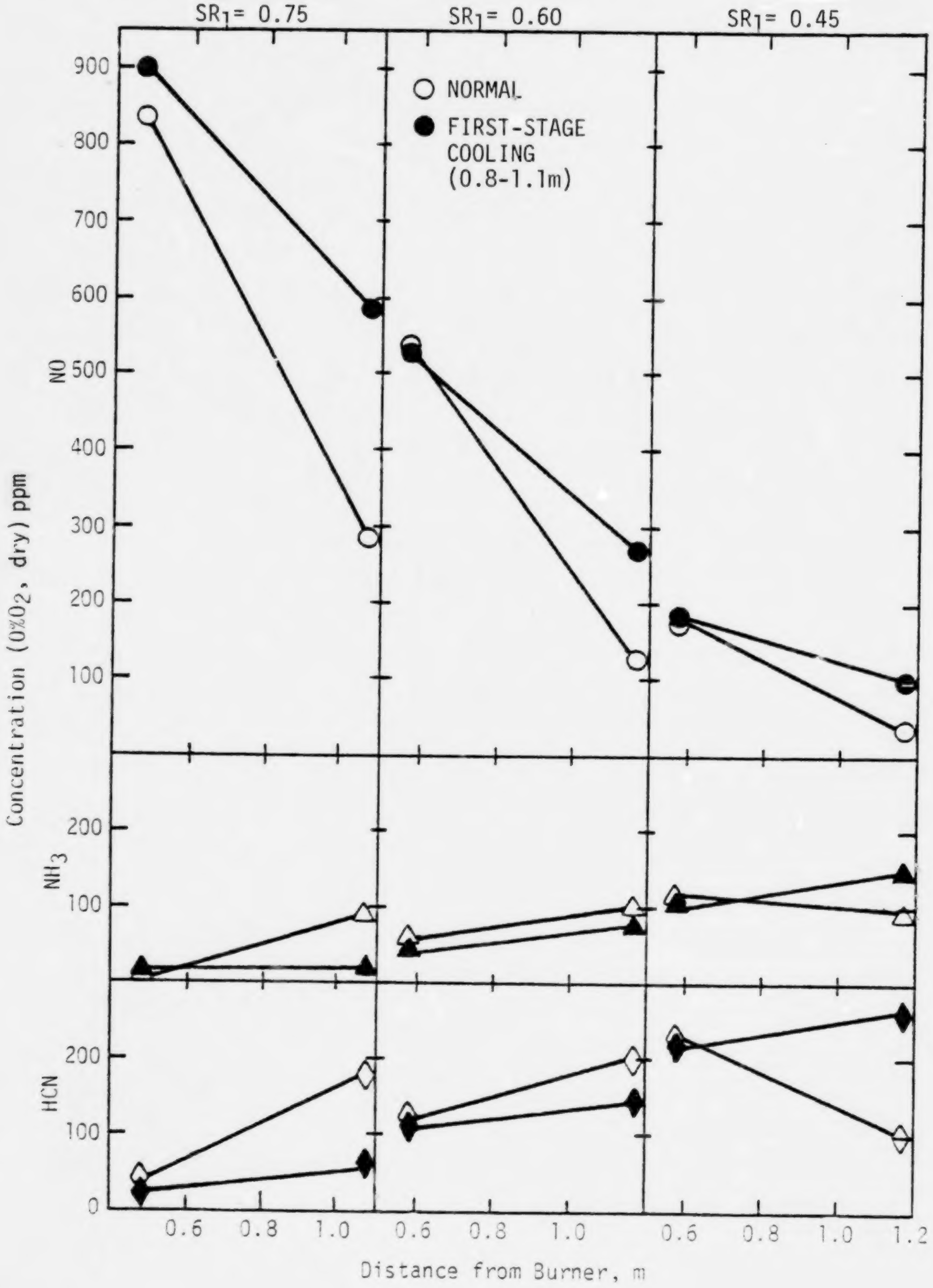

Figure 3-30. Effect of First-Stage Cooling on TFN Concentration With Coal.

(#45). The cooling coil reduced the gas temperature approximately 350°K and appeared to have reduced the NO decaying rate. Even though the growth of HCN and NH_3 species was somewhat suppressed, the total fixed nitrogen leaving the first stage was higher when heat was removed prior to the addition of staged air.

Figure 3-31 shows the percent of initial carbon and nitrogen retained in the char at the exit of the first stage under both conditions. Cooling increased both the total solids loading and the amount of solid-phase nitrogen being carried into the second stage.

Thus, based simply upon first-stage consideration, increasing rich zone heat removal does not appear attractive since it increases both TFN and solid-phase nitrogen entering the second stage. However, as shown in the next section, first-stage cooling can be beneficial in minimizing the exit NO emissions.

3.4.4 Second Stage Conversion

The second stage of the staged combustion system can be considered as an air flame burning partially-oxidized combustion products from the first stage. The ultimate yield of NO will be dependent upon the second-stage reactants (fuel composition, gas-phase nitrogen content and char nitrogen content) as well as combustion parameters such as the second stage air injection rate and the second-stage flame temperature. The previous sections define the influence of fuel properties and combustion parameters on the amount and chemical operation of the gas- and solid-phase nitrogen leaving the first stage. This section will consider the second stage parameters which control the exhaust NO emissions and discuss the conversion of both the XN species and char nitrogen in the second stage.

Combustion Parameters. The influence of the second-stage flame temperature on the ultimate NO production is illustrated in Figure 3-32. Cooling the second stage (with cooling coil located immediately downstream of the air injection position) resulted in lower emissions. Since the first-stage conditions were identical for both cases, cooling apparently reduced the conversion efficiency of the oxidizable nitrogen to NO.

Besides flame temperature, the rate at which the second-stage air is added is the other combustion parameters. Figure 3-33 shows data comparing exhaust emissions as a function of the first stage stoichiometry for two methods of staged air injection. The lower emissions were obtained with a

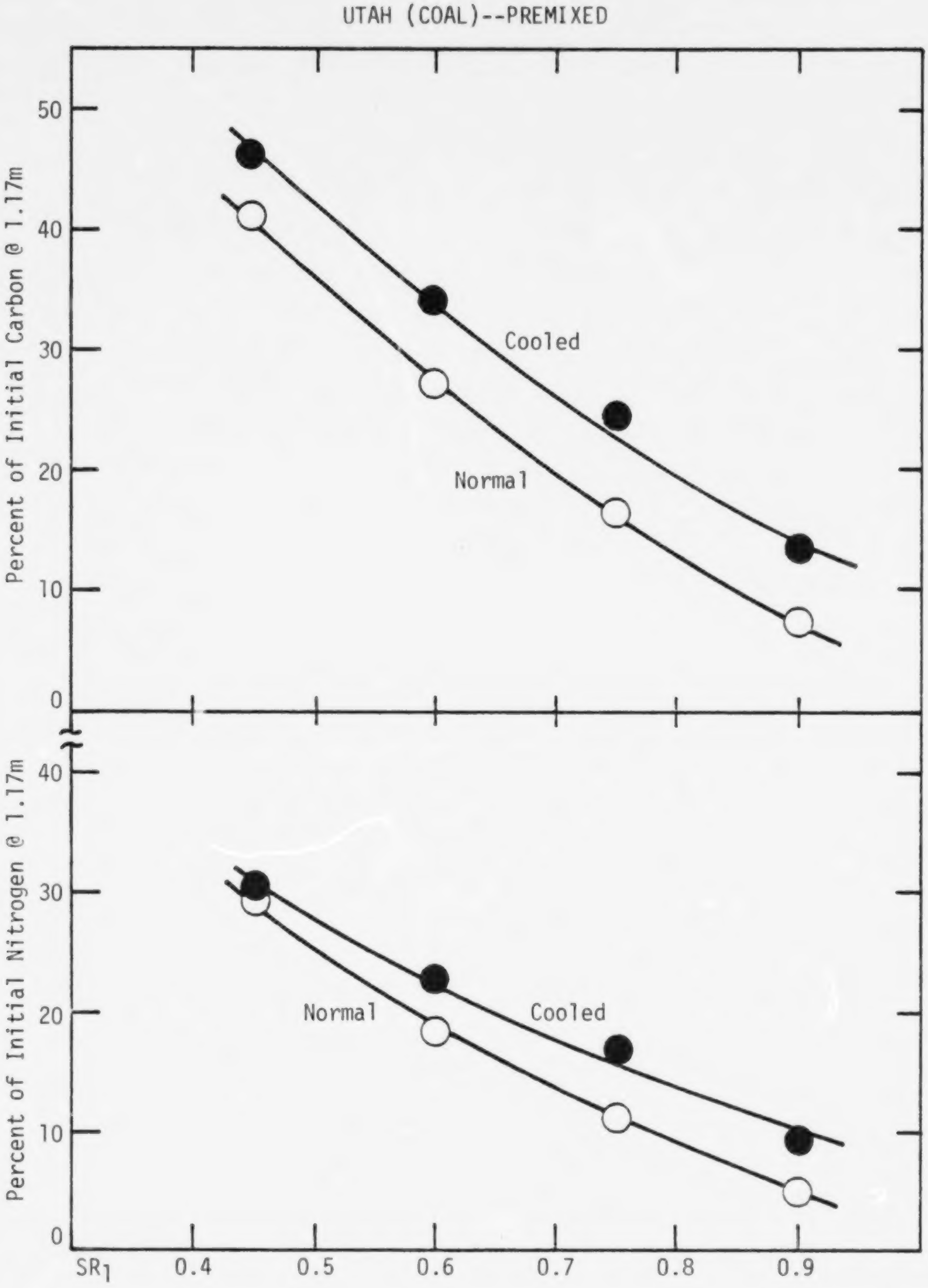

Figure 3-31. Effect of First-Stage Cooling on Solids Composition.

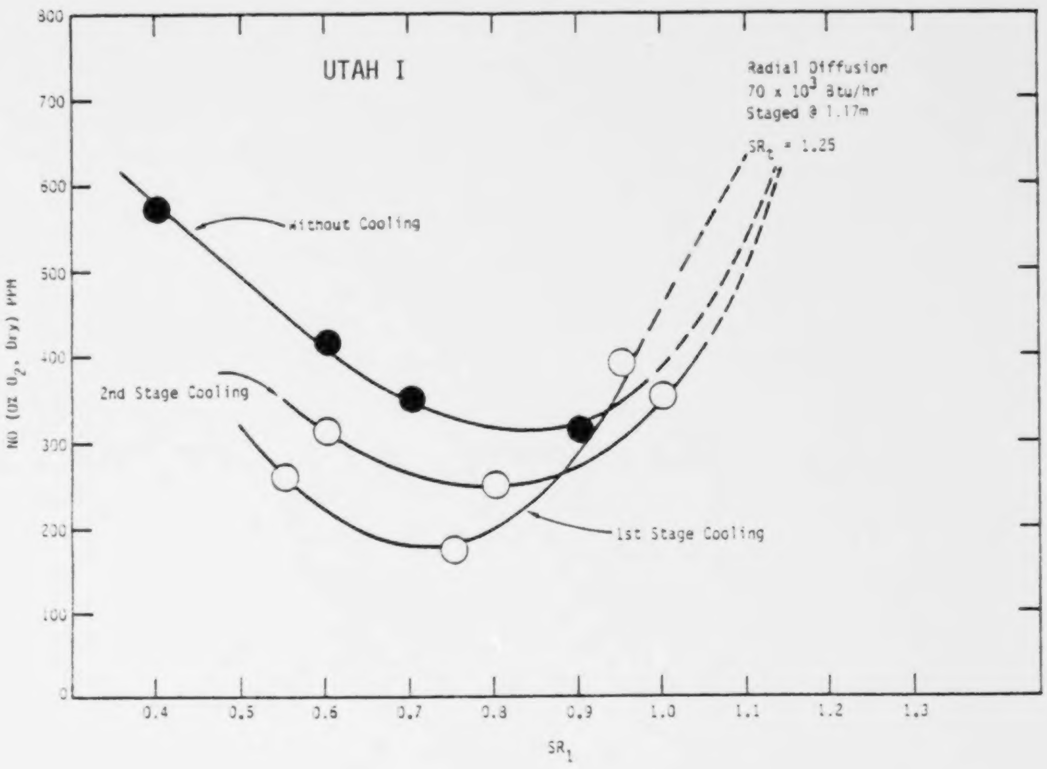

Figure 3-32. Effect of Cooling in the First or Second Stage Upon NO Emissions.

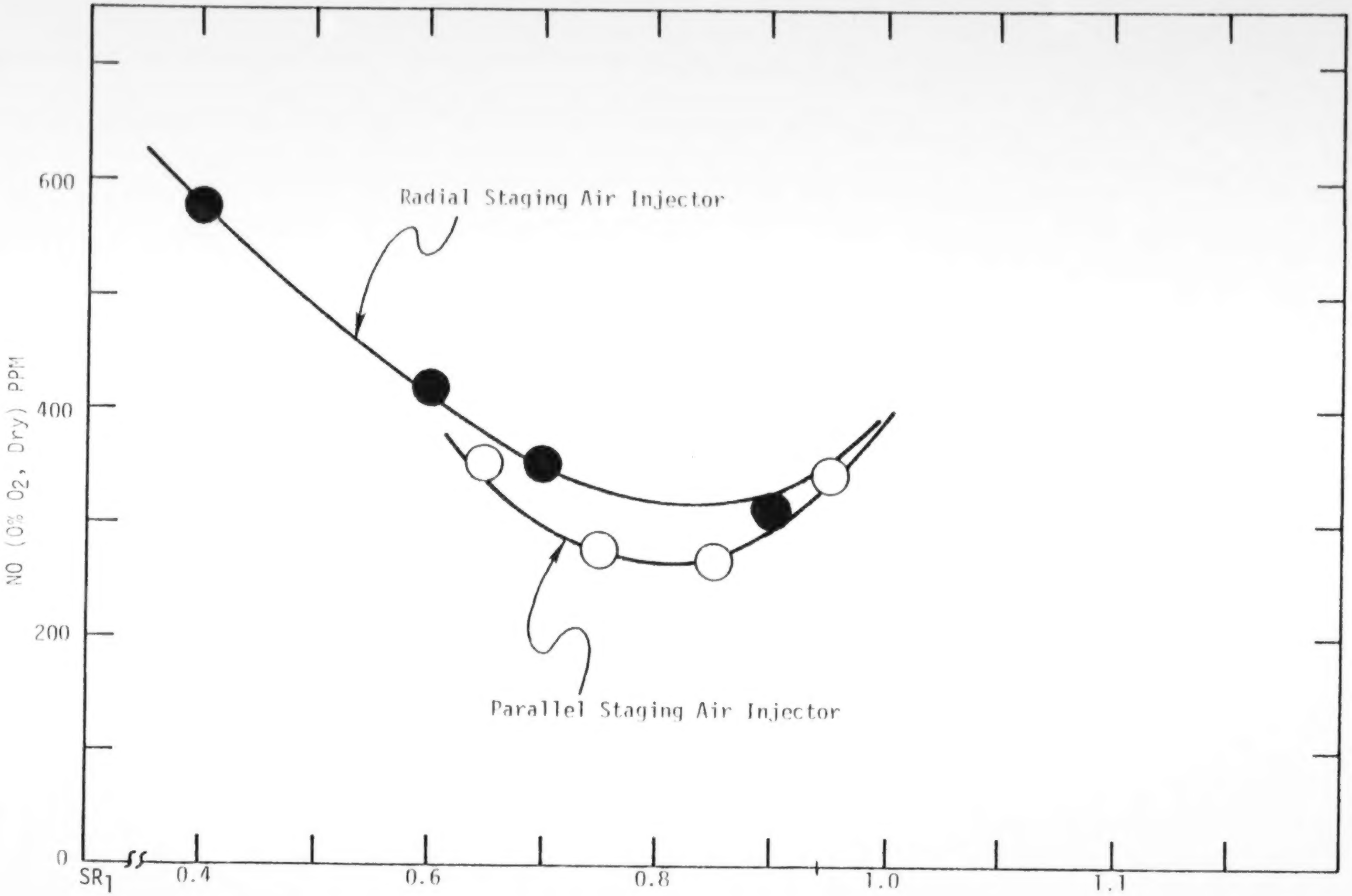

Figure 3-33. Impact of Second-Stage Air Addition Method on Exhaust Emissions.

parallel staging system which reduced the mixing rate by injecting second-stage air parallel to the oncoming first-stage effluent. Emissions were only slightly higher, however, when air was added radially at the staging choke. All of the data used in the following assessment of second-stage conversion was obtained with the radial staged-air injection. The radial system was selected for these tests because it provided a more well-defined staging location (first-stage residence time), and it helped ensure complete carbon burnout.

The next part of the section will discuss the conversion of the gas-phase nitrogen species and char nitrogen in the second stage as well as the impact of thermal environment on the conversion efficiency.

XN Species Conversion. The conversion of the gas-phase nitrogen species was investigated first without the complication of the solid phase, i.e., char. A series of experiments using propane/ammonia and propane/nitric oxide was carried out under staged conditions. The propane flow and the fuel nitrogen content in both flames were identical. XN species distribution at the first-stage exit is shown in Figure 3-34. The percent conversion of these XN species to NO in the second stage is shown in Figure 3-35. The results indicate that under relatively mild staging conditions where NO is the dominant TFN species (generally $SR_1 > 0.75$), the second-stage conversion (retention) of TFN to NO is very high (~90 percent) and relatively insensitive to total TFN level over the range of interest. Under these conditions, only a small amount of the combustion is actually occurring in the second-stage, and the second-stage "fuel" is primarily CO. However, as the first-stage stoichiometry is reduced further and the dominant TFN species become NH_3 and HCN, the second-stage conversion decreases dramatically and becomes inversely dependent on the TFN level. Figure 3-36 shows that the transition from NO to HCN + NH_3 dominance corresponds to the onset of hydrocarbon formation/carryover from the first stage. Thus, it is likely that the decrease in second-stage TFN conversion is a direct result of the second-stage "fuel" changing from CO to hydrocarbons and char.

Figure 3-35 also shows data on second-stage TFN conversions in char/C_3H_8 flames with and without NH_3. (By measuring TFN and exhaust NO in both flames, it was possible to infer a mean TFN conversion). These results show trends similar to those observed with the gas flames and suggest that the

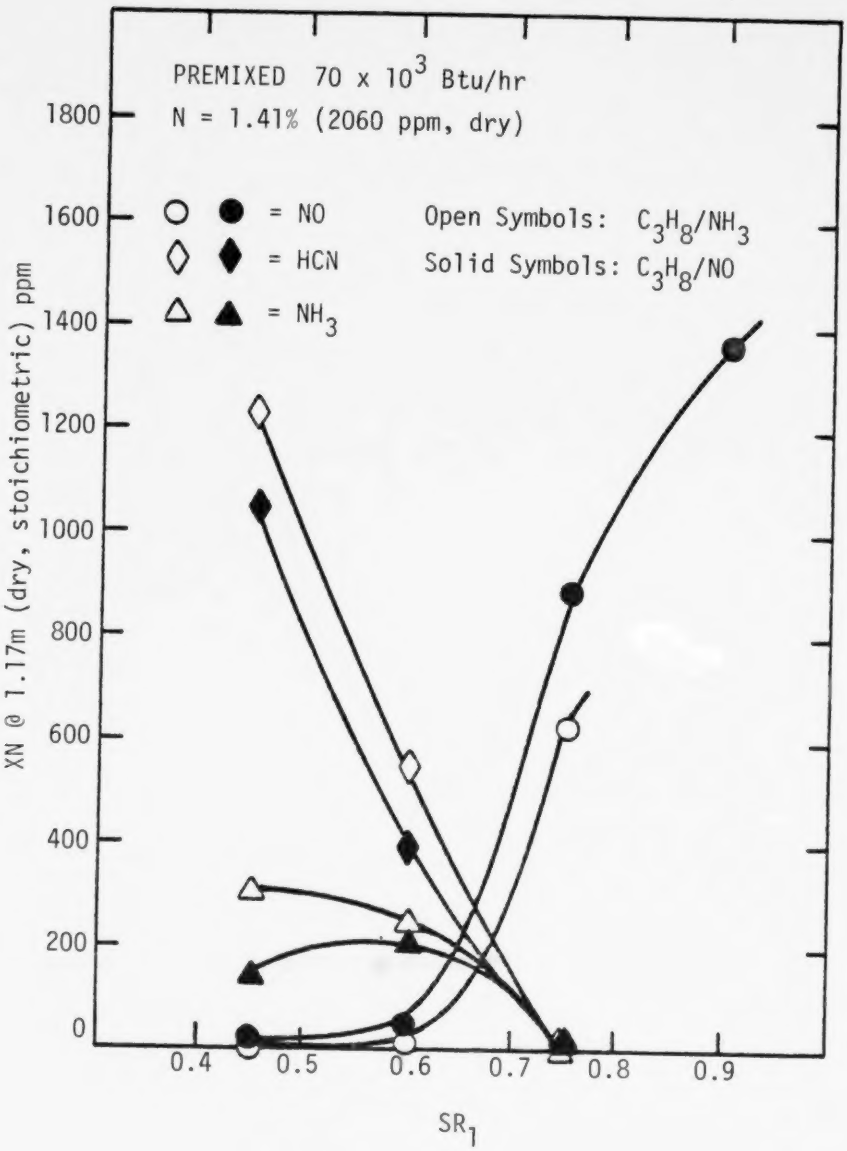

Figure 3-34. XN Species Distribution at Exit of First Stage.

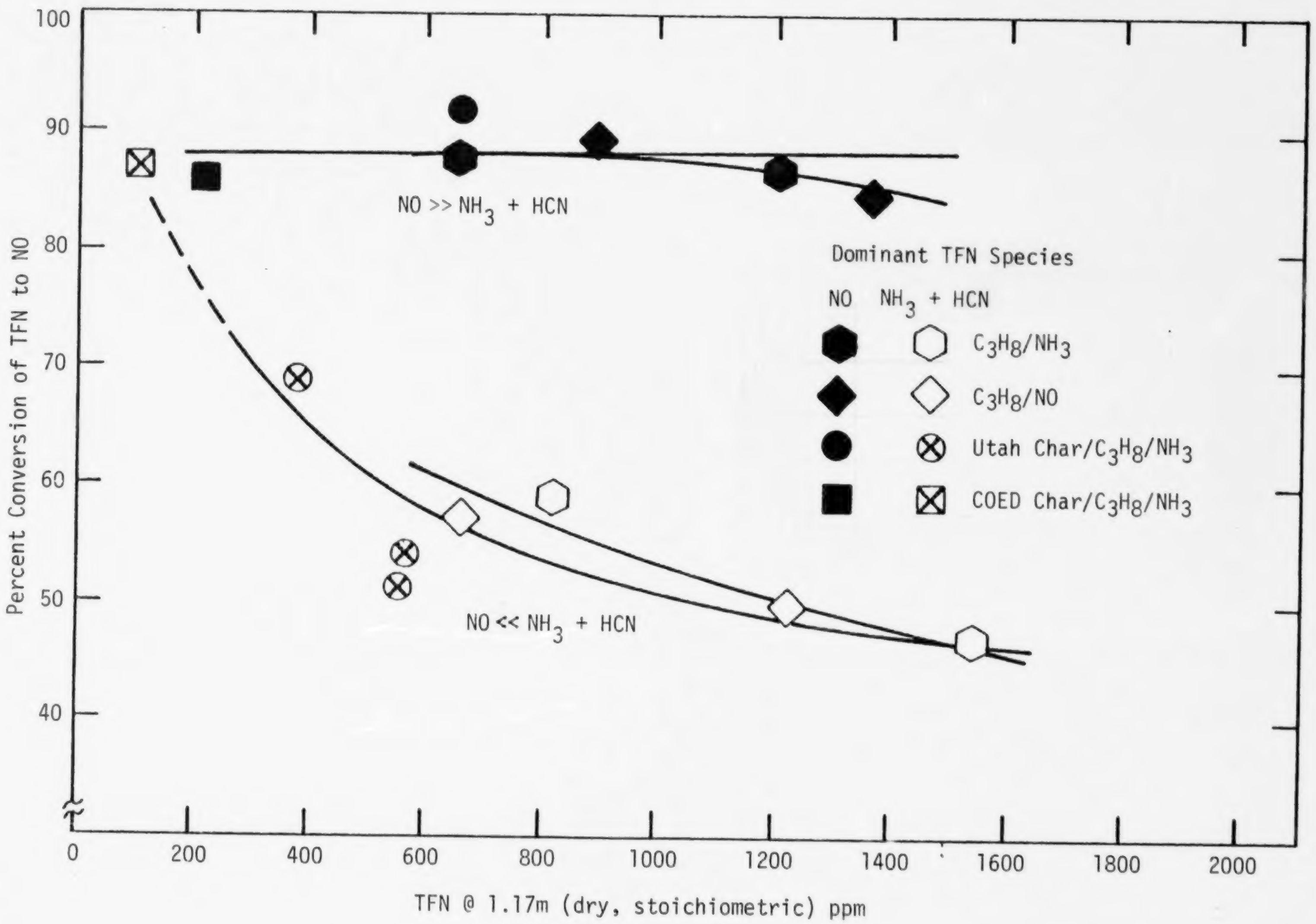

Figure 3-35. Second-Stage Conversion of TFN Species.

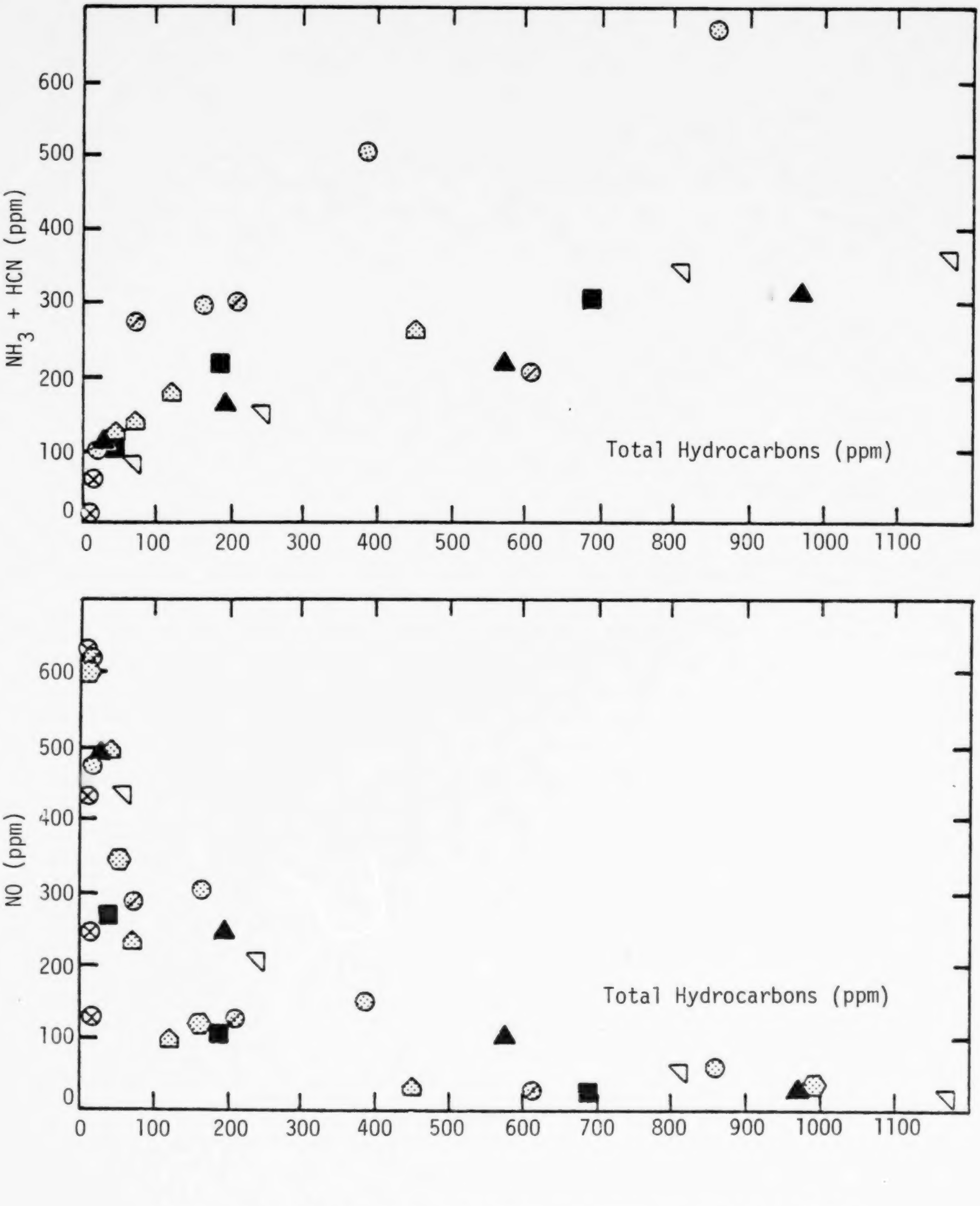

Figure 3-36. Relationship Between Hydrocarbon Content of Gas Entering Second Stage and TFN Species.

solid phase has relatively little effect on the TFN conversion in the second stage. This is an apparent contradiction with the excess-air results (Figure 3-17). It should, however, be remembered that in the results shown in Figure 3-35 the char entering the second stage is completely devolatilized due to it being subjected to flame temperatures for over one second. Assuming no heterogeneous reactions between the NO and char surface it is therefore more likely to act as an inert material.

Experiments were also carried out to investigate the thermal effect on the conversion of these gas-phase nitrogen species. Cooling coil was placed immediately upstream of the staging choke and the same propane/ammonia fuel as discussed above was used for these experiments. Figures 3-37, 3-38, and 3-39 compare results obtained with the cooling coil and those without the cooling coil. As shown in Figure 3-37, heat extraction in the first stage did not change the distribution of XN species at the first-stage exit. However, the results shown in Figure 3-38 indicate that exhaust NO emissions were lower with cooling at richer stoichiometries, i.e., $SR_1 = 0.45$. Thus, it appeared that, as shown in Figure 3-39, the retention of first-stage NO species was nearly temperature independent; but the conversion efficiency of NH_3 and HCN species to NO was lower in colder environment.

Because the propane/NH_3 results (Figure 3-39) suggested that the form of the TFN species was of primary importance, a special series of experiments was conducted with the Utah coal. NO or NH_3 was injected into the second-stage flame (with the staging air), and the effect of cooling was again studied. The second-stage inlet temperature was decreased approximately 400^0K (Figure 3-40a), and this had essentially no effect on the conversion of added NO (Figure 3-40b). However, when NH_3 was added, a significant thermal effect was observed at all stoichiometries.

Figure 3-41 shows the results of a similar test series where the fuel was COED char/propane, and where 1360 ppm NH_3 was injected directly into the second stage. Cooling the flame again decreased the second-stage TFN conversion, particularly at $SR_1 = 0.9$ where the data indicate that when the temperature of the second-stage flame was reduced, the overall emissions were lower than in the case without NH_3 addition (hence the apparent negative conversion). These data suggest that reducing the temperature of the second-stage flame may decrease overall exhaust emissions because it shifts the

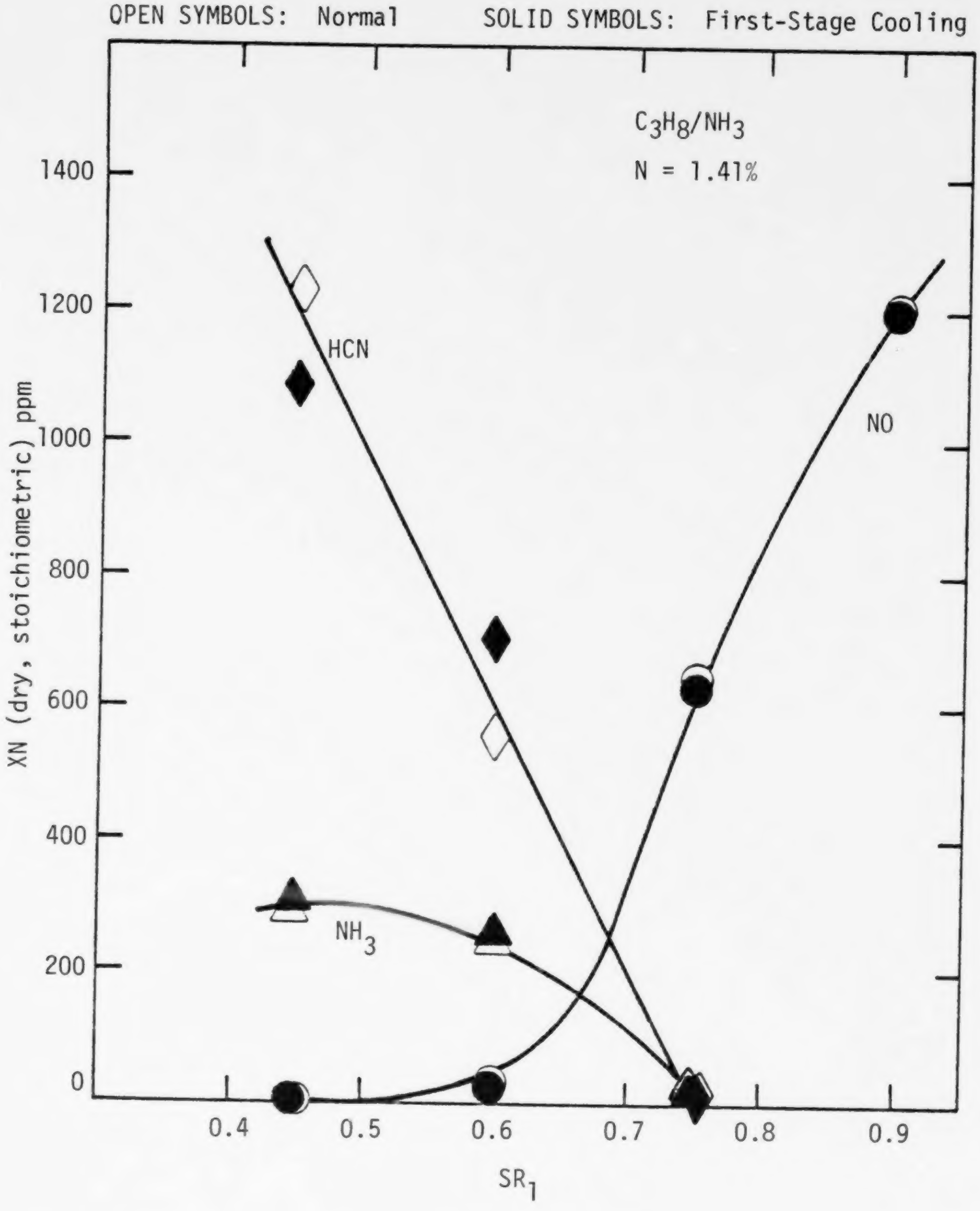

Figure 3-37. XN Species Distribution - With and Without First-Stage Cooling.

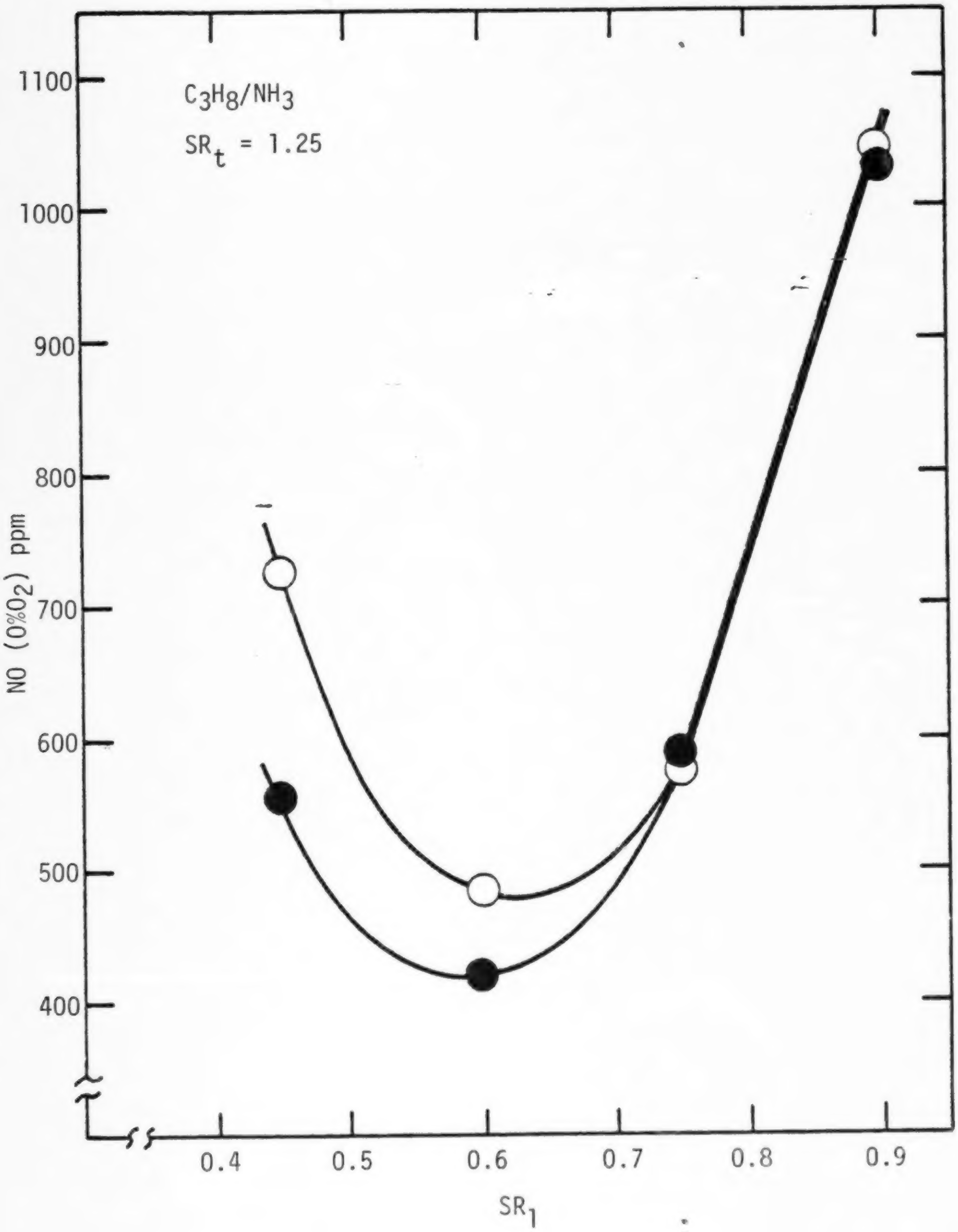

Figure 3-38. Exhaust NO Emissions - With and Without First-Stage Cooling.

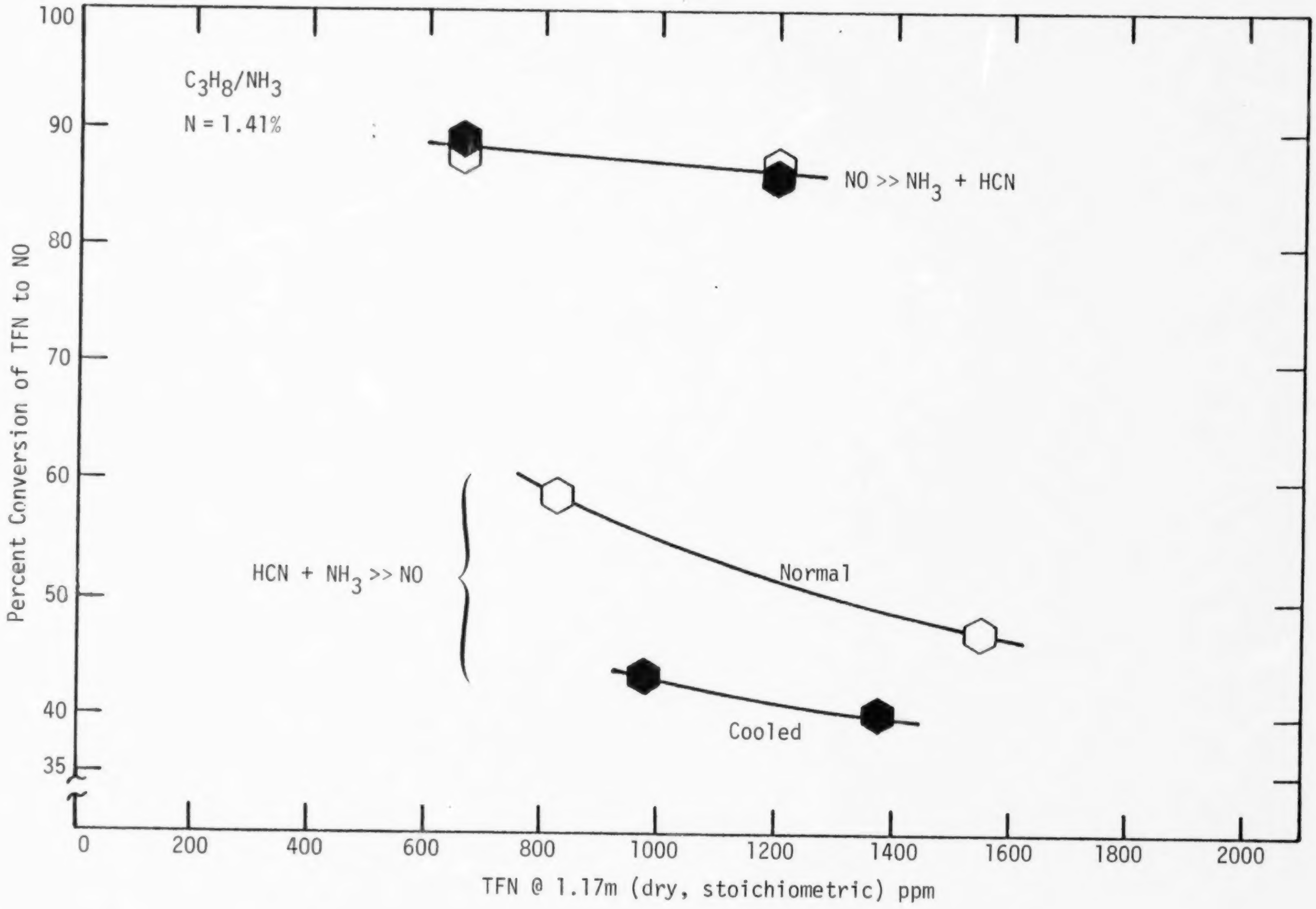

Figure 3-39. Influence of Cooling on Second-Stage TFN Conversion - C_3H_8/NH_3 Flames.

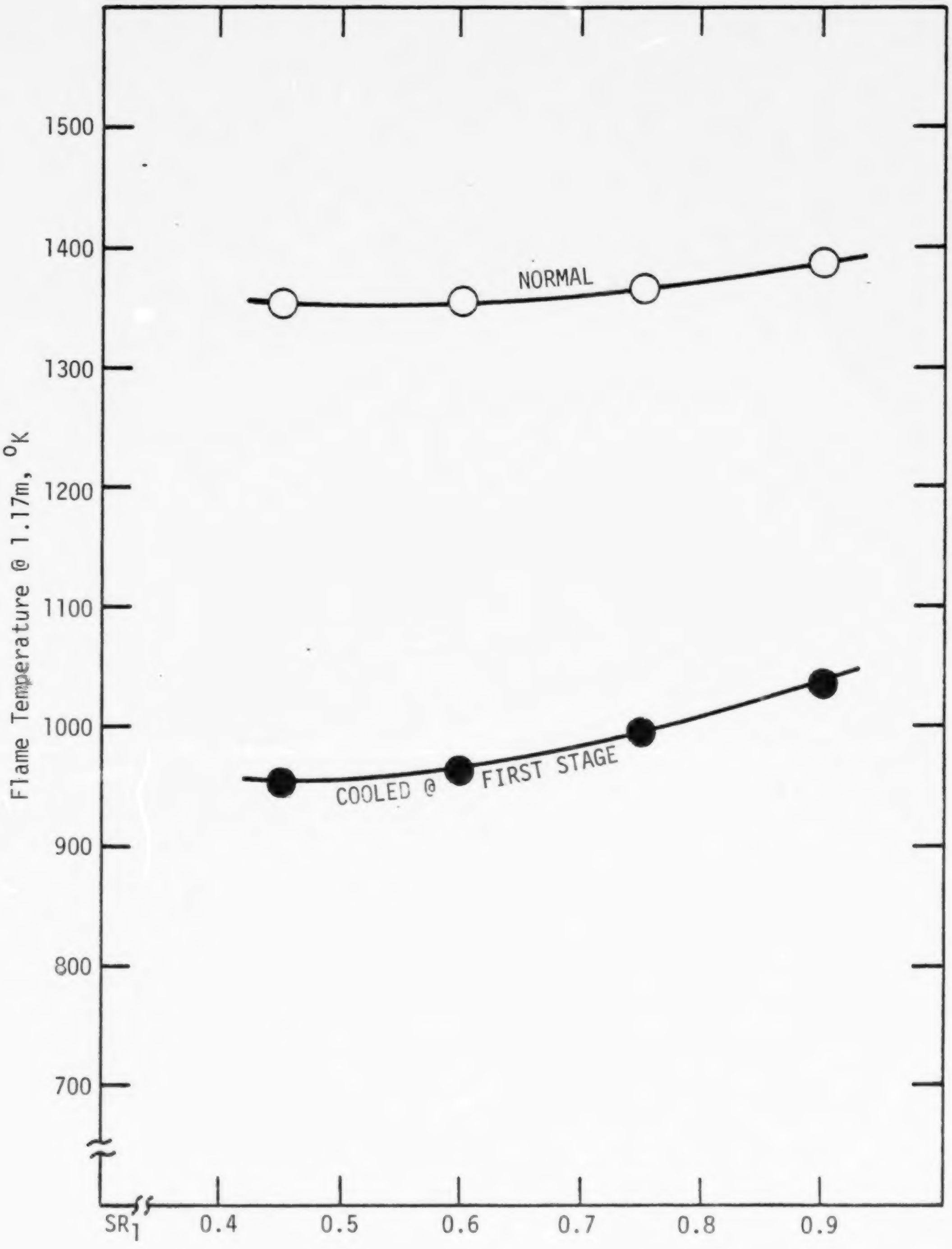

Figure 3-40(a). Influence of Cooling on Gas Temperature at First-Stage Exit - Utah Coal Flames.

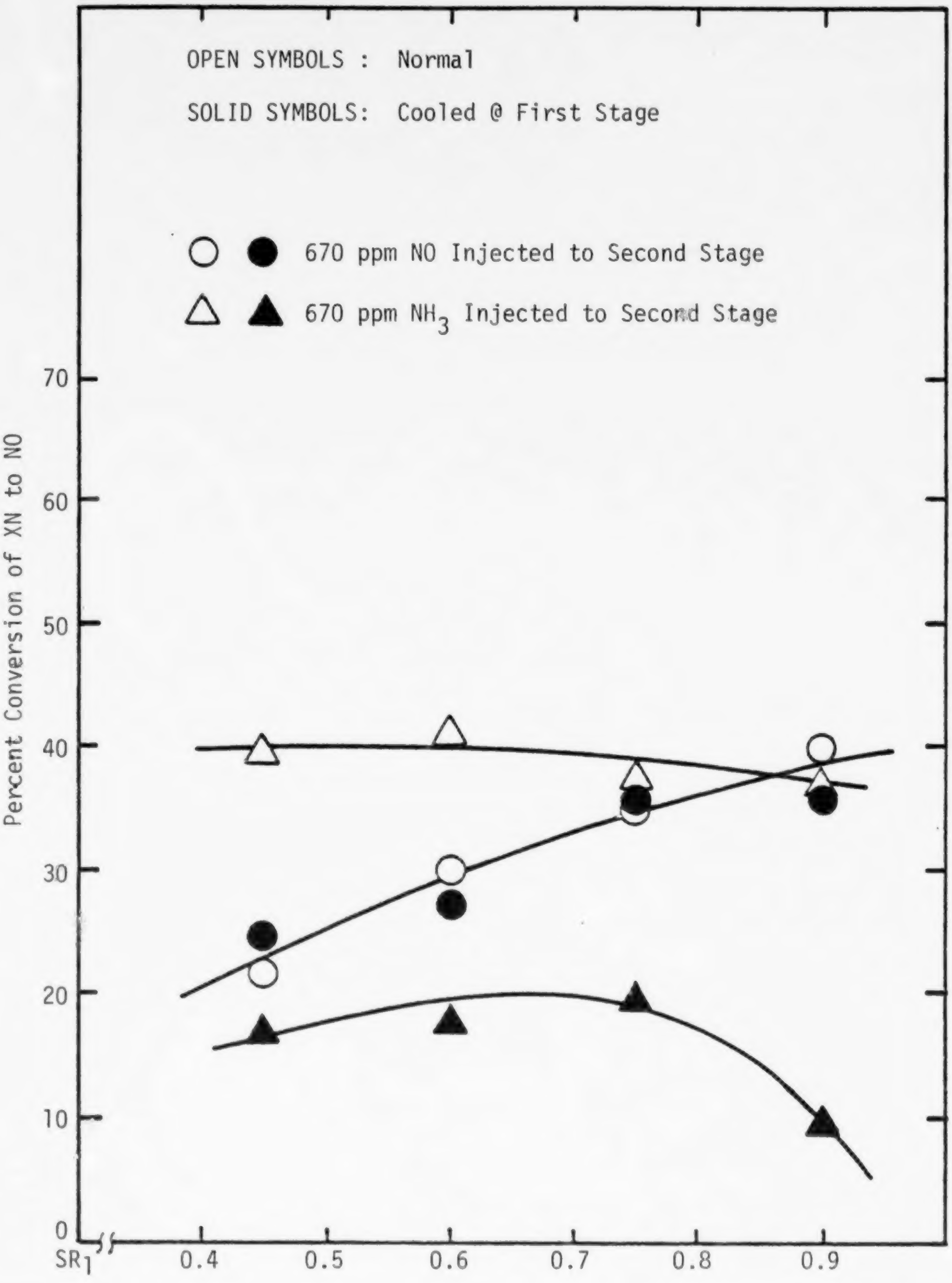

Figure 3-40(b). Influence of Cooling on Second-Stage TFN Conversion - Utah Coal Flames.

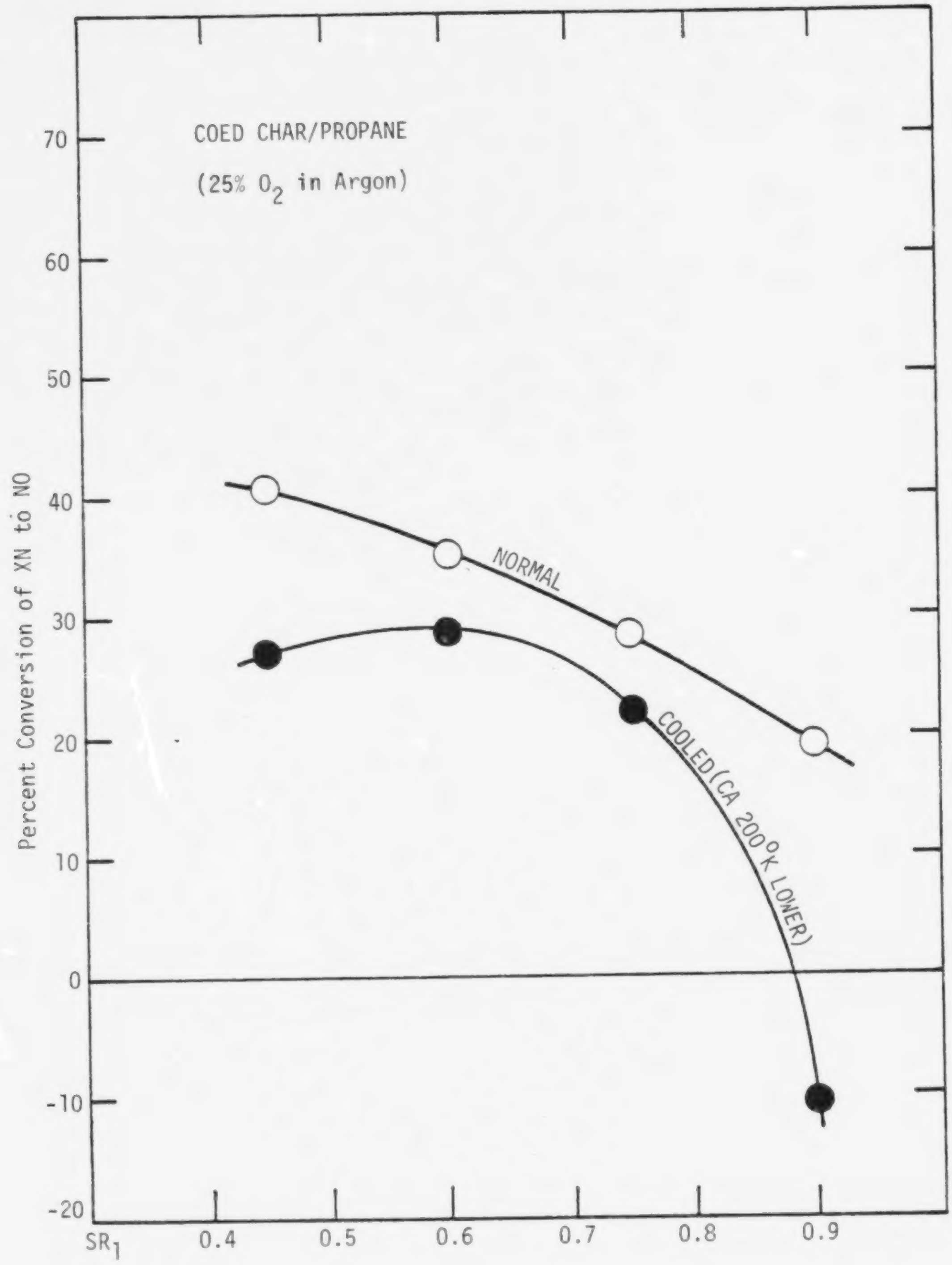

Figure 3-41. Influence of Cooling on Second-Stage TFN Conversion-NH_3 Additions to Char/C_3H_8 Flames.

gas-phase chemistry into a temperature region where NH_i species can selectively react with NO formed previously.

Oxidation of Char Nitrogen. To investigate the thermal effect on the conversion of char nitrogen in the second stage, a low-volatile char (COED char) mixed with propane was used as the fuel. The mixture was burned with an oxidant containing 25 percent oxygen and 75 percent argon to exclude the formation of thermal NO and to ensure complete burnout of char in cooled environment. The exhaust NO emissions and first-stage exit XN species distribution for both the cooled and the uncooled situations are shown in Figure 3-42 and Figure 3-43, respectively. As the first stage stoichiometry decreased, the TFN at the exit became negligible for both cases; thus, the char nitrogen carried into the second stage was the major contributor to exhaust NO emissions. Identical exhaust emissions obtained under both conditions indicate that temperature has little effect on char nitrogen conversion.

Figure 3-44 (upper plot) shows the concentrations of char nitrogen carried into the second stage of the COED char/propane system. The calculated conversion data based upon the exhaust NO emissions are shown in the lower plot. (The error bars are associated with the uncertainty in the conversion of the small amounts of TFN.) These results suggest that the conversion of the char nitrogen to NO in the second-stage flame is 20 percent or less and the conversion appears to increase slightly with decreasing first-stage stoichiometry.

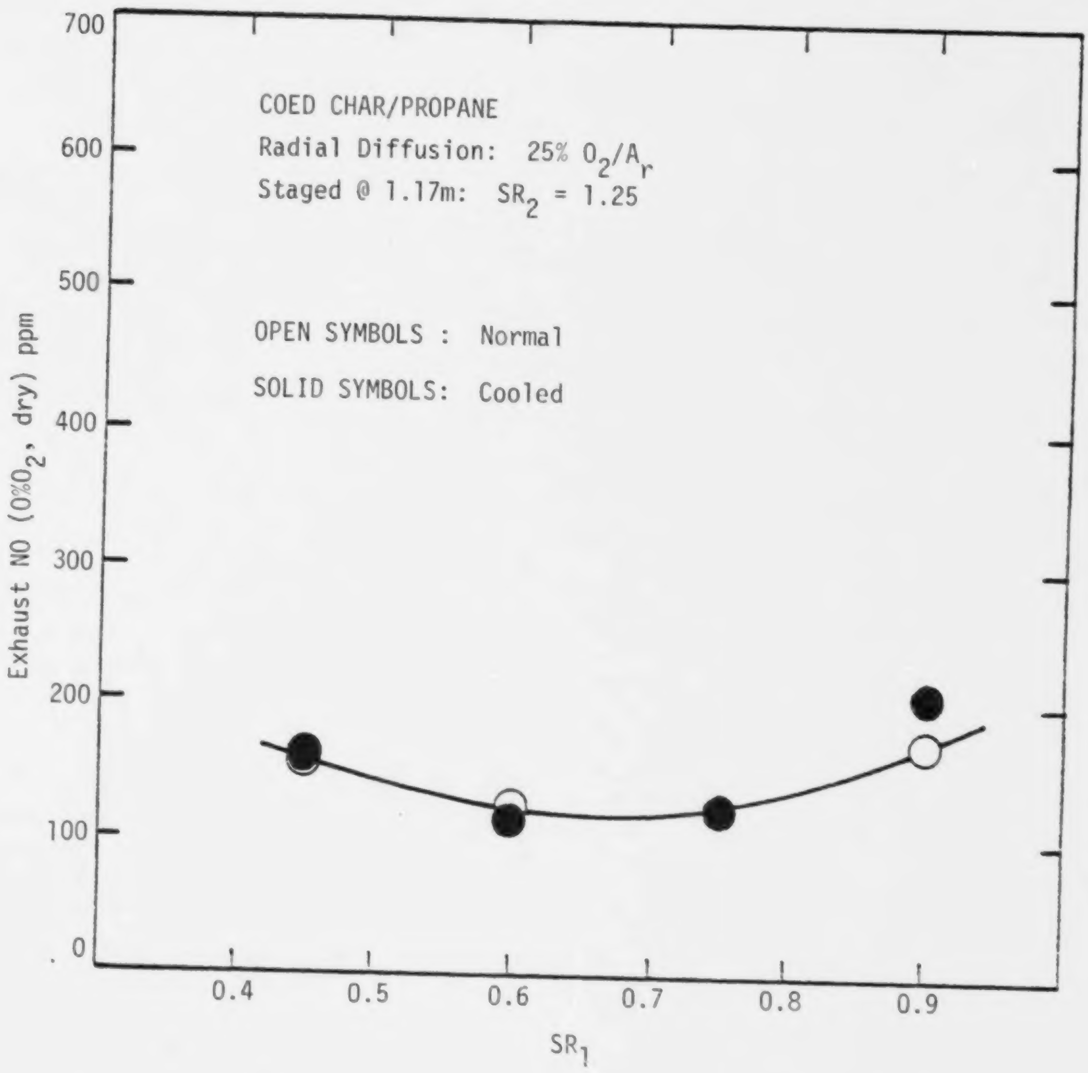

Figure 3-42. Exhaust NO Emissions.

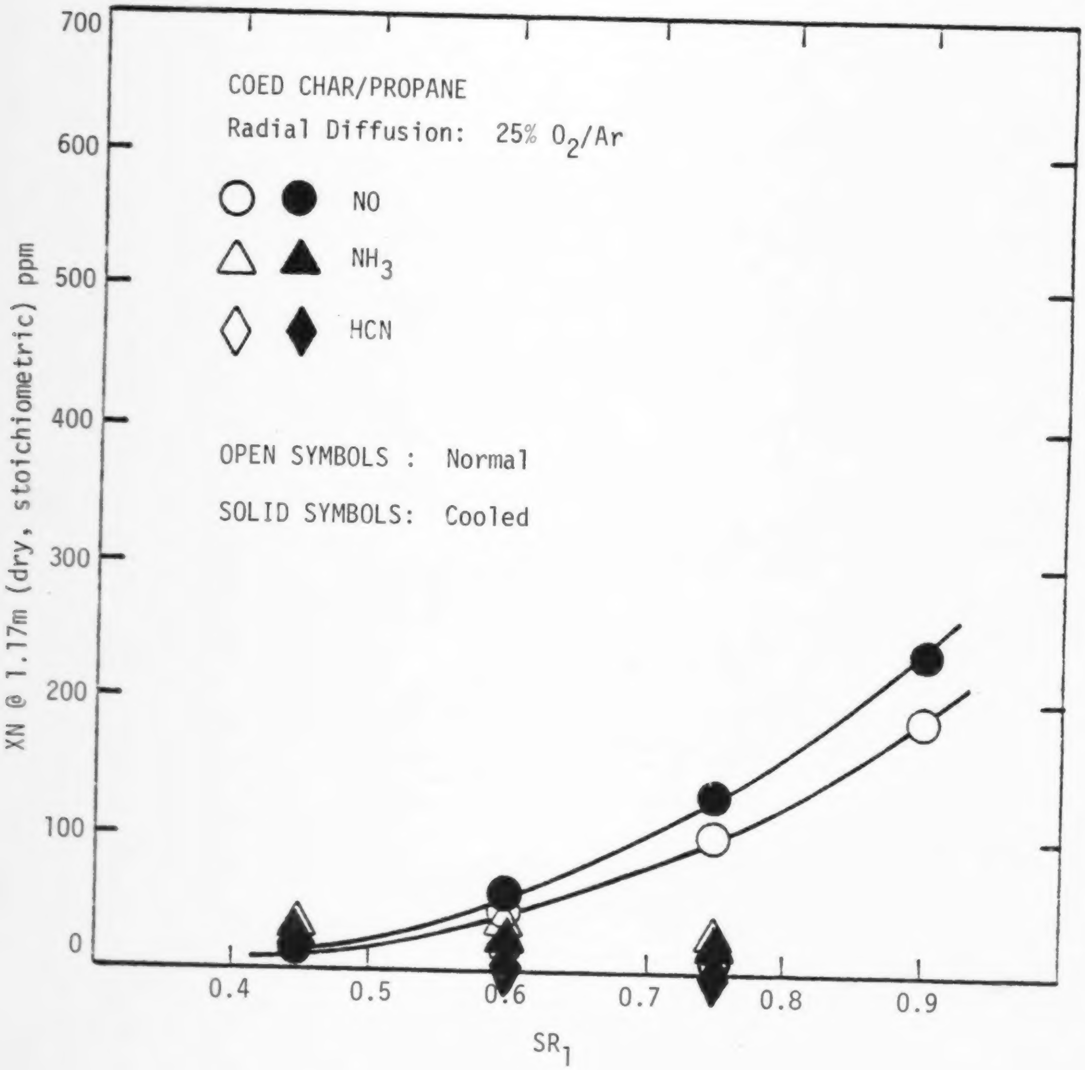

Figure 3-43. XN Species at First-Stage Exit.

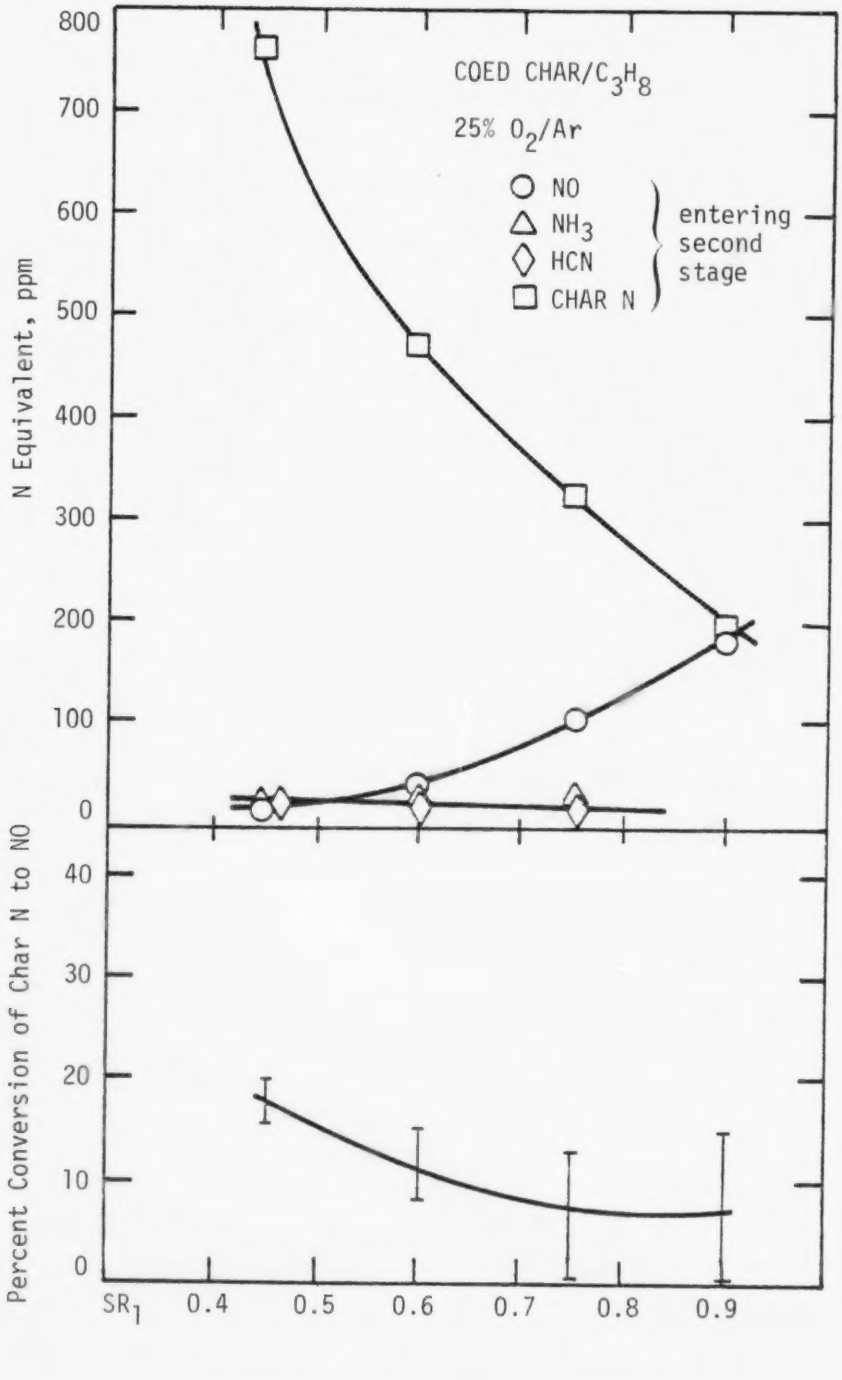

Figure 3-44. Solid-Phase Nitrogen Conversion in the Second Stage.

4.0 BENCH-SCALE STUDIES TO ASSESS THE IMPACT OF COAL TYPE AND SORBENTS ON SO_x EMISSIONS

Based on the results presented in previous Annual Reports showing the potential for achieving large SO_2 reductions in the furnace using dry limestone, a study was initiated to verify and develop the technical information to extend the results to an operating boiler system. An initial step of this effort was to verify the measurement techniques by obtaining a sulfur balance (i.e., input = output) under both gas-phase and heterogeneous combustion conditions.

4.1 Gas-Phase Measurements--Analytical Methods/Instrumentation

The ability to reliably measure both H_2S and SO_2 continuously was developed. The analytical method of choice for SO_2 measurements (nondispersive ultraviolet--NDUV--light absorption using an instrument manufactured by DuPont) has been compared with the basic EPA wet method under both cold-flow and furnace combustion conditions. Data generated by the two methods compares within acceptable limits and is not a function of either SO_2 or water vapor concentration.

H_2S is measured by oxidizing the H_2S to SO_2 under controlled conditions and measuring the resulting SO_2 concentration with the DuPont instrument. The H_2S converter system was tested with a standard mixture of H_2S in N_2 gas. As shown in Figure 4-1, the H_2S measured as SO_2 matched the H_2S expected (based on dilution) within 2 percent.

Other lightweight gaseous sulfur species may be measured on a noncontinuous basis using a gas chromatograph (G.C.). The G.C. is equipped with a sulfur specific flame photometric detector and a column which separates the low molecular weight sulfur compounds. The G.C. system has been tested with a mixture of SO_2, H_2S, COS, CS_2, and thiophene gases which have been shown to be present in coal flames. The system gives good separation of these gases and may be calibrated for each compound. The results show that this system is adequate for quantitative analysis of a mixture containing H_2S, SO_2, COS, CS_2, and thiophene in combustion gases.

The measurement of sulfur compounds in a combustion system poses several special problems in sample acquisition and conditioning. A sample probe and a conditioning system have been constructed and tested. The system consists

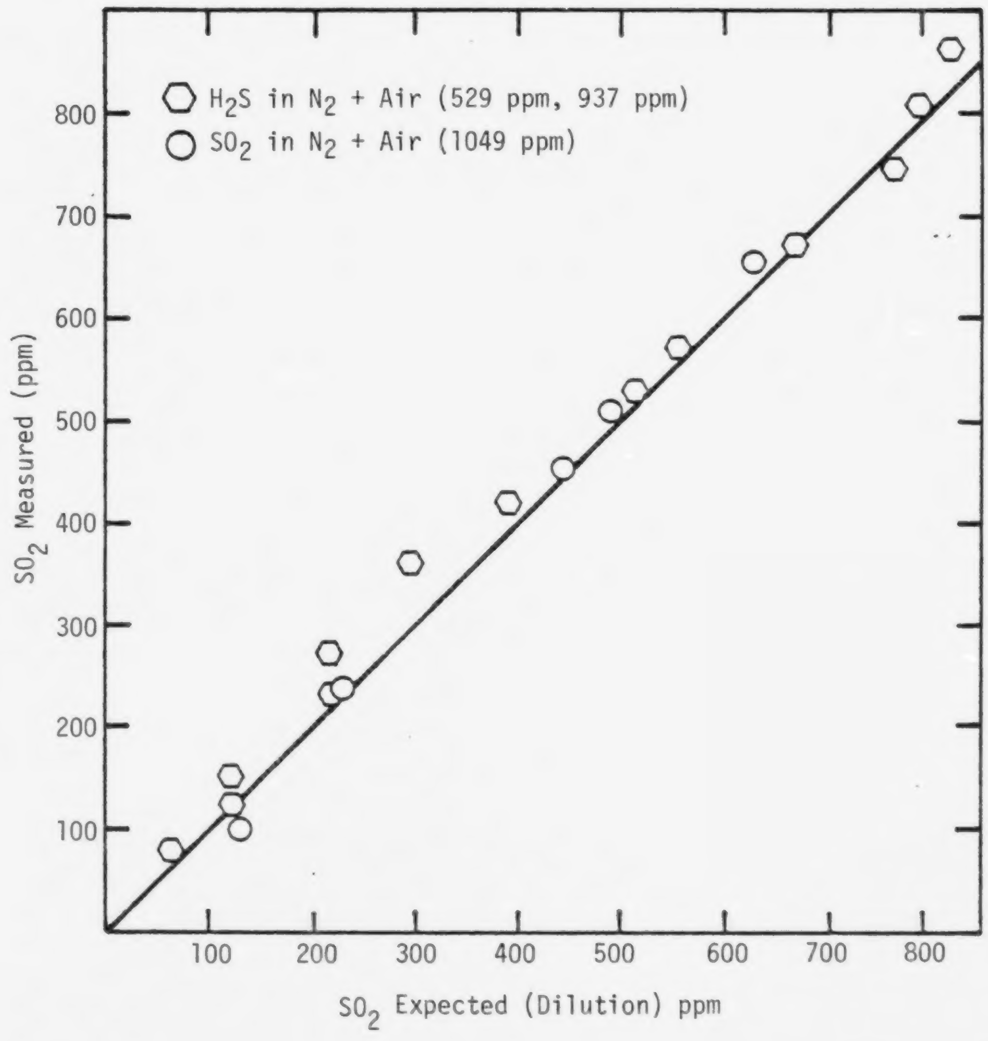

Figure 4-1. H_2S Converter Test.

of a sample probe inside a removable water-cooled jacket (the water may be heated to control sample temperature) and a conditioning system which removes water from the sample immediately after the probe. The sample is kept hot and is under vacuum (15" H_g) until the water is removed. Water vapor is selectively removed from the sample by a permeation tube drier using dry nitrogen as the dry gas medium. The permeation drier was tested with mixed gases containing known concentrations of SO_2 and water removal without affecting the concentration of other gases (SO_2, CO_2, CO, NO_x) in the test sample. No "breakthrough" of other combustion gases, such as NO, into the dry nitrogen side of the drier could be detected.

The overall sample system was tested using samples drawn from the furnace flue. SO_2 was added to the combustion air, the SO_2 concentration in the flue was measured. The measured SO_2 concentration compared to that calculated from the inlet SO_2 concentration and an overall sulfur balance to within 10 percent was obtained. The sulfur balance was improved to within 3 percent when measurements of SO_3 in the flue were also made. This ability to balance sulfur in and out of the furnace implies that the sampling system is functioning properly and that reliable measurements of SO_2 in the gas phase can be made employing this system.

4.2 Heterogeneous Systems--Probe Sampling System/Analysis. The measurement of sulfur compounds in a system containing reactive solids has required the development and testing of a new sampling system. The system contains a new "phase discrimination" probe which was designed to draw a gas-phase sample from the furnace. The solid particles are inertially separated from the gas sample at the probe tip by routing the gas around a baffle as shown in Figure 4-2. This phase discrimination probe has been tested under limited experimental conditions. Tests were run when SO_2 was added to the furnace directly ahead of the probe while a solid sample was added at the burner; and, secondly, both a gas sample of SO_2 and a solid sorbent were added to the furnace at the burner. The results showed that the added solids did not affect the measured SO_2 concentration when the SO_2 was added directly ahead of the probe and that the measured SO_2 in the flue was reduced when both the solids and SO_2 were added at the burner and passed through the furnace. These results imply that the sulfur/sorbent reaction takes place in the furnace and not in the sample system.

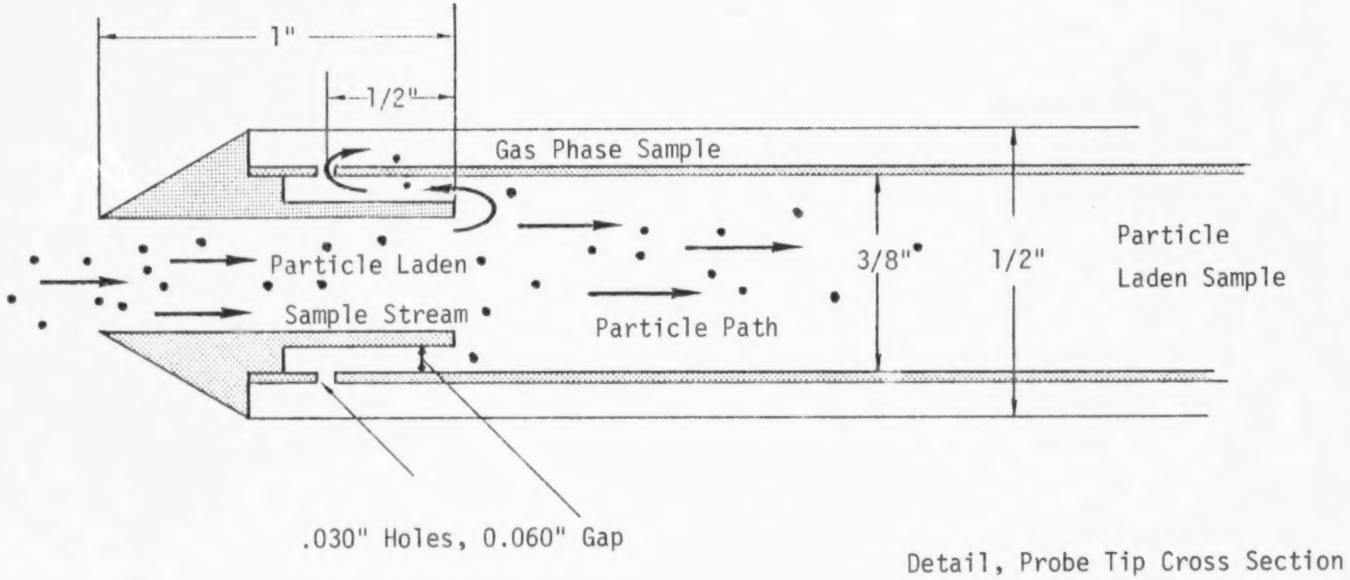

Figure 4-2. Schematic of Phase Discrimination Used for Sampling SO_2 in the Presence of Limestone.

The effect on sorbent characteristics of the experimental parameters which influence sulfur capture are also being assessed. The sorbent characteristics of interest are particle size distribution, surface area, and sulfur content. The instrument used at EER for measuring the sulfur content of solids is manufactured by Leco. This instrument burns the solid sample at high temperatures, >2400^{0}F, in an oxygen-enriched atmosphere and measures the SO_2 evolved from the solid. The instrument is equipped with a microprocessor which automatically converts measured SO_2 concent of the burnt gases to equivalent sulfur content of the solid burnt. The ability to measure the sulfur content of noncombustible solids, including calcium salts and coal ashes has been developed and validated. Measurement of sulfur in a noncombustible solid requires the use of a combustion accelerator. Several combustion accelerators were tested, including V_20_5, Al_20_3, and M_g0; V_20_5 gave the most repeatable results and the fastest instrument response and V_20_5 was therefore selected as the accelerator for all subsequent sulfur measurements.

Calcium sulfate ($CaSO_4$), pure reagent grade, was used to prepare standards for analysis by the Leco (and for subsequent use as calibration standards). The $CaSO_4$ was mixed in known proportions (by mass) with pure, dry, unreacted calcium carbonate. The sulfur content of these standards was measured on the Leco and compared to the expected sulfur content. There was good agreement between the measured and expected values, as shown in Figure 4-3. Each point plotted is an average of at least six measurements of sulfur content. Blanks, containing pure $CaCO_3$ or $Ca\ (OH)_2$, were run before each measurement. At the beginning of each day the system was conditioned with several runs of pure $CaSO_4$ before initiating testing.

The surface area of the solid sorbent powders has been determined by gas adsorption. EER has an instrument manufactured by Quartachrome which measures powder surface area by determining the monolay capacity of an adsorbent. The monolay capacity is conventionally determined by the Brunauer-Emmett-Teller (BET) equation which relates the monolayer capacity of the sorbent to the volume of gas adsorbed, the adsorption conditions, and the properties of the adsorbate. The BET surface areas of porous and nonporous adsorbents are conventionally determined from N_2 adsorption isotherms measured at 77^{0}K. The "Quantasorb" instrument is capable of doing

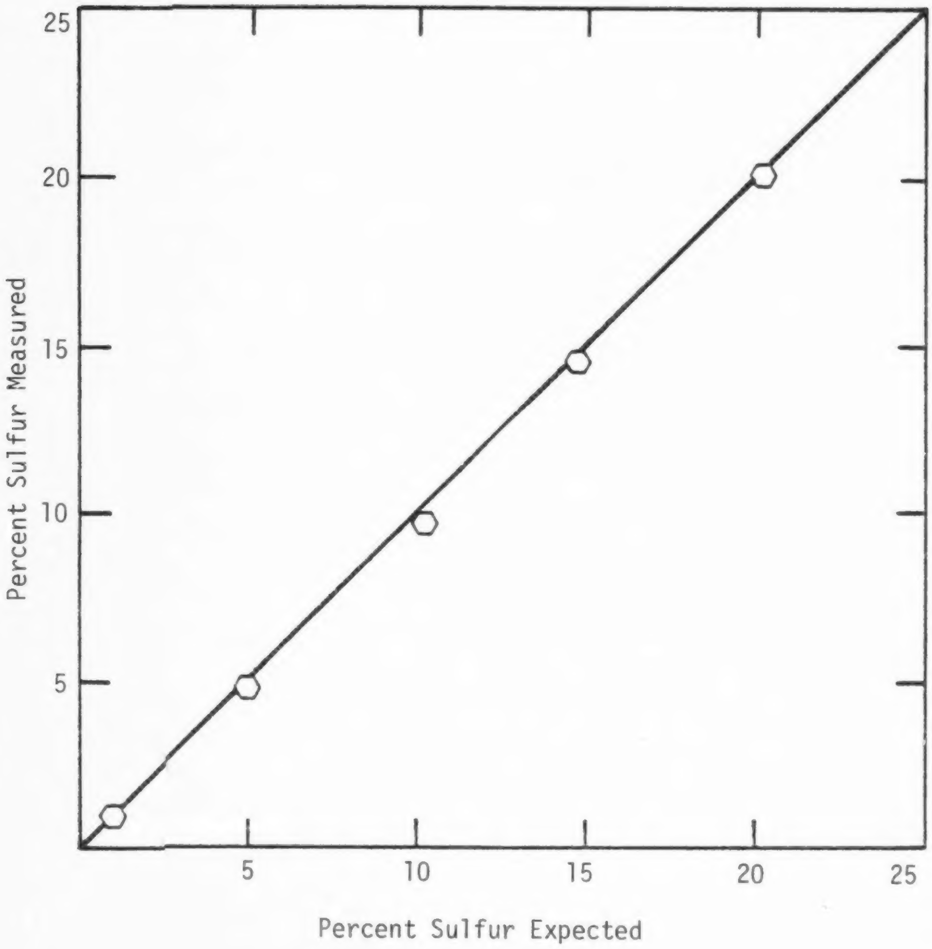

Figure 4-3. Solid Sulfur Measurement Validation.

single and multipoint BET surface area measurements with either N_2 or CO_2 as the adsorbate. These conditions were selected on the basis of simplicity of method and time for analysis after it had been determined that the out-gassing method (thermal or repetitive cycling) and the adsorbate (N_2 or CO_2) made little difference in the measured surface areas of sorbents. Future solid surface area measurements will be done with a two-point BET rather than a three-point BET because the preliminary studies show that these solids behave in a nearly ideal fashion, so that the two-point BET surface area is essentially the same as the measured three-point area.

Solid samples were taken from the flue using the solids probe cyclone system described earlier. The sulfur content and surface area of the collected sample were measured as described above. The sulfur measured in the samples collected was higher than that expected from mass balance calculations, possibly because some segregation of particle size (due to a 90^0 turn) take place before the sampling point in the flue.

5.0 BOILER SIMULATOR FURNACE

Overview

The Boiler Simulator Furnace (BSF) is designed to study the combustion processes in utility boilers. Fired at 1 x 10^6 Btu/hr, the experimental facility will simulate the time, temperature, and stoichiometry history, instead of the hardware, of various boiler firing schemes, such as:

- Wall Firing
- Tangential Firing
- Turbo
- Arch
- Tower
- Steamer
- Cyclone.

The BSF is a cost-effective tool to study formation of pollutants and to develop advanced concepts for their control. The furnace is sufficiently large to produce conditions typical of commercial practice. It is flexible, yet controllable, and can be used for a wide range of experiments. Specifically, it is supporting continuing studies in the following areas:

- Sulfur-Sorbent Interaction
- Formations and Fate of NO_x
- Solid Pollutants.

The BSF meets the experimental needs with these special designed features:

- Radiant, post-flame and convective furnace modules to simulate boiler process.
- Five independently-controlled and heated combustion air streams for distributed mixing.
- Modular burner with variable swirl.
- Variable heat extraction rate in all furnace parts.
- Variable residence time by adding or removing furnace modules.

- Solid sorbent injection.
- Gas and solid sampling ports throughout the furnace.

The following sections describe the final designs and specifications of the test facility.

5.1 Design

The BSF is sized to fire at 1 x 10^6 Btu/hr continuously and consists of these systems:

- Furnace
- Burner
- Fuel
- Combustion Air
- Sorbent and Additive
- Sampling and Measurement
- Cleanup
- Data Acquisition.

These systems have been designed for flexibility and ease of operation to minimize the downtime and experiment labor costs.

5.1.1 Furnace

The furnace is the heart of the test facility. It consists of the radiant, post-flame and convective sections. These simulate the burner zone, the volume above the burners and the convective passages of a boiler, respectively. The major parameters considered in the design include residence times, gas velocities, thermal environment, and confinement. The BSF concept is illustrated in Figure 5-1. The simulation is based on the combustion and subsequent processes rather than the hardware in a boiler.

The radiant furnace is a horizontal, refractory-lined cylinder made up of four modules. The chamber is 24 inches in diameter and 96 inches long, giving a residence time of 1-2 seconds at nominal operating conditions. Modules of two wall constructions will be used. One is designed for minimum

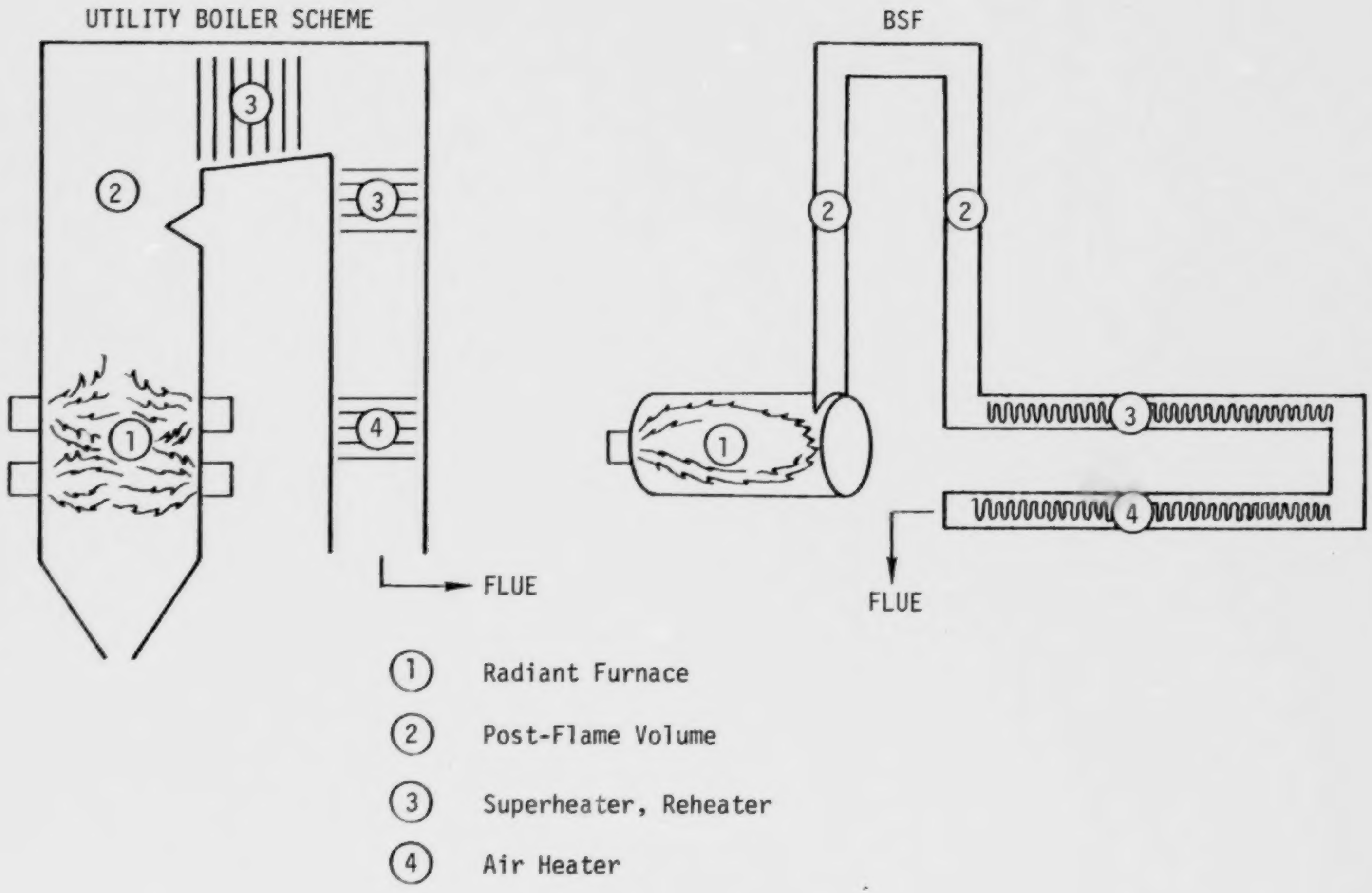

Figure 5-1. Boiler Simulator Concept.

conduction heat loss by backing the high-density refractory lining with vacuum-formed Kaowool fibre cylinders. The other is designed for high heat removal by cooling the refractory lining externally with circulating water. Figure 5-2 and Table 5-1 illustrate the design and specifications of the radiant furnace, respectively.

The post-flame section provides a reaction volume similar to the space above the burner zone in a boiler. The major parameters are gas velocities, residence time, and temperature. As shown in Figure 5-3, seven modules make up the post-flame sections. The inside is 9 x 9 inches and 32 feet 4 inches long, giving a residence time of approximately 0.9 seconds. The designed bulk gas velocity is about 32 ft/sec, and is similar to that of the gases leaving the burner zone of utility boilers and hence will deposit bottom ash similarly. The walls are insulated with B&W Kaowool ceramic boards (2300^{O}F, 2600^{O}F, 3000^{O}F) to minimize uncontrolled heat loss. Additional heat is removed by inserting water-cooled tube banks along the wall to give the desired gas temperature profile. The detailed specifications are listed in Table 5-2.

The convective sections in the BSF simulates the superheaters and air heaters of a boiler. The important parameters in the convective section include gas velocity, residence time, heat extraction rate, tube geometry, and orientation. A series of six open-top refractory-lined (Cast-O-Lite 30) modules, each six feet long, makes up the convective section. Banks of air-cooled 3/8" O.D. stainless steel tubes are inserted into the flow path from the top. To obtain the desired gas temperature history, the heat extracted will be varied by adjusting the cooling air flow rates. The flow areas of the convective passages are reduced from 8 x 8 inches to 8 x 6 inches to maintain the gas velocity between 34 and 41 ft/sec as the gas temperature decreases. Figure 5-4 and Table 5-3 illustrate the design of the convective sections.

5.1.2 Burner

The test burner designed for the BSF has these features:

- Modular construction.
- Interchangeable throat section for variable throat velocity and geometry.

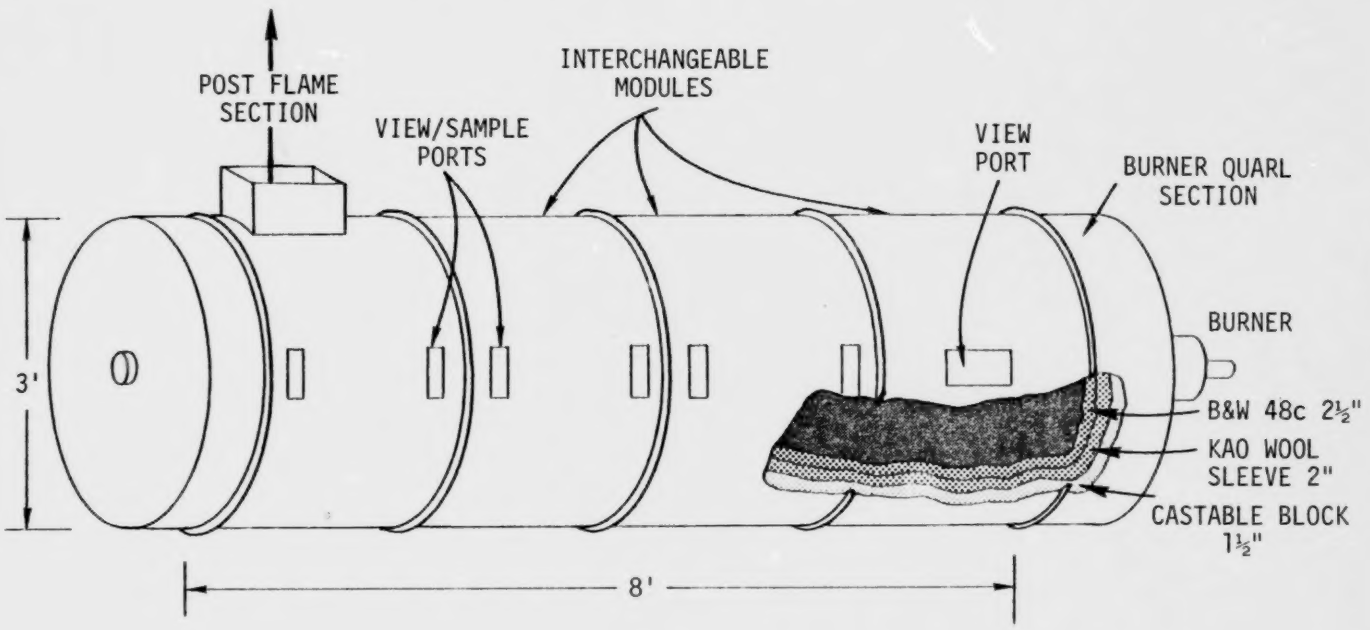

Figure 5-2. Boiler Simulator Radiant Furnace.

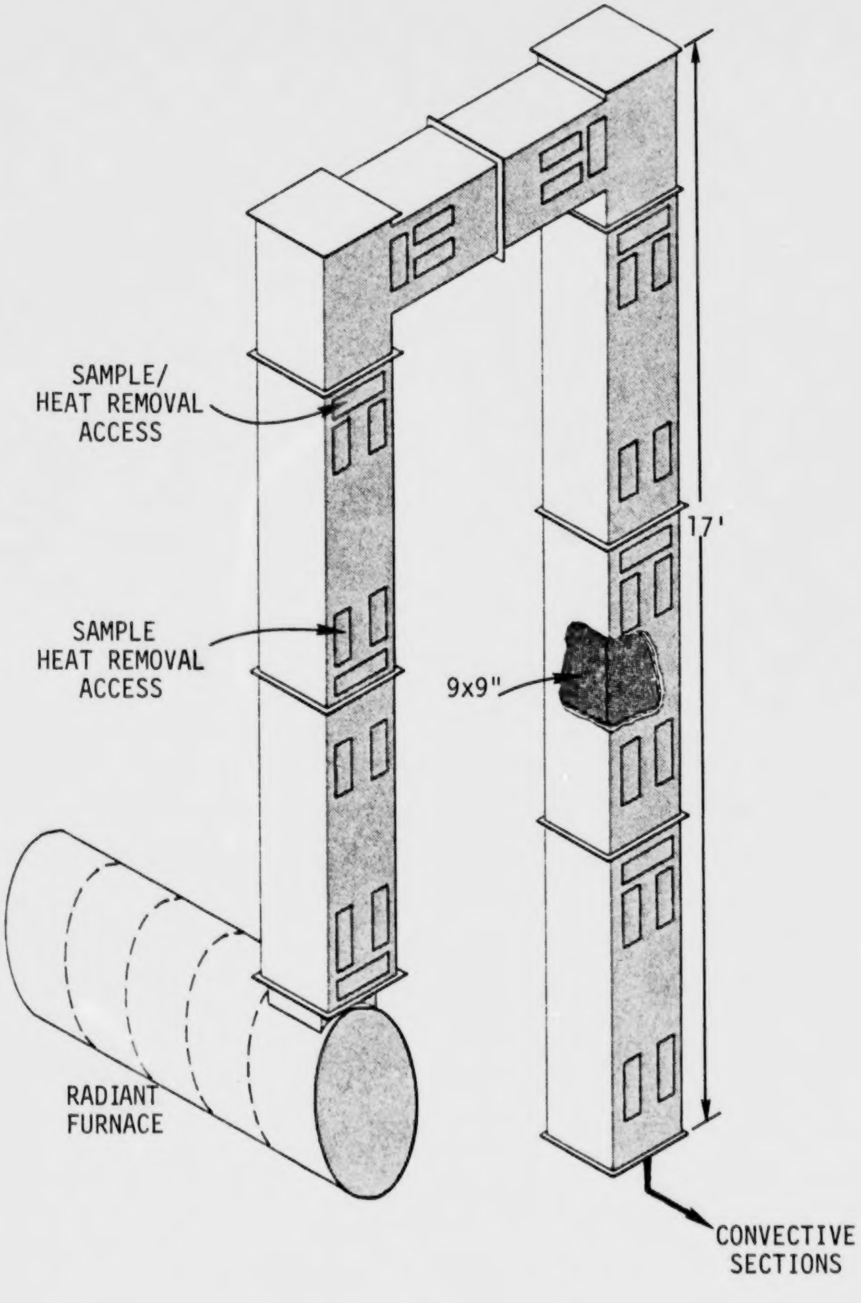

Figure 5-3. Post-Flame Section.

Table 5-1. Radiant Section Design Specifications

GENERAL	
Internal Dimensions	24" ID x 96" Long
External Dimensions	36" OD x 102 " Long
Orientation	Horizontal
Max. Designed Gas Temp	3200 °F
Furnace Volume	24.4 cu ft.
Internal Surface Area	55.0 sq. ft.
No. Of Modules	One (1) Burner Module Two (2) Regular Modules One (1) Exhaust Module
Wall Construction	- Adiabatic Modules and Exhaust Module Consist of 4 Wall Layers: (inside to outside) 2½" B&W Mix 48C (or similar) 2" 3000°F Insulation Cylinder 1½" Castablock Insulation 1/8" Carbon Steel Shell
Heat Extraction	- 3 watercooled probes inserted from rear wall; variable insertion depth; up to 200 K Btu/hr heat removal.
Residence Time @ 1 x 10^6 BTU/HR, SR_T=1·2. Tmean = 2800°F	1.2 Seconds
Total Port Area/%	177 sq. in./ 2.24%

Table 5-2. Post-Flame Section Design Specifications

Internal Dimensions	LEG #1 : 9"x9" Section x 10'0" LEG #2 : 9"x9" Section x 7'4" LEG #3 : 9"x9" Section x 15'0"
External Dimensions	LEG #1 : 15"x15" Section x 10'0" LEG #2 : 15"x15" Section x 7'4" LEG #3 : 15"x15" Section x 15'0"
Total Volume	18·19 cu. ft
Flow Area	81 sq. in (0·5625 sq. ft.)
Internal Surface Area	97 sq. ft.
External Surface Area	162 sq. ft.
Orientation	LEG #1 : Vertical Up LEG #2 : Horizontal Across LEG #3 : Vertical Down
Design Temp	Inlet 2900 ^{O}F Maximum Outlet 2200 ^{O}F Maximum
Overall Conduction Heat Transfer Coef.	0·667 $\frac{BTU}{hr \cdot ft^2 \cdot F}$
Heat Loss Estimate	1700 $\frac{BTU}{ft^2 \cdot hr}$
Total Heat Loss Estimate	166,000 $\frac{BTU}{hr}$
Wall Construction	- 1" 3000 ^{O}F Kaowool Board 2" 2600^{O}F Kaowool Board - 1/8" Thick Steel Casing
Res Time @ $1x10^6 \frac{BTU}{hr}$ SR_T= 1·20, Tmean = 2550 ^{O}F	- 0·9 Seconds
Gas Velocity	35 ft/sec
Estimated Weight	1800 lb

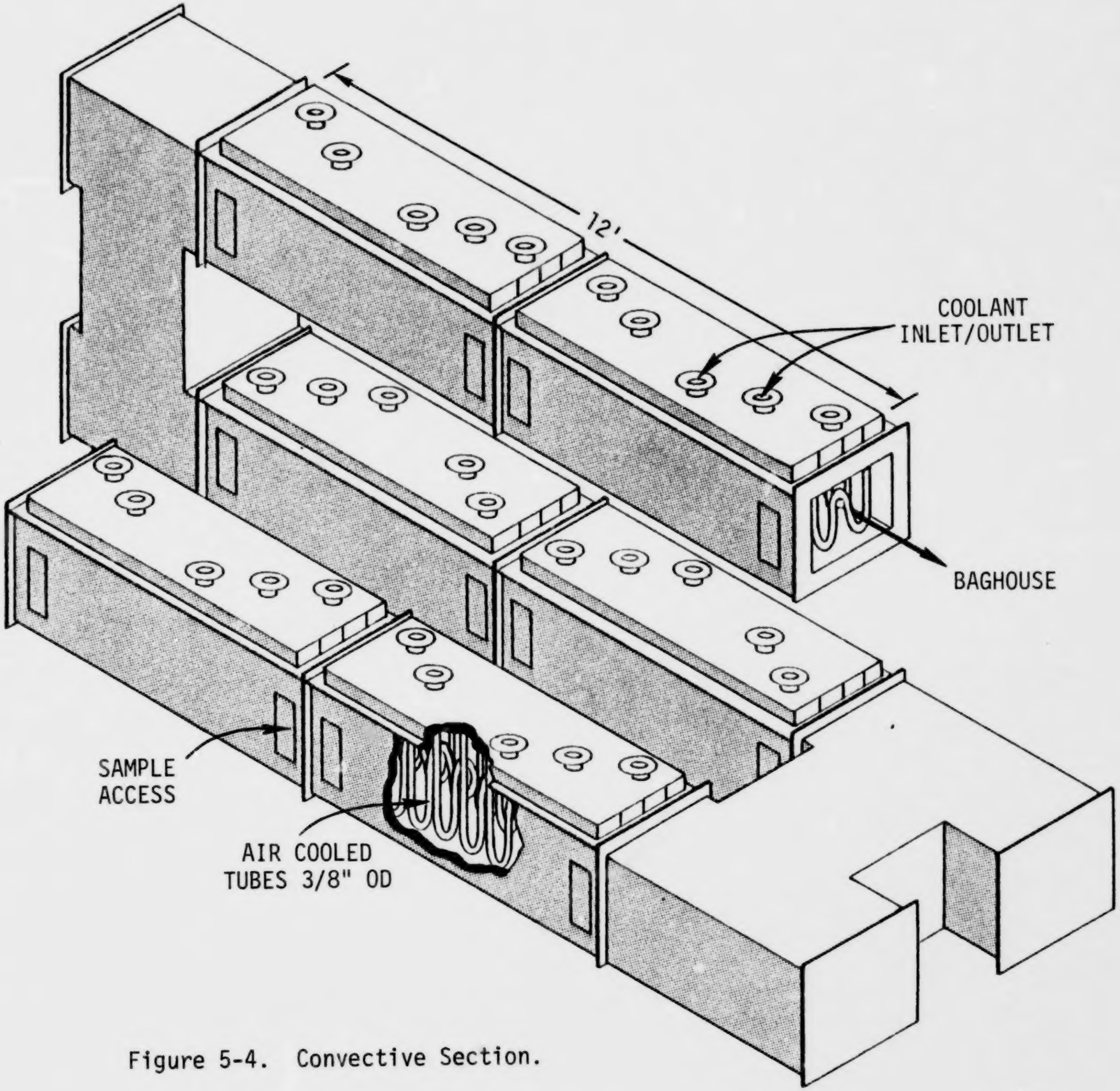

Figure 5-4. Convective Section.

Table 5-3. Convective Sections Design Specifications

GENERAL	SUPERHEATER	REHEATER
Internal Dimension	8"x8" Section x 14'0"	8"x7" Section x 14'0"
External Dimension	14"x16" Section x 14'0"	14"x15" Section x 14'0"
Total Volume	6·22 cu. ft	5·44 cu. ft
Internal Surface Area	37·3 sq. ft	35·0 sq. ft
External Surface Area	70·0 sq. ft	67·7 sq. ft
Orientation	Horizontal	Horizontal
Design Gas Temp	2200 ^{o}F - 1500 ^{o}F	1500 ^{o}F - 850 ^{o}F
Wall Construction	3" Cast-O-Lite 30	3" Cast-O-Lite 30
Modules	(2) Adaptor=1'Long (2) Regular=6'Long	(2) Adaptor = 1' Long (2) Regular = 6' Long
HEAT TRANSFER TUBE BUNDLES		
Tube Arrangement	Cross Flow Banks	Cross Flow Banks
Tubing Size	3/8"	3/8"
Wall Thickness	0·035"	0.035"
Tubing Spacing		
Perpendicular to Flow	2·0"	2·0"
Parallel to Flow	0·85"	0.85"
No of Rows	148	148
Tube Length Per Row	31"	27"
Total Length	382 ft	333 ft
Total Exchange Surface Area	37.5 sq. ft	32.7 sq. ft
Estimated Heat Transfer Coef	7·1 $\frac{BTU}{hr \cdot ft^2 \cdot {}^oF}$	7·1 $\frac{BTU}{hr \cdot ft^2 \cdot {}^oF}$
Estimated Heat Extraction Rate	472,000 $\frac{BTU}{hr}$	250,400 $\frac{BTU}{hr}$
X-Section Area of Tube	11·6 sq. in	10·1 sq. in
Free Flow Area (gas side)	52·4 sq. in	38·9 sq. in.
% Tube Area	18·2 %	20·6 %
Gas Velocity	41 ft/sec	39 ft/sec
Estimated Resid. Time	0·34 sec	0·37 sec

Table 5-3. Convective Section Design Specifications (Concluded)

GENERAL	
Internal Dimensions	8" x 6" Section x 14'0"
External Dimensions	14"x14" Section x 14'0"
Total Volume	4.67 cu ft
Internal Surface Area	32.7 sq. ft
External Surface Area	65.3 sq. ft
Orientation	Horizontal
Design Gas Temp	850 °F - 250 °F
Wall Construction	3" Cast-O-Lite 30
Module:	(2) Adaptor = 1' Long (2) Regular = 6' Long
Heat Transfer Tube Bundles:	
Tube Arrangement	Cross Flow Banks
Tube Size	3/8"
Wall Thickness	0.035"
Tube Spacing Perpendicular To Flow	2·0"
Parallel To Flow	0.85"
No Of Rows	148
Length Per Row	23"
Total Tube Length	284
Total Tube Surface Area	27.8 sq. ft.
Estimated Heat Transfer Coef.	7·1 $\frac{\text{BTU}}{\text{hr}\cdot\text{ft}^2\cdot{}^\circ\text{F}}$
Estimated Heat Extractions Rate	109,000 $\frac{\text{BTU}}{\text{hr}}$
X-Section Area Of Tube	8.6 sq. in
Free Flow Area	27.4 sq. in.
% Tube Area	23.9 %
Gas Velocity	34 ft/sec
Estimated Residence Time	0·58 Second

- Variable swirl.
- Multiple fuel firing by changing fuel nozzles.
- Tertiary air ports.

A schematic of the test burner is shown in Figure 5-5. The modular construction of the air chambers enables adaptation to the dual register configuration if the need arises. The swirl intensity is variable by the distribution of independently controlled combustion air through the axial and swirl generators. The baseline swirl generator can produce swirl numbers from 0 to 3.8. Swirl intensities out of this range are obtained by replacing the swirl generator with a different device.

The water-cooled throat section is removable from the burner quarl and the air chambers. Throats of different designs can be installed to produce different exit velocities. The throat used in the early phase of experiments is five inces in diameter and gives a nominal exit velocity of about 50 ft/sec. Metal sleeves can be inserted in the throat to increase the exit velocity.

The quarl section is constructed of castable refractory and is integrated with the furnace front plate. The quarl diverges at a half angle of 25^{o} from 5.0 inches to 9.66 inches with a length-to-diameter ratio (L/D) of 1.0.

The fuel nozzles for coal, oil, and gas are removable from the back of the burner. The axial position of the nozzle is variable and is referenced at the entrance of the quarl. The coal nozzle is a 1½-inch Schedule 40 pipe with a spreader at the tip. The nominal velocity is 44 ft/sec with 18 percent theoretical air in the primary stream. This is changed by varying the primary air flow or replacing the coal nozzle.

Four tertiary air ports, each 2½ inches in diameter, are spaced evenly on the furnace front plate at 10 inches from the burner axis. The ports are sized for minimum velocities of 30 ft/sec with 80 percent theoretical air at 600^{o}F preheat. Sleeves or special nozzles can be installed to change the direction and velocity of the tertiary air.

5.1.3 Fuel System

Solid, liquid, and gaseous fuels are being burned in the BSF. Since solid fuels are the primary test fuels, requirements on their production, storage,

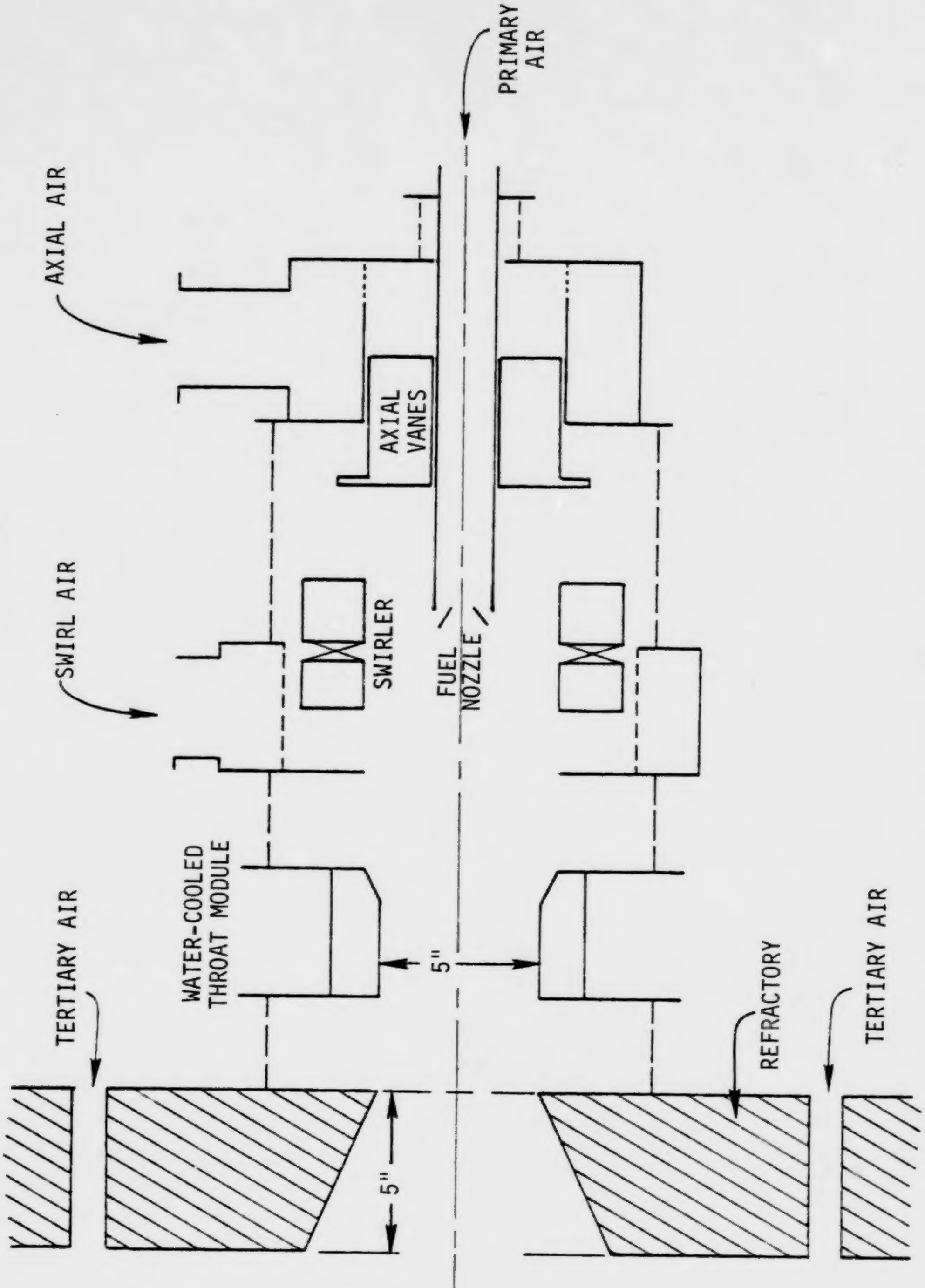

Figure 5-5. Test Burner Schematic.

delivery, and general handling are the most stringent. No. 6 and No. 2 fuel oils are used for overnight firing. Propane is used for ignition and as back-up overnight fuel. All three fuel systems are supervised by a flame monitor (ultraviolet detectors) and are shut off on loss of flame.

Coal is pulverized using an 8000-lb/hr Raymond Bowl mill. The coal powder is separated from the transport air with a bag filter and then stored in air-tight aluminum bins topped with carbon dioxide. The 74 cu ft bins are transported to the BSF coal loading station with a fork lift truck. On demand, the pulverized coal is auger-fed to the small hopper of the gravimetric feeder.

A K-Tron gravimetric feeder (model LWF3-35), which has a twin-screw, delivers the pulverized coal at the operator-selected rate based on the loss-in-weight principle. The manufacturer of the feeder claims it to be accurate to ± one-half percent with an operation range from 0.05 to 35 cu ft/hr (2.5 to 1750 lb/hr for 50 lb/cu ft material). The BSF, depending on coal types used, consumes coal at 70 to 125 lbs/hr and therefore requires the accuracy of the feeder for determination of fuel input.

Primary air flowing through an eductor removes the metered coal powder from the feeder discharge. Two regulating valves at the eductor air and coal inlets are used to adjust the static pressure at the feeder discharge. This is needed to prevent coal stoppage and induced coal flow due to excessive negative pressure. Tests have shown that this arrangement works adequately.

The heart of the oil system is a Zenith variable-speed gear pump (Model BMC-534-11). Pump speed is set by the operator to give the proper fuel flow according to applicable calibration curves. Nominal fuel flow is 8 gph when fired at 1×10^6 Btu/hr. The maximum delivery of the pump is 17 gph at 500 psig. This pump system is adequate for both light and heavy fuel oils. Consistent delivery of viscous fuel oils is assured by controlling the fluid temperature with electrical heat tracing.

Propane is supplied from a 2000-gallon storage tank via a pressure regulator. Independent rotameters (Dwyer RMC-Series) and regulating valves control the pilot and the main propane flows. Maximum capacity of the main propane system is 600 CFH (1.5×10^6 Btu/hr) at a system pressure of 15 psig.

5.1.4 Combustion Air System

Firing coal at 1 x 10^6 Btu/hr requires approximately 260 SCFM of combustion air. A rotary screw compressor (Ingersol-Rand Model SSR 350L), with 350 CFM capacity at 110 psig, supplies the combustion air and other system air demands. The air is dried by a refrigeration dryer (Hankinson Model 80400) to a dew point of 35°F and filtered with a coalescent filter (Hankinson Model 1317). The clean dry air is necessary to insure the accuracy of the flow meters of the combustion air system.

The compressed air is delivered to a common manifold at 15 psig. From the manifold, five independently-controlled and metered air streams supply the primary transport, sorbent transport, in addition to two main and one staging air streams. The capacities of the streams are selected at optimum metering accuracy and are listed in Table 5-4. Pneumatically actuated valves regulate the air flows which are indicated by the pressure drop across factory-calibrated laminar flow elements (Meriam Instrument). The pressure drop signals (0.6 in W.C.) are displayed by inclined manometers (Dwyer Model 264) for manual data recording. They are also fed to a scan valve (Scanivalve Model W1260/1P-12T) which allows the five differential pressures and the manifold pressure to be measured with pressure transducers (Validyne DP45). The transducers and demodulators system, outputs voltage signals to the automatic data acquisition system.

Each combustion air stream is preheated by a propane-fired radiant heat exchanger for maximum 900°F preheat. A temperature controller fires the propane burner when the exit air temperature falls below the operator-selected setpoint. Provision is included to retrieve a part of the exhaust waste heat from the main furnace by the two largest air streams before they are heated at the preheaters.

5.1.5 Sorbent and Additive System

Sulfur and sorbent interaction is a central part of the experiments with the BSF system. The sorbent delivery system is based on a maximum rate of 64 lb/hr of limestone. It consists of a volumetric feeder (K-Tron T-20 with 6300 controller) and associated piping. Nozzles have been developed as the study progresses. The twin screw feeder can deliver between 0.002 to 3.5 cu ft/hr of solids. This converts to 0.3 to 525 lb/hr of powdered limestone.

Table 5-4. Air System

Air Stream	Maximum Flow % T.A.	Maximum Flow Rate SCFM (70°F)	Maximum Temp. °F	Meriam Flowmeter Model
Primary	30	52	900	50 MW 20-2
Additive	50	86	900	50 MW 20-2
Outboard	80	138	900	50 MY 15-4
Secondary I	140	241	900	50 MR 2-2
Secondary II	110	189	900	50 MY 15-3

T.A. - Theoretical Air

The sorbent is pneumatically transported and injected at the burner, the radiant furnace, the post-flame section, and other desired points in the furnace system.

5.1.6 Sampling and Measurement

Sampling and measurement are the most important elements of the experiments. Different methods are required for determining the species concentrations of interest; namely, O_2, CO, CO_2, SO_x, NO_x, HC, HCN and solids, etc. Table 5-5 summarizes the sampling and measurement techniques that are used for the gas-phase measurements during the BSF experiments.

Three probe designs are used; namely, solid rejection, water-cooled, and water-spray. The solid rejection, or phase discrimination probe, is suitable for sampling gas-phase sulfur species and has been described in detail in Section 4. The water-cooled probe is used to extract samples which are relatively stable and do not require rapid quenching or separation of the solid from the gas. (It is only used for O_2, CO, and CO_2 measurements.) A water-spray probe quenches the sample rapidly and also removes the solids and soluble gases and is used for sampling NO_x in a reactive environment. Also, by metering the water-spray and gas-sample rates, the concentrations of nitrogen compounds are also determined by specific ion electrodes.

5.1.7 Cleanup

Coal-firing systems pose a serious ash cleanup problem. Particulates in the radiant, post-flame, convective sections and the stack gas will be handled differently according to their characteristics.

Radiant furnace ash is of the fused or running type because of the high furnace temperature (above 2500°F). By firing the furnace at a higher rate, molten slag is formed and can be removed from the furnace bottom.

Deposits on the convective tubes depend on the tube temperature, ash composition, and the combustion characteristics in the flame zone. Sequentially-activated high-pressure air jets blow the loose ash deposits from the tube surfaces. Periodically, the tube bundles are removed from the convective passages and manually cleaned.

Table 5-5. Gas-Phase Measurements

Species	Probe	RD	Instrument	Range
O_2	WC, SR	RD	BECKMAN 755 Paramagnetic	0-5, 0-10 0-25 %
CO	WC, SR	RD	LOW-ANARAD 500R NDIR HIGH-ANARAD 600 NDIR	0-500 ppm 0-1, 0-10%
CO_2	WC, SR	RD	ANARAD 600 NDIR	0-20%
NO, NO_x	WC, WS	RD	TECO 10R Chemiluminescent	0-5 ppm to 0-10,000 ppm
SO_2	SR	PD	DuPont 400 Photometric	0-400 0-4000 ppm

WC - water cooled
WS - Water spray
SR - Solid rejection
RD - Refrigeration dried
PD - Permapure drier

Solids that remain suspended in the flue gas are separated from the gas with a bag filter (Mickopulsair) sized for 700 ACFM of gas throughput. The baghouse is constructed of stainless steel and uses high-temperature bags (up to 500^{o}F). The fly ash collected in the baghouse is periodically manually removed.

5.1.8 Data Acquisition System

The BSF is a complex facility and can only be fully characterized if a complete set of system conditions is recorded for every data point. Although the BSF can be operated without an automated data acquisition system, data rate and quality are greatly enhanced by such a system.

The BSF has an automatic data acquisition system which is backed up by a system of switches, meters, and chart recorders so that experiments can be carried out should the automatic system fail.

The automatic data acquisition system (Figure 5-6) centers around a LSI-11/23 computer. Via an IEEE-488 interface link, it communicates with a measurement and control module (Fluke 2400) which performs the analog to digital (ADC) and digital to analog (DAC) conversions. The test program resident in the computer memory requests data from the measurement and control module (MCM), performs computations, and displays system conditions on a CRT terminal. Selected information is printed on paper or recorded on a flexible magnetic disc.

The LSI-11/23 computer has 128 K bytes of memory and operates under Digital Equipment Corporation's (DEC) RT-11, Fortran IV and Basic 11 software. This operating system supports two users simultaneously. The experimentation user has top priority (foreground). In the background, a user may develop programs or retrieve experimental data. If further need arises, multi-user capabilities can be implemented by adding a hard disc drive, expanding the memory to 256 bytes, and changing to the RSX-11M software.

The measurement and control module (MCM) consists of a main chasis and ancillary plug-in modules to measure and output voltages, currents and resistances. It can also handle status imputs and outputs. The MCM is programmed by the LSI-11/23 computer; thereafter, it functions independently.

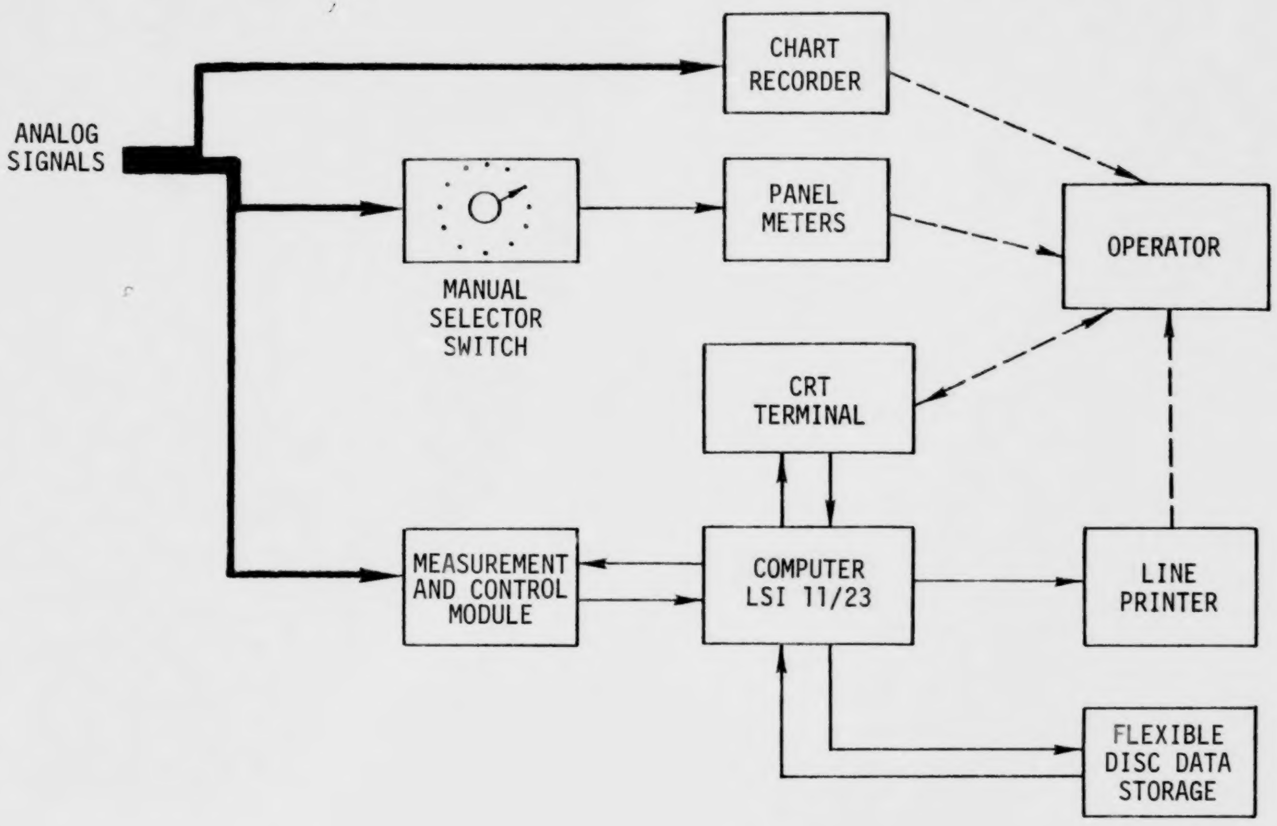

Figure 5-6. Data Acquisition System.

System parameters are updated and stored in the MCM's memory continuously.

The computer is free to perform other tasks until it requests data from the MCM in a burst mode. This "distributed processing" configuration maximizes the system efficiency, particularly when the computer has to support several users.

5.2 Experimental Approach

The BSF facility is scheduled to be on-line and available for coal/sorbent injection studies in April 1981. Data from the BSF will bridge the gap between the small-scale furnaces ($\sim$100 x 10^3 Btu/hr) and the larger furnaces ($>$10 x 10^6 Btu/hr).

The initial efforts will concentrate on the characterization of the furnace; specifically, residence time distributions, temperature profiles, operation limits will be determined and changes made as necessary. Following the system characterization phase, and the definition of baseline operating conditions, studies on SO_x-sorbent interaction, NO_x and particulates will commence. Initially, a test plan comprising three series of experiments is envisaged:

- Series A - Combustion parameter screening studies.
- Series B - Influence of thermal environment.
- Series C - Fuel and sorbent effects.

The series A studies are intended to provide a screening of parameters to determine gross effects of major variables on SO_x capture. These studies will be carried out with one coal and one sorbent type, only, and will investigate the parameters

- firing rate (load)
- "burner zone" stoichiometry
- flame zone heat extraction
- excess air
- sorbent injection location and velocity
- Ca/S ratio.

Since temperature has been shown to be an important combustion parameter which has a strong influence on sulfur/sorbent interaction, the Series B experiments will investigate more thoroughly the influence of thermal environment. More specifically, this series will examine the detailed effects of sorbent particle temperature-time profiles. The Series C experiments will extend the studies to establish the relationship between optimum combustion conditions and the properties of both the sorbent and the fuel used.

6.0 CONCLUDING REMARKS

6.1 Bench-Scale Studies to Assess the Impact of Coal Type on NO_x Formation

Twenty-eight different coals as well as several simulated coals, i.e., char/propane and char/propane/ammonia or nitric oxide, were tested under excess air and staged conditions to study the effects of fuel properties on the fate of fuel-bound nitrogen during combustion. Detailed measurements of first-stage and exhaust species concentrations were performed for 14 different coals to investigate the parameters controlling a staged combustion process.

Results obtained have pointed to the following conclusion and implications.

6.1.1 Excess Air

NO formation during pulverized coal combustion can be attributed to the nitrogen in both the volatiles and the char. The conversion of nitrogen which remains in the solid phase during devolatilization is inherently low. The conversion of nitrogen evolved with the volatiles appears to be higher than that of the char nitrogen. The presence of hydrocarbon volatiles, however, enhances the conversion of char nitrogen. On the other hand, the presence of solid phase is believed to suppress the conversion of volatile nitrogen. Initial fuel/air contacting rate controls the oxygen availability for both fuel nitrogen fractions. It appears that the volatile nitrogen conversion increases with increasing mixing rate, but the conversion of char nitrogen is less sensitive to change in the initial air distribution.

Thus, those coals which evolve more volatile nitrogen are expected to produce higher NO emissions under well mixed conditions. Data obtained under excess air conditions indicate that with premixed or rapidly mixed system, fuel NO formation increases with increasing fuel nitrogen content; however, other fuel properties also significantly affect the fate of coal nitrogen. Attempts to correlate these data on the basis of the nitrogen lost in the ASTM volatile determination or with such basic fuel properties as percent nitrogen, percent volatiles or coal rank prove unsuccessful.

An experiment has been developed in another EPA-support program to define the reactive volatile nitrogen fraction of coals. Six of the very different coals tested in the bench scale reactor were pyrolyzed under inert conditions at 1370°K and the volatile nitrogen species which were converted to HCN were measured. Figure 6-1 shows that the data obtained in this quartz reactor pyrolysis experiment agree qualitatively with the experimental results obtained with the premixed burner. The Savage lignite has the highest percentage conversion of fuel nitrogen to NO in the combustion experiments, and also the highest fractional volatile reactive nitrogen yield in the inert pyrolysis study. Likewise, the Beulah lignite was the lowest of both experiments. The slope of the correlation decreases with decreasing mixing rate (premixed or radial diffusion) and the axial diffusion data do not correlate well. This may be because the pyrolysis experiment does not characterize char nitrogen. Therefore, it can be concluded that under excess air conditions fuel nitrogen conversion is proportionally greater with coals containing a high fraction of volatile, reactive nitrogen.

6.1.2 Staged Combustion

Detailed measurements of first stage and exhaust species concentrations suggest that a staged combustion system must be optimized with respect to first-stage stoichiometry and residence time, fuel properties and heat extraction rate. As first-stage stoichiometry is decreased, the NO formed in the first stage decreases, but other oxidizable gas-nitrogen species increase as does nitrogen retention in the char. Total fixed nitrogen (TFN = NO + NH_3 + HCN) generally increases with increasing fuel nitrogen and correlates well with excess-air exhaust emissions. Increasing the residence time in the fuel-rich stage allows TFN species to decay toward low equilibrium values and thus reduces exhaust NO emissions.

The distribution of the TFN species leaving the first stage is strongly dependent upon the coal composition. Of the 12 coals tested in detail, only two produced high HCN concentrations. Figure 6-2 shows the percent of input fuel nitrogen exiting the first stage as NO, NH_3 or HCN at $SR_1 = 0.70$. The German bituminous coal (Saar) correlates well with American bituminous coals. The anthracite and the Utah char (classified as semianthracite according to the criteria outlined in ASTM Method D 388) produced relatively large amounts of first stage NO. This could be due to the increased oxygen partial pressure in the early stages of combustion. With low volatile fuels, the rate of consumption was reduced due to decreased hydrocarbon evolution. For all the bituminous coals except the Indiana bituminous both NH_3 and HCN usually

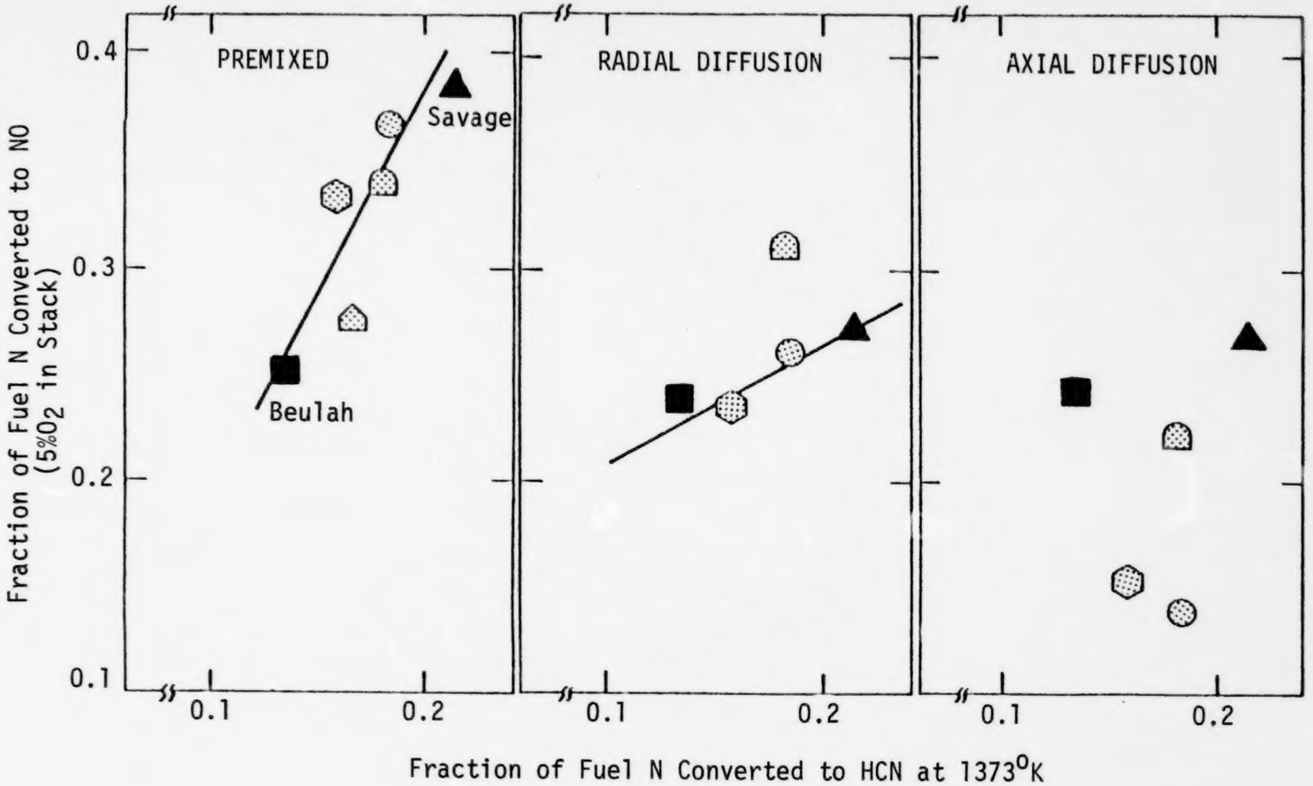

Figure 6-1. Fuel NO Correlation.

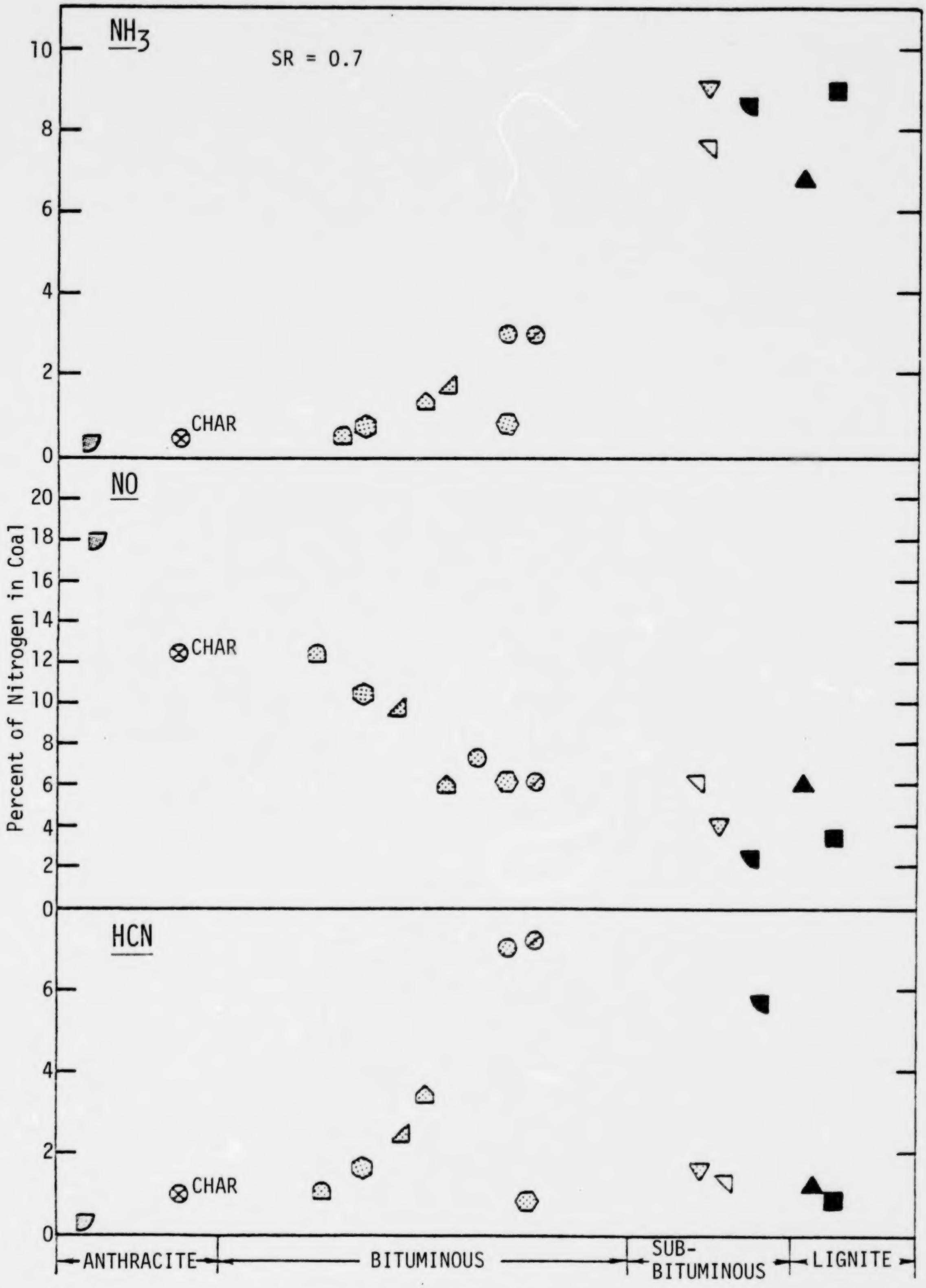

Figure 6-2. Influence of Coal Rank on Gas-Phase Nitrogen Species Exiting First Stage.

increased with increasing fuel volatility. HCN concentrations were higher than NH_3 for all the bituminous coals. However, for sub-bituminous and lignite coals HCN concentrations were significantly less than NH_3 levels at all stoichiometries.

In general, NO at the exit of the first stage appears to decrease with decreasing coal rank from anthracite to lignite. Conversely, the relative amounts of NH_3 grow with decreasing rank. The percent of initial nitrogen leaving the first stage as HCN was below 4 percent for most of the coals tested.

Second-stage TFN conversion decreases as the TFN distribution shifts in favor of HCN and NH_3, and as the hydrocarbon content of the second-stage reactants increases. The percentage conversion of char nitrogen to NO in the second stage is low (<20 percent). First-stage cooling decreases the TFN decay in the fuel-rich zone and, hence, increases the TFN and char nitrogen carryover into the second stage. Reduced second-stage flame temperatures have little effect on solid-phase nitrogen conversion, but they dramatically decrease gas-phase TFN conversion due to a shift in controlling flame chemistry.

The exhaust NO emissions depend on first stage stoichiometry, on the amount and speciation of the TFN entering the second stage and on the amount of char nitrogen. Thus the exhaust NO data can be correlated with a model of the form:

$\text{NO exhaust} = X_1\,(\text{NO}) + X_2\,(NH_3 + \text{HCN}) + X_3\,(C_N) + NO_{Th}$ where

X_1 = conversion of NO.
X_2 = conversion of NH_3 and HCN,
X_3 = conversion of char nitrogen, and
NO_{Th} = thermal NO formation

in the second stage flame. The TFN concentrations were correlated in ppm, dry 0% O_2 based on the detailed measurements at the end of the first stage. The char nitrogen (C_N) was used as equivalent ppm based on stoichiometric conversion of the remaining nitrogen.

As noted previously, NO conversion in the second stage flame did not appear to be a strong function of NO concentration; however, it was found to depend on first-stage stoichiometry (probably specifically on the hydrocarbon content of the second stage flame). Data from pairs of Utah char/C_3H_8/NH_3 experiments indicated that as the SR was reduced from 0.9 to 0.6, NO conversion dropped from approximately 89 percent conversion to 51 percent with no change in HCN or NH_3 concentrations. Therefore, NO conversion was modeled as:

$$X_1 = \alpha\text{-SR}$$

where α = correlation constant.

Figure 3-35 indicates that the conversion of HCN and NH_3 decreases with increasing TFN content; hence, a reciprocal model was used for these conversions:

$$X_2 = \frac{1}{\beta + \gamma(NH_3 + HCN)}$$

Char nitrogen conversion was assumed to be approximately constant: $X_3 = \delta$ as was the contribution of thermal NO formation, NO_{Th}.

A multivariable linear regression program was used to calculate the required parameters. The resulting correlation was:

$$NO_{EX} = 0.8(SR)\ (NO) + \frac{1}{2 + 0.007\ (HN_3 + HCN)}\ (NH_3 + HCN) + 0.2\ C_N + 5$$

Figure 6-3 shows the results of this correlation plotted against the measured exhaust NO and indicates that the agreement is reasonable considering the wide range of coals (lignite - bituminous) and conditions (SR_1 = 0.45 - 0.90) which were included. The overall correlation coefficient (r^2) was 0.93.

The equation suggests that first stage NO has a very significant impact on the ultimate exhaust NO concentration; even at SR = 0.45, the retention of NO is predicted to be 36 percent. NH_3 and HCN conversions are predicted to decrease from 50 percent at low concentrations to 18 percent at 500 ppm of HCN + NH_3. Char nitrogen conversion was estimated to be approximately 20 percent and thermal NO was predicted to be relatively low in this system (5 ppm).

The above correlation, which is valid when the first stage operates without cooling, suggests that optimum staged combustion technology will minimize first stage NO formation and attempt to maximize the TFN decay in the first stage. Char NO formation in the second stage flame can also be significant if large amounts of nitrogen are allowed to remain in the solid phase; hence, this should be avoided. Results indicate that increasing the rate of heat extraction from a staged combustion system reduces NO emissions via a more complex reaction.

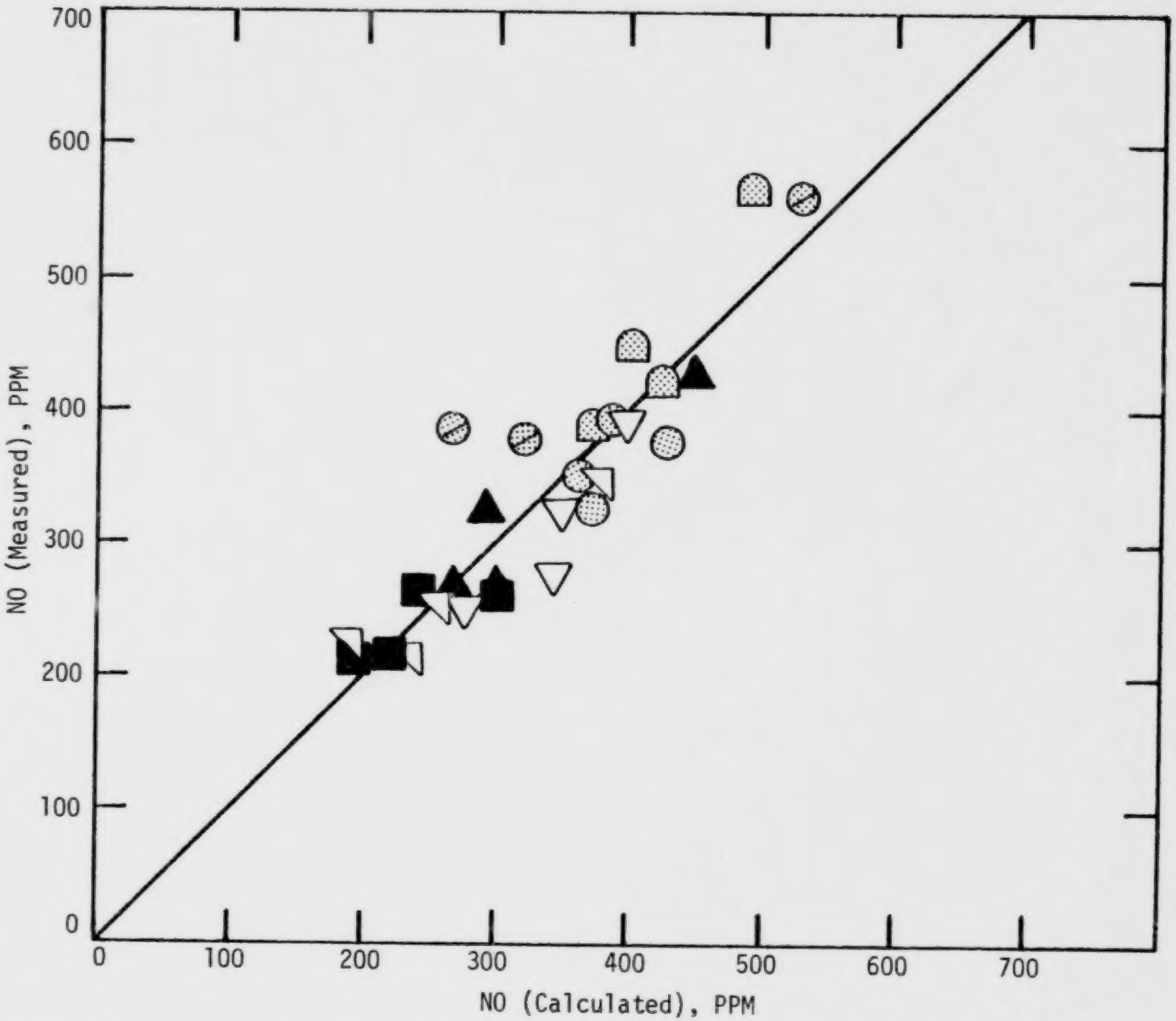

Figure 6-3. Exhaust NO Can be Calculated by $NO_{ex} = 0.8(SR)(NO) + \frac{HCN + NH_3}{2 + 0.007\ (HCN+NH_3)} + 0.2\ (Char\ N) + 5.$

6.2 Bench-Scale Studies to Assess the Impact of Coal Type on SO_x Emissions and Sorbents for SO_x Emissions Reduction

This effort has only been recently initiated and the results should be considered preliminary at this time. The general conclusions that can be drawn from this effort are:

- Uniform dispersion of limestone in the combustion zone is critical to obtaining high sorbent utilization.
- Results suggest that proper control of temperature/time/stoichiometry can produce significant SO_2 removal from combustion products.
- Experimental measurement methods can be designed which provide sufficient accuracy that reasonable sulfur balances can be obtained.

7.0 APPENDICES

APPENDIX A

SUMMARY OF BENCH-SCALE DATA

Fuel and Thermal NO Emissions as a Function of Excess Air and Burner Type

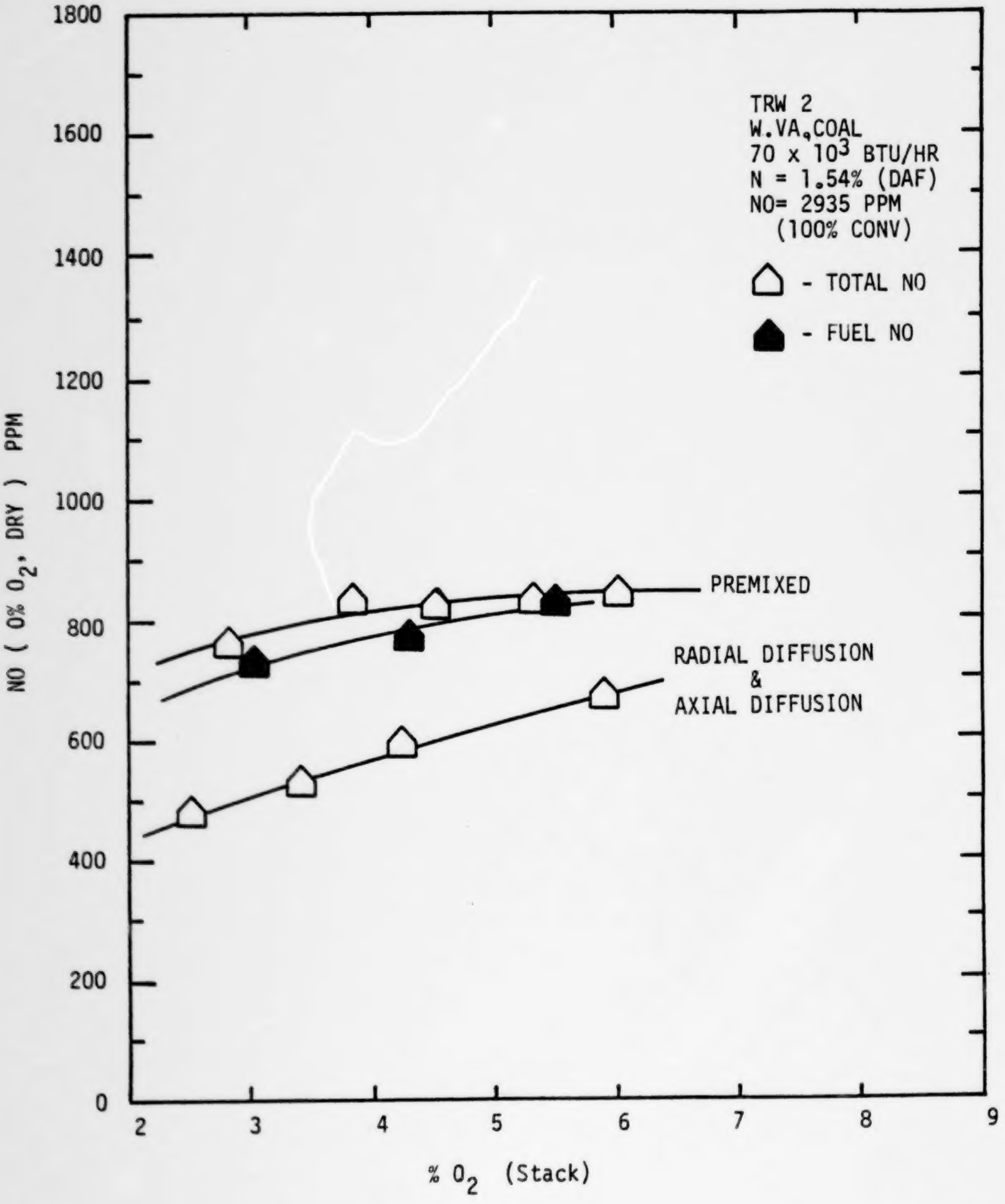
1800
1600
1400
1200
1000
800
600
400
200
0
2
3
4
5
6
7
8
9
NO (0% O_2, DRY) PPM
% O_2 (Stack)
TRW 2
W.VA. COAL
70 x 10^3 BTU/HR
N = 1.54% (DAF)
NO= 2935 PPM
(100% CONV)
- TOTAL NO
- FUEL NO
PREMIXED
RADIAL DIFFUSION
&
AXIAL DIFFUSION

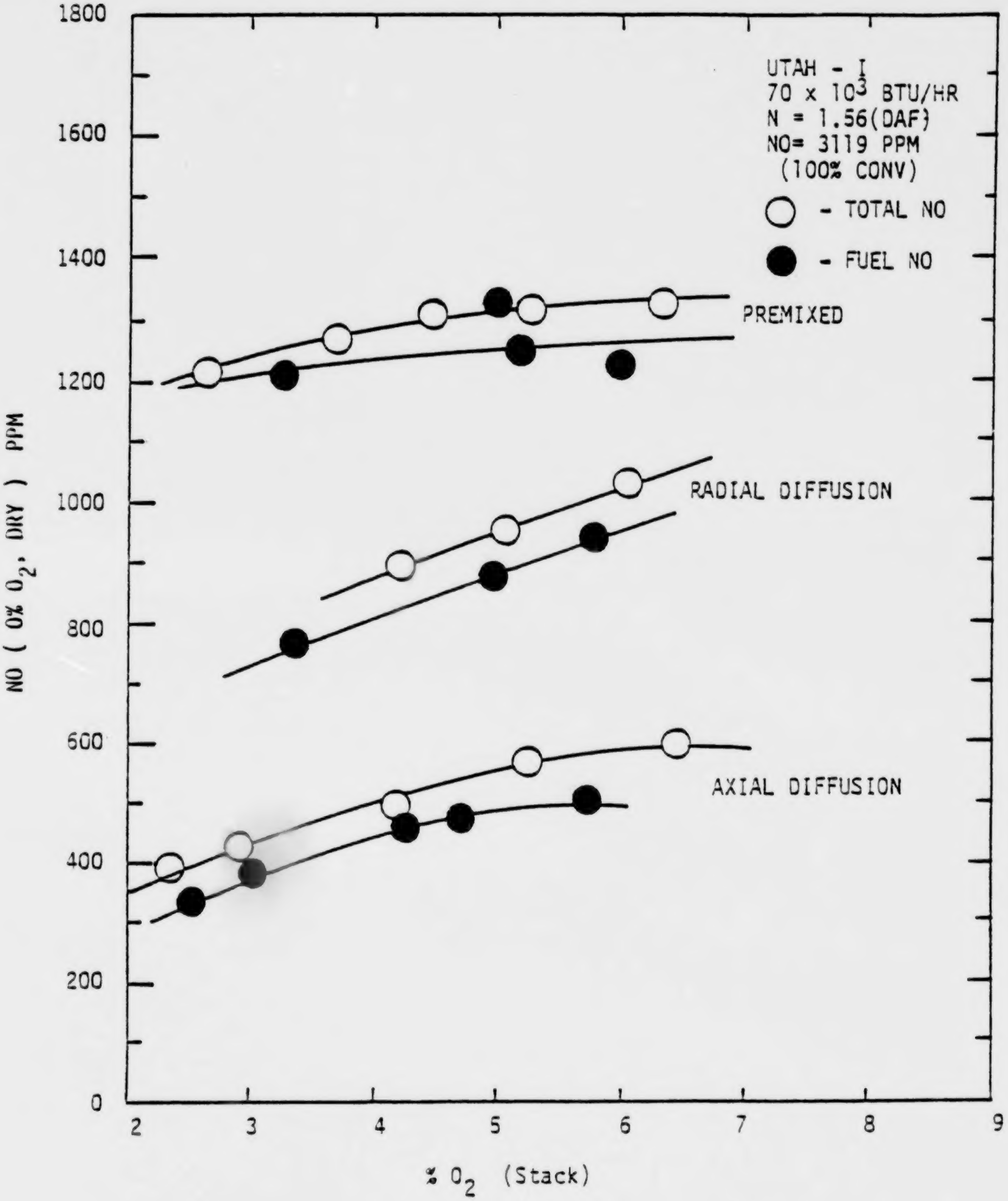
UTAH - I
70 x 10^3 BTU/HR
N = 1.56(DAF)
NO= 3119 PPM
(100% CONV)
○ - TOTAL NO
● - FUEL NO
PREMIXED
RADIAL DIFFUSION
AXIAL DIFFUSION
NO (0% O_2, DRY) PPM
1800
1600
1400
1200
1000
800
600
400
200
0
2
3
4
5
6
7
8
9
% O_2 (Stack)

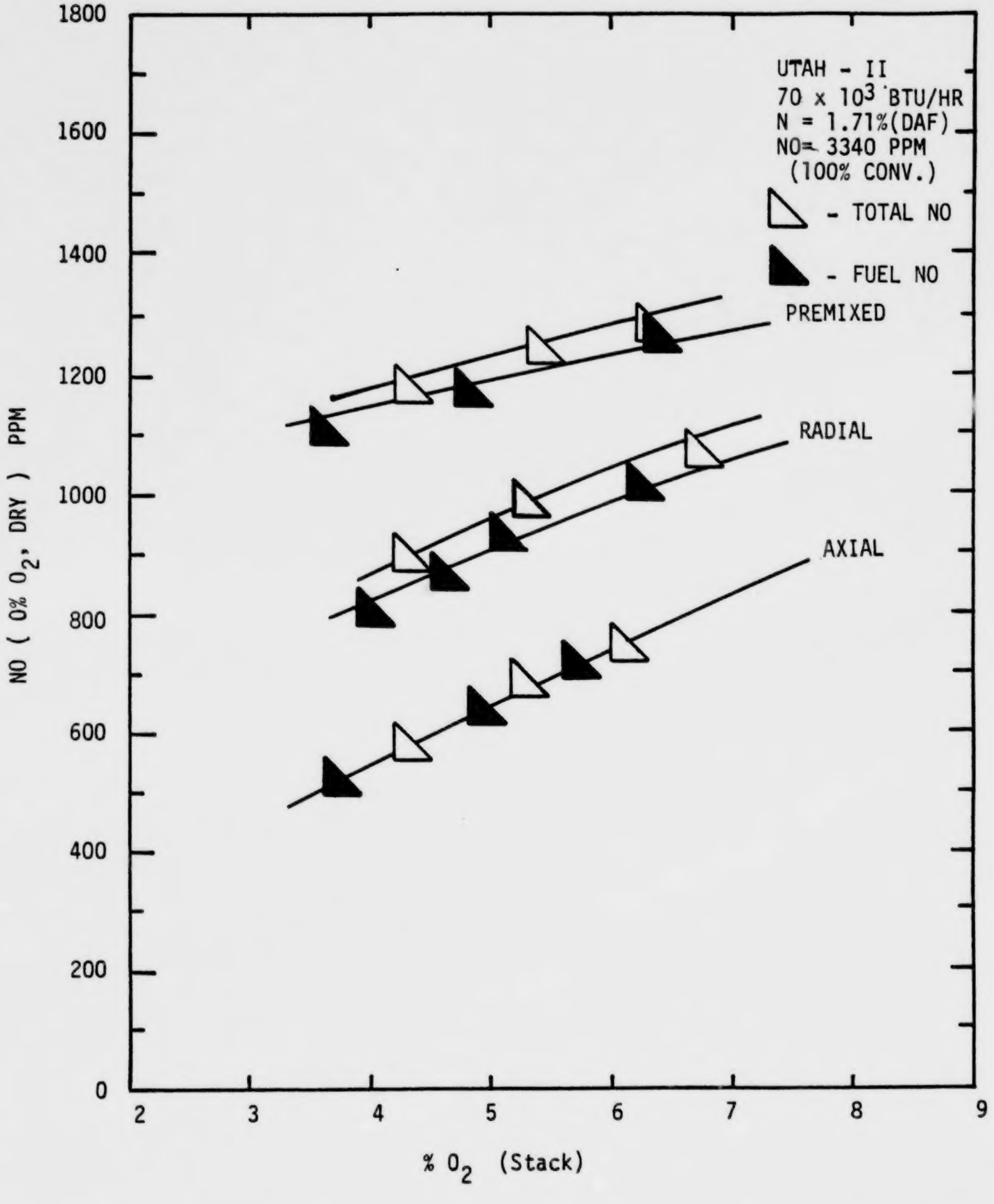
1800
1600
1400
1200
1000
800
600
400
200
0
2
3
4
5
6
7
8
9
NO (0% O_2, DRY) PPM
% O_2 (Stack)
UTAH - II
70 x 10^3 BTU/HR
N = 1.71%(DAF)
NO= 3340 PPM
(100% CONV.)
△ - TOTAL NO
▲ - FUEL NO
PREMIXED
RADIAL
AXIAL

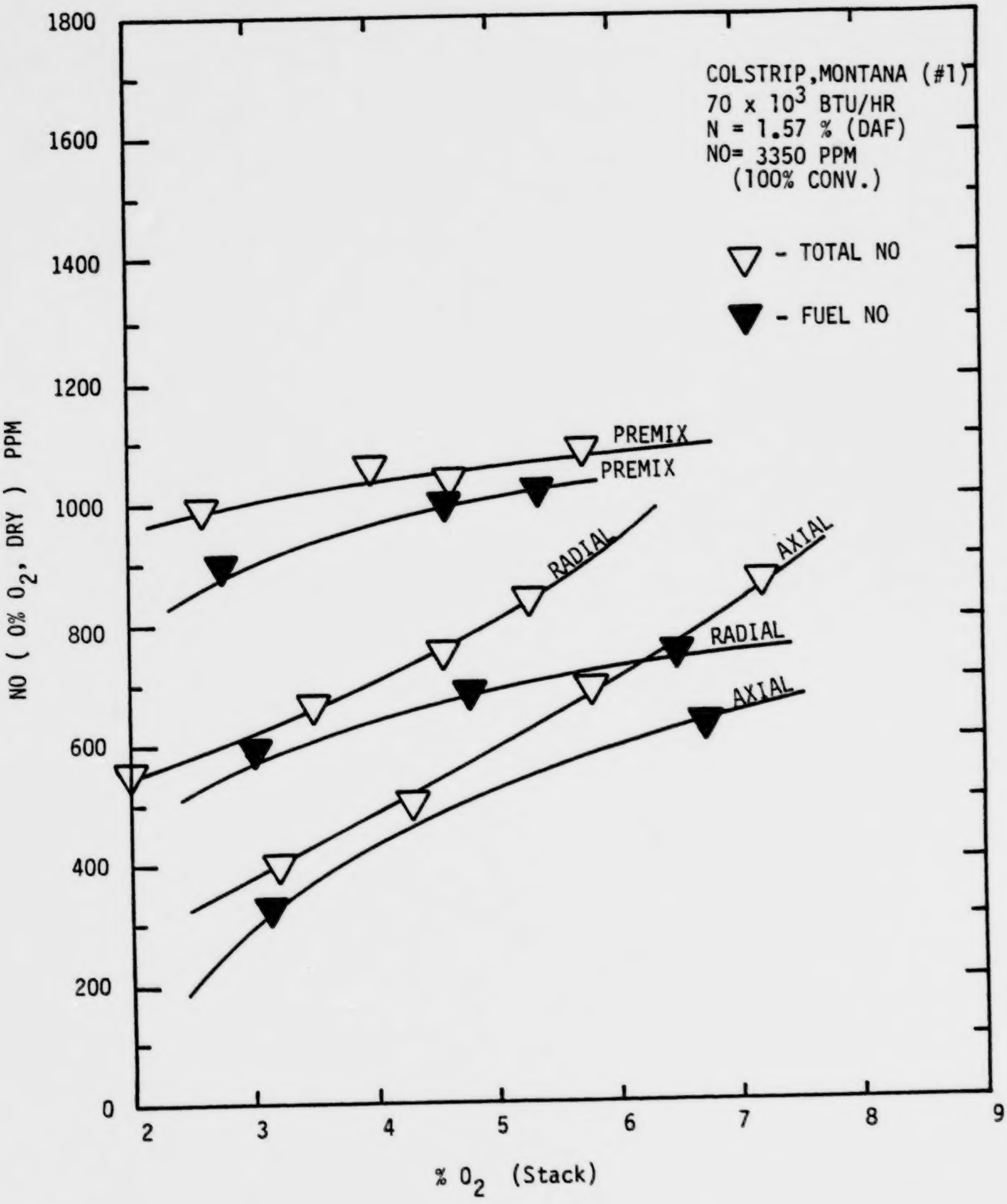

COLSTRIP,MONTANA (#1)
70 x 10^3 BTU/HR
N = 1.57 % (DAF)
NO= 3350 PPM
(100% CONV.)
▽ - TOTAL NO
▼ - FUEL NO
PREMIX
PREMIX
RADIAL
RADIAL
AXIAL
AXIAL
NO (0% O_2, DRY) PPM
% O_2 (Stack)
0
200
400
600
800
1000
1200
1400
1600
1800
2
3
4
5
6
7
8
9

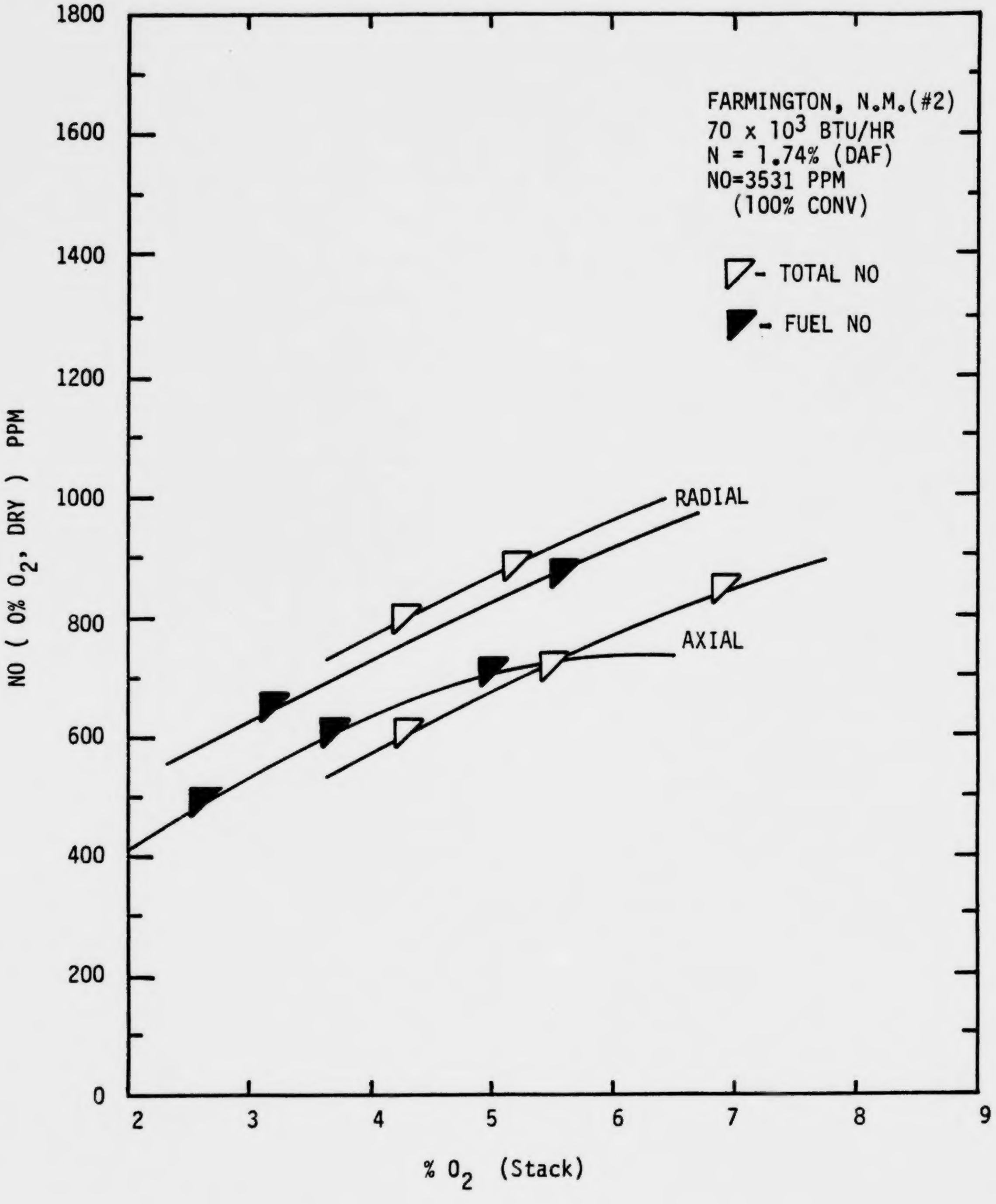
FARMINGTON, N.M.(#2)
70 x 10³ BTU/HR
N = 1.74% (DAF)
NO=3531 PPM
(100% CONV)
▽- TOTAL NO
▼- FUEL NO
RADIAL
AXIAL
NO (0% O₂, DRY) PPM
% O₂ (Stack)
0
200
400
600
800
1000
1200
1400
1600
1800
2
3
4
5
6
7
8
9

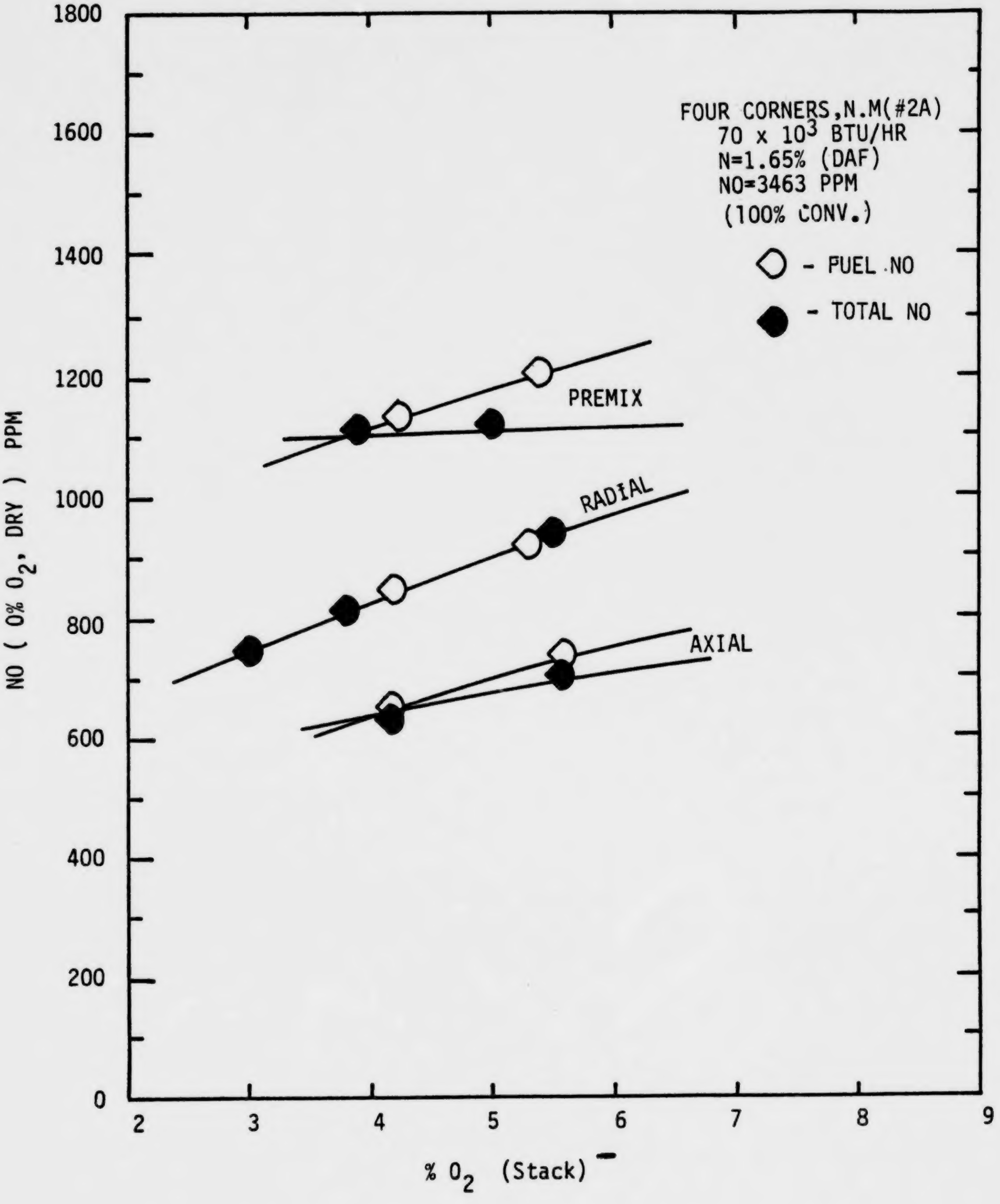
FOUR CORNERS,N.M(#2A)
70 x 10³ BTU/HR
N=1.65% (DAF)
NO=3463 PPM
(100% CONV.)
◇ - FUEL NO
● - TOTAL NO
PREMIX
RADIAL
AXIAL
NO (0% O₂, DRY) PPM
% O₂ (Stack)
1800
1600
1400
1200
1000
800
600
400
200
0
2
3
4
5
6
7
8
9

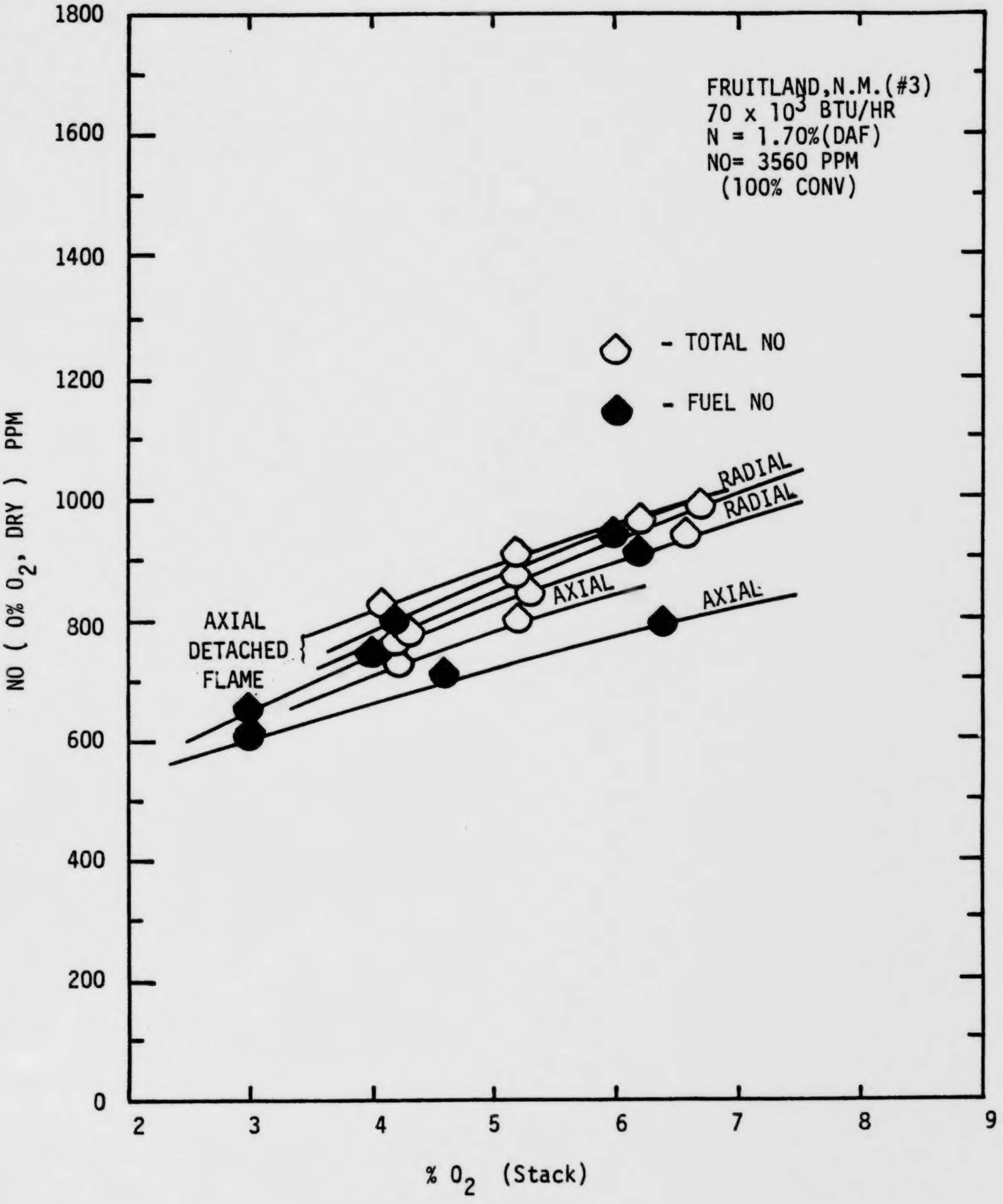
FRUITLAND,N.M.(#3)
70 x 10^3 BTU/HR
N = 1.70%(DAF)
NO= 3560 PPM
(100% CONV)
- TOTAL NO
- FUEL NO
RADIAL
RADIAL
AXIAL
AXIAL
AXIAL DETACHED FLAME
NO (0% O_2, DRY) PPM
1800
1600
1400
1200
1000
800
600
400
200
0
2
3
4
5
6
7
8
9
% O_2 (Stack)

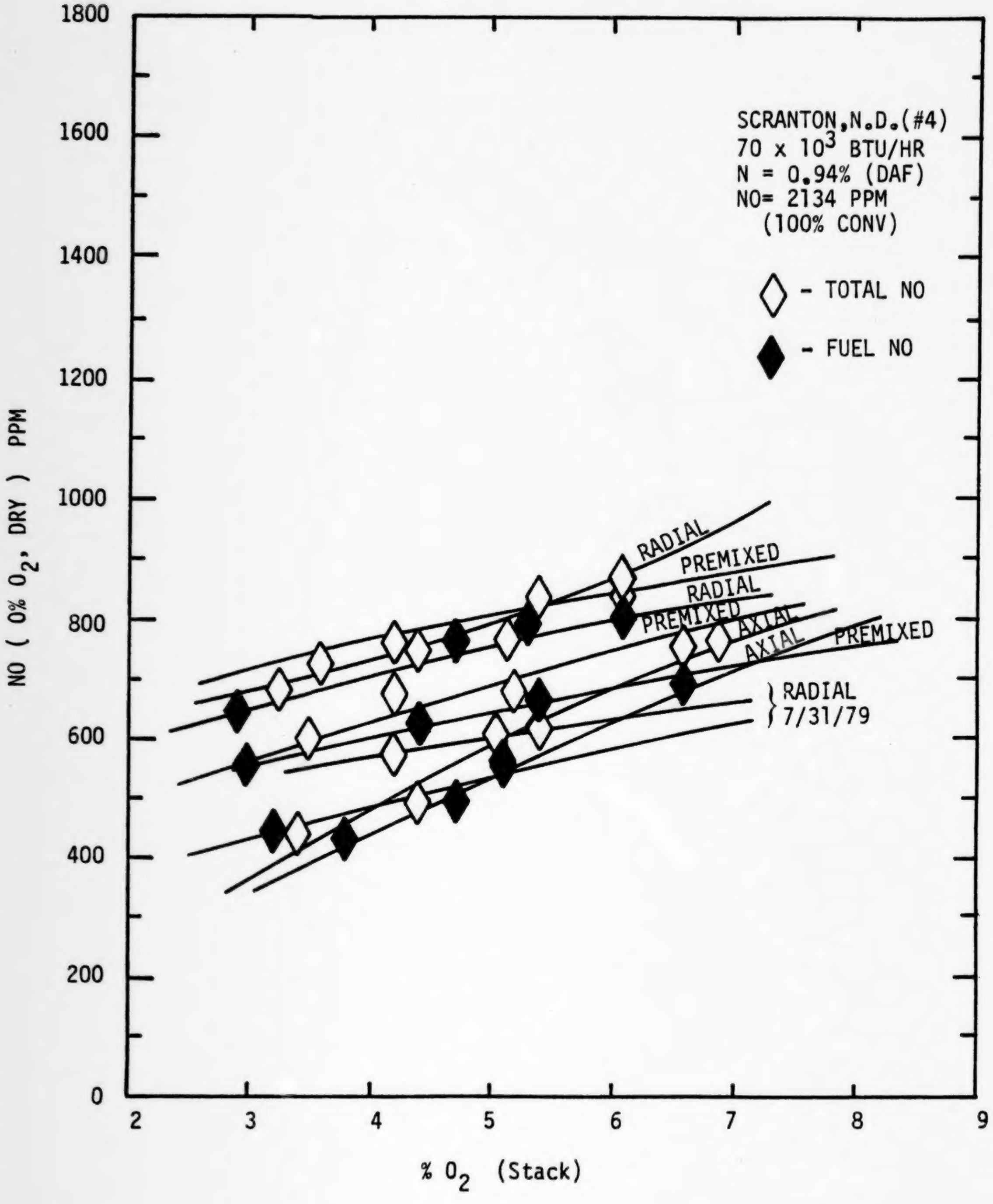
SCRANTON, N.D. (#4)
70 x 10^3 BTU/HR
N = 0.94% (DAF)
NO= 2134 PPM
(100% CONV)
◇ - TOTAL NO
◆ - FUEL NO
RADIAL
PREMIXED
RADIAL
PREMIXED
AXIAL
AXIAL
PREMIXED
RADIAL
7/31/79
NO (0% O2, DRY) PPM
0
200
400
600
800
1000
1200
1400
1600
1800
% O2 (Stack)
2
3
4
5
6
7
8
9

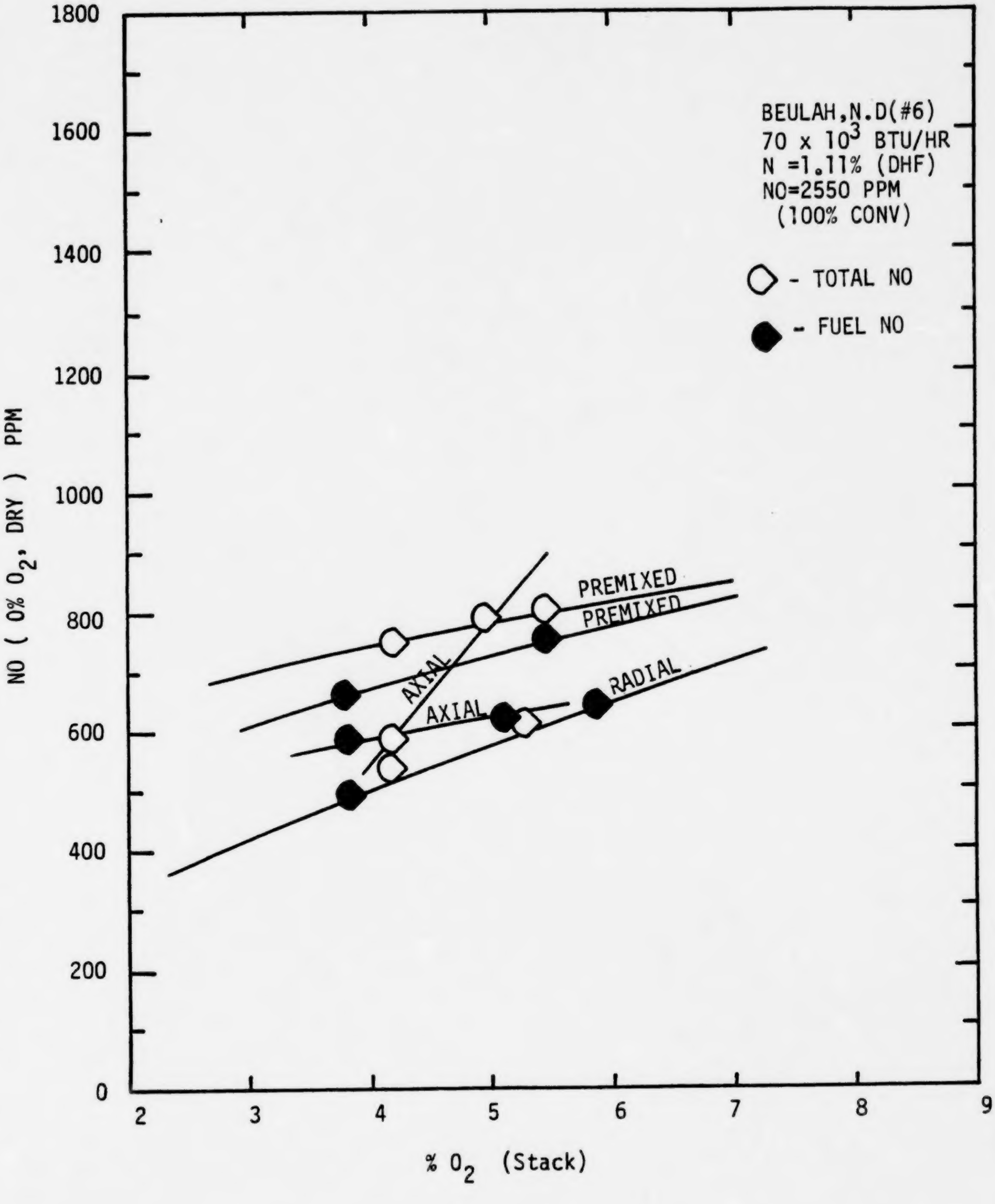
BEULAH,N.D(#6)
70 x 10^3 BTU/HR
N =1.11% (DHF)
NO=2550 PPM
(100% CONV)
○ - TOTAL NO
● - FUEL NO
PREMIXED
PREMIXED
AXIAL
AXIAL
RADIAL
1800
1600
1400
1200
1000
800
600
400
200
0
2
3
4
5
6
7
8
9
NO (0% O2, DRY) PPM
% O2 (Stack)

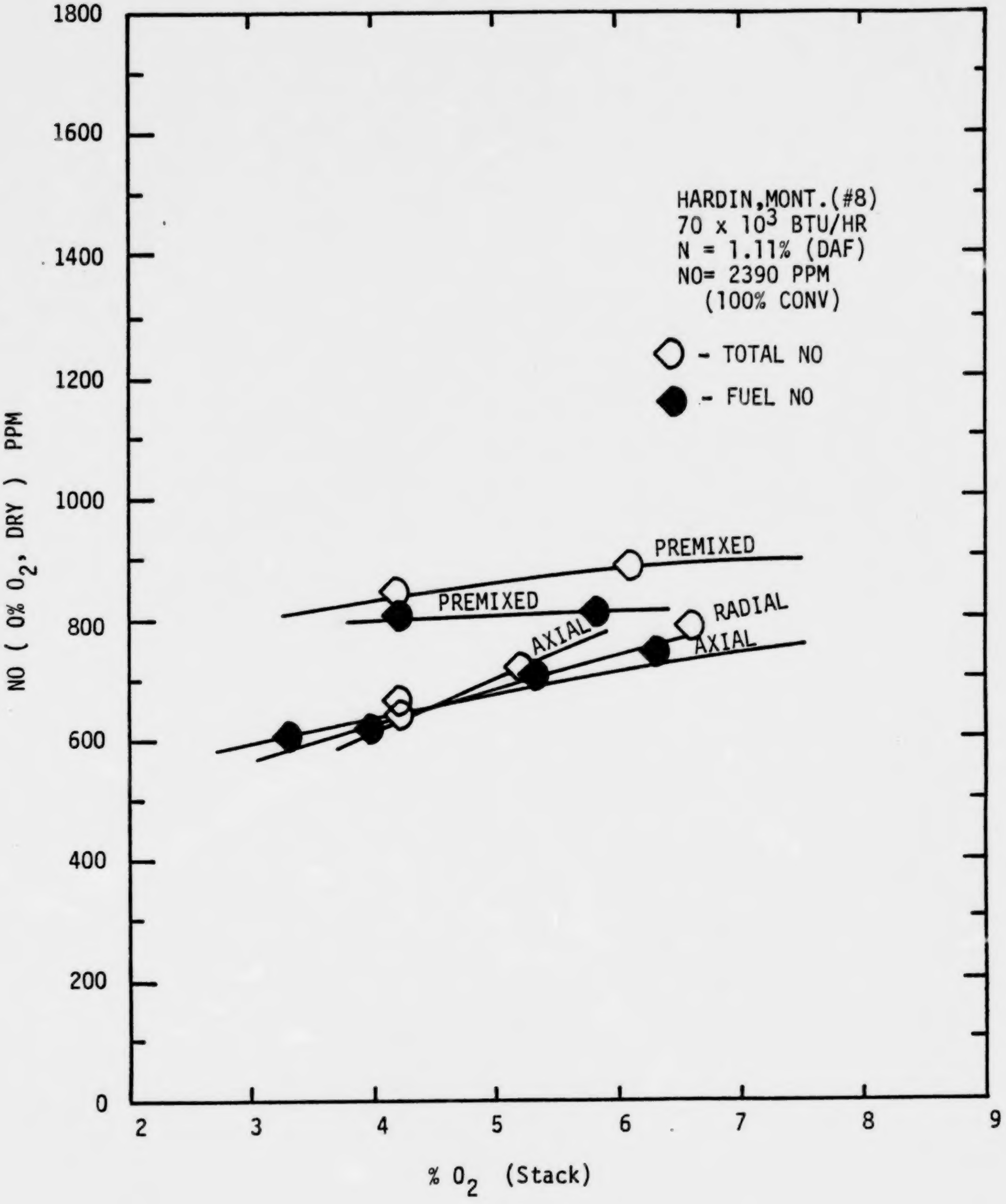
HARDIN,MONT.(#8)
70 x 10^3 BTU/HR
N = 1.11% (DAF)
NO= 2390 PPM
(100% CONV)
◇ - TOTAL NO
◆ - FUEL NO
PREMIXED
PREMIXED
RADIAL
AXIAL
AXIAL
NO (0% O_2, DRY) PPM
% O_2 (Stack)
0
200
400
600
800
1000
1200
1400
1600
1800
2
3
4
5
6
7
8
9

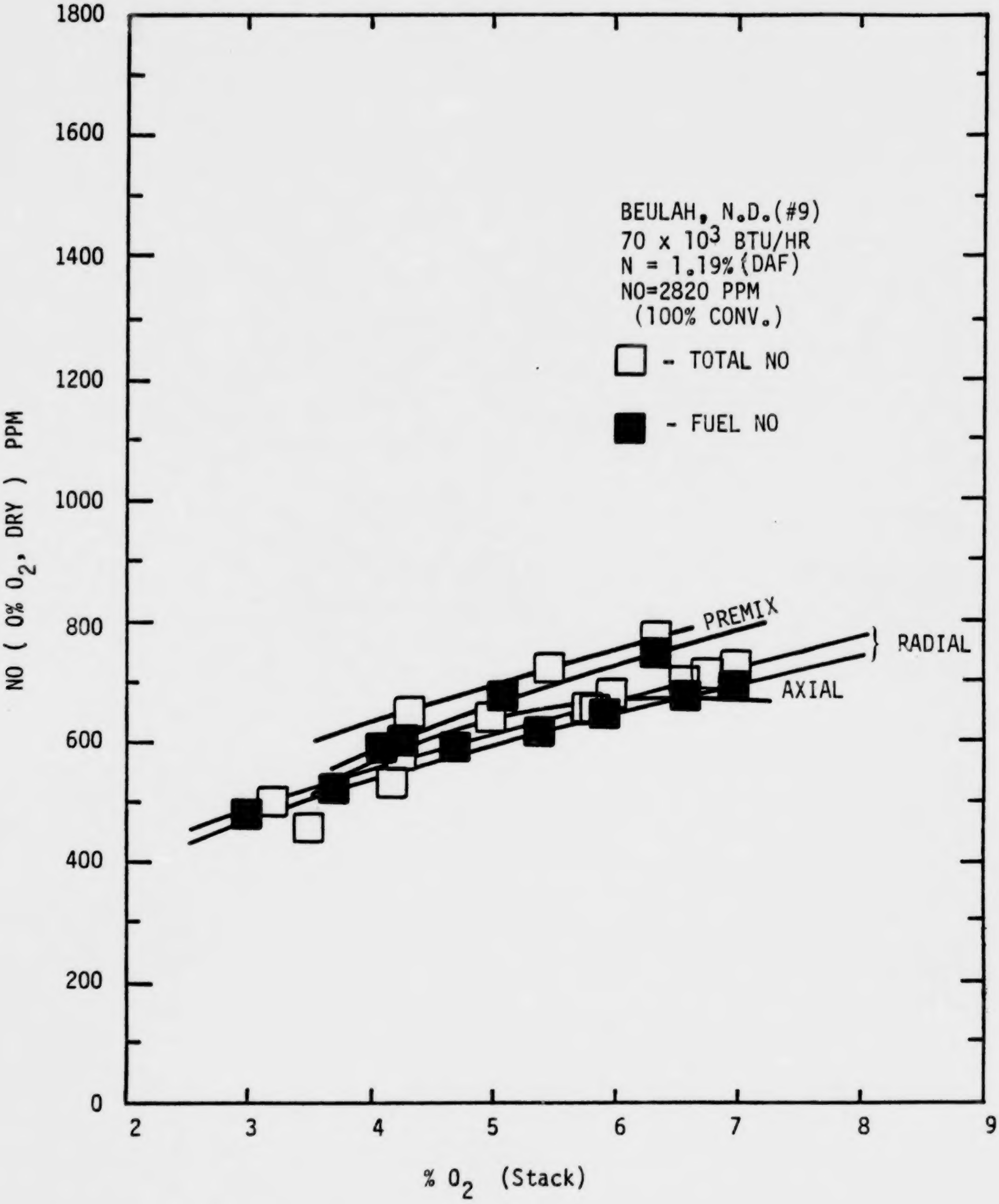
1800
1600
1400
1200
1000
800
600
400
200
0
2
3
4
5
6
7
8
9
NO (0% O_2, DRY) PPM
% O_2 (Stack)
BEULAH, N.D.(#9)
70 x 10^3 BTU/HR
N = 1.19% (DAF)
NO=2820 PPM
(100% CONV.)
□ - TOTAL NO
■ - FUEL NO
PREMIX
RADIAL
AXIAL

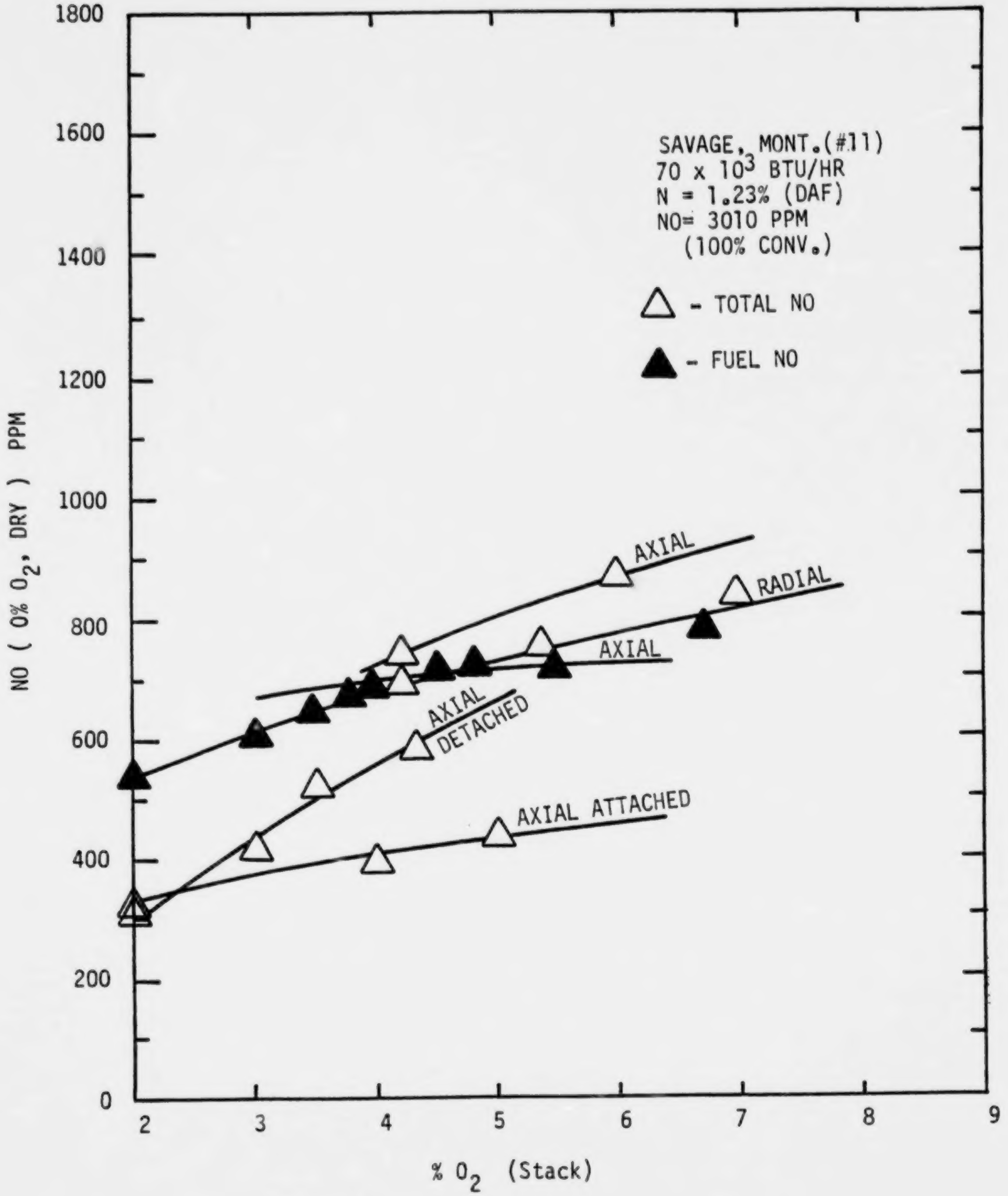

SAVAGE, MONT.(#11)
70 x 10³ BTU/HR
N = 1.23% (DAF)
NO= 3010 PPM
(100% CONV.)
△ - TOTAL NO
▲ - FUEL NO
AXIAL
RADIAL
AXIAL
AXIAL DETACHED
AXIAL ATTACHED
NO (0% O2, DRY) PPM
% O2 (Stack)
0
200
400
600
800
1000
1200
1400
1600
1800
2
3
4
5
6
7
8
9

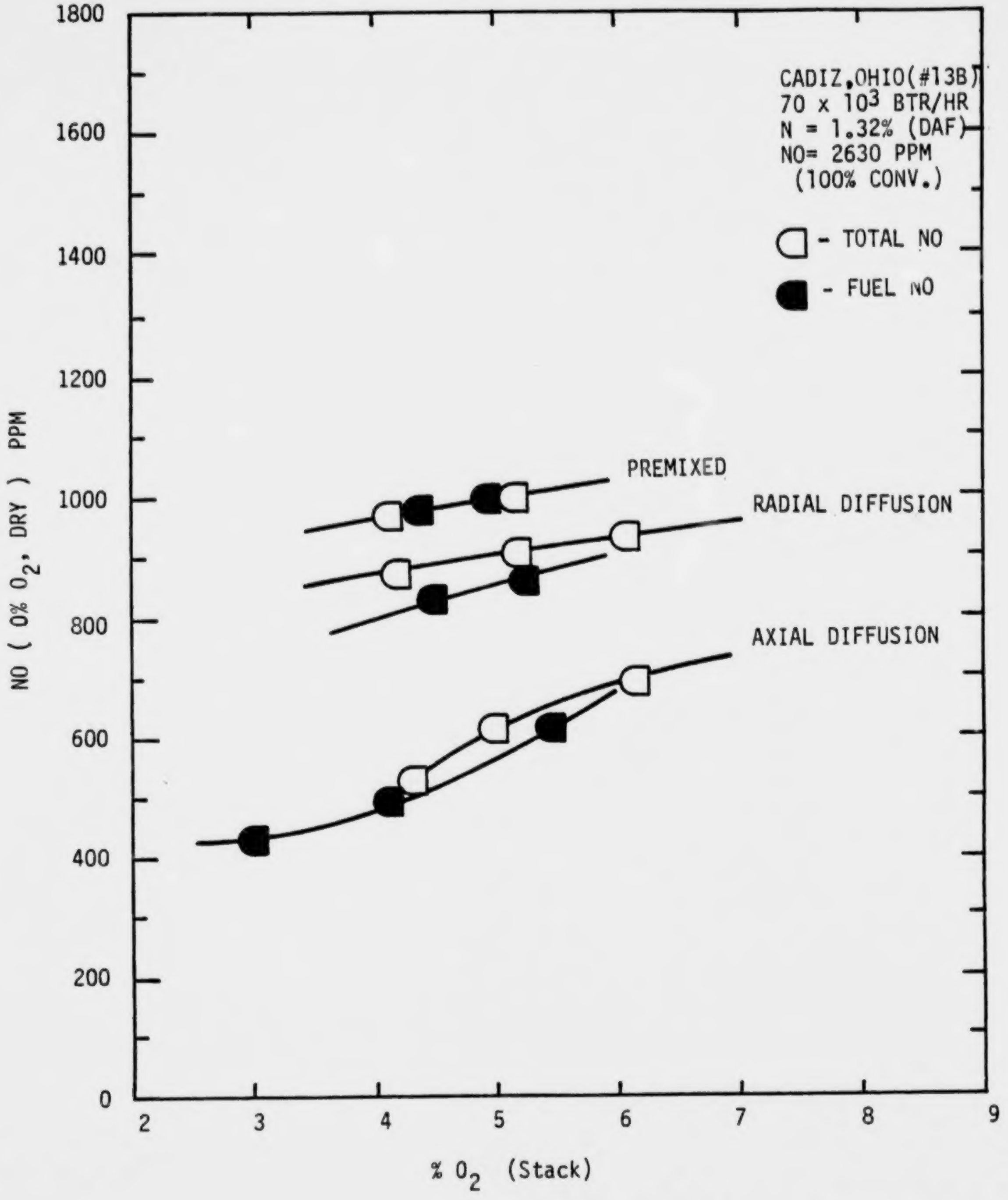

1800
1600
1400
1200
1000
800
600
400
200
0
NO (0% O_2, DRY) PPM
2
3
4
5
6
7
8
9
% O_2 (Stack)
CADIZ,OHIO(#13B)
70 x 10^3 BTR/HR
N = 1.32% (DAF)
NO= 2630 PPM
(100% CONV.)
- TOTAL NO
- FUEL NO
PREMIXED
RADIAL DIFFUSION
AXIAL DIFFUSION

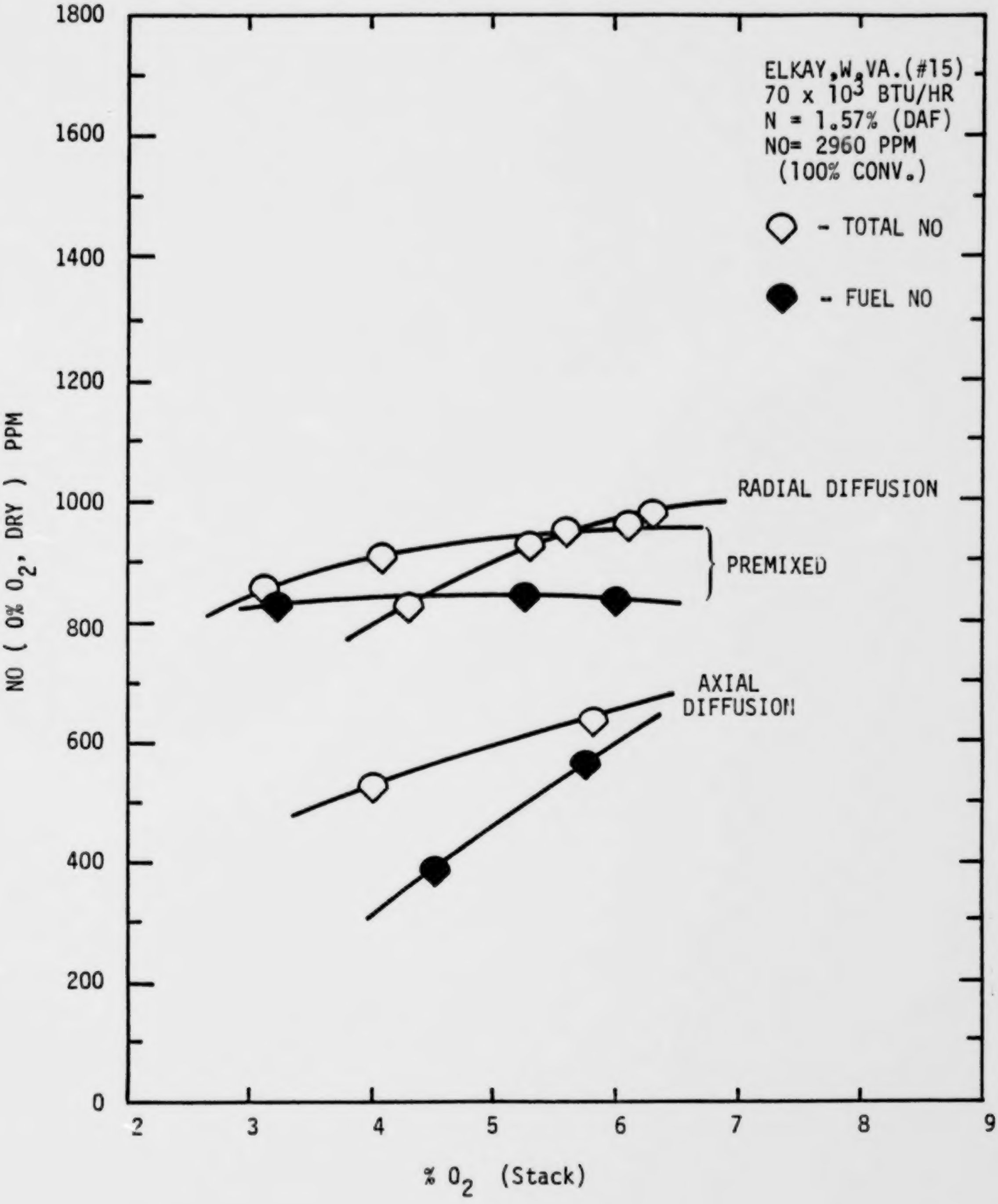ELKAY,W.VA.(#15)
70 x 10^3 BTU/HR
N = 1.57% (DAF)
NO= 2960 PPM
(100% CONV.)
○ - TOTAL NO
● - FUEL NO
RADIAL DIFFUSION
PREMIXED
AXIAL DIFFUSION
NO (0% O_2, DRY) PPM
% O_2 (Stack)
0
200
400
600
800
1000
1200
1400
1600
1800
2
3
4
5
6
7
8
9

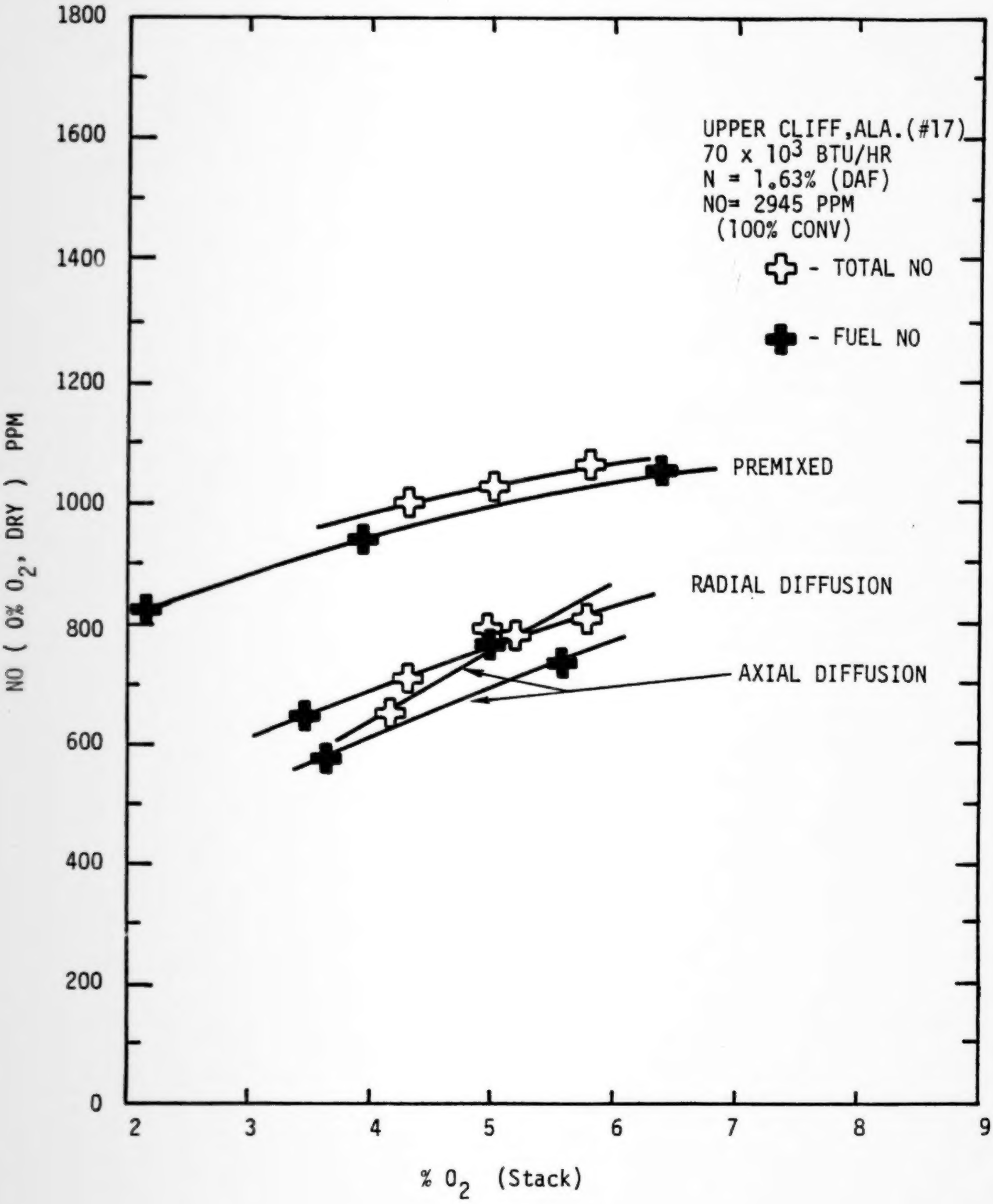
UPPER CLIFF,ALA.(#17)
70 x 10^3 BTU/HR
N = 1.63% (DAF)
NO= 2945 PPM
(100% CONV)
✛ - TOTAL NO
✚ - FUEL NO
PREMIXED
RADIAL DIFFUSION
AXIAL DIFFUSION
NO (0% O_2, DRY) PPM
1800
1600
1400
1200
1000
800
600
400
200
0
2
3
4
5
6
7
8
9
% O_2 (Stack)

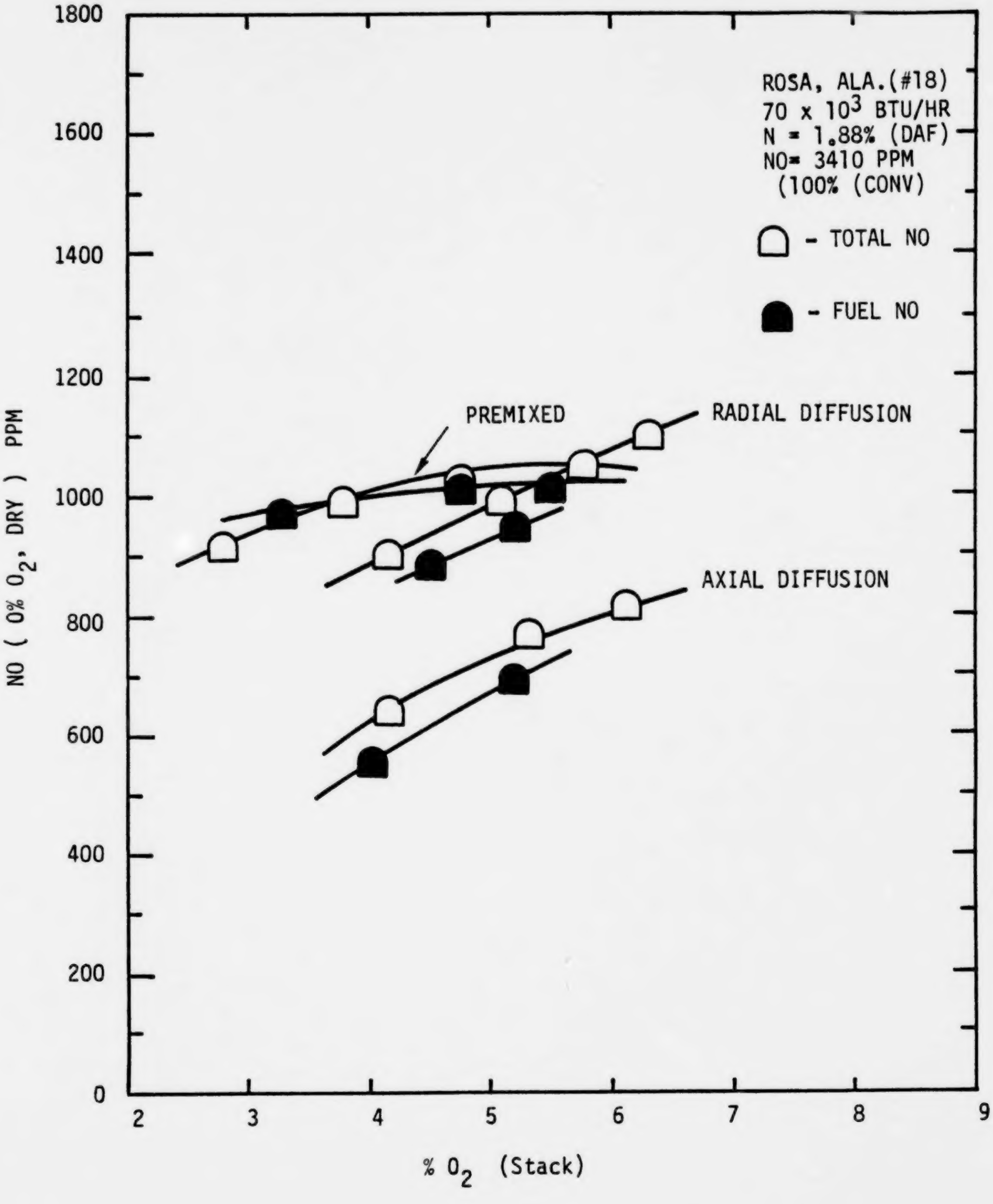

1800
1600
1400
1200
1000
800
600
400
200
0
NO (0% O_2, DRY) PPM
2
3
4
5
6
7
8
9
% O_2 (Stack)
ROSA, ALA.(#18)
70 x 10^3 BTU/HR
N = 1.88% (DAF)
NO= 3410 PPM
(100% (CONV)
○ - TOTAL NO
● - FUEL NO
PREMIXED
RADIAL DIFFUSION
AXIAL DIFFUSION

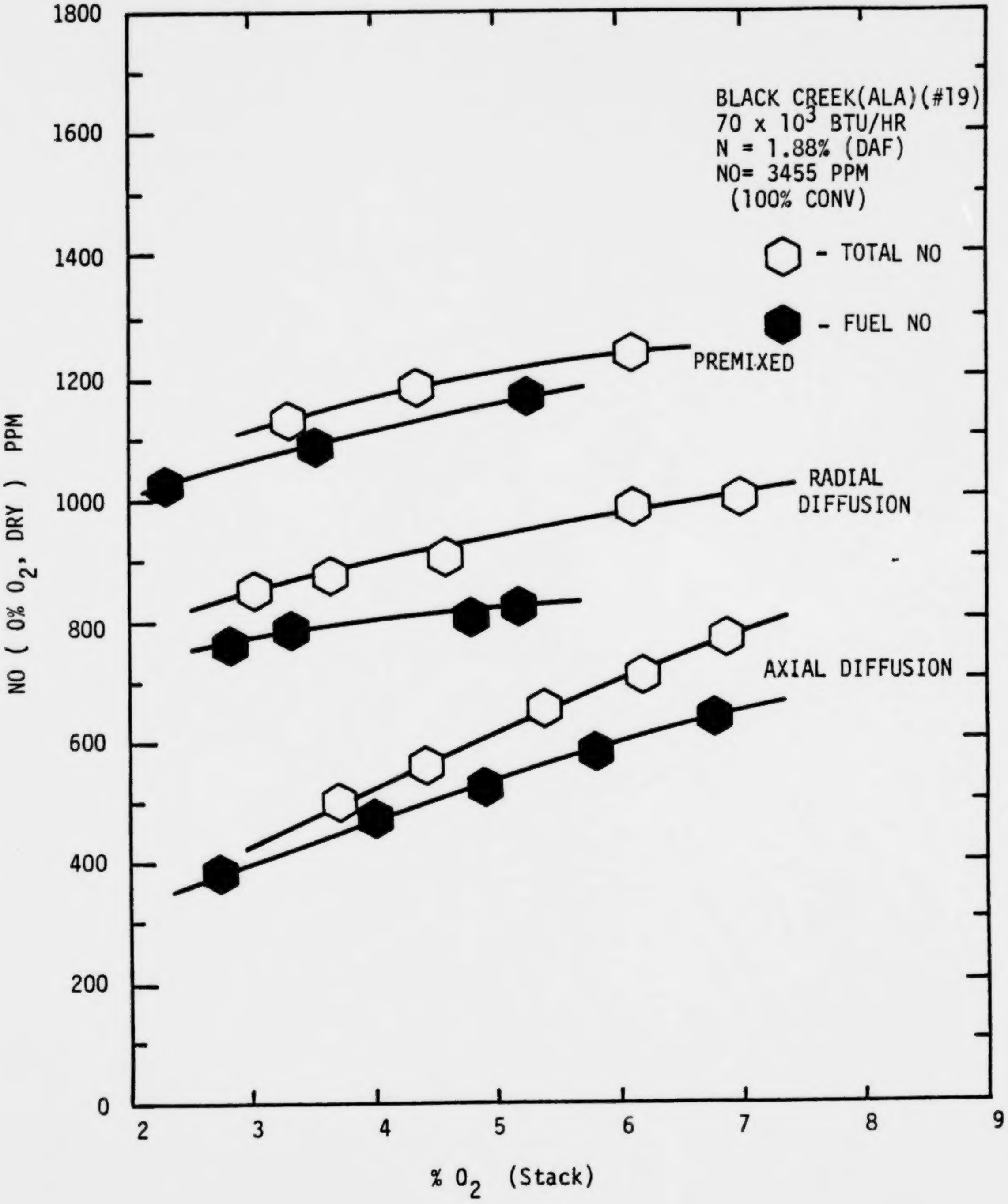
BLACK CREEK(ALA)(#19)
70 x 10³ BTU/HR
N = 1.88% (DAF)
NO= 3455 PPM
(100% CONV)
⬡ - TOTAL NO
⬢ - FUEL NO
PREMIXED
RADIAL DIFFUSION
AXIAL DIFFUSION
NO (0% O2, DRY) PPM
% O2 (Stack)
0
200
400
600
800
1000
1200
1400
1600
1800
2
3
4
5
6
7
8
9

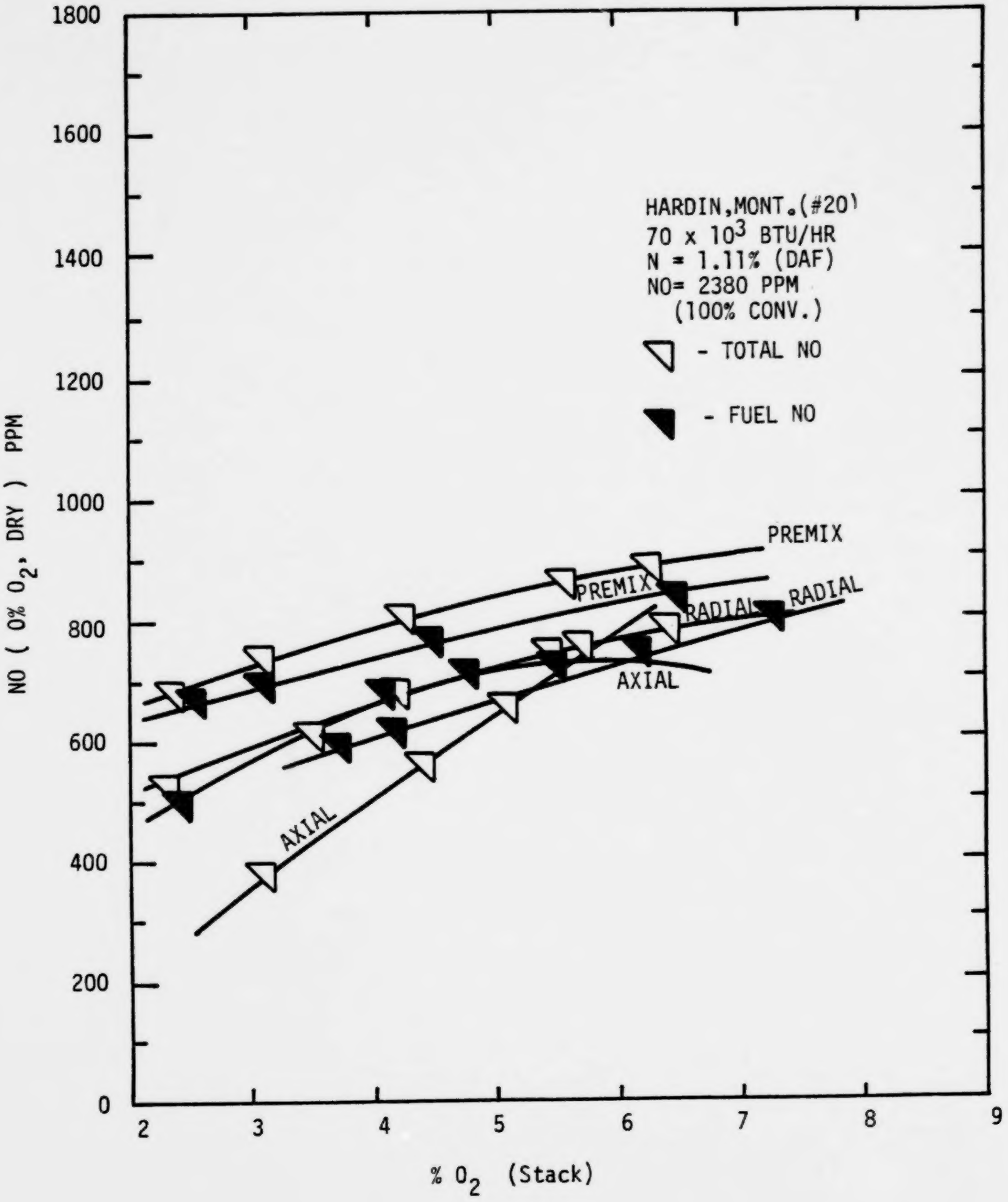
HARDIN,MONT.(#20)
70 x 10^3 BTU/HR
N = 1.11% (DAF)
NO= 2380 PPM
(100% CONV.)
▽ - TOTAL NO
▼ - FUEL NO
PREMIX
PREMIX
RADIAL
RADIAL
AXIAL
AXIAL
NO (0% O2, DRY) PPM
% O2 (Stack)
0
200
400
600
800
1000
1200
1400
1600
1800
2
3
4
5
6
7
8
9

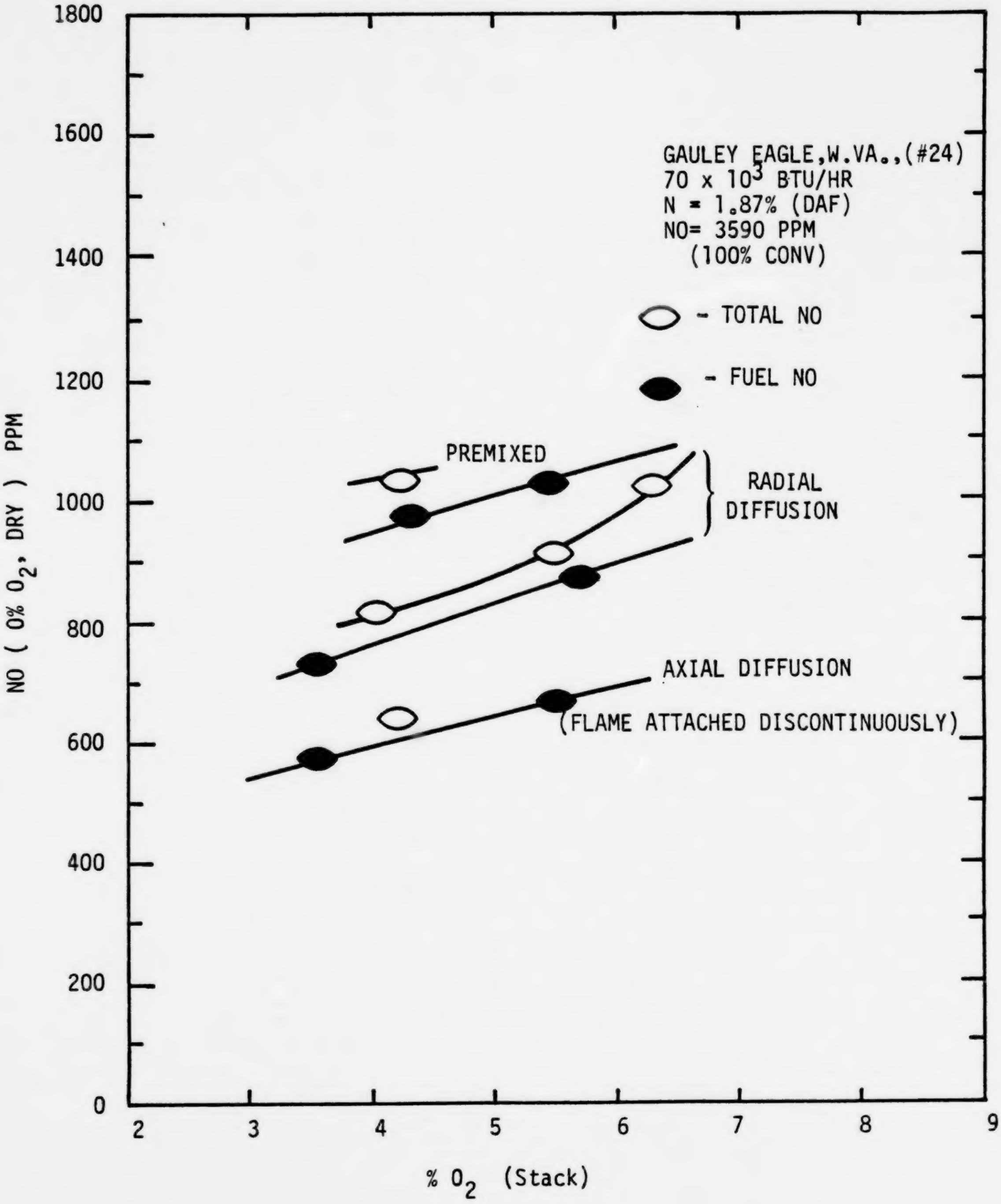
1800
1600
1400
1200
1000
800
600
400
200
0
2
3
4
5
6
7
8
9
NO (0% O_2, DRY) PPM
% O_2 (Stack)
GAULEY EAGLE, W.VA., (#24)
70 x 10^3 BTU/HR
N = 1.87% (DAF)
NO= 3590 PPM
(100% CONV)
○ - TOTAL NO
● - FUEL NO
PREMIXED
RADIAL
DIFFUSION
AXIAL DIFFUSION
(FLAME ATTACHED DISCONTINUOUSLY)

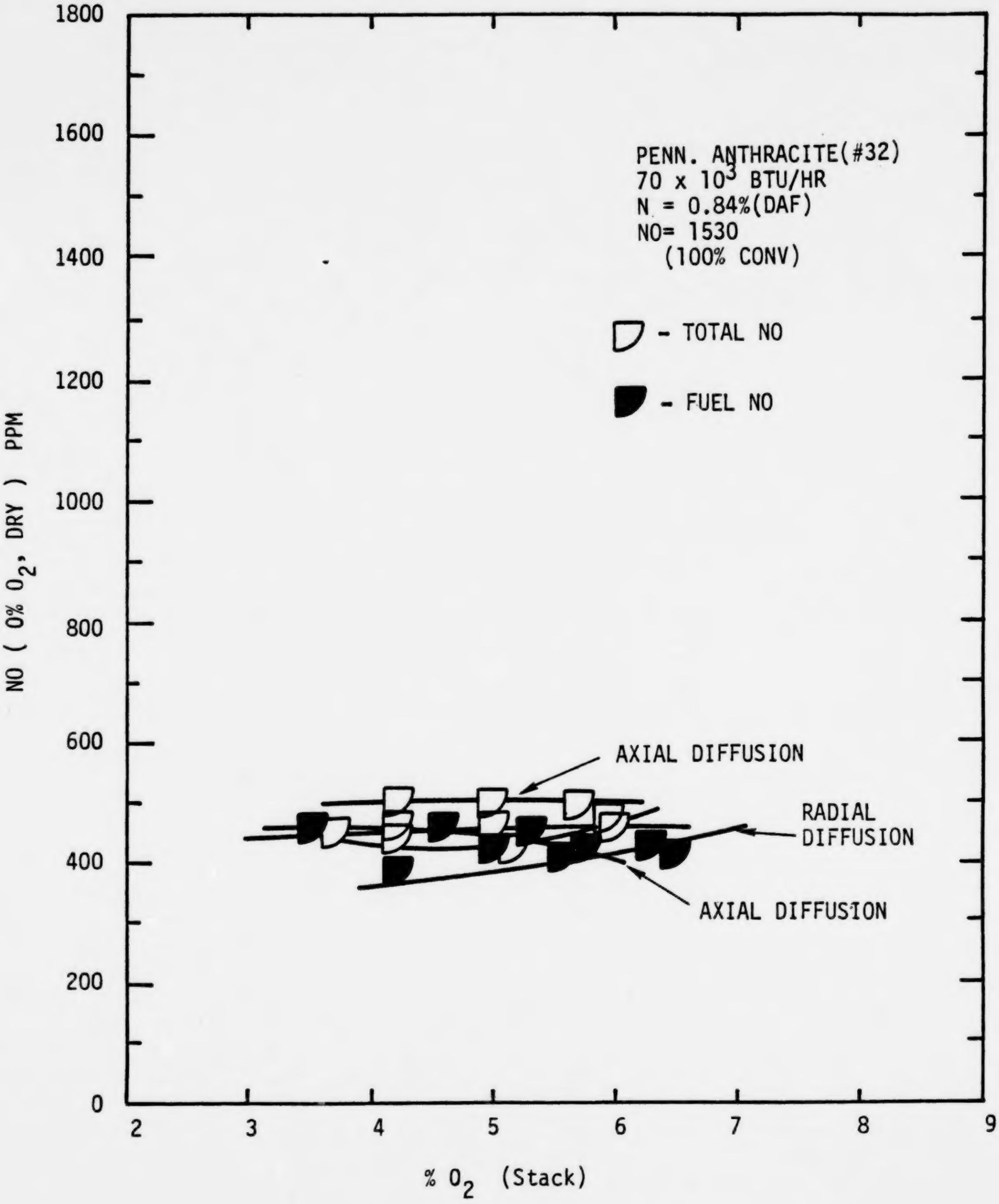
1800
1600
1400
1200
1000
800
600
400
200
0
NO (0% O_2, DRY) PPM
2
3
4
5
6
7
8
9
% O_2 (Stack)
PENN. ANTHRACITE(#32)
70 x 10^3 BTU/HR
N = 0.84%(DAF)
NO= 1530
(100% CONV)
- TOTAL NO
- FUEL NO
AXIAL DIFFUSION
RADIAL DIFFUSION
AXIAL DIFFUSION

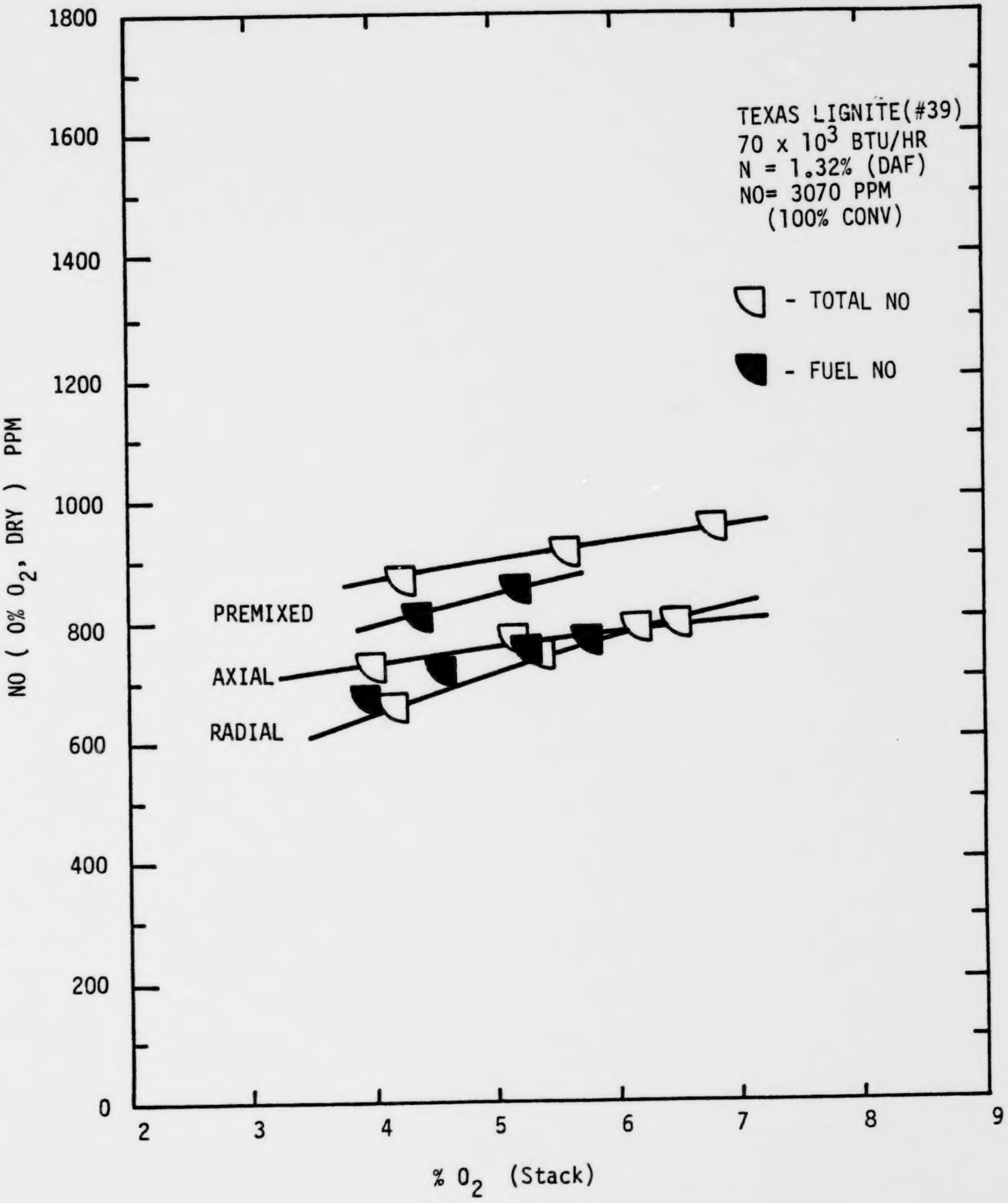
TEXAS LIGNITE(#39)
70 x 10^3 BTU/HR
N = 1.32% (DAF)
NO= 3070 PPM
(100% CONV)
◻ - TOTAL NO
◼ - FUEL NO
PREMIXED
AXIAL
RADIAL
NO (0% O2, DRY) PPM
% O2 (Stack)
0
200
400
600
800
1000
1200
1400
1600
1800
2
3
4
5
6
7
8
9

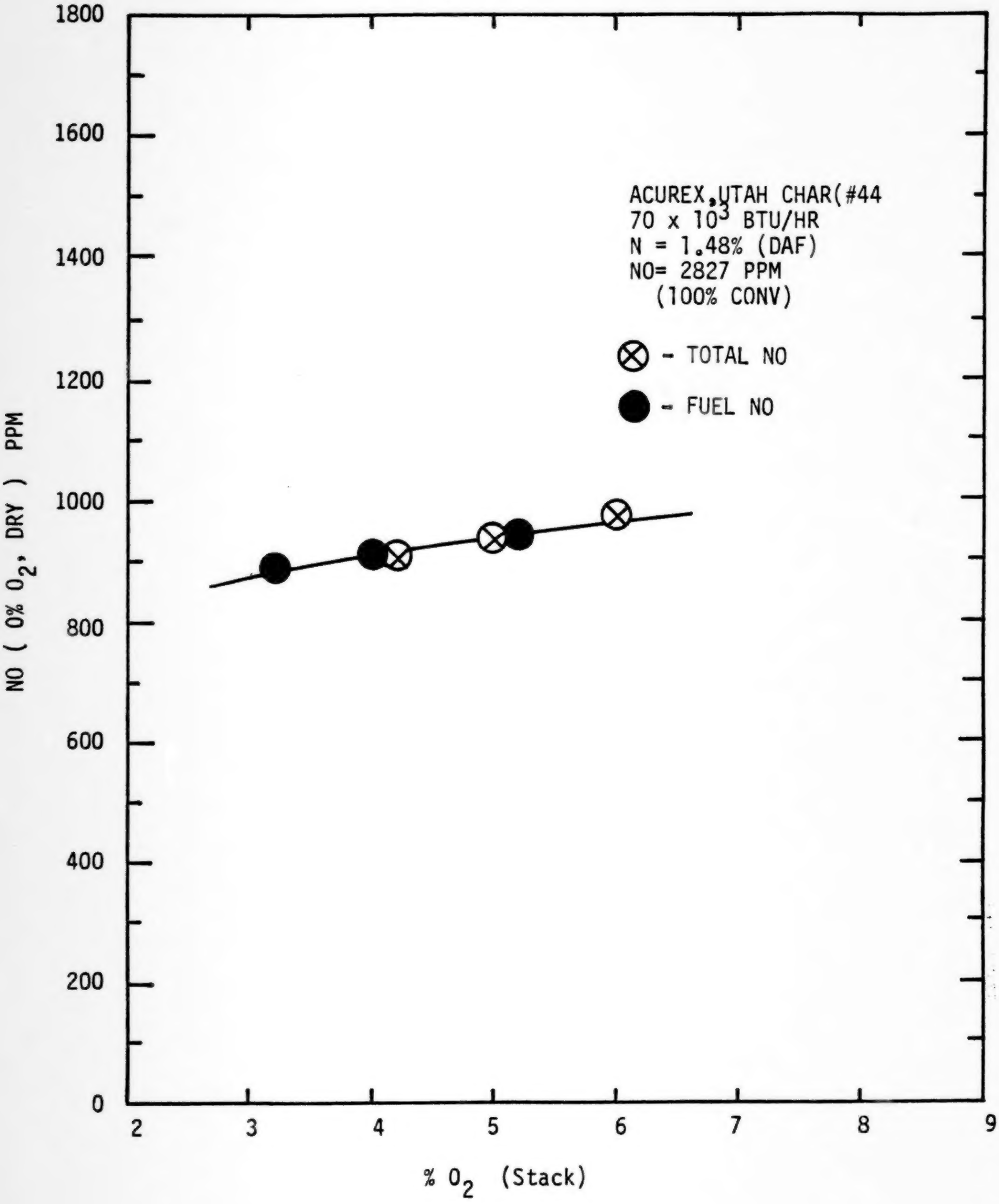

1800
1600
1400
1200
1000
800
600
400
200
0
2
3
4
5
6
7
8
9
NO (0% O_2, DRY) PPM
% O_2 (Stack)
ACUREX,UTAH CHAR(#44
70 x 10^3 BTU/HR
N = 1.48% (DAF)
NO= 2827 PPM
(100% CONV)
⊗ - TOTAL NO
● - FUEL NO

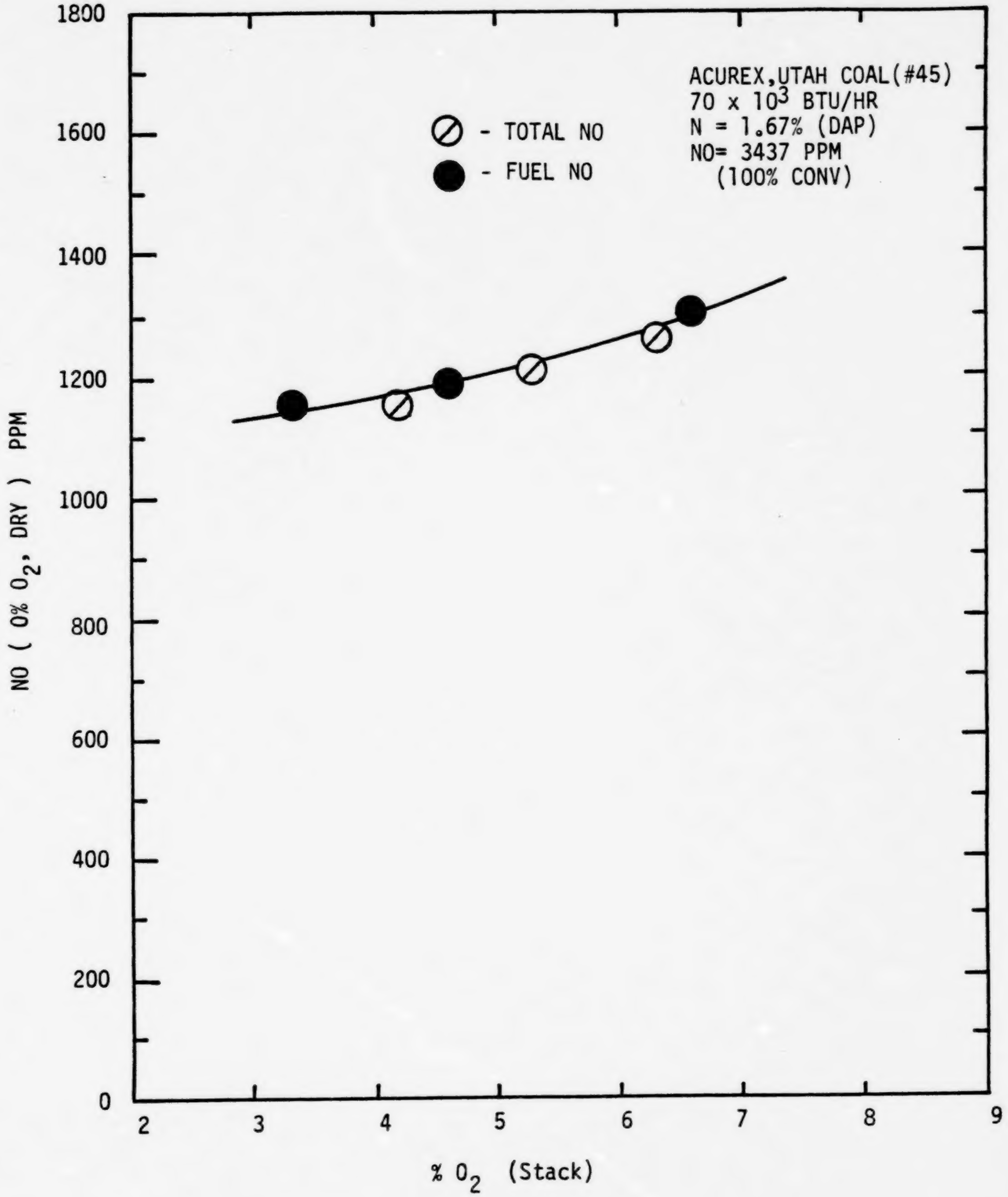ACUREX,UTAH COAL(#45)
70 x 10³ BTU/HR
N = 1.67% (DAP)
NO= 3437 PPM
(100% CONV)
⊘ - TOTAL NO
● - FUEL NO
NO (0% O2, DRY) PPM
% O2 (Stack)
0
200
400
600
800
1000
1200
1400
1600
1800
2
3
4
5
6
7
8
9

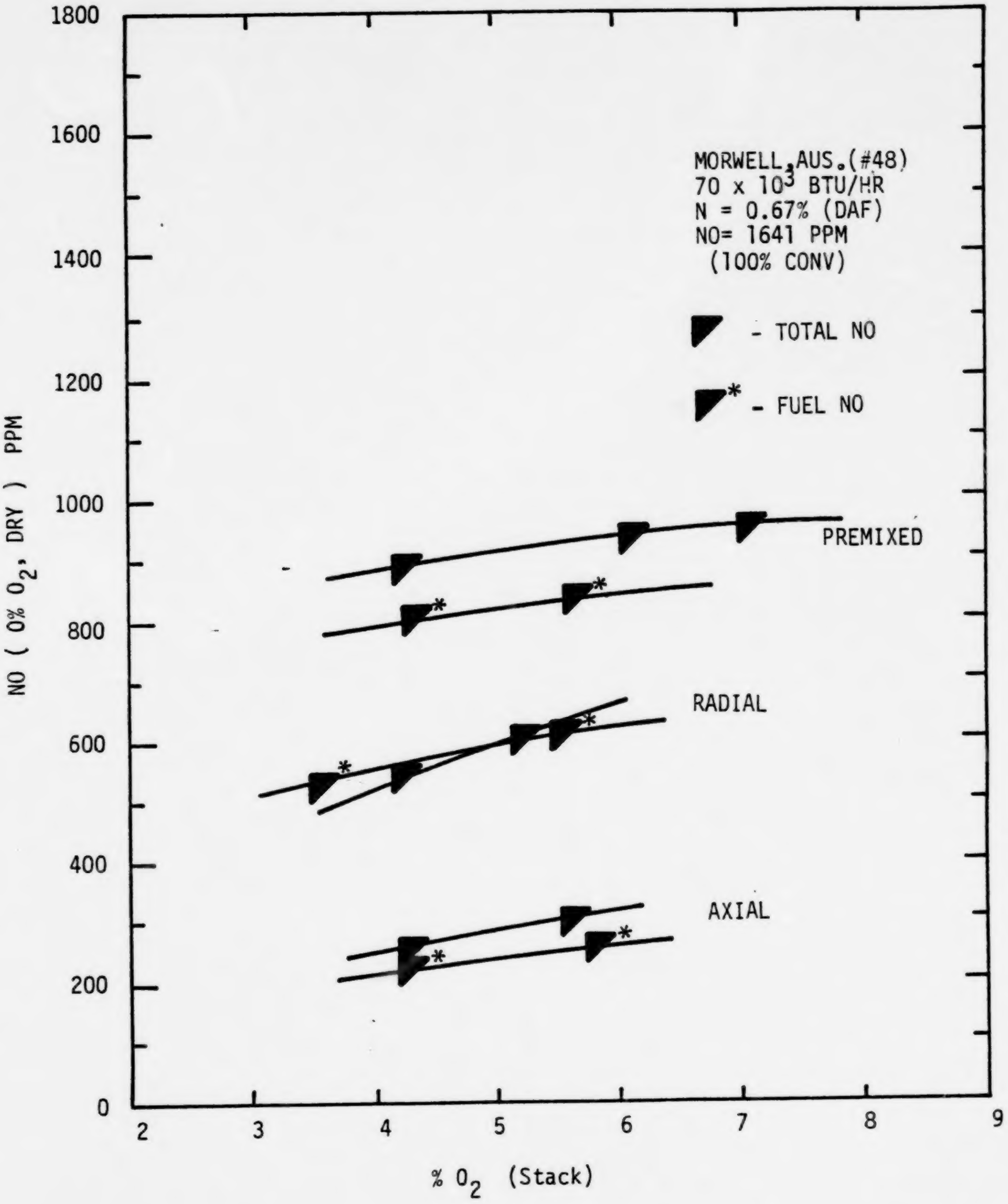
MORWELL, AUS. (#48)
70 x 10^3 BTU/HR
N = 0.67% (DAF)
NO= 1641 PPM
(100% CONV)
◤ - TOTAL NO
◤* - FUEL NO
PREMIXED
RADIAL
AXIAL
NO (0% O_2, DRY) PPM
% O_2 (Stack)
0
200
400
600
800
1000
1200
1400
1600
1800
2
3
4
5
6
7
8
9

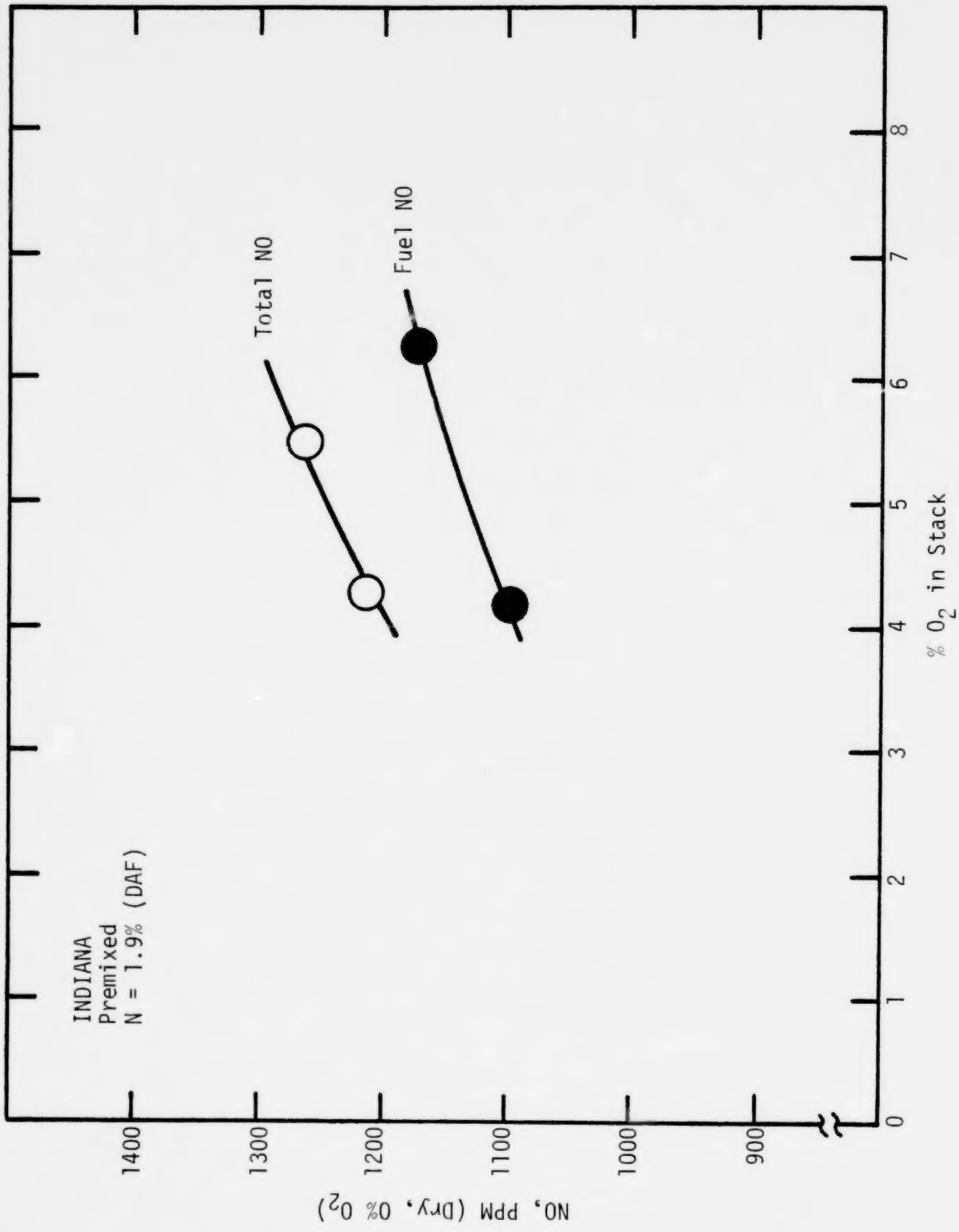
INDIANA
Premixed
N = 1.9% (DAF)
Total NO
Fuel NO
NO, PPM (Dry, 0% O_2)
1400
1300
1200
1100
1000
900
% O_2 in Stack
0
1
2
3
4
5
6
7
8

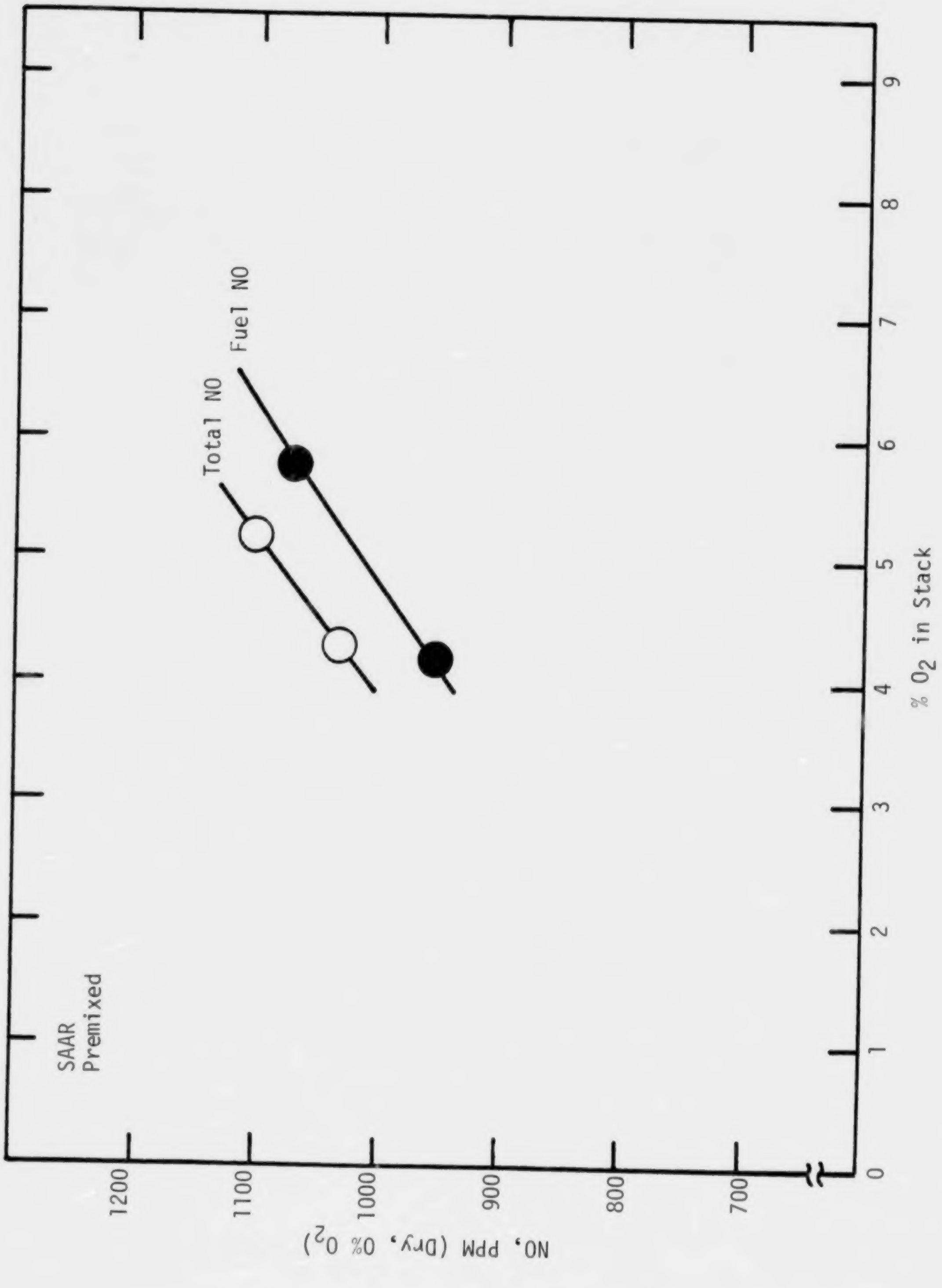
SAAR
Premixed
Total NO
Fuel NO
NO, PPM (Dry, 0% O2)
1200
1100
1000
900
800
700
0
1
2
3
4
5
6
7
8
9
% O2 in Stack

APPENDIX B

Summary of Bench-Scale Data

- Fuel NO as a Function of % CO_2 in the Oxidant

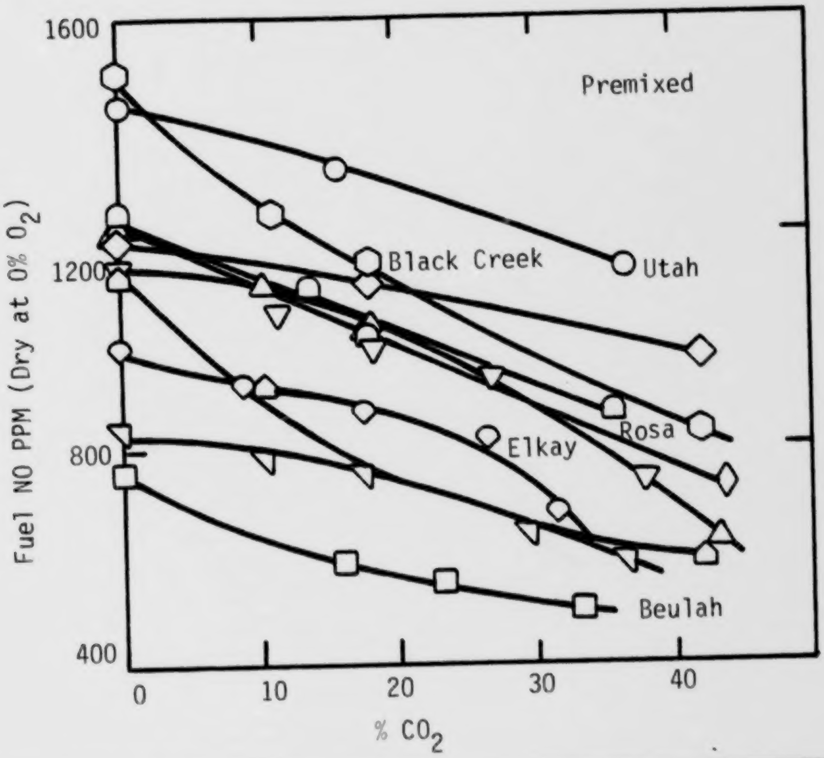
Premixed
Black Creek
Utah
Rosa
Elkay
Beulah
1600
1200
800
400
0
10
20
30
40
Fuel NO PPM (Dry at 0% O_2)
% CO_2

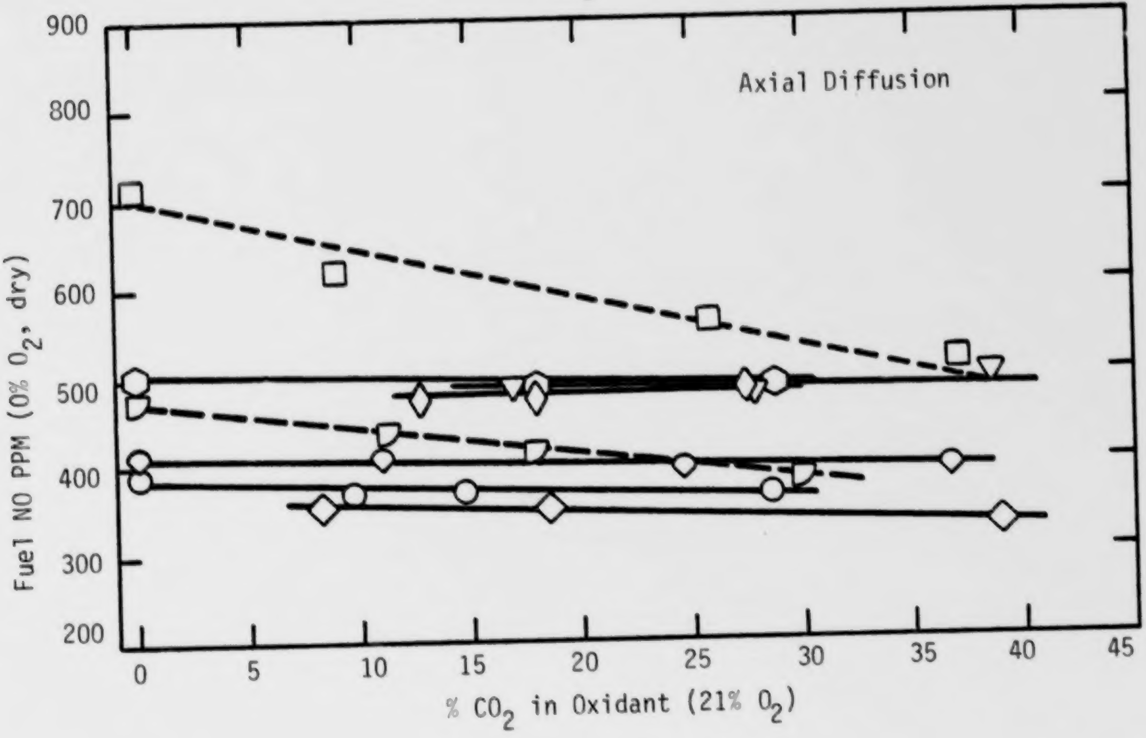
Axial Diffusion
900
800
700
600
500
400
300
200
0
5
10
15
20
25
30
35
40
45
Fuel NO PPM (0% O_2, dry)
% CO_2 in Oxidant (21% O_2)

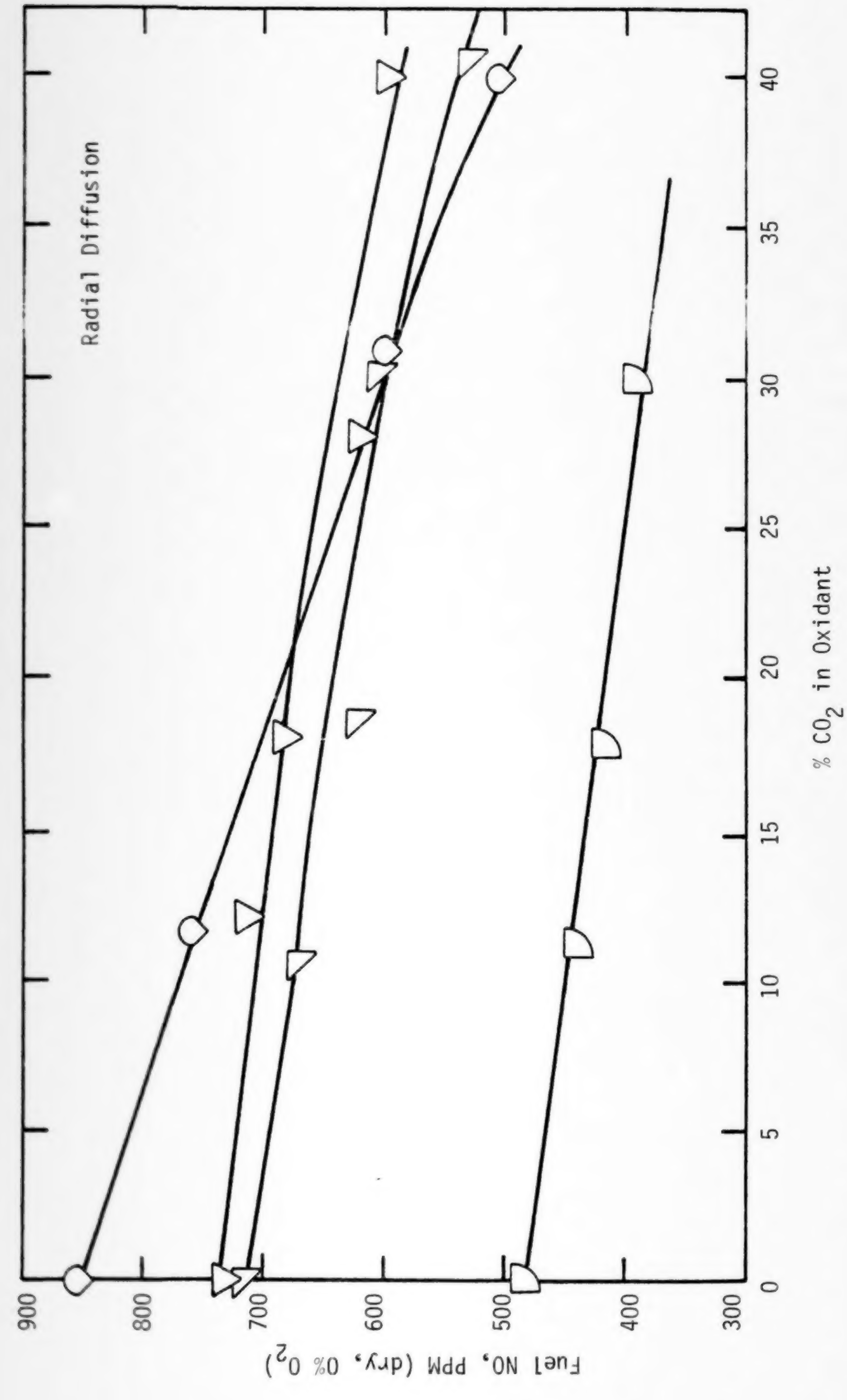
Radial Diffusion
Fuel NO, PPM (dry, 0% O$_2$)
900
800
700
600
500
400
300
% CO$_2$ in Oxidant
0
5
10
15
20
25
30
35
40

APPENDIX C

Summary of Bench-Scale Data

(NO Produced Under Two-Stage Conditions)

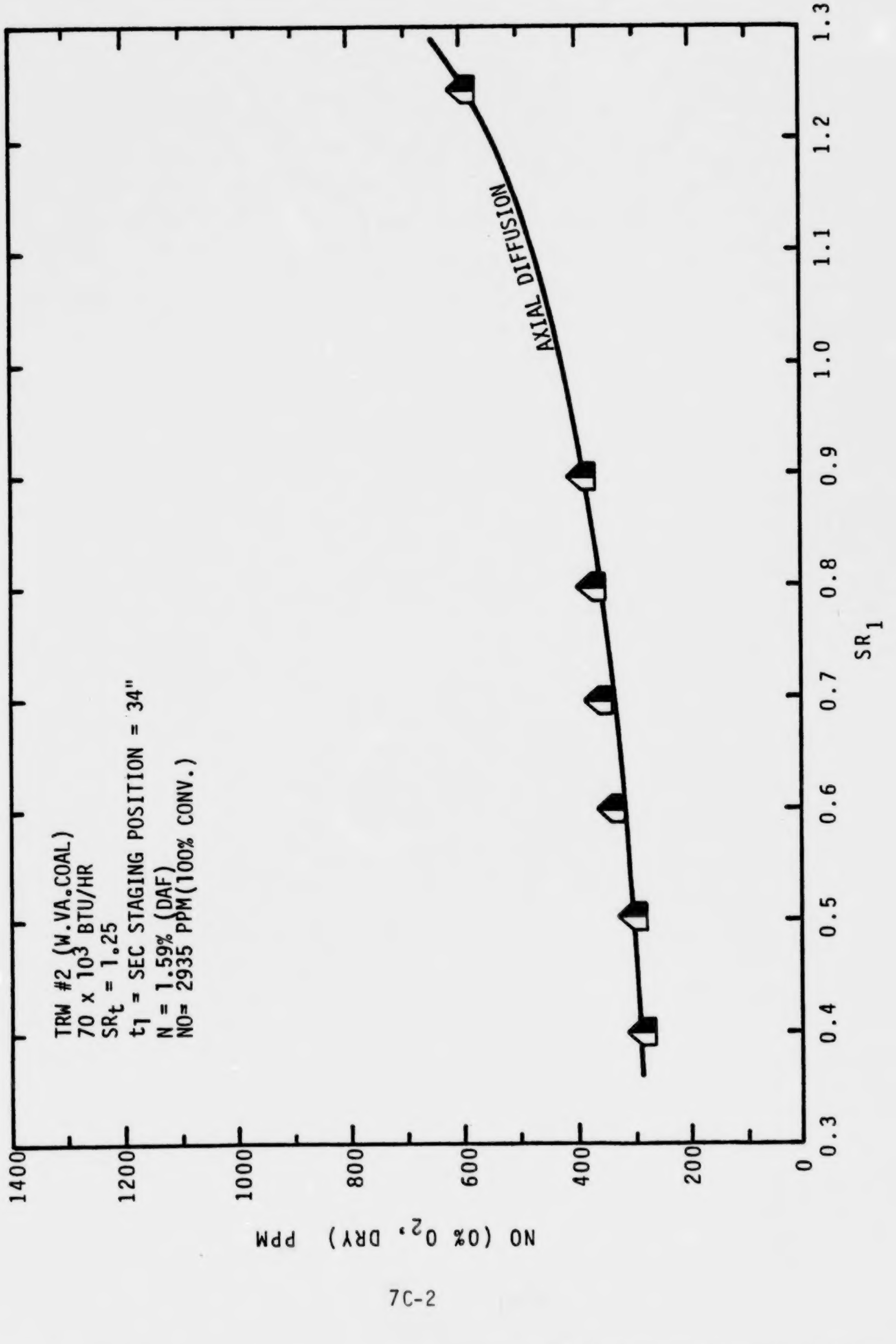
TRW #2 (W.VA.COAL)
70 x 10^3 BTU/HR
SR$_t$ = 1.25
t_1 = SEC STAGING POSITION = 34"
N = 1.59% (DAF)
NO= 2935 PPM(100% CONV.)
AXIAL DIFFUSION
NO (0% O$_2$, DRY) PPM
0
200
400
600
800
1000
1200
1400
SR$_1$
0.3
0.4
0.5
0.6
0.7
0.8
0.9
1.0
1.1
1.2
1.3

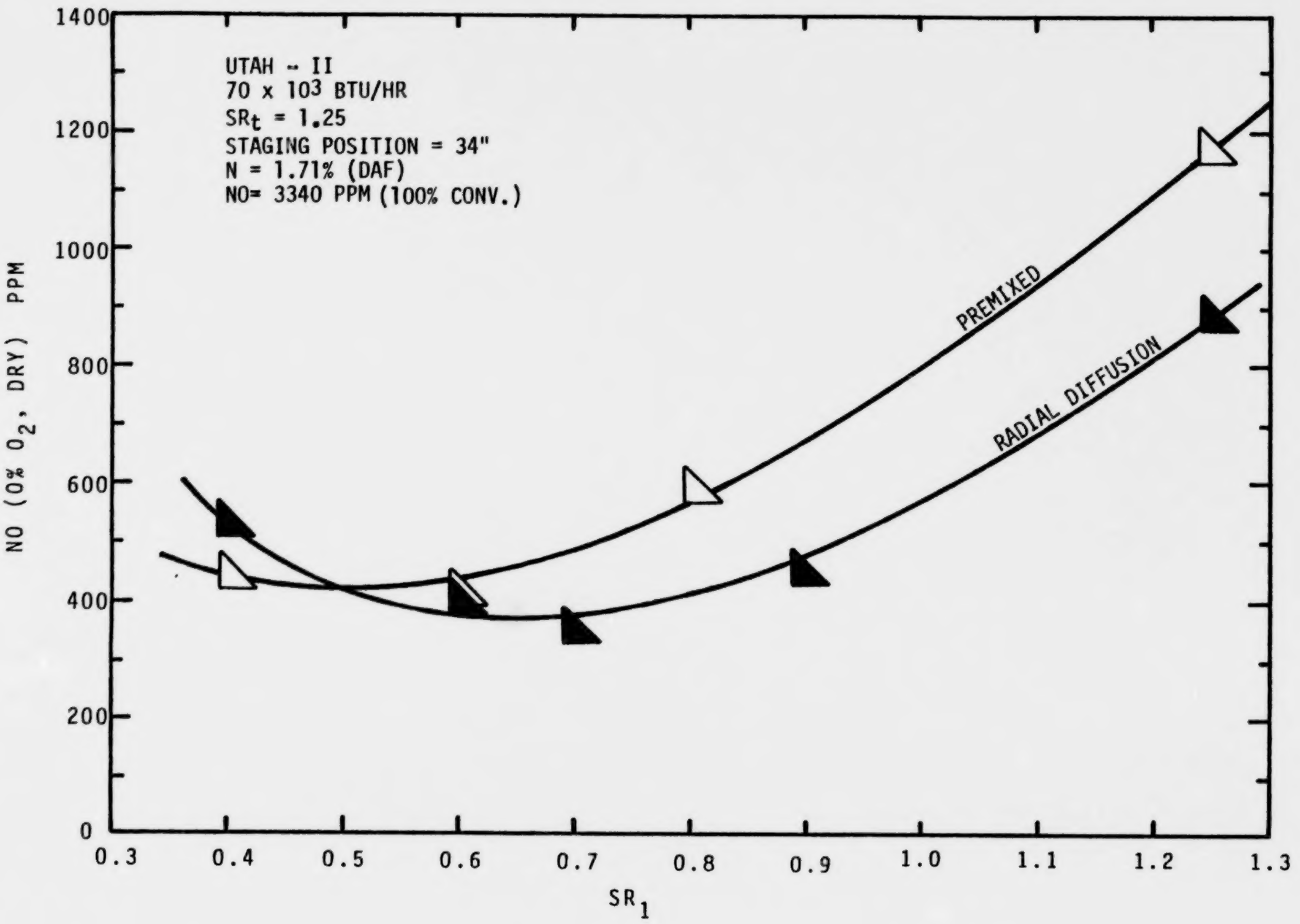
UTAH – II
70 x 10³ BTU/HR
SRt = 1.25
STAGING POSITION = 34"
N = 1.71% (DAF)
NO= 3340 PPM (100% CONV.)
PREMIXED
RADIAL DIFFUSION
NO (0% O2, DRY) PPM
1400
1200
1000
800
600
400
200
0
0.3
0.4
0.5
0.6
0.7
0.8
0.9
1.0
1.1
1.2
1.3
SR1

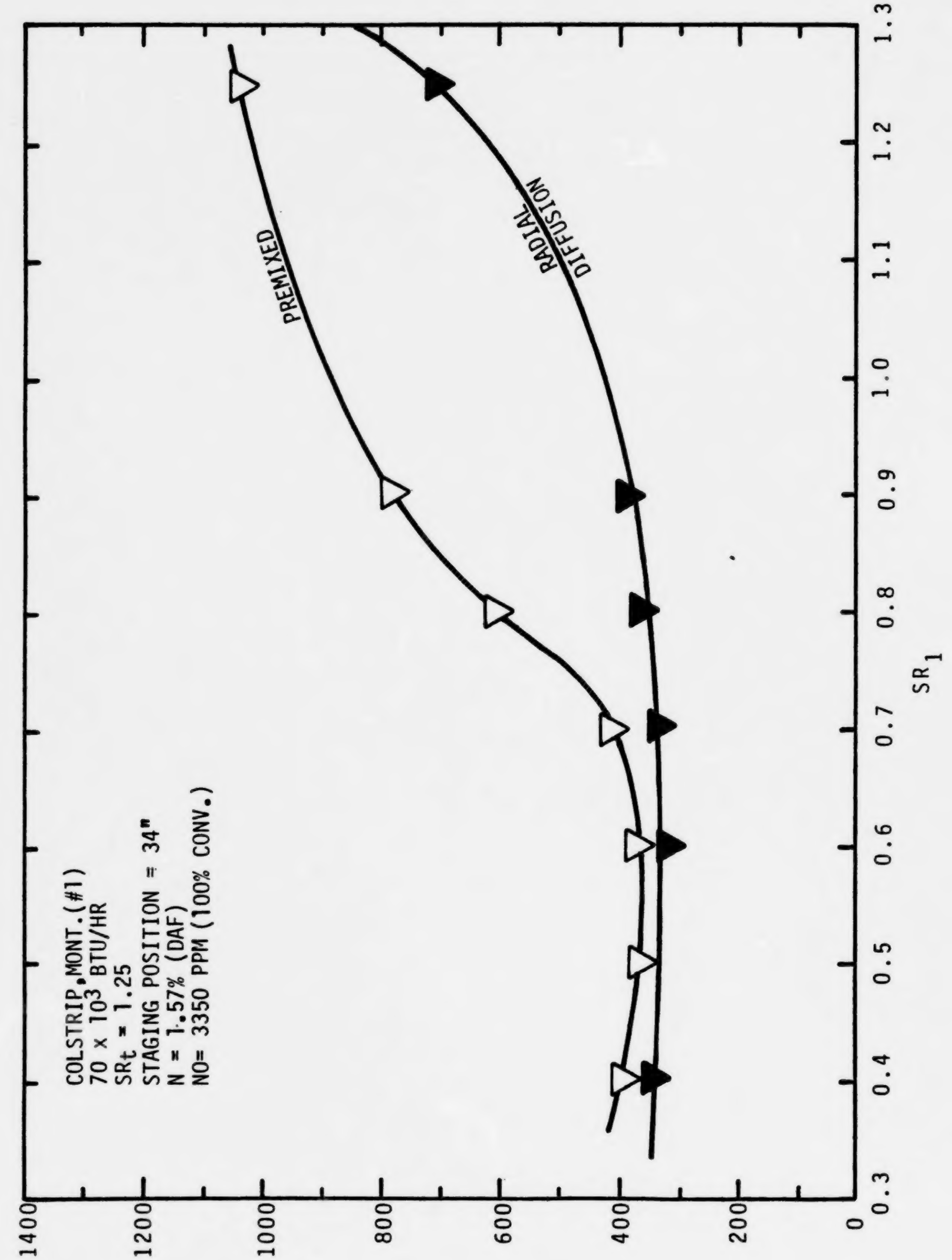
COLSTRIP, MONT. (#1)
70 x 10^3 BTU/HR
SRt = 1.25
STAGING POSITION = 34"
N = 1.57% (DAF)
NO= 3350 PPM (100% CONV.)
PREMIXED
RADIAL DIFFUSION
NO (0% O2, DRY) PPM
0
200
400
600
800
1000
1200
1400
SR1
0.3
0.4
0.5
0.6
0.7
0.8
0.9
1.0
1.1
1.2
1.3

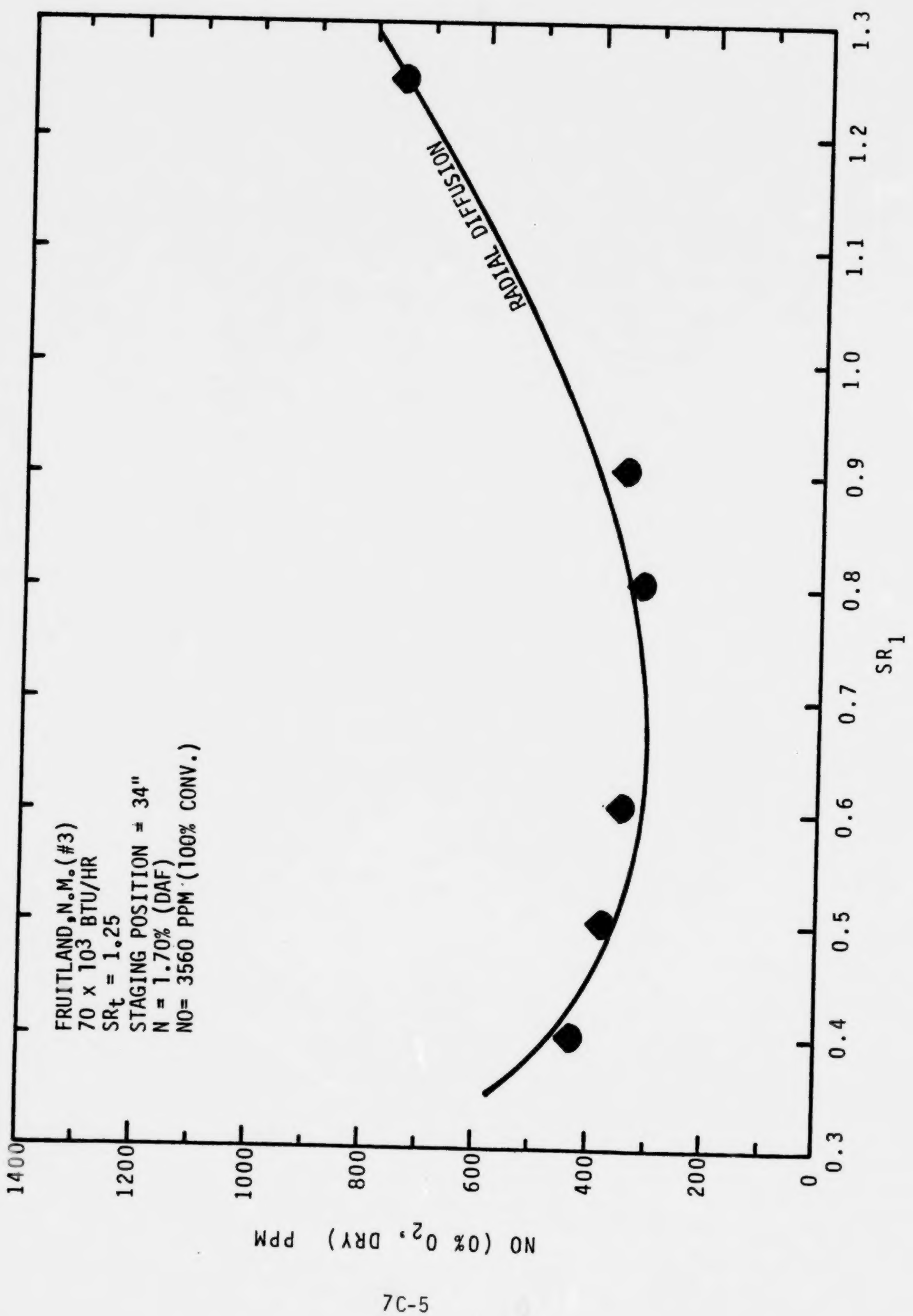
FRUITLAND, N.M. (#3)
70 x 10^3 BTU/HR
SR_t = 1.25
STAGING POSITION = 34"
N = 1.70% (DAF)
NO= 3560 PPM (100% CONV.)
RADIAL DIFFUSION
NO (0% O2, DRY) PPM
0
200
400
600
800
1000
1200
1400
SR1
0.3
0.4
0.5
0.6
0.7
0.8
0.9
1.0
1.1
1.2
1.3

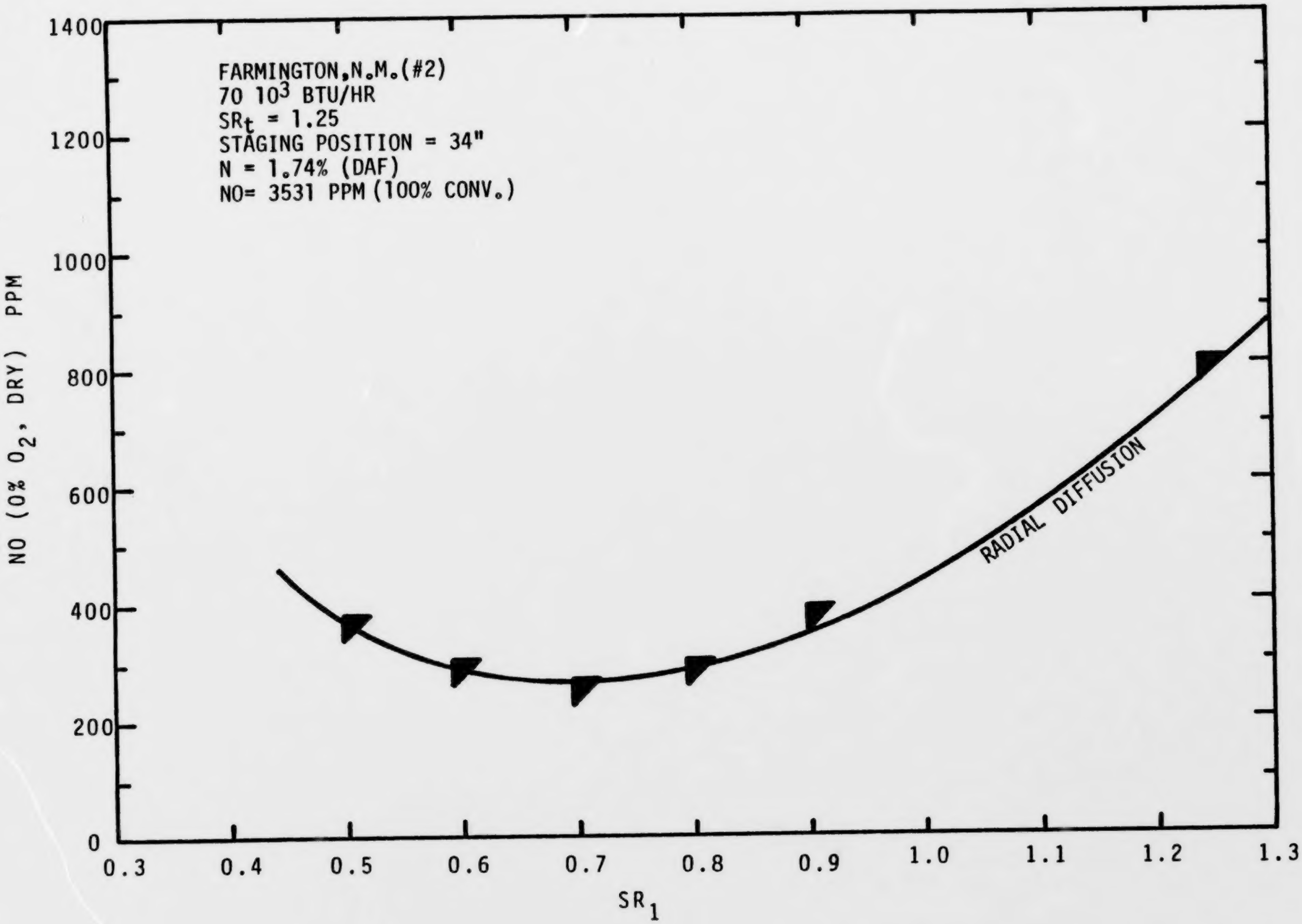
FARMINGTON,N.M.(#2)
70 10³ BTU/HR
SRt = 1.25
STAGING POSITION = 34"
N = 1.74% (DAF)
NO= 3531 PPM (100% CONV.)
RADIAL DIFFUSION
NO (0% O2, DRY) PPM
0
200
400
600
800
1000
1200
1400
SR1
0.3
0.4
0.5
0.6
0.7
0.8
0.9
1.0
1.1
1.2
1.3

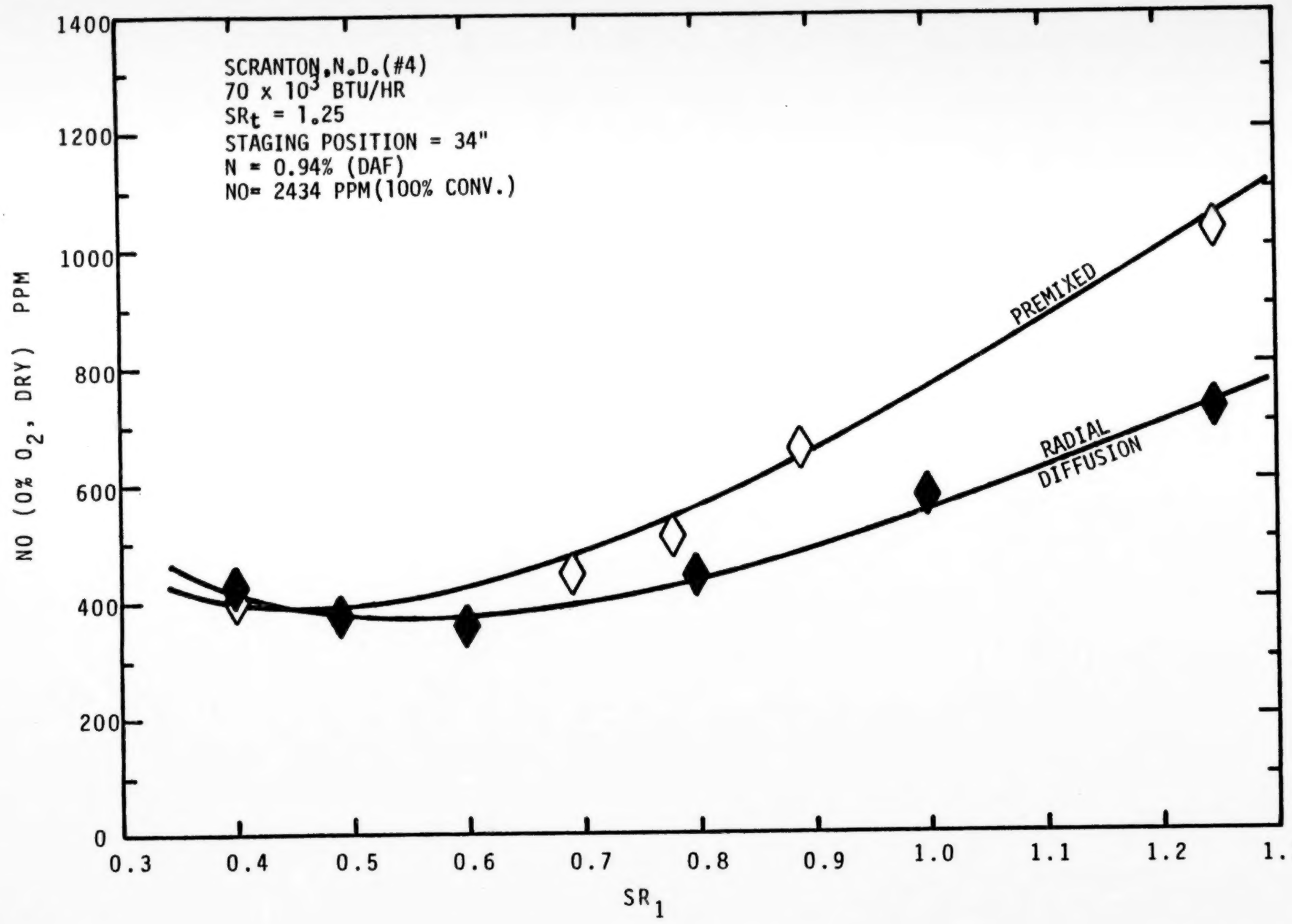
SCRANTON,N.D.(#4)
70 x 10³ BTU/HR
SRt = 1.25
STAGING POSITION = 34"
N = 0.94% (DAF)
NO= 2434 PPM(100% CONV.)
PREMIXED
RADIAL DIFFUSION
NO (0% O2, DRY) PPM
0
200
400
600
800
1000
1200
1400
SR1
0.3
0.4
0.5
0.6
0.7
0.8
0.9
1.0
1.1
1.2
1.3

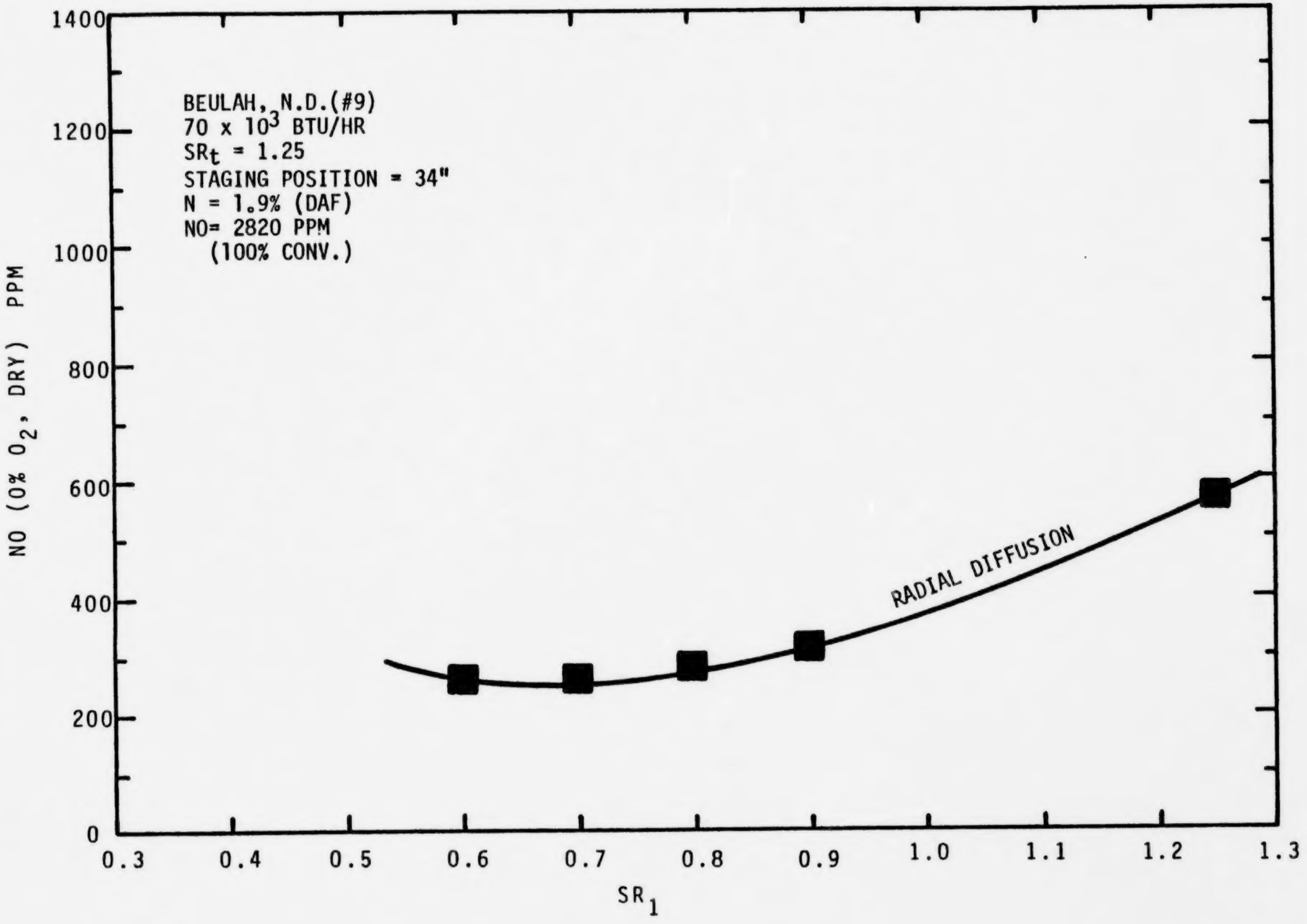
BEULAH, N.D.(#9)
70 x 10^3 BTU/HR
SR_t = 1.25
STAGING POSITION = 34"
N = 1.9% (DAF)
NO= 2820 PPM
(100% CONV.)
RADIAL DIFFUSION
NO (0% O_2, DRY) PPM
1400
1200
1000
800
600
400
200
0
0.3
0.4
0.5
0.6
0.7
0.8
0.9
1.0
1.1
1.2
1.3
SR_1

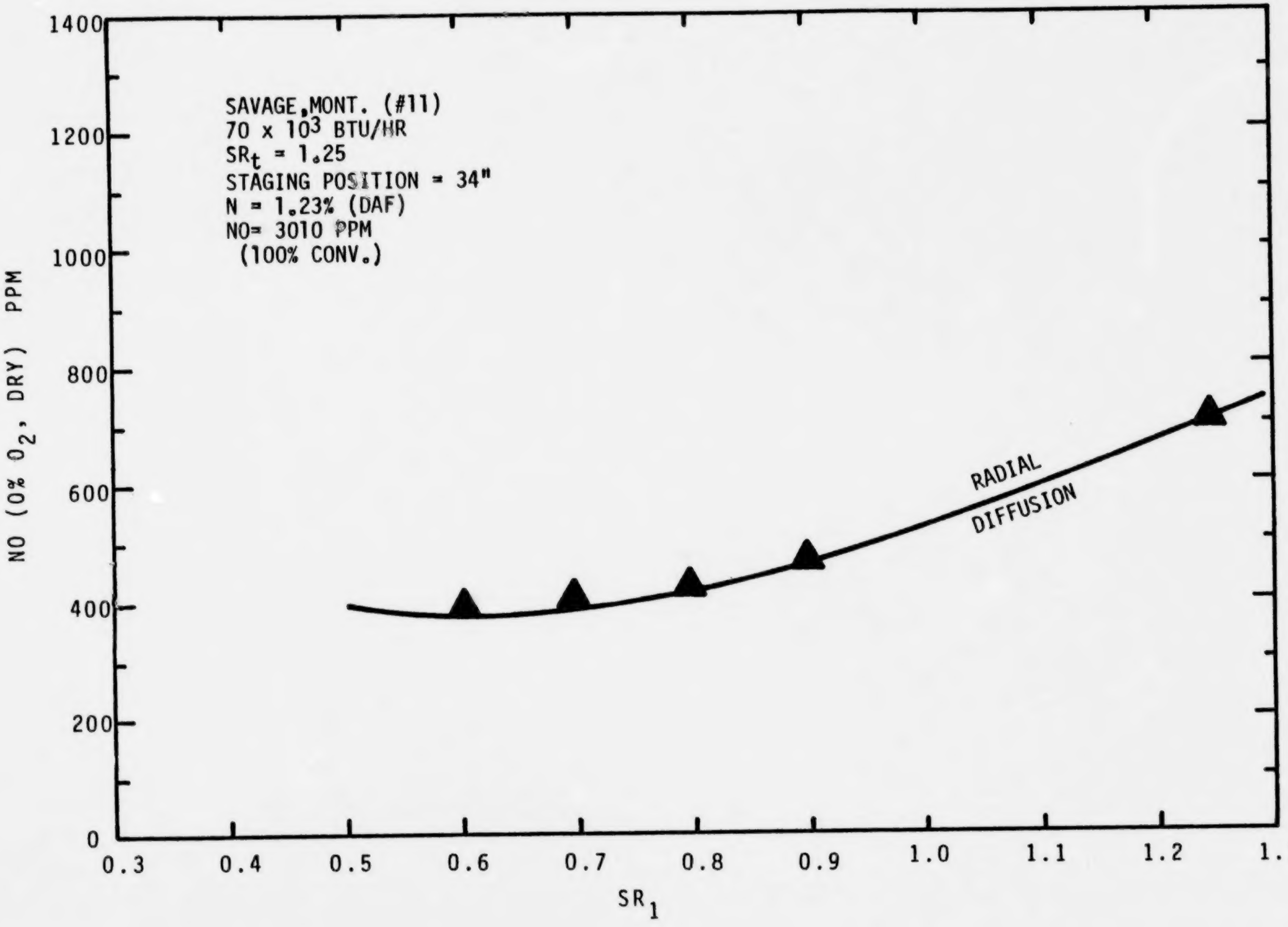
SAVAGE, MONT. (#11)
70 x 10³ BTU/HR
SRt = 1.25
STAGING POSITION = 34"
N = 1.23% (DAF)
NO= 3010 PPM
(100% CONV.)
RADIAL DIFFUSION
NO (0% O2, DRY) PPM
1400
1200
1000
800
600
400
200
0
0.3
0.4
0.5
0.6
0.7
0.8
0.9
1.0
1.1
1.2
1.3
SR1

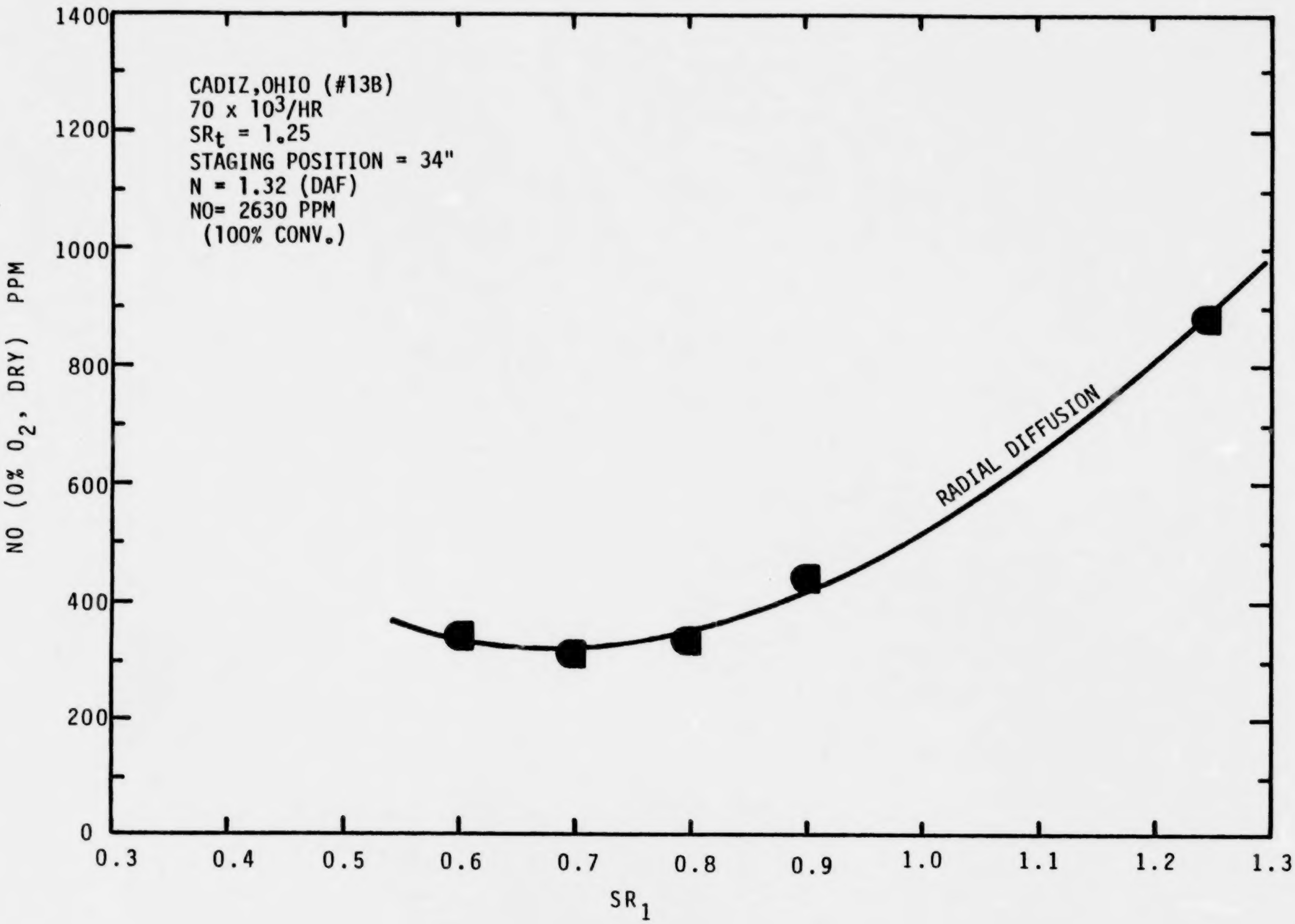
CADIZ,OHIO (#13B)
70 x 10³/HR
SRt = 1.25
STAGING POSITION = 34"
N = 1.32 (DAF)
NO= 2630 PPM
(100% CONV.)
RADIAL DIFFUSION
NO (0% O2, DRY) PPM
0
200
400
600
800
1000
1200
1400
0.3
0.4
0.5
0.6
0.7
0.8
0.9
1.0
1.1
1.2
1.3
SR1

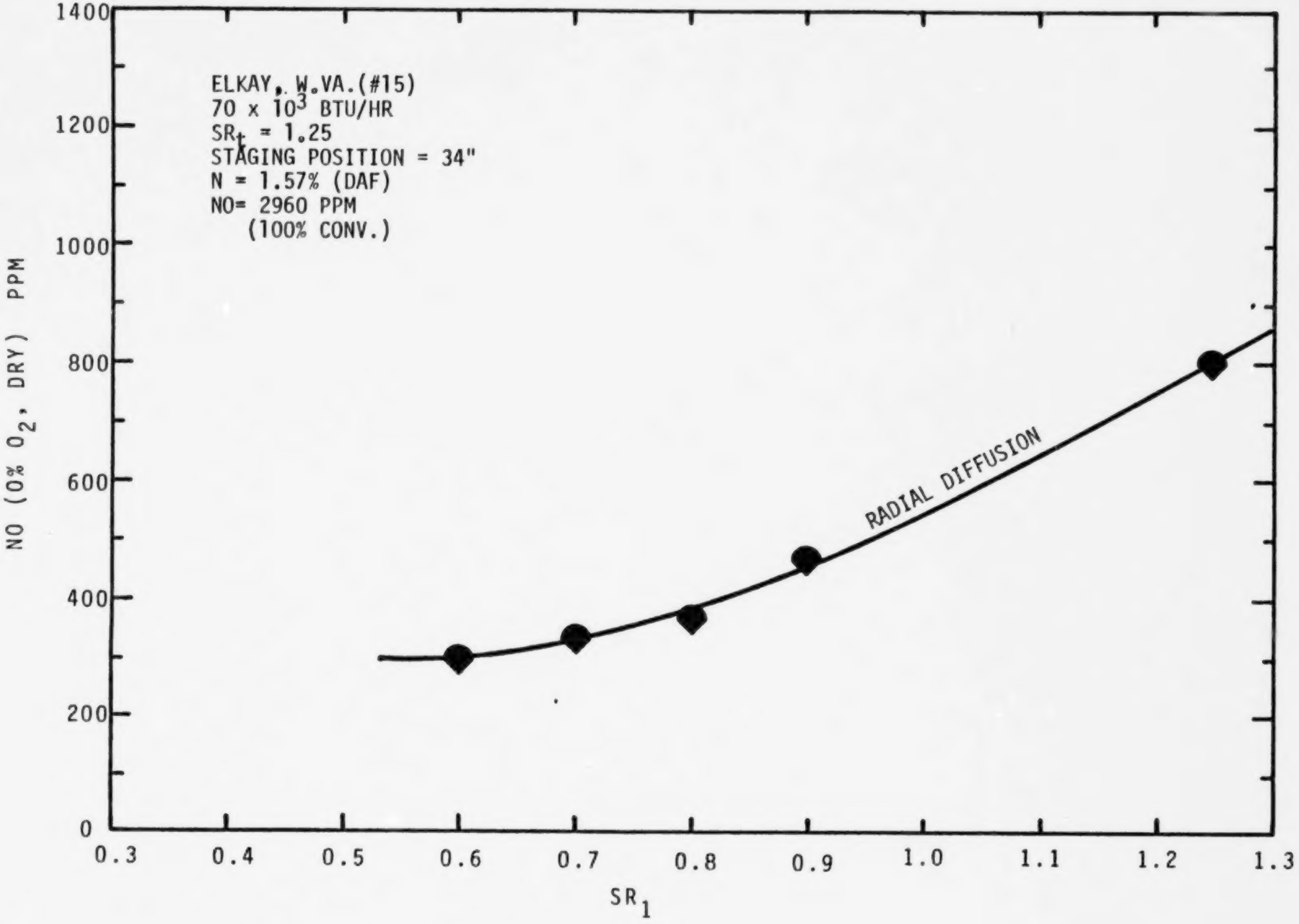
ELKAY, W.VA. (#15)
70 x 10³ BTU/HR
SRₜ = 1.25
STAGING POSITION = 34"
N = 1.57% (DAF)
NO= 2960 PPM
(100% CONV.)
RADIAL DIFFUSION
NO (0% O₂, DRY) PPM
1400
1200
1000
800
600
400
200
0
0.3
0.4
0.5
0.6
0.7
0.8
0.9
1.0
1.1
1.2
1.3
SR₁

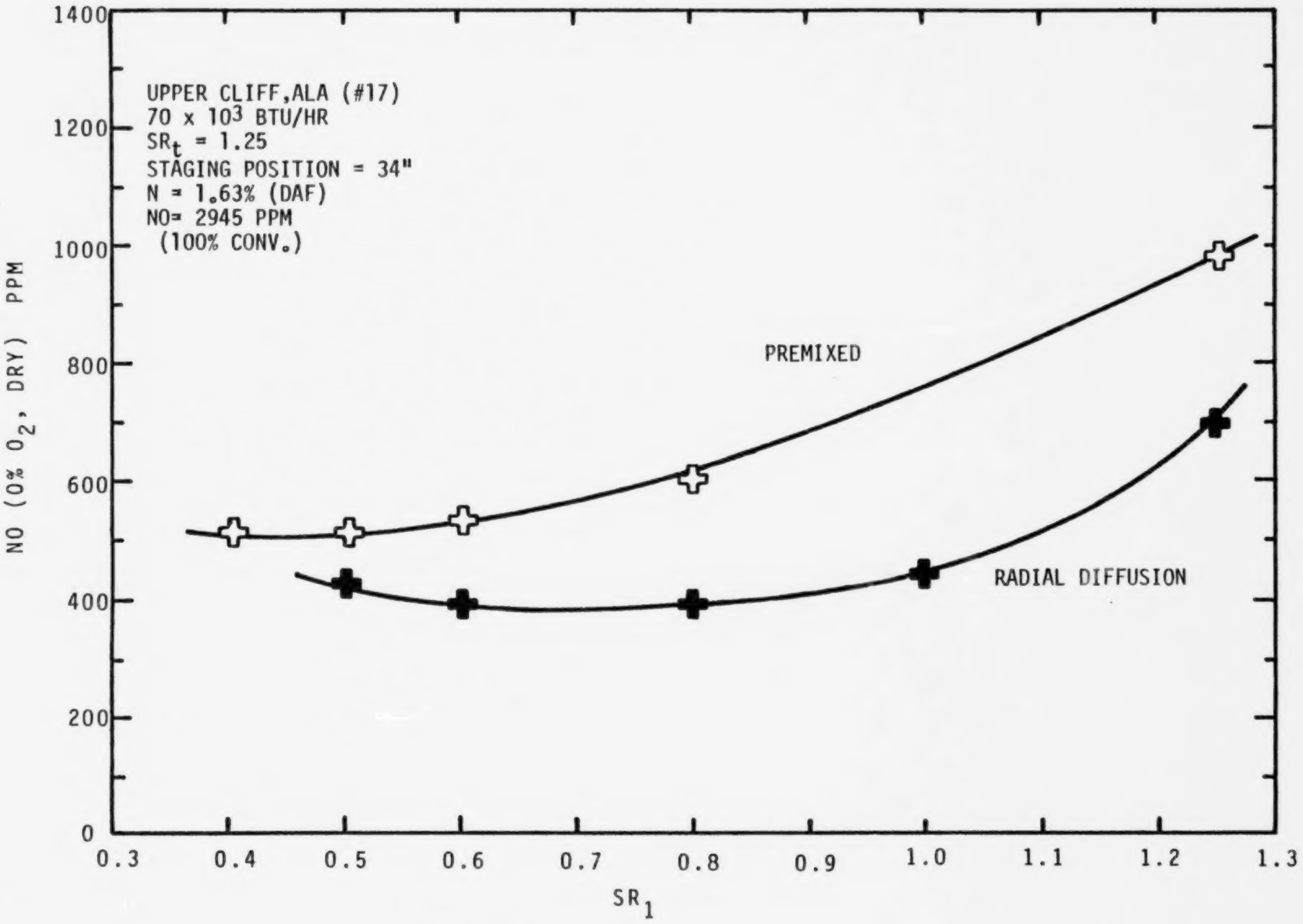
UPPER CLIFF,ALA (#17)
70 x 10^3 BTU/HR
SR_t = 1.25
STAGING POSITION = 34"
N = 1.63% (DAF)
NO= 2945 PPM
(100% CONV.)
PREMIXED
RADIAL DIFFUSION
NO (0% O_2, DRY) PPM
1400
1200
1000
800
600
400
200
0
0.3
0.4
0.5
0.6
0.7
0.8
0.9
1.0
1.1
1.2
1.3
SR_1

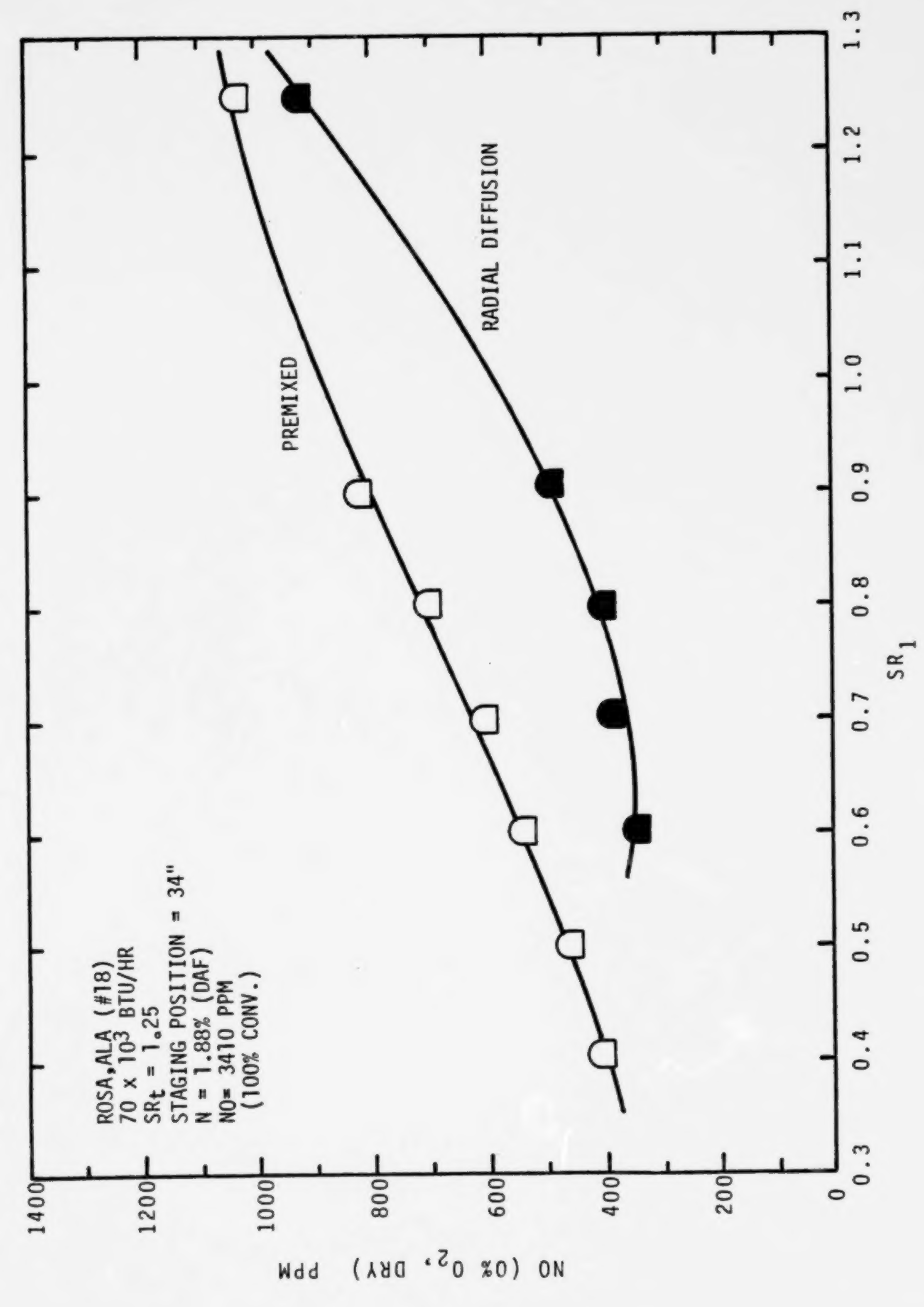
ROSA,ALA (#18)
70 x 10^3 BTU/HR
SR$_t$ = 1.25
STAGING POSITION = 34"
N = 1.88% (DAF)
NO= 3410 PPM
(100% CONV.)
PREMIXED
RADIAL DIFFUSION
NO (0% O$_2$, DRY) PPM
0
200
400
600
800
1000
1200
1400
SR$_1$
0.3
0.4
0.5
0.6
0.7
0.8
0.9
1.0
1.1
1.2
1.3

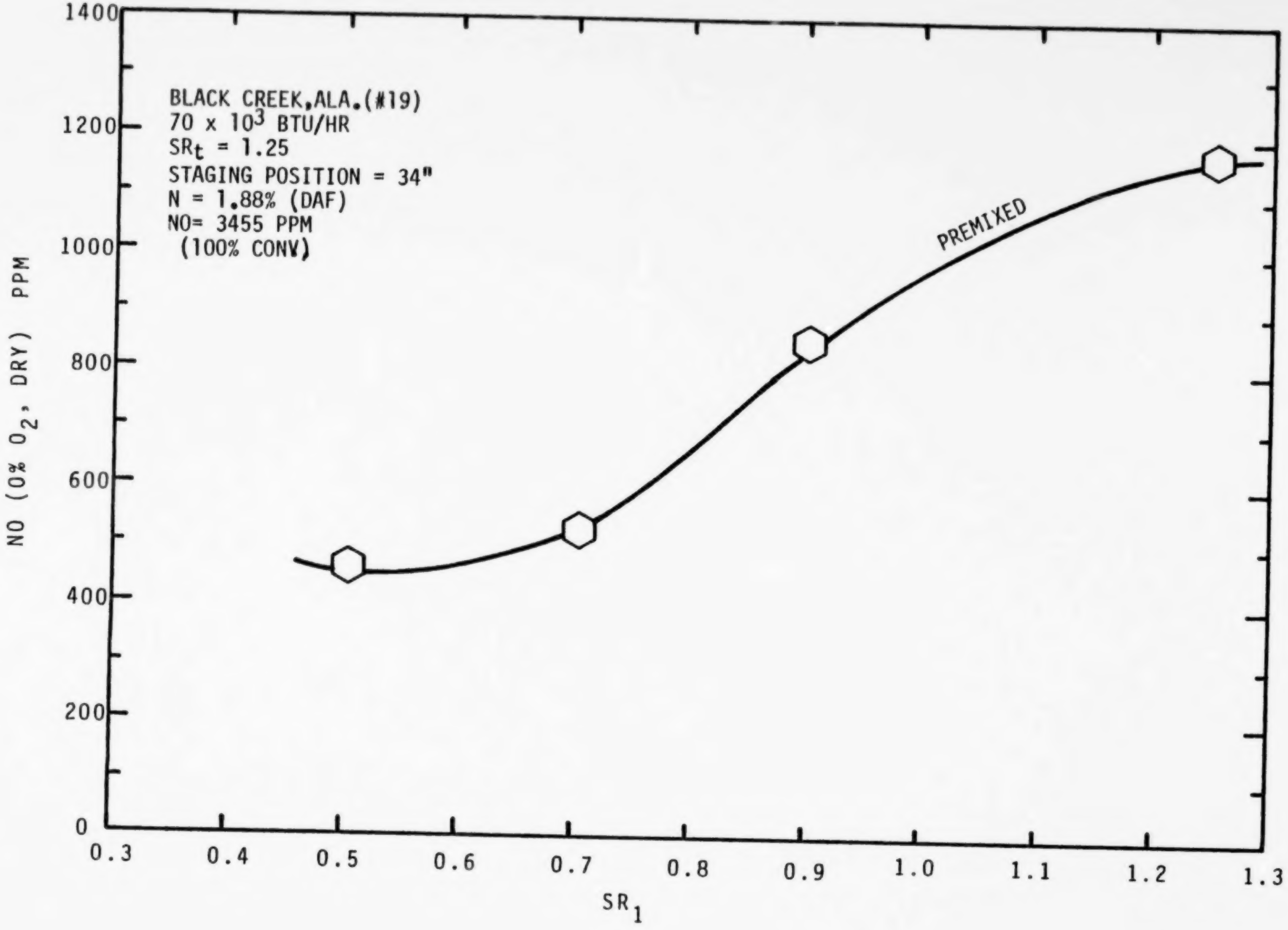
BLACK CREEK,ALA.(#19)
70 x 10^3 BTU/HR
SR_t = 1.25
STAGING POSITION = 34"
N = 1.88% (DAF)
NO= 3455 PPM
(100% CONV)
PREMIXED
NO (0% O_2, DRY) PPM
0
200
400
600
800
1000
1200
1400
0.3
0.4
0.5
0.6
0.7
0.8
0.9
1.0
1.1
1.2
1.3
SR_1

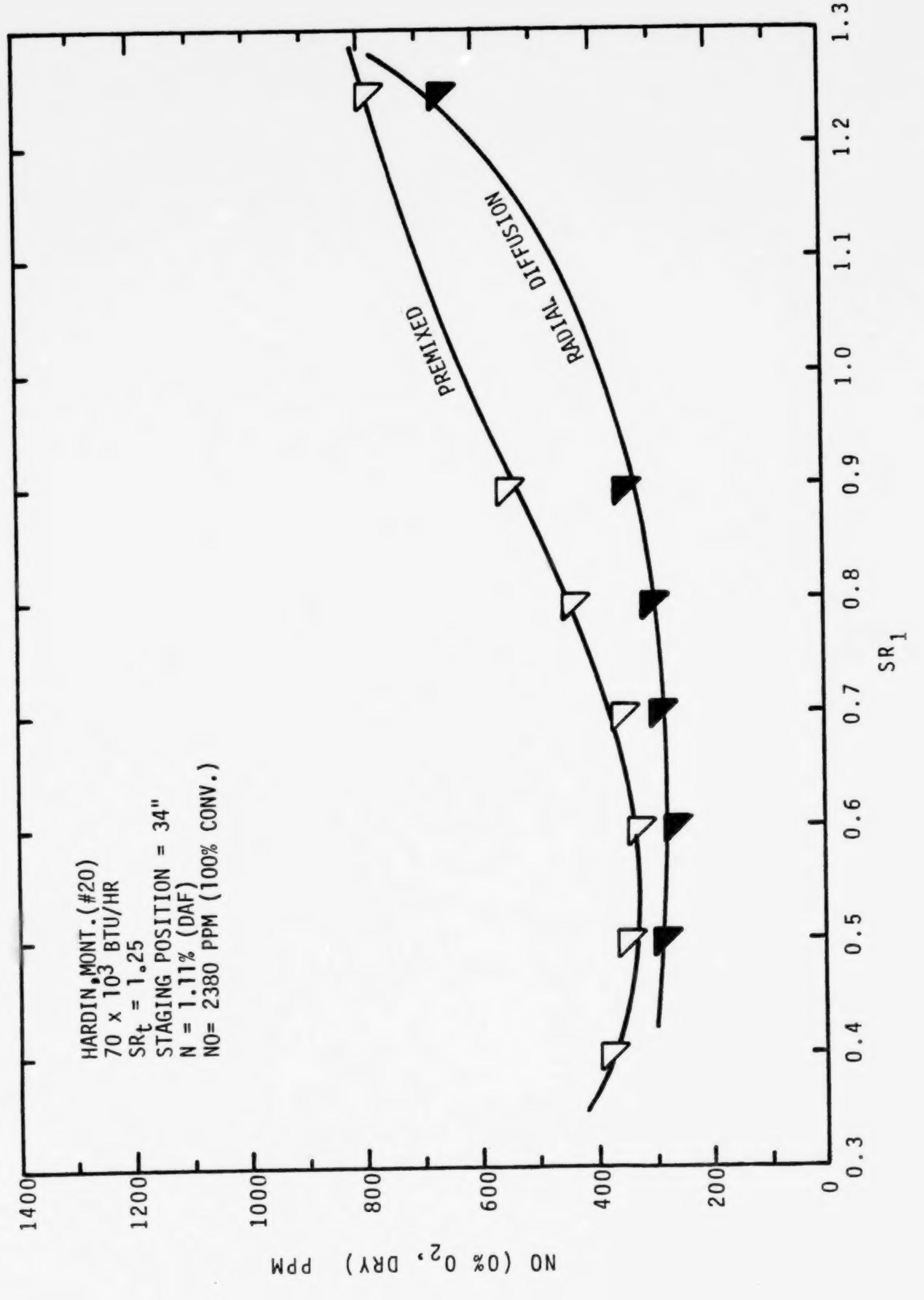
HARDIN MONT. (#20)
70 x 10^3 BTU/HR
SR$_t$ = 1.25
STAGING POSITION = 34"
N = 1.11% (DAF)
NO= 2380 PPM (100% CONV.)
PREMIXED
RADIAL DIFFUSION
NO (0% O$_2$, DRY) PPM
0
200
400
600
800
1000
1200
1400
SR$_1$
0.3
0.4
0.5
0.6
0.7
0.8
0.9
1.0
1.1
1.2
1.3

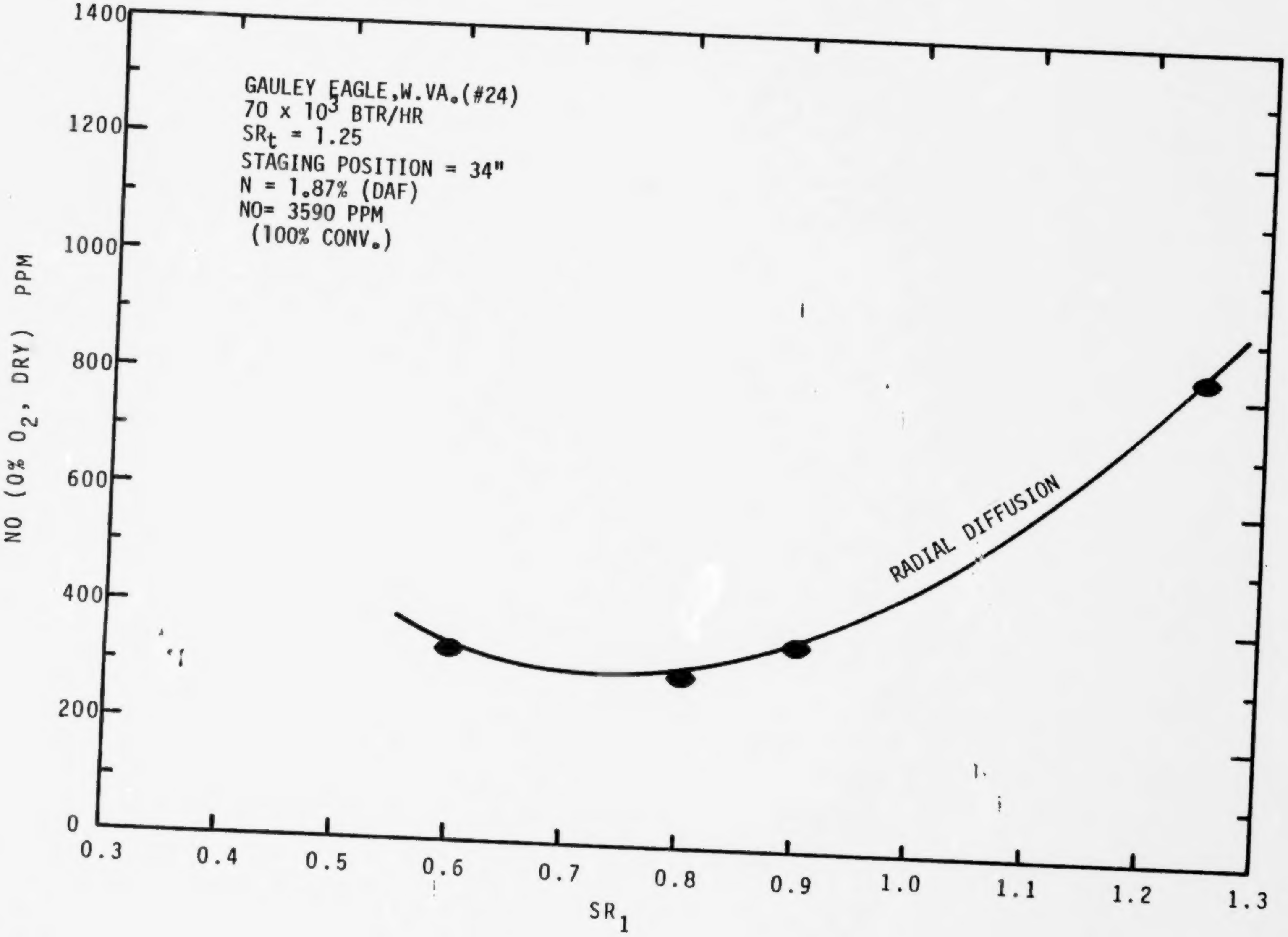
GAULEY EAGLE,W.VA.(#24)
70 x 10^3 BTR/HR
SR$_t$ = 1.25
STAGING POSITION = 34"
N = 1.87% (DAF)
NO= 3590 PPM
(100% CONV.)
RADIAL DIFFUSION
NO (0% O$_2$, DRY) PPM
0
200
400
600
800
1000
1200
1400
SR$_1$
0.3
0.4
0.5
0.6
0.7
0.8
0.9
1.0
1.1
1.2
1.3

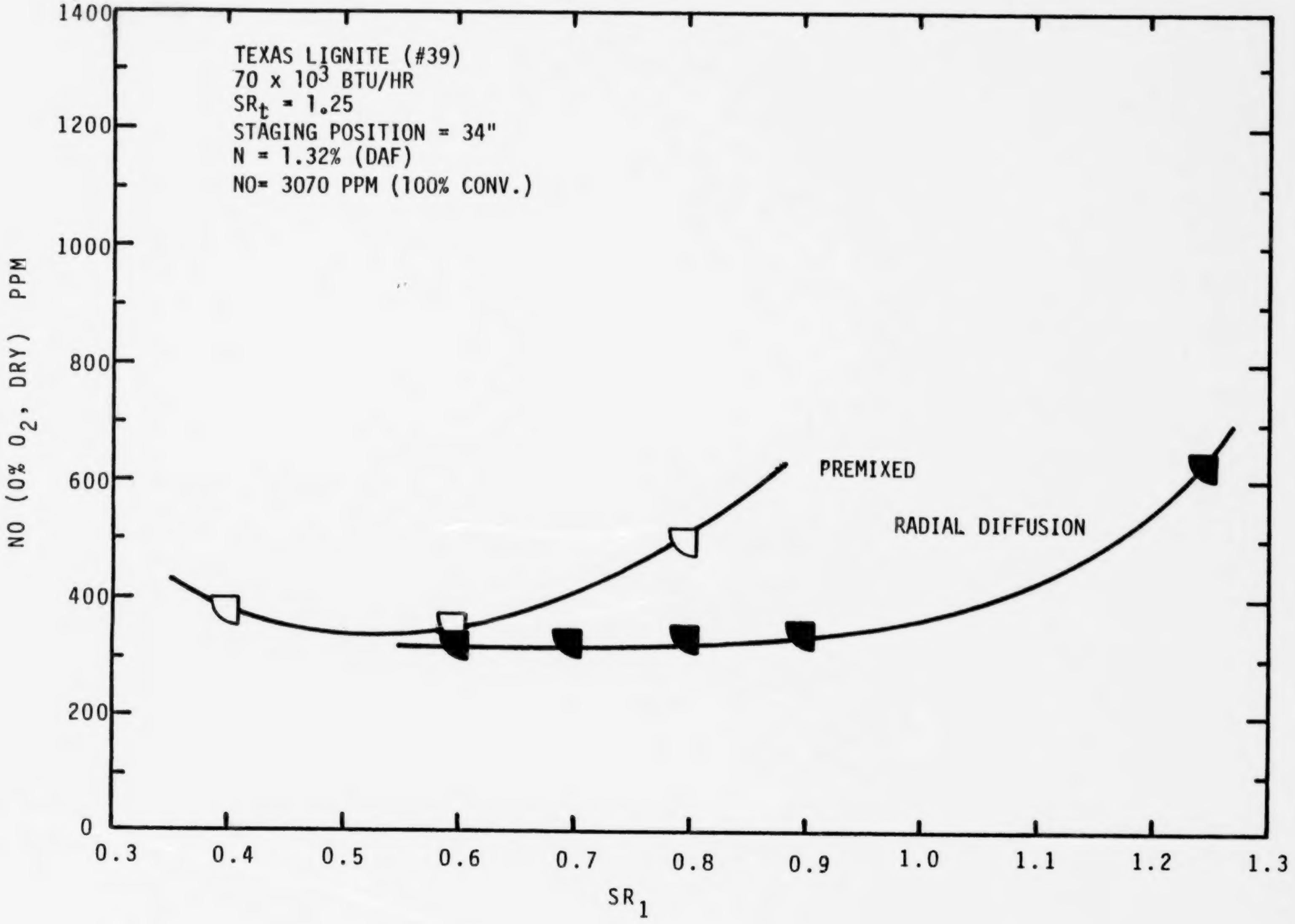
TEXAS LIGNITE (#39)
70 x 10³ BTU/HR
SR_t = 1.25
STAGING POSITION = 34"
N = 1.32% (DAF)
NO= 3070 PPM (100% CONV.)
PREMIXED
RADIAL DIFFUSION
NO (0% O₂, DRY) PPM
1400
1200
1000
800
600
400
200
0
0.3
0.4
0.5
0.6
0.7
0.8
0.9
1.0
1.1
1.2
1.3
SR₁

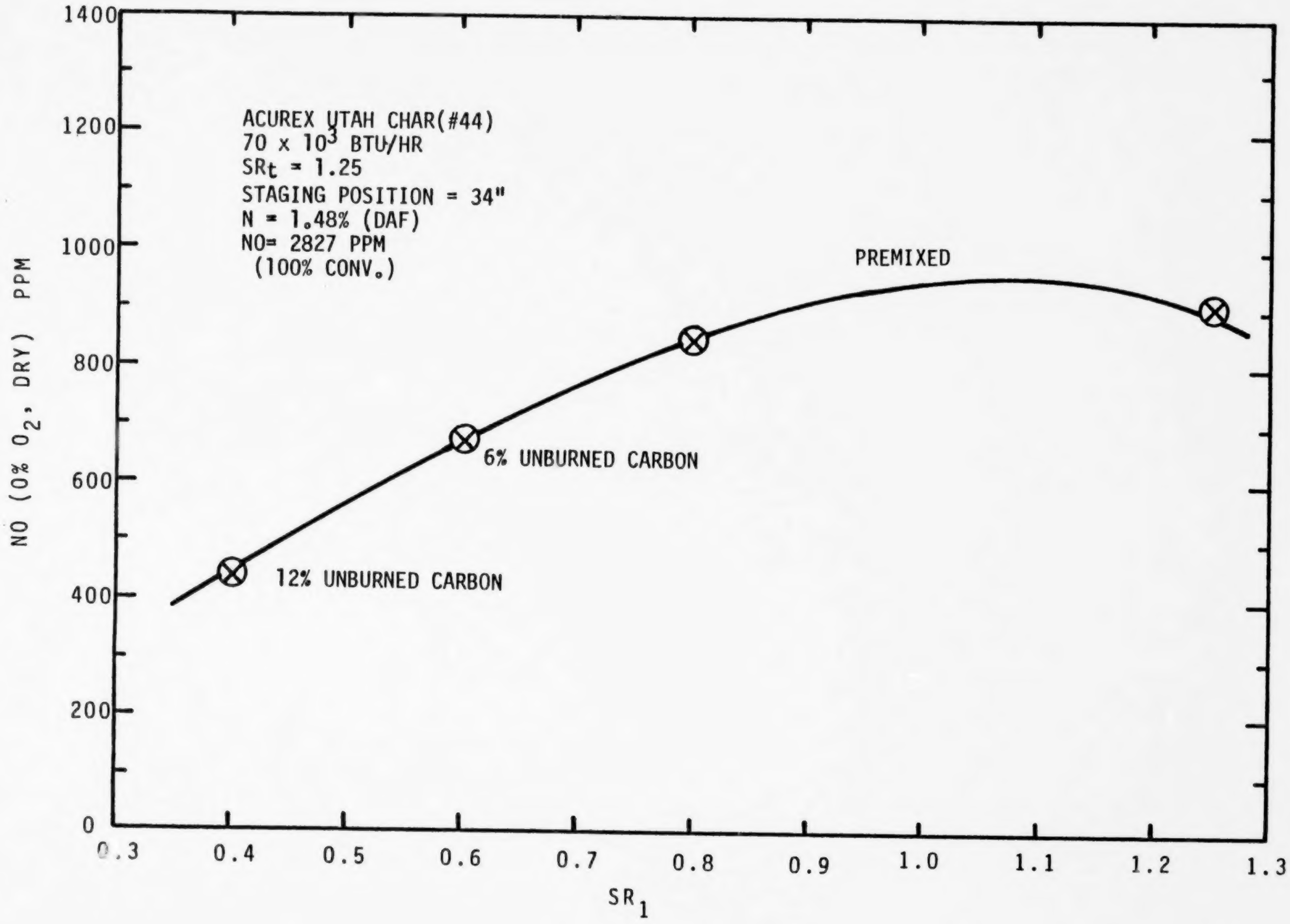
ACUREX UTAH CHAR(#44)
70 x 10³ BTU/HR
SRt = 1.25
STAGING POSITION = 34"
N = 1.48% (DAF)
NO= 2827 PPM
(100% CONV.)
PREMIXED
6% UNBURNED CARBON
12% UNBURNED CARBON
NO (0% O2, DRY) PPM
1400
1200
1000
800
600
400
200
0
0.3
0.4
0.5
0.6
0.7
0.8
0.9
1.0
1.1
1.2
1.3
SR1

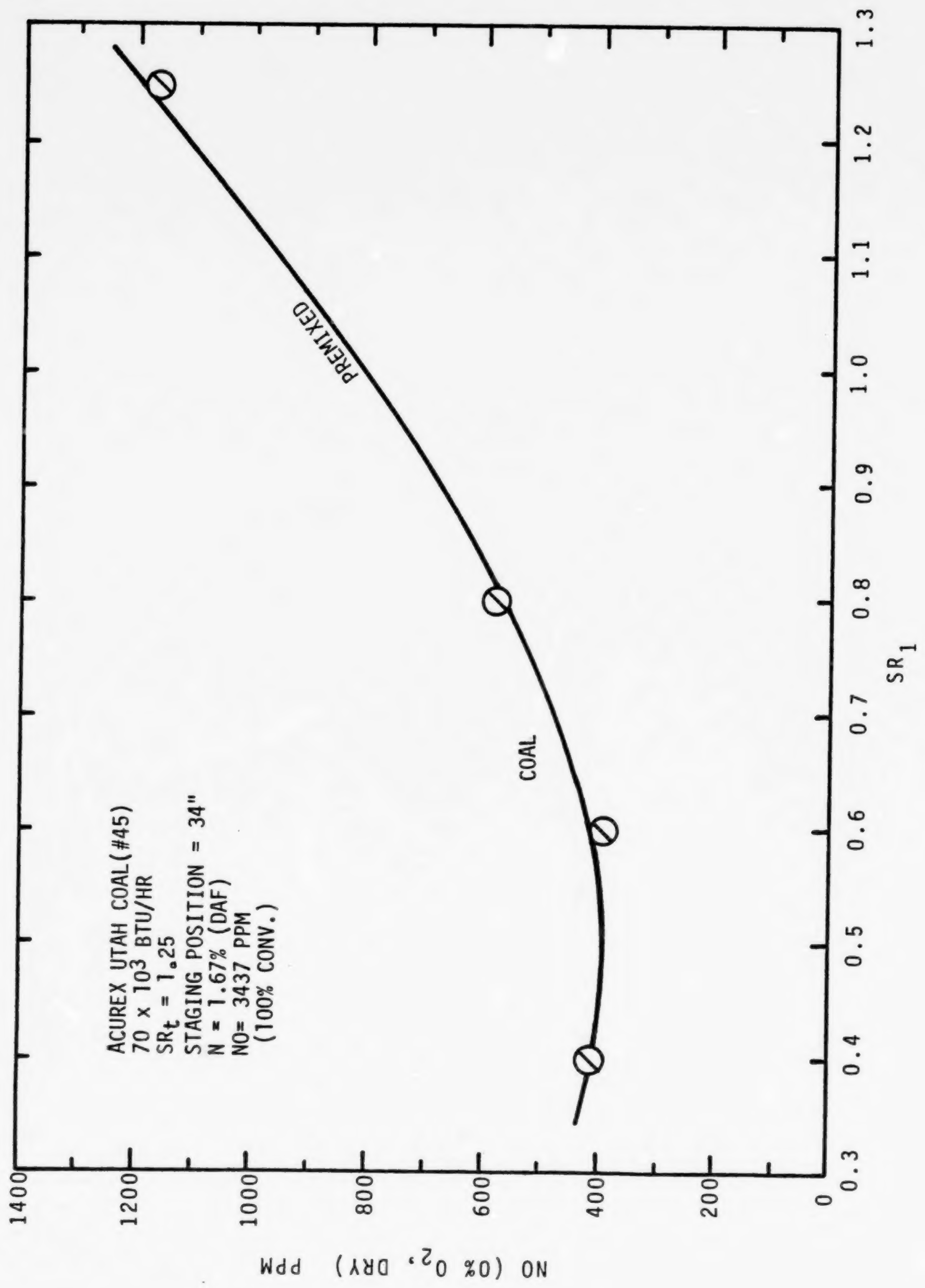
ACUREX UTAH COAL(#45)
70 x 10^3 BTU/HR
SR$_t$ = 1.25
STAGING POSITION = 34"
N = 1.67% (DAF)
NO= 3437 PPM
(100% CONV.)
PREMIXED
COAL
NO (0% O$_2$, DRY) PPM
1400
1200
1000
800
600
400
200
0
0.3
0.4
0.5
0.6
0.7
0.8
0.9
1.0
1.1
1.2
1.3
SR$_1$

APPENDIX D

Summary of Bench-Scale Data

- NO Produced Under Three-Stage Conditions

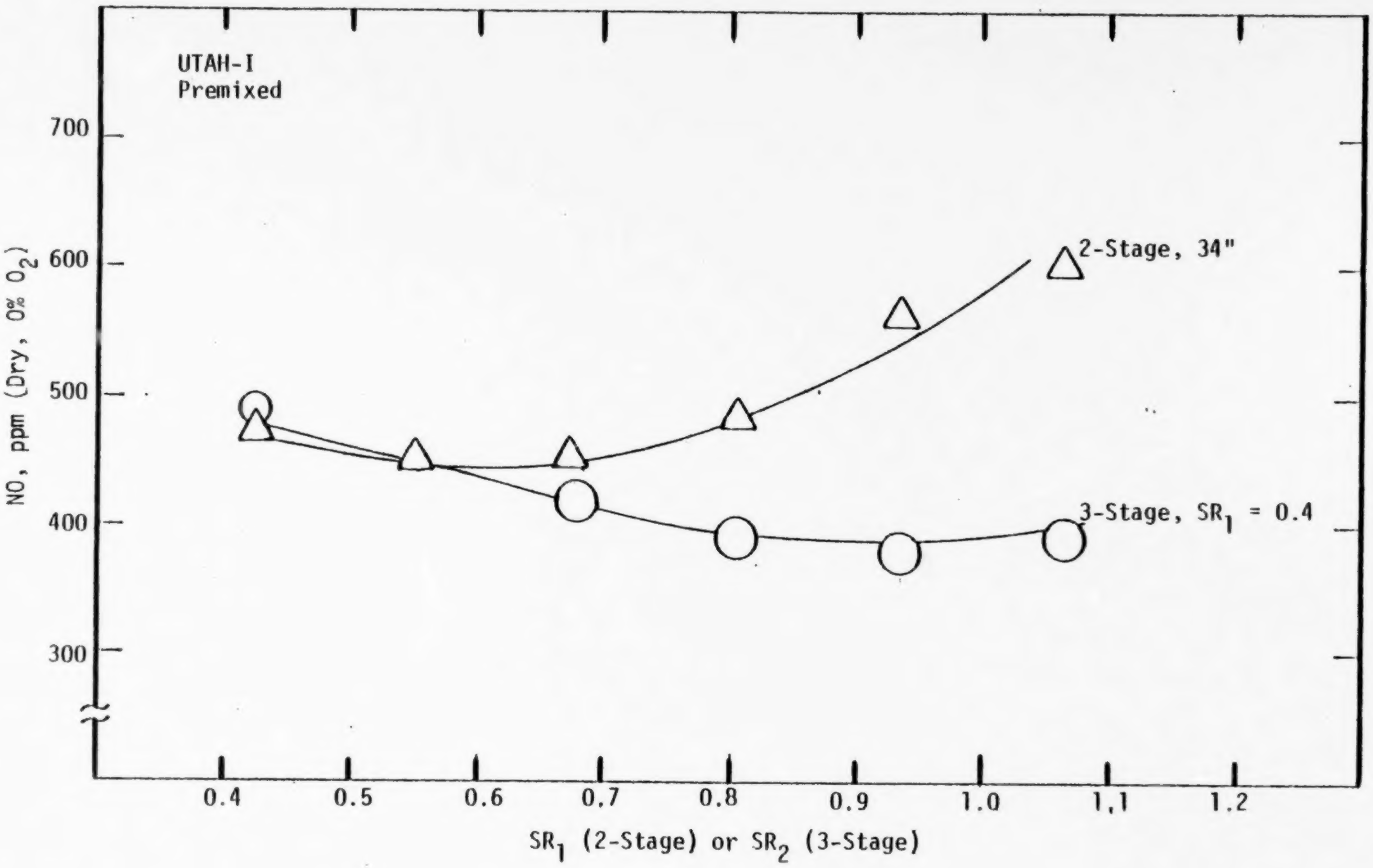UTAH-I
Premixed
NO, ppm (Dry, 0% O_2)
700
600
500
400
300
2-Stage, 34"
3-Stage, SR_1 = 0.4
0.4
0.5
0.6
0.7
0.8
0.9
1.0
1.1
1.2
SR_1 (2-Stage) or SR_2 (3-Stage)

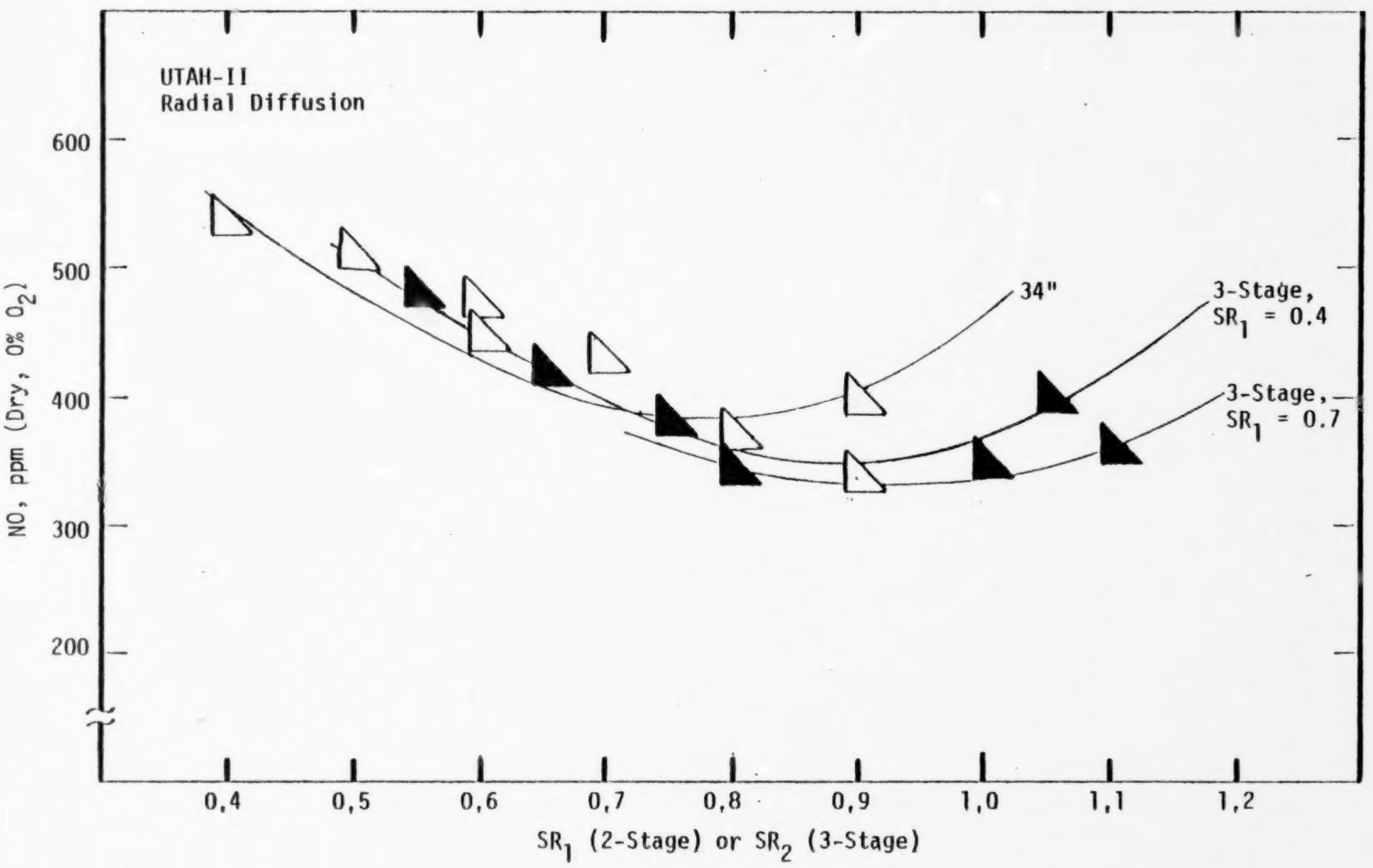
UTAH-II
Radial Diffusion
600
500
400
300
200
NO, ppm (Dry, 0% O$_2$)
0,4
0,5
0,6
0,7
0,8
0,9
1,0
1,1
1,2
SR$_1$ (2-Stage) or SR$_2$ (3-Stage)
34"
3-Stage, SR$_1$ = 0.4
3-Stage, SR$_1$ = 0.7

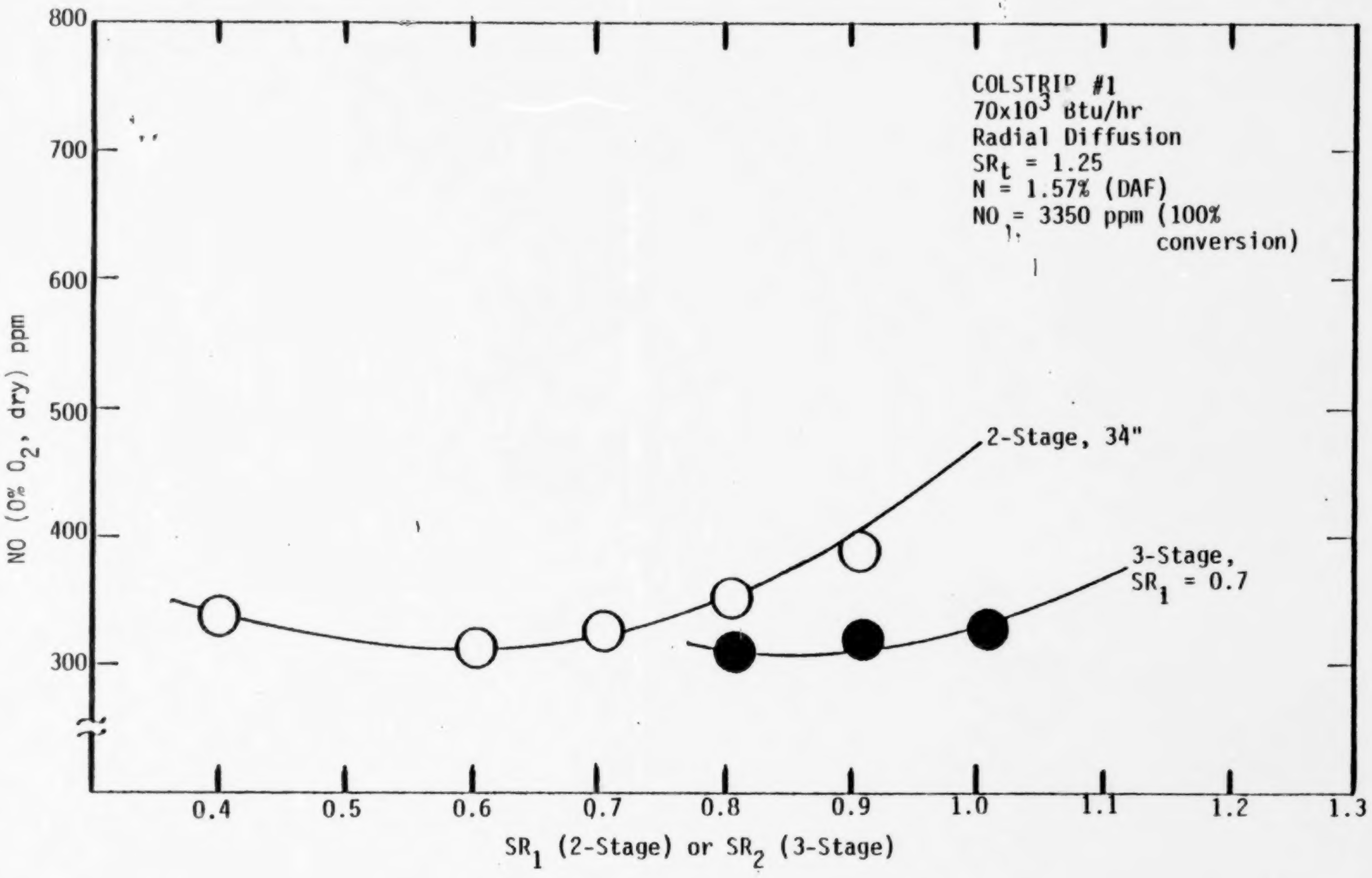
COLSTRIP #1
70x10³ Btu/hr
Radial Diffusion
SRt = 1.25
N = 1.57% (DAF)
NO = 3350 ppm (100% conversion)
2-Stage, 34"
3-Stage, SR1 = 0.7
NO (0% O2, dry) ppm
800
700
600
500
400
300
0.4
0.5
0.6
0.7
0.8
0.9
1.0
1.1
1.2
1.3
SR1 (2-Stage) or SR2 (3-Stage)

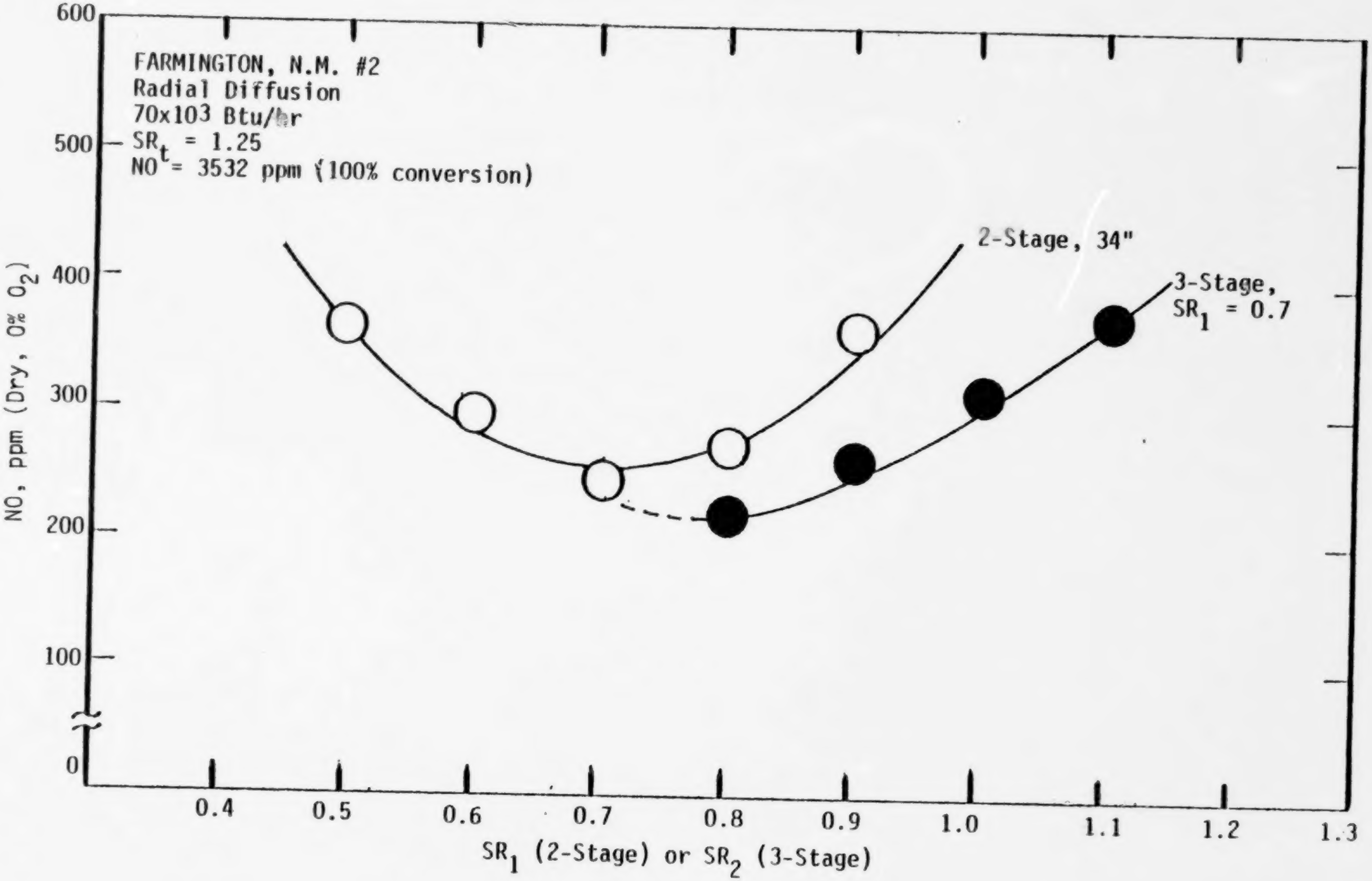
FARMINGTON, N.M. #2
Radial Diffusion
70x103 Btu/hr
SR_t = 1.25
NO = 3532 ppm (100% conversion)
2-Stage, 34"
3-Stage, SR_1 = 0.7
NO, ppm (Dry, 0% O_2)
600
500
400
300
200
100
0
0.4
0.5
0.6
0.7
0.8
0.9
1.0
1.1
1.2
1.3
SR_1 (2-Stage) or SR_2 (3-Stage)

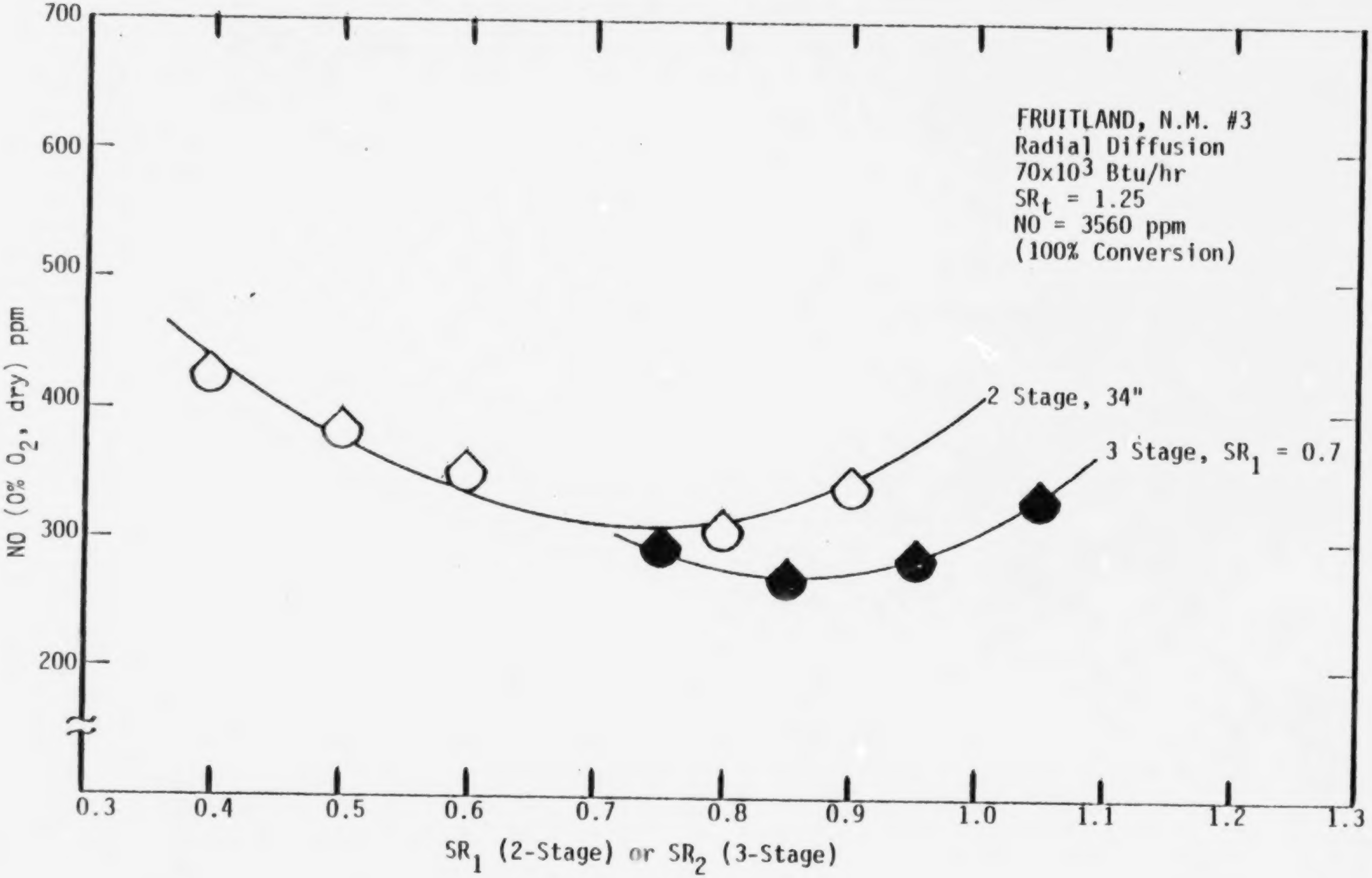
FRUITLAND, N.M. #3
Radial Diffusion
70x10^3 Btu/hr
SR_t = 1.25
NO = 3560 ppm
(100% Conversion)
2 Stage, 34"
3 Stage, SR_1 = 0.7
NO (0% O_2, dry) ppm
700
600
500
400
300
200
0.3
0.4
0.5
0.6
0.7
0.8
0.9
1.0
1.1
1.2
1.3
SR_1 (2-Stage) or SR_2 (3-Stage)

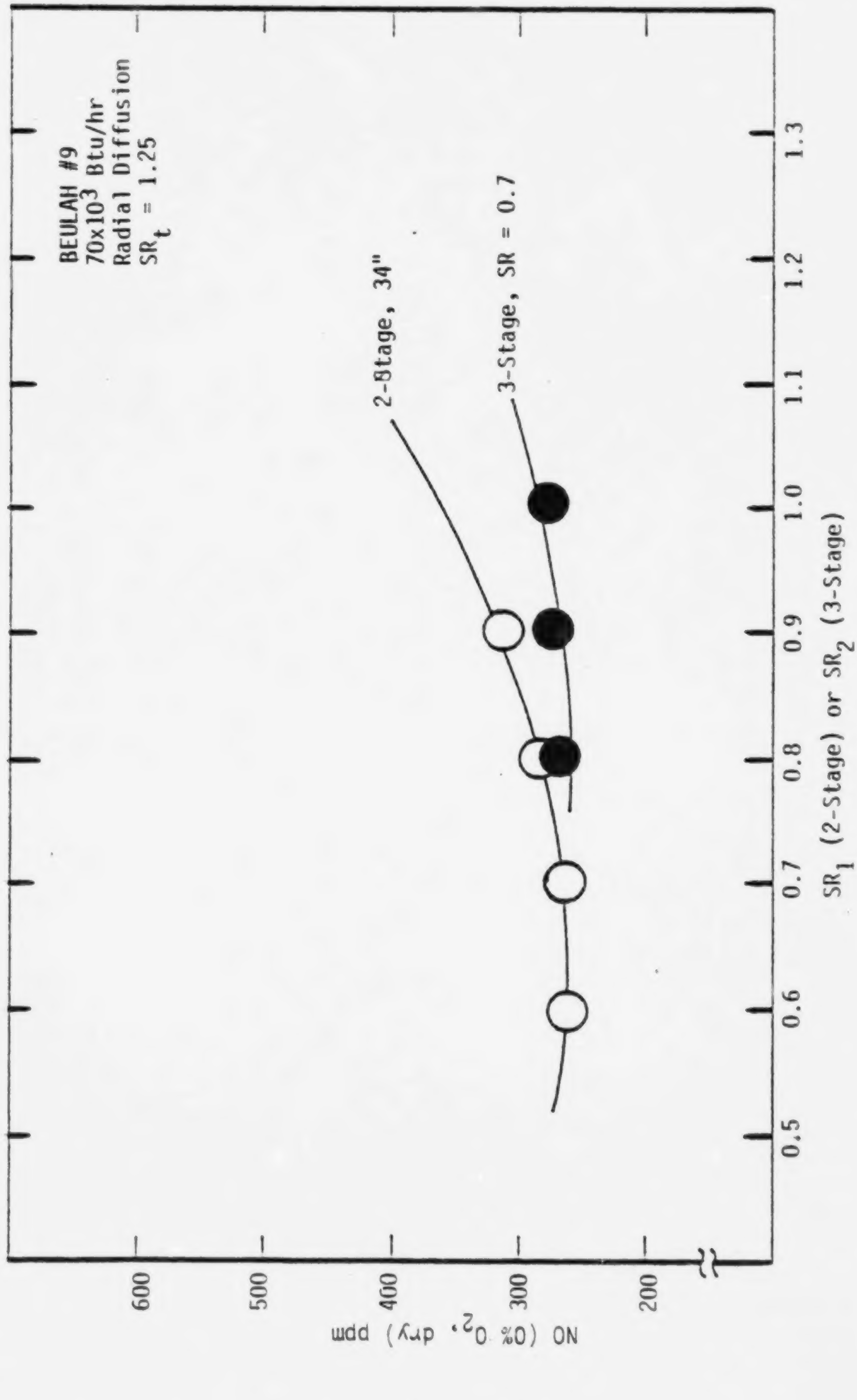
BEULAH #9
70x10^3 Btu/hr
Radial Diffusion
SR_t = 1.25
2-Stage, 34"
3-Stage, SR = 0.7
600
500
400
300
200
NO (0% O_2, dry) ppm
0.5
0.6
0.7
0.8
0.9
1.0
1.1
1.2
1.3
SR_1 (2-Stage) or SR_2 (3-Stage)

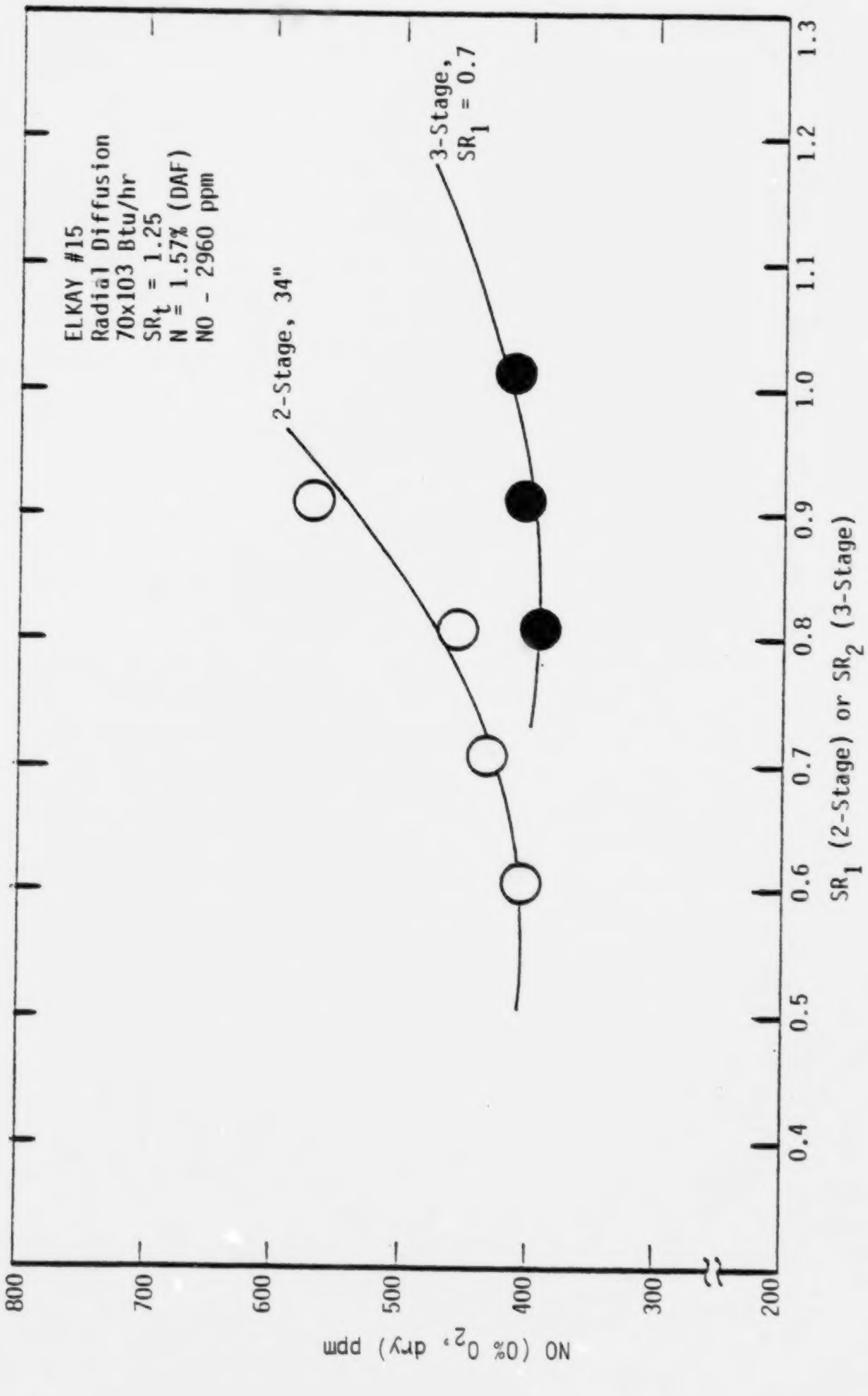
ELKAY #15
Radial Diffusion
70x103 Btu/hr
SR_t = 1.25
N = 1.57% (DAF)
NO - 2960 ppm
2-Stage, 34"
3-Stage, SR_1 = 0.7
NO (0% O_2, dry) ppm
800
700
600
500
400
300
200
0.4
0.5
0.6
0.7
0.8
0.9
1.0
1.1
1.2
1.3
SR_1 (2-Stage) or SR_2 (3-Stage)

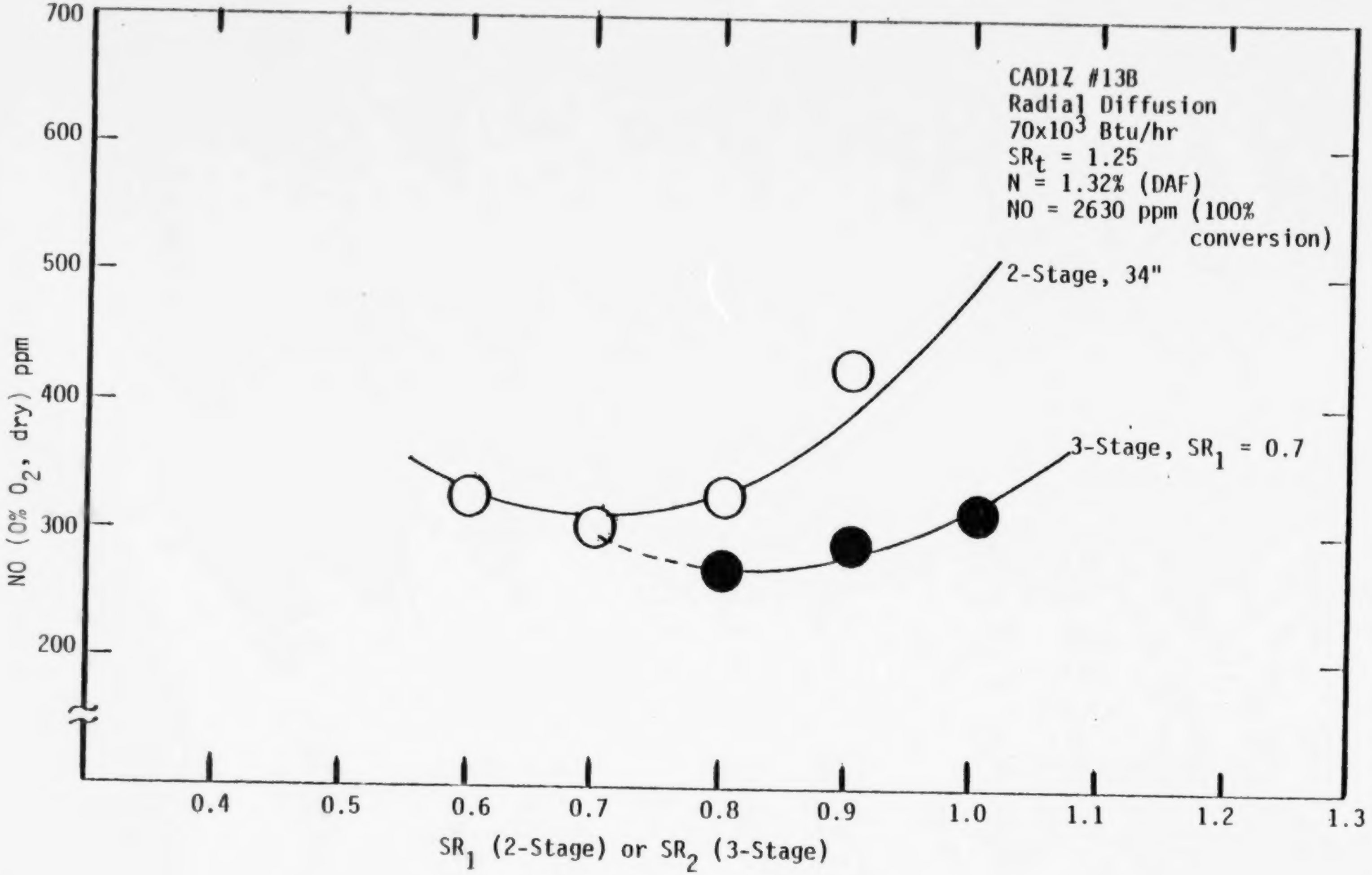
CADIZ #13B
Radial Diffusion
70×10^3 Btu/hr
$SR_t = 1.25$
N = 1.32% (DAF)
NO = 2630 ppm (100% conversion)
2-Stage, 34"
3-Stage, $SR_1 = 0.7$
700
600
500
400
300
200
NO (0% O_2, dry) ppm
0.4
0.5
0.6
0.7
0.8
0.9
1.0
1.1
1.2
1.3
SR_1 (2-Stage) or SR_2 (3-Stage)

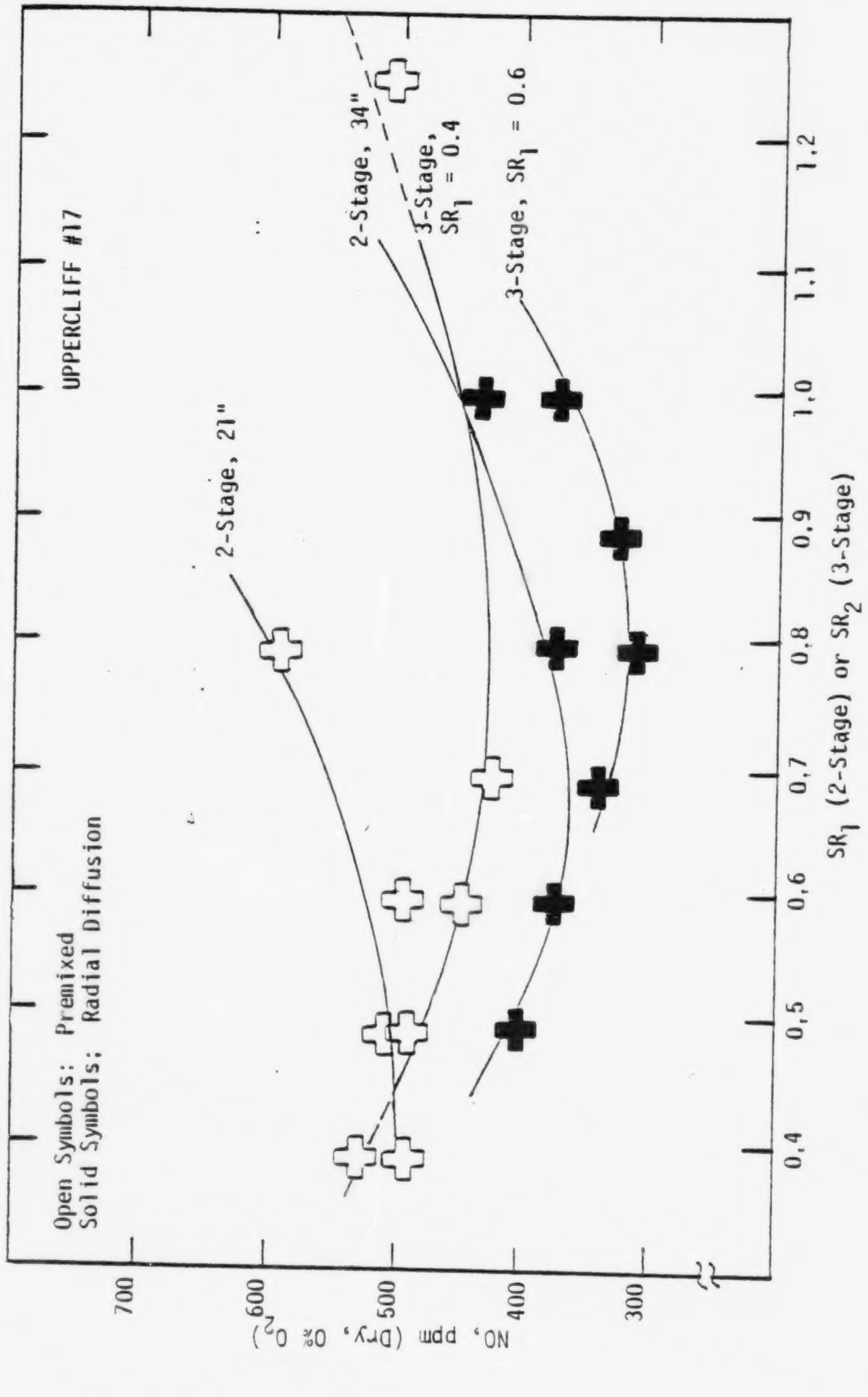
UPPERCLIFF #17
Open Symbols: Premixed
Solid Symbols: Radial Diffusion
2-Stage, 21"
2-Stage, 34"
3-Stage, SR_1 = 0.4
3-Stage, SR_1 = 0.6
NO, ppm (Dry, 0% O_2)
700
600
500
400
300
SR_1 (2-Stage) or SR_2 (3-Stage)
0.4
0.5
0.6
0.7
0.8
0.9
1.0
1.1
1.2

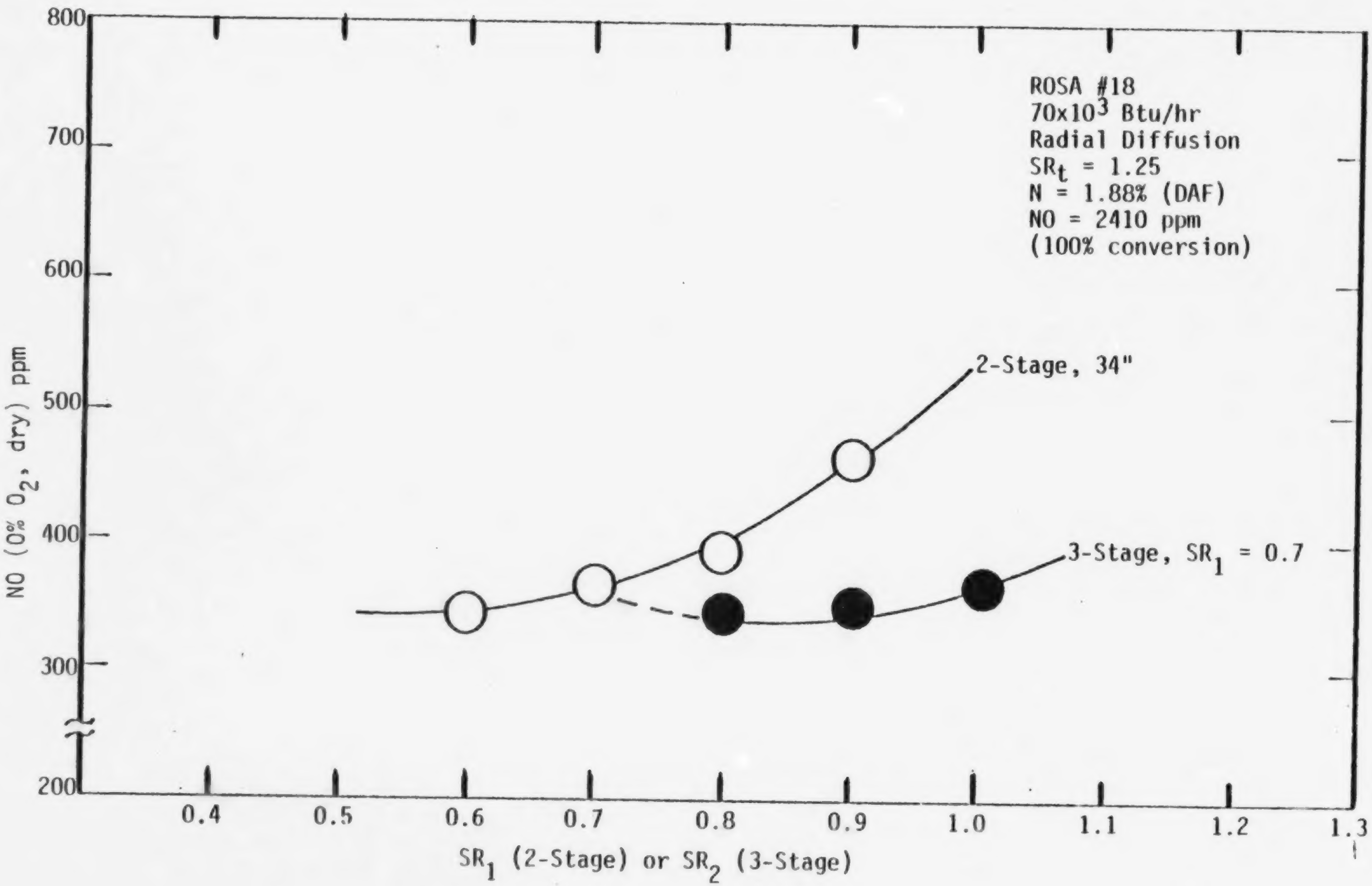
ROSA #18
70×10^3 Btu/hr
Radial Diffusion
$SR_t = 1.25$
N = 1.88% (DAF)
NO = 2410 ppm
(100% conversion)
2-Stage, 34"
3-Stage, $SR_1 = 0.7$
NO (0% O_2, dry) ppm
800
700
600
500
400
300
200
0.4
0.5
0.6
0.7
0.8
0.9
1.0
1.1
1.2
1.3
SR_1 (2-Stage) or SR_2 (3-Stage)

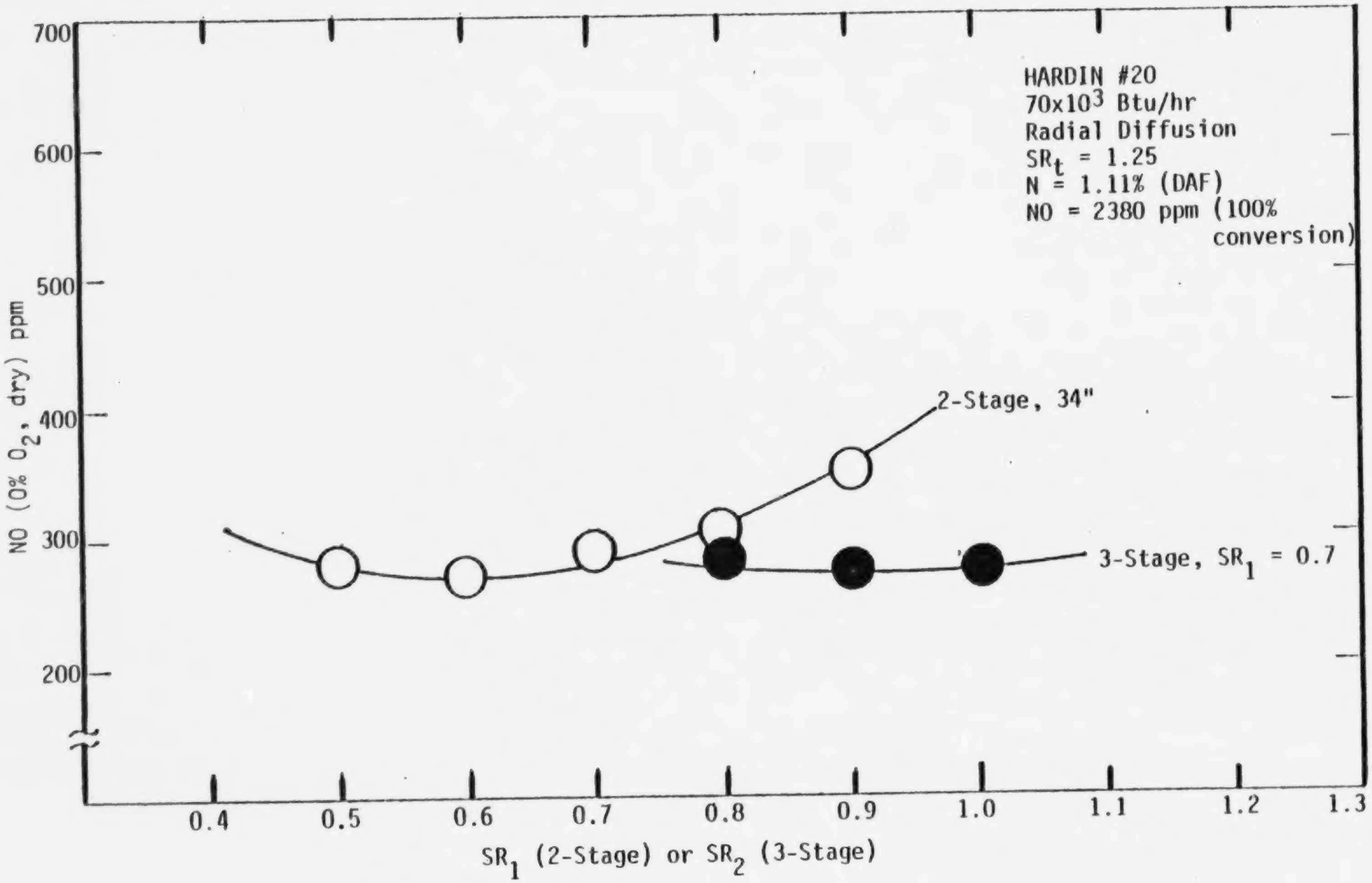
HARDIN #20
70x10^3 Btu/hr
Radial Diffusion
SR_t = 1.25
N = 1.11% (DAF)
NO = 2380 ppm (100% conversion)
2-Stage, 34"
3-Stage, SR_1 = 0.7
NO (0% O_2, dry) ppm
700
600
500
400
300
200
0.4
0.5
0.6
0.7
0.8
0.9
1.0
1.1
1.2
1.3
SR_1 (2-Stage) or SR_2 (3-Stage)

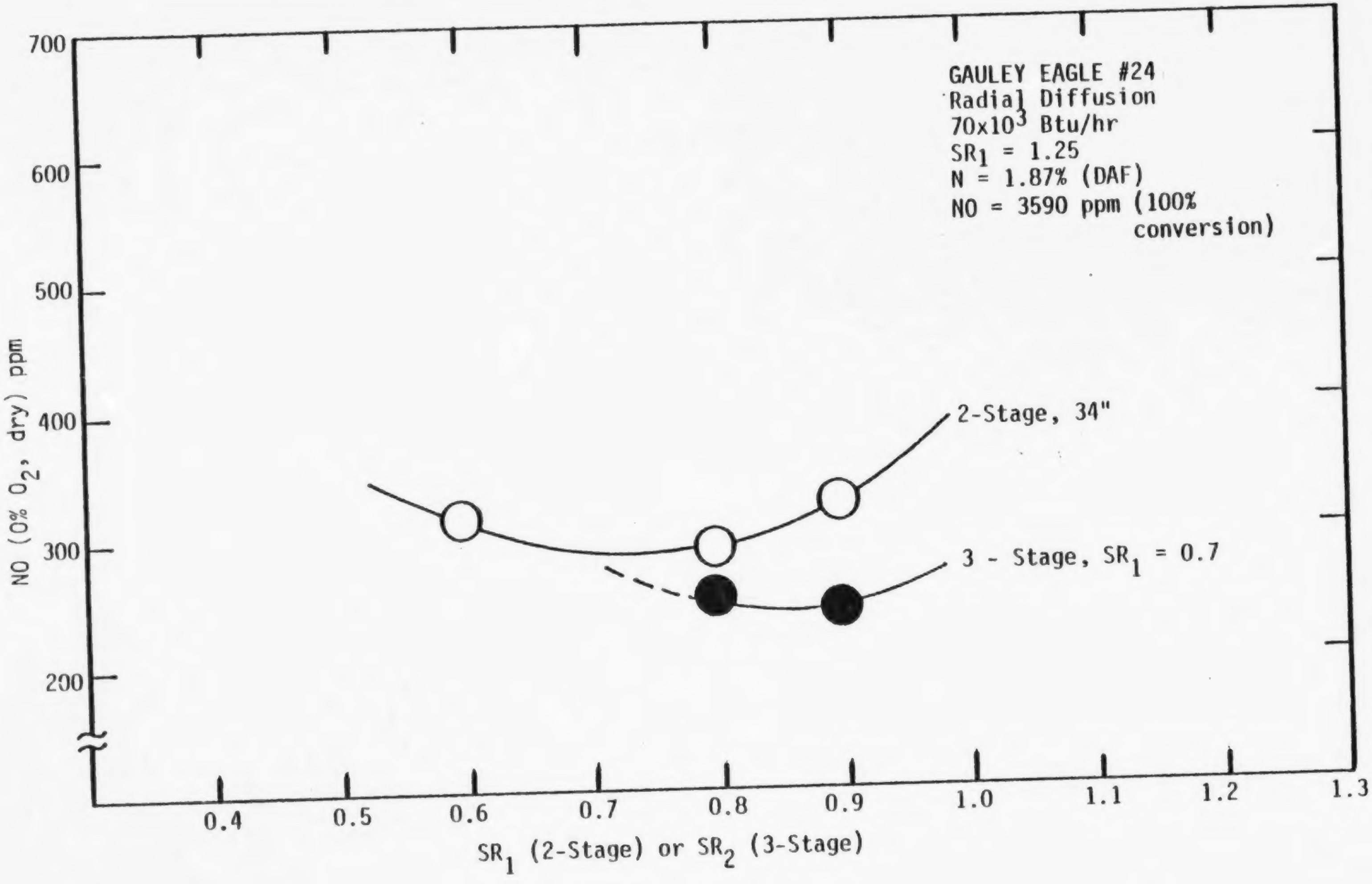
GAULEY EAGLE #24
Radial Diffusion
70x10^3 Btu/hr
SR$_1$ = 1.25
N = 1.87% (DAF)
NO = 3590 ppm (100% conversion)
2-Stage, 34"
3 - Stage, SR$_1$ = 0.7
NO (0% O$_2$, dry) ppm
700
600
500
400
300
200
0.4
0.5
0.6
0.7
0.8
0.9
1.0
1.1
1.2
1.3
SR$_1$ (2-Stage) or SR$_2$ (3-Stage)

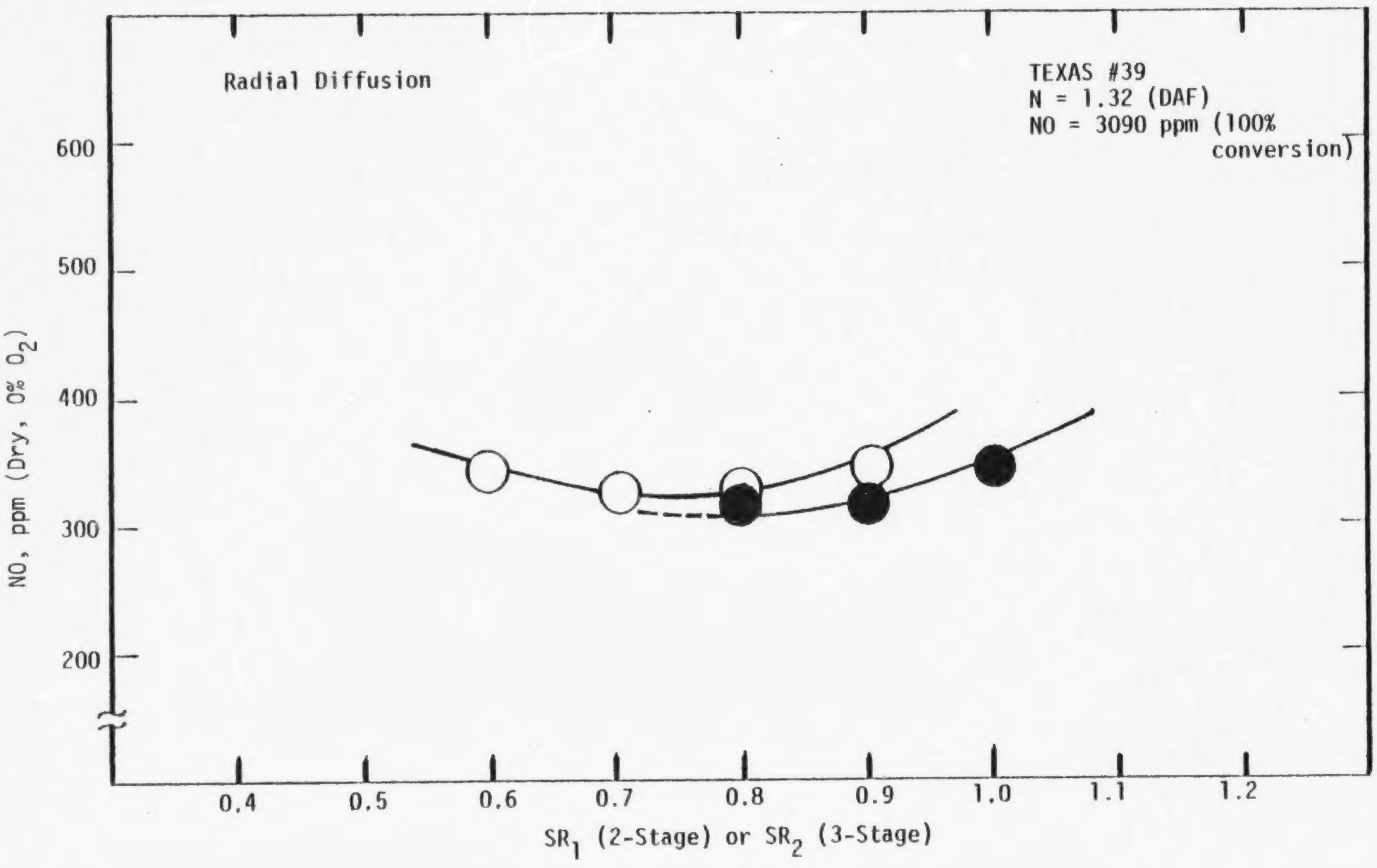
Radial Diffusion
TEXAS #39
N = 1.32 (DAF)
NO = 3090 ppm (100% conversion)
600
500
400
300
200
NO, ppm (Dry, 0% O_2)
0.4
0.5
0.6
0.7
0.8
0.9
1.0
1.1
1.2
SR_1 (2-Stage) or SR_2 (3-Stage)

APPENDIX E

Summary of Bench-Scale Data

- TFN Species Distribution at the Exit of the First Stage and Exhaust NO Concentrations

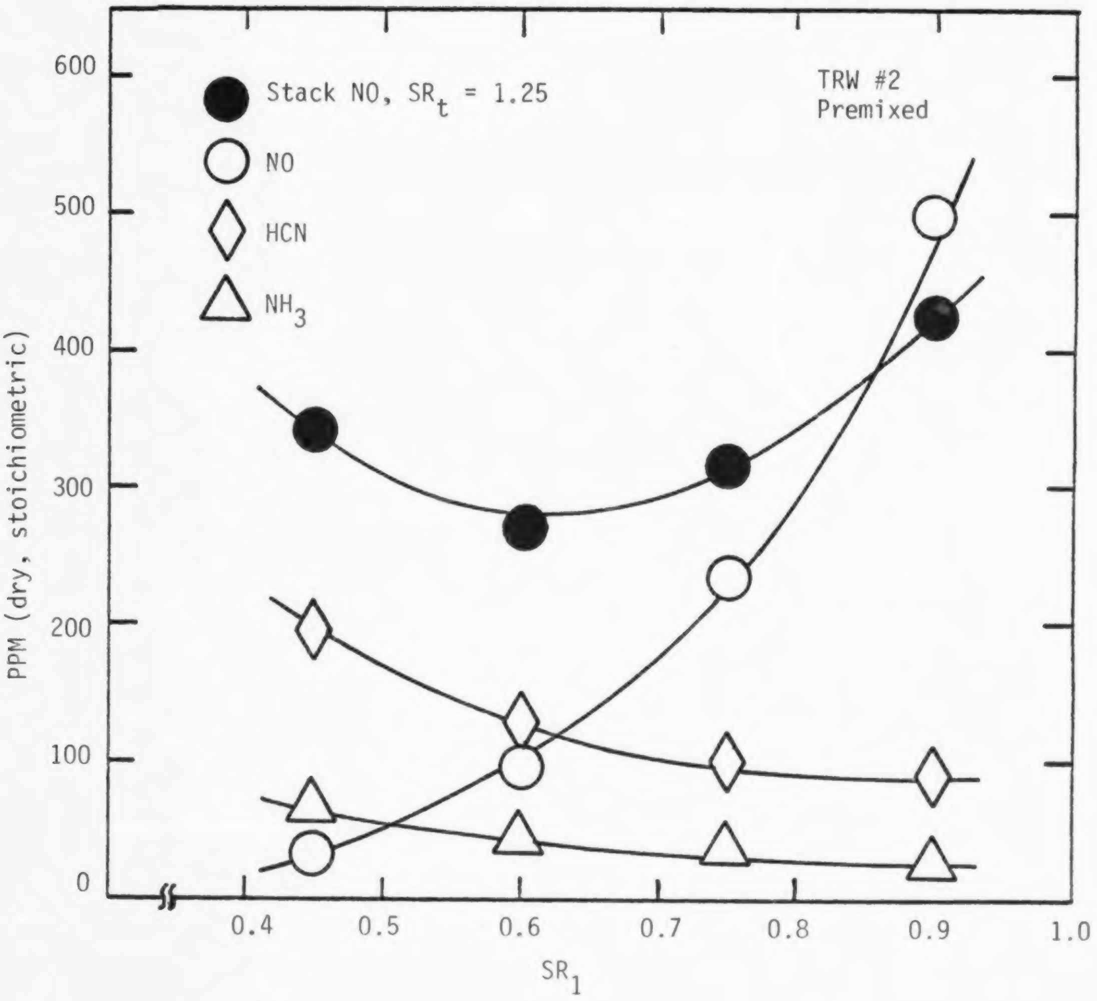

600
500
400
300
200
100
0
PPM (dry, stoichiometric)
● Stack NO, SR_t = 1.25
○ NO
◇ HCN
△ NH_3
TRW #2
Premixed
0.4
0.5
0.6
0.7
0.8
0.9
1.0
SR_1

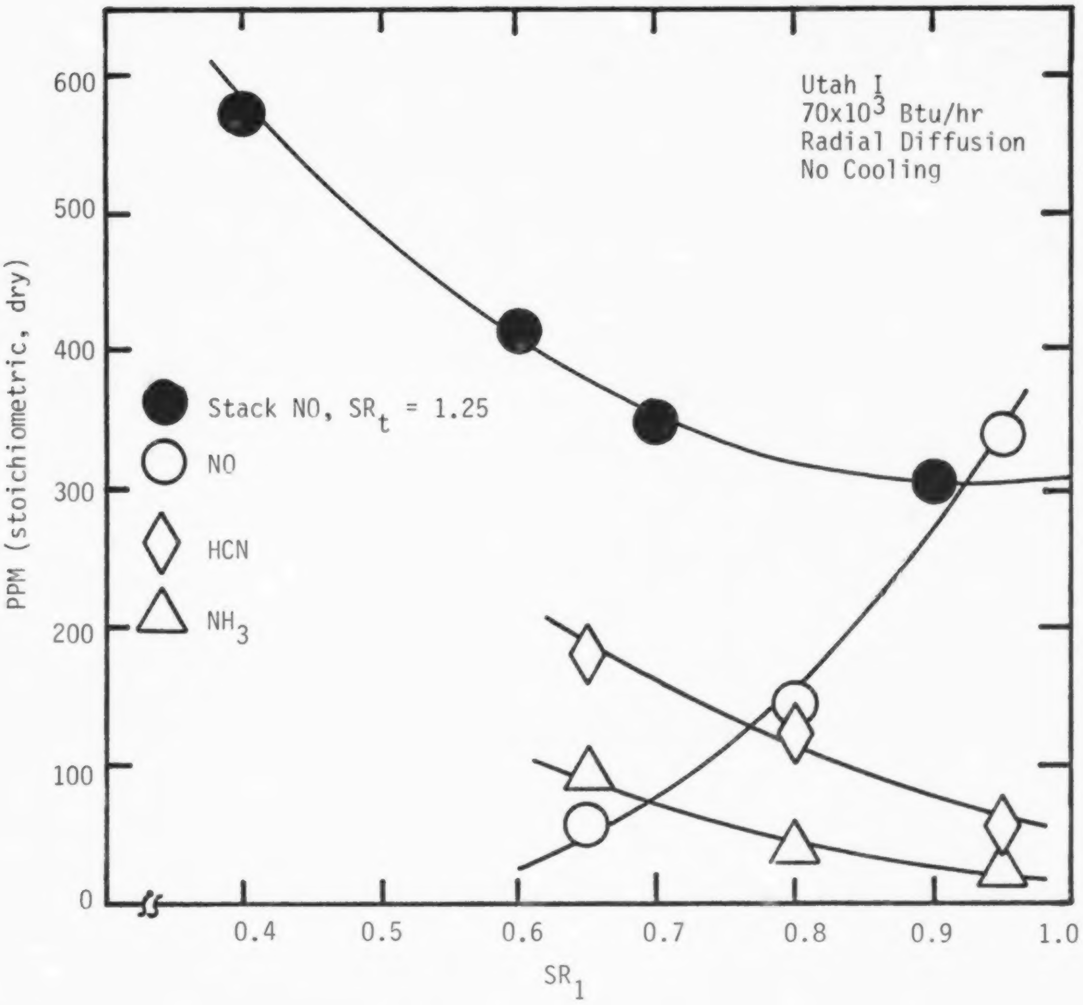
Utah I
70x10^3 Btu/hr
Radial Diffusion
No Cooling
● Stack NO, SR_t = 1.25
○ NO
◇ HCN
△ NH_3
PPM (stoichiometric, dry)
600
500
400
300
200
100
0
0.4
0.5
0.6
0.7
0.8
0.9
1.0
SR_1

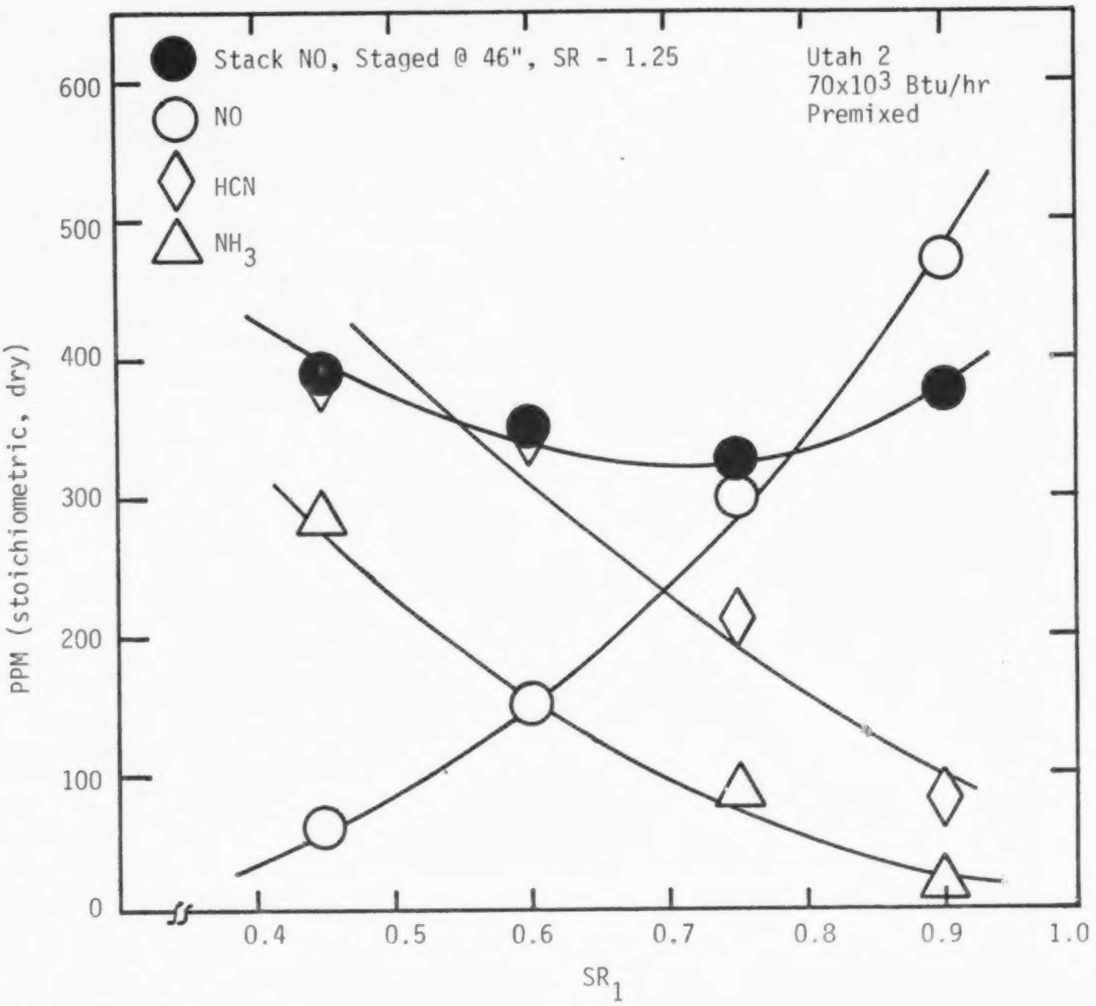
Stack NO, Staged @ 46", SR - 1.25
NO
HCN
NH$_3$
Utah 2
70x10^3 Btu/hr
Premixed
PPM (stoichiometric, dry)
0
100
200
300
400
500
600
0.4
0.5
0.6
0.7
0.8
0.9
1.0
SR$_1$

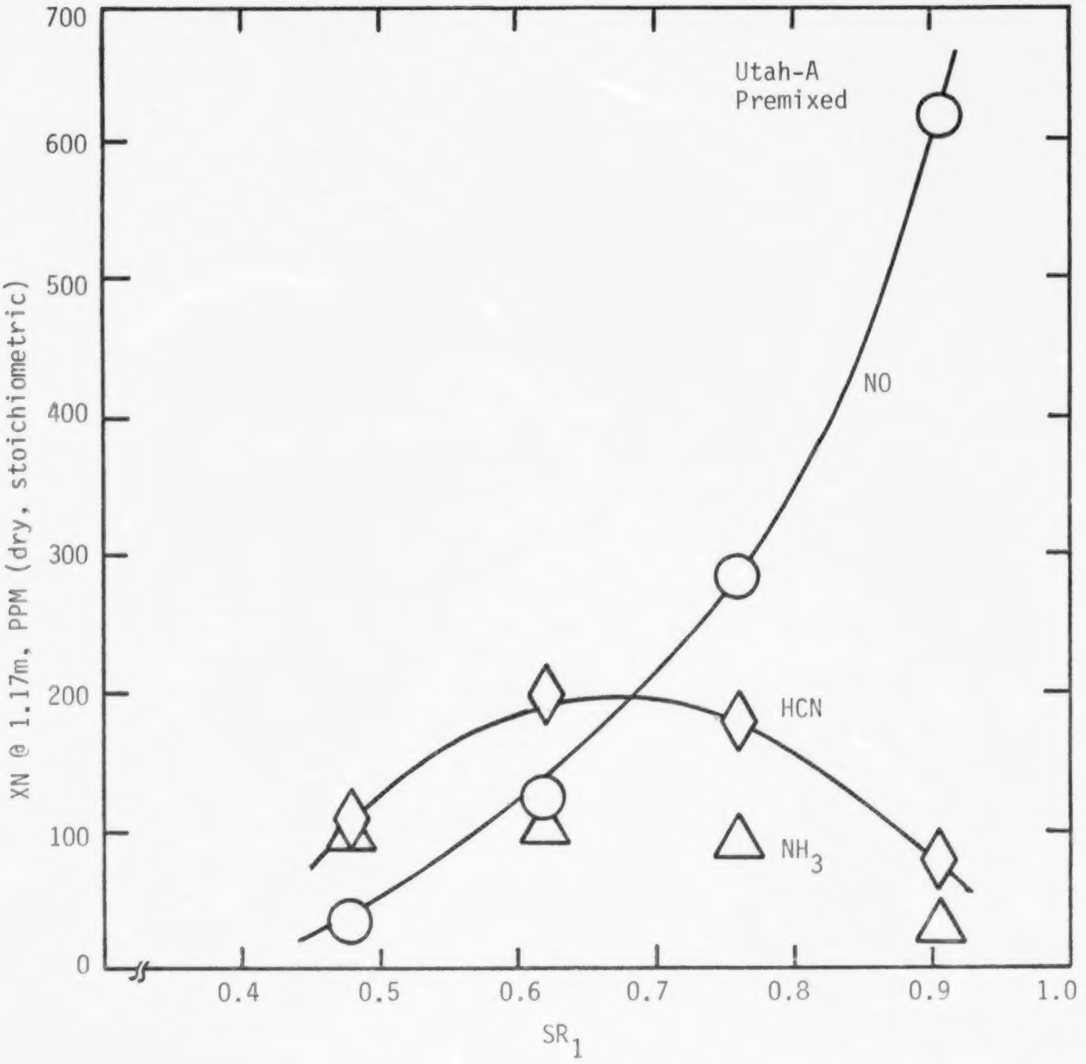
700
600
500
400
300
200
100
0
0.4
0.5
0.6
0.7
0.8
0.9
1.0
SR_1
XN @ 1.17m, PPM (dry, stoichiometric)
Utah-A
Premixed
NO
HCN
NH_3

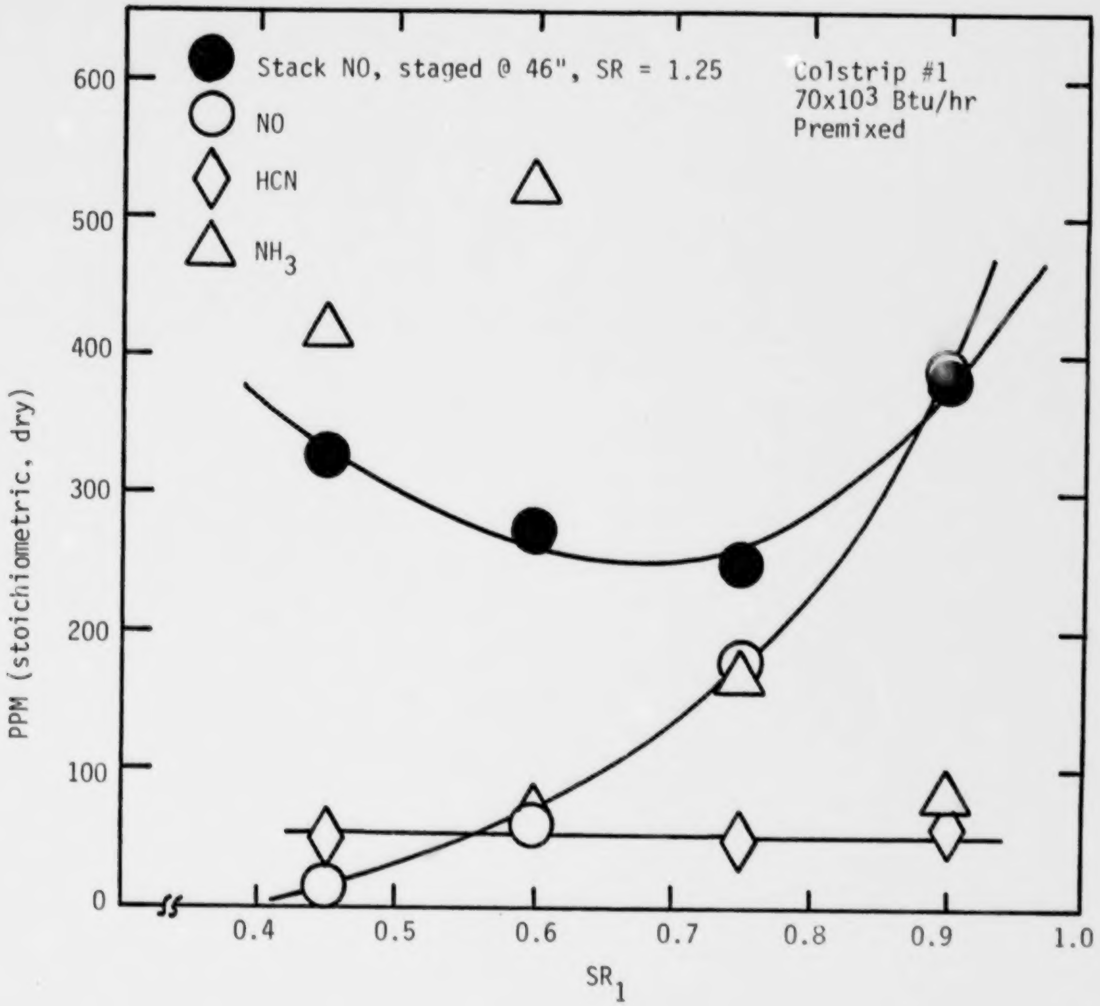
● Stack NO, staged @ 46", SR = 1.25
○ NO
◇ HCN
△ NH3
Colstrip #1
70x10³ Btu/hr
Premixed
PPM (stoichiometric, dry)
600
500
400
300
200
100
0
0.4
0.5
0.6
0.7
0.8
0.9
1.0
SR1

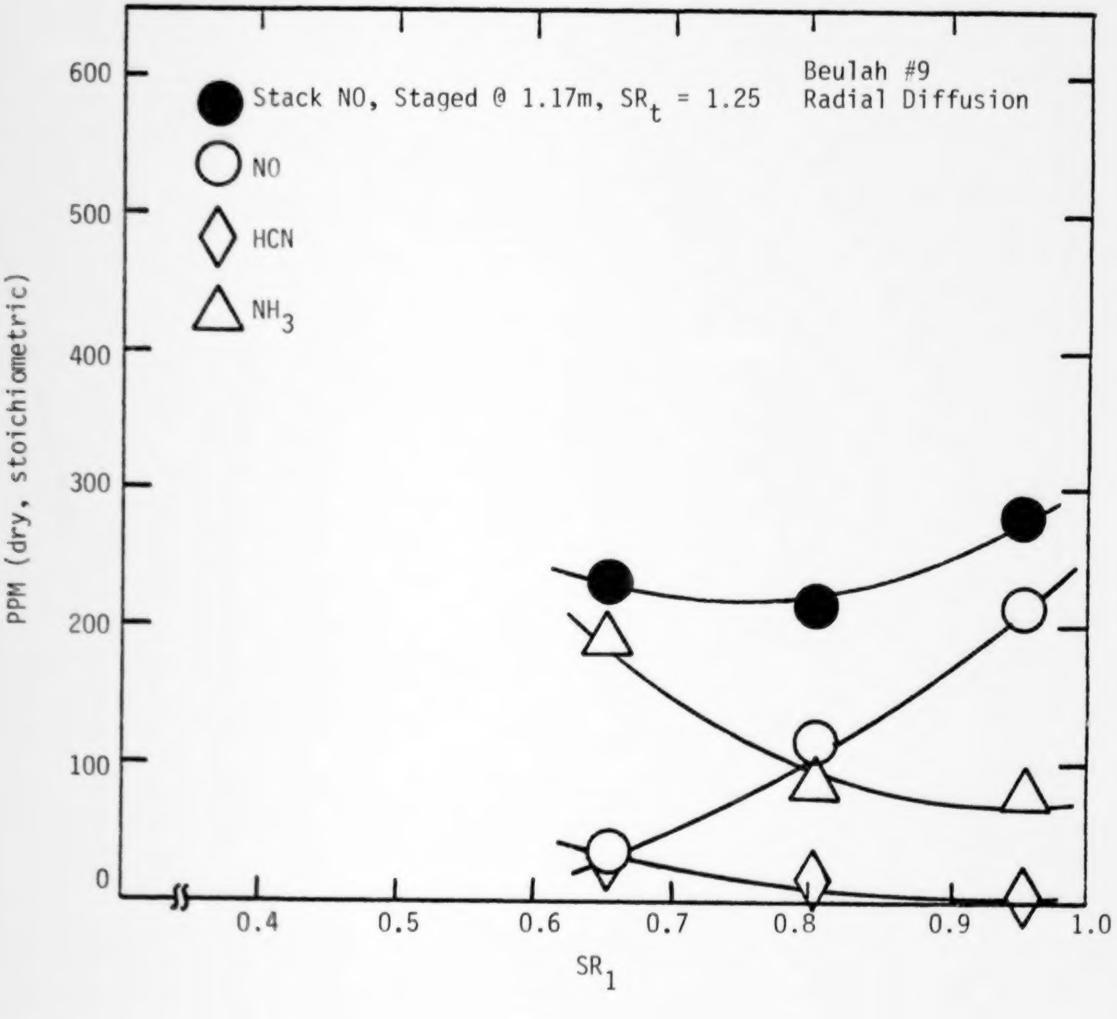
Stack NO, Staged @ 1.17m, SR_t = 1.25
NO
HCN
NH_3
Beulah #9
Radial Diffusion
PPM (dry, stoichiometric)
600
500
400
300
200
100
0
0.4
0.5
0.6
0.7
0.8
0.9
1.0
SR_1

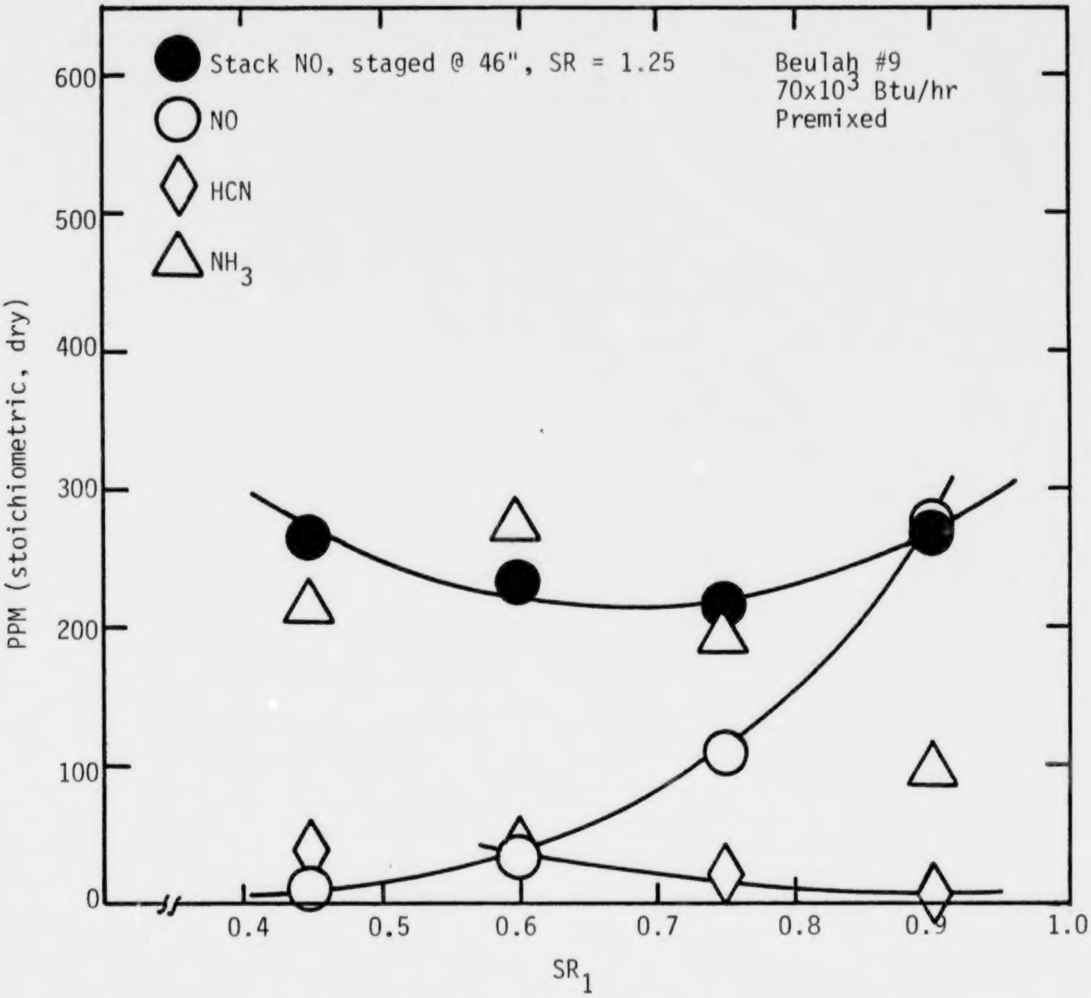
● Stack NO, staged @ 46", SR = 1.25
○ NO
◇ HCN
△ NH_3
Beulah #9
70×10^3 Btu/hr
Premixed
PPM (stoichiometric, dry)
600
500
400
300
200
100
0
0.4
0.5
0.6
0.7
0.8
0.9
1.0
SR_1

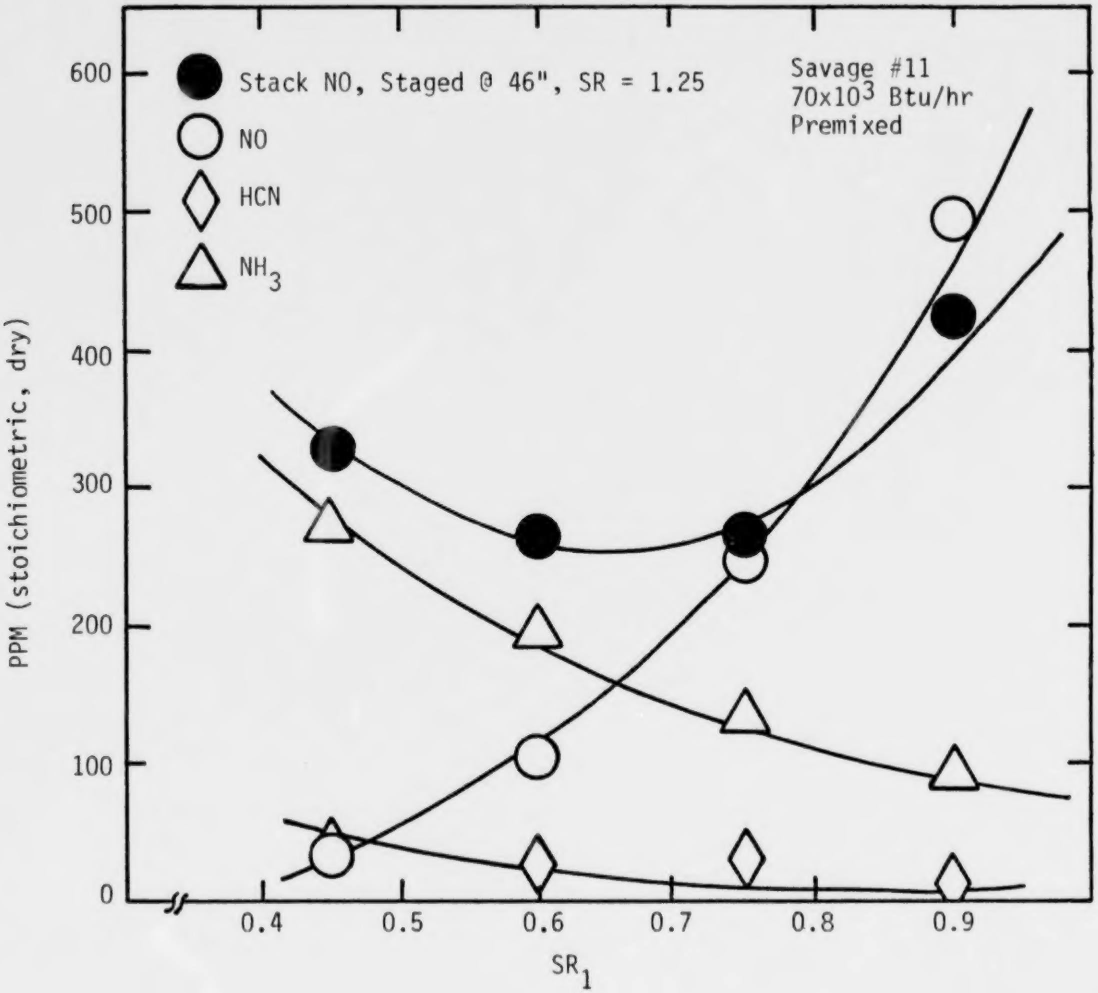
● Stack NO, Staged @ 46", SR = 1.25
○ NO
◇ HCN
△ NH_3
Savage #11
70×10^3 Btu/hr
Premixed
PPM (stoichiometric, dry)
0
100
200
300
400
500
600
0.4
0.5
0.6
0.7
0.8
0.9
SR_1

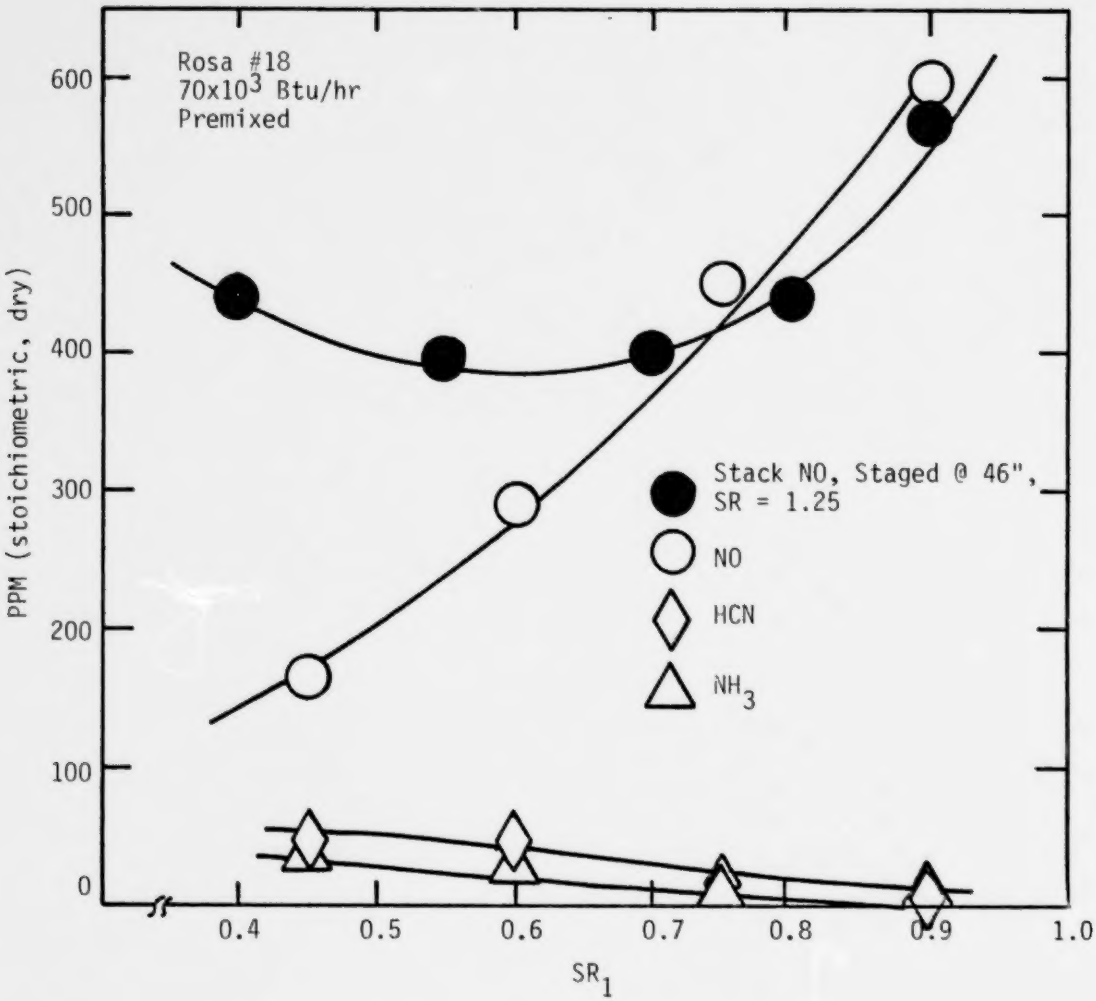
Rosa #18
70×10^3 Btu/hr
Premixed
PPM (stoichiometric, dry)
600
500
400
300
200
100
0
0.4
0.5
0.6
0.7
0.8
0.9
1.0
SR_1
● Stack NO, Staged @ 46", SR = 1.25
○ NO
◇ HCN
△ NH_3

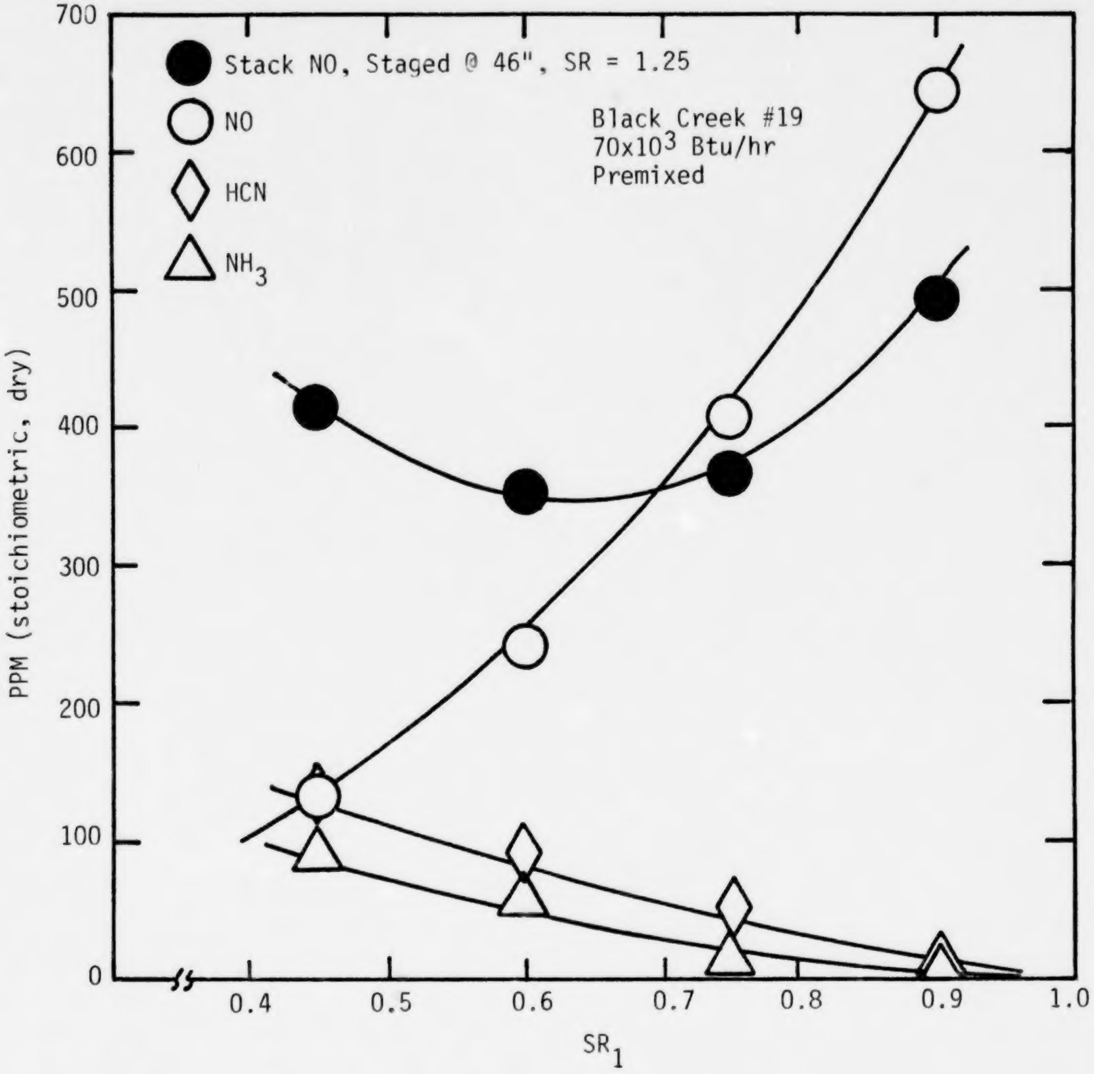
Stack NO, Staged @ 46", SR = 1.25
NO
HCN
NH_3
Black Creek #19
70x10^3 Btu/hr
Premixed
PPM (stoichiometric, dry)
700
600
500
400
300
200
100
0
0.4
0.5
0.6
0.7
0.8
0.9
1.0
SR_1

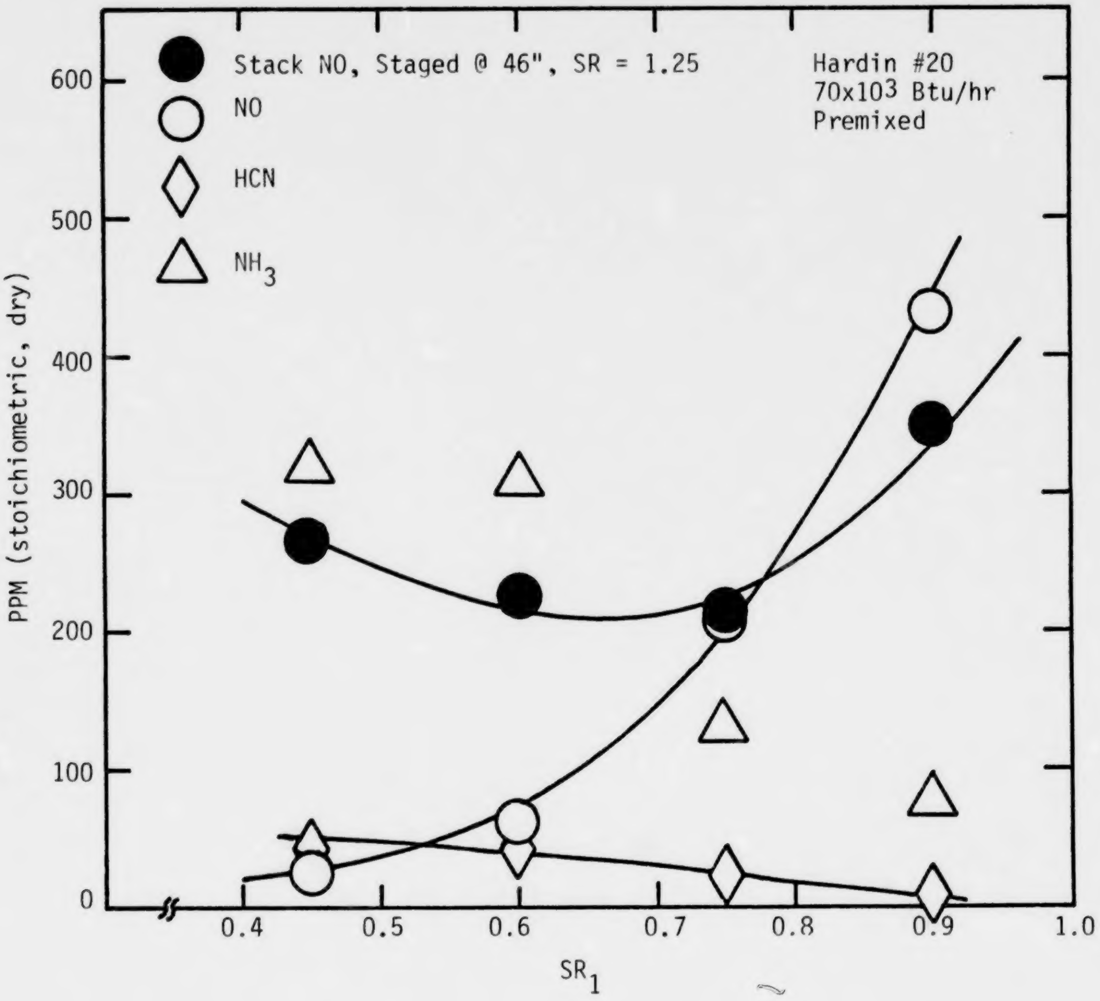

● Stack NO, Staged @ 46", SR = 1.25
○ NO
◊ HCN
△ NH_3
Hardin #20
70x10^3 Btu/hr
Premixed
PPM (stoichiometric, dry)
600
500
400
300
200
100
0
0.4
0.5
0.6
0.7
0.8
0.9
1.0
SR_1

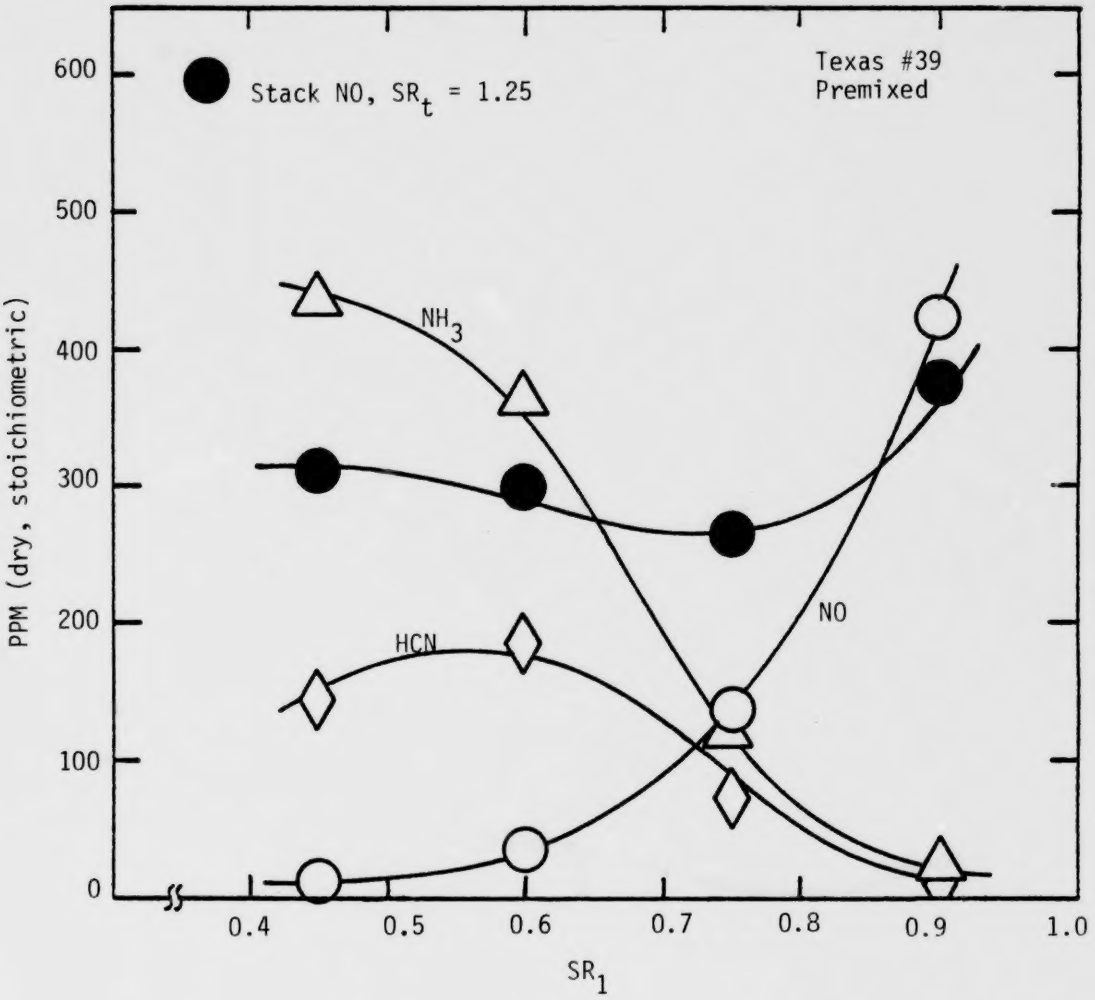
● Stack NO, SR_t = 1.25
Texas #39
Premixed
NH_3
NO
HCN
PPM (dry, stoichiometric)
0
100
200
300
400
500
600
0.4
0.5
0.6
0.7
0.8
0.9
1.0
SR_1

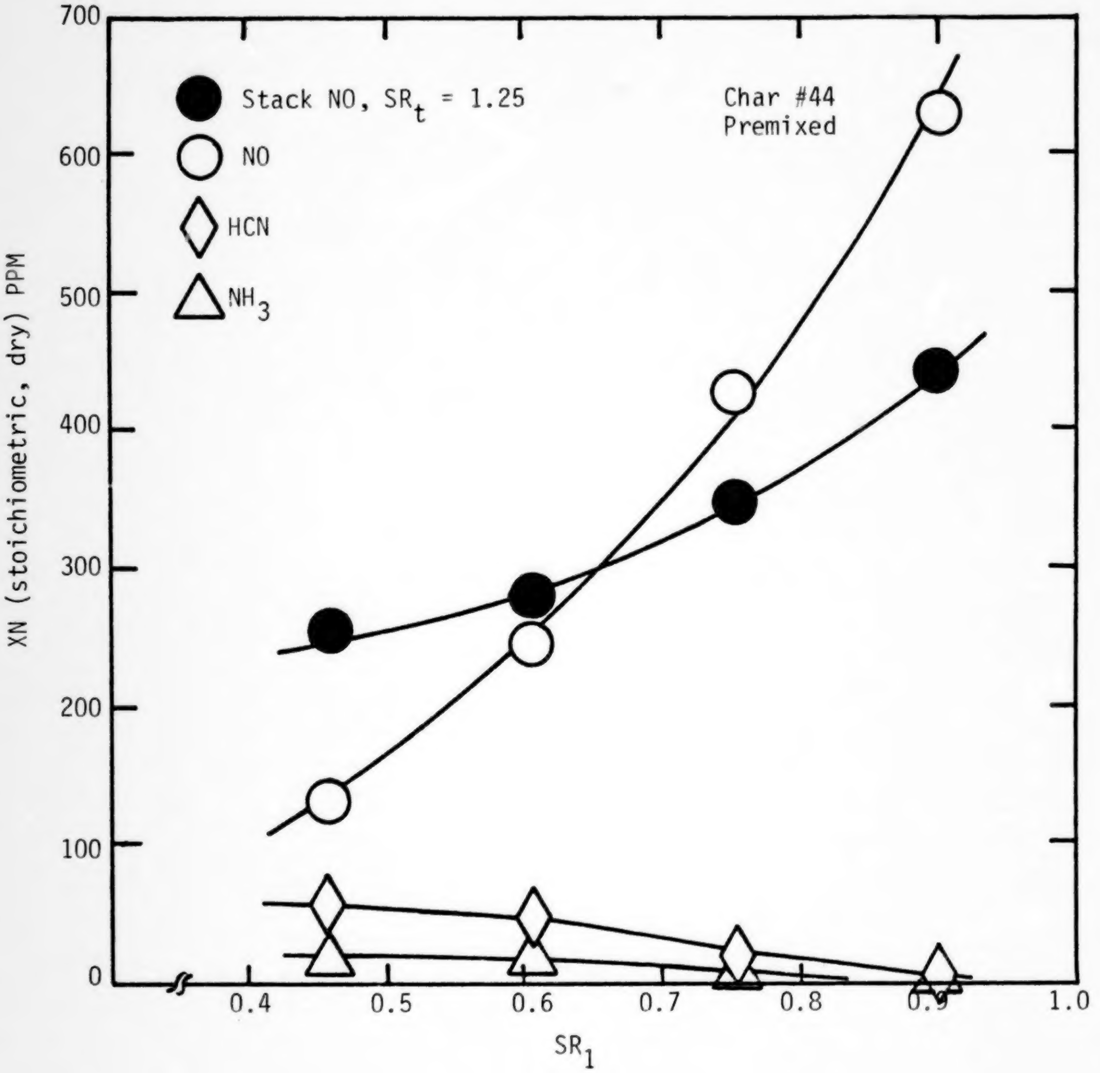

700
600
500
400
300
200
100
0
XN (stoichiometric, dry) PPM
● Stack NO, SR_t = 1.25
○ NO
◇ HCN
△ NH_3
Char #44
Premixed
0.4
0.5
0.6
0.7
0.8
0.9
1.0
SR_1

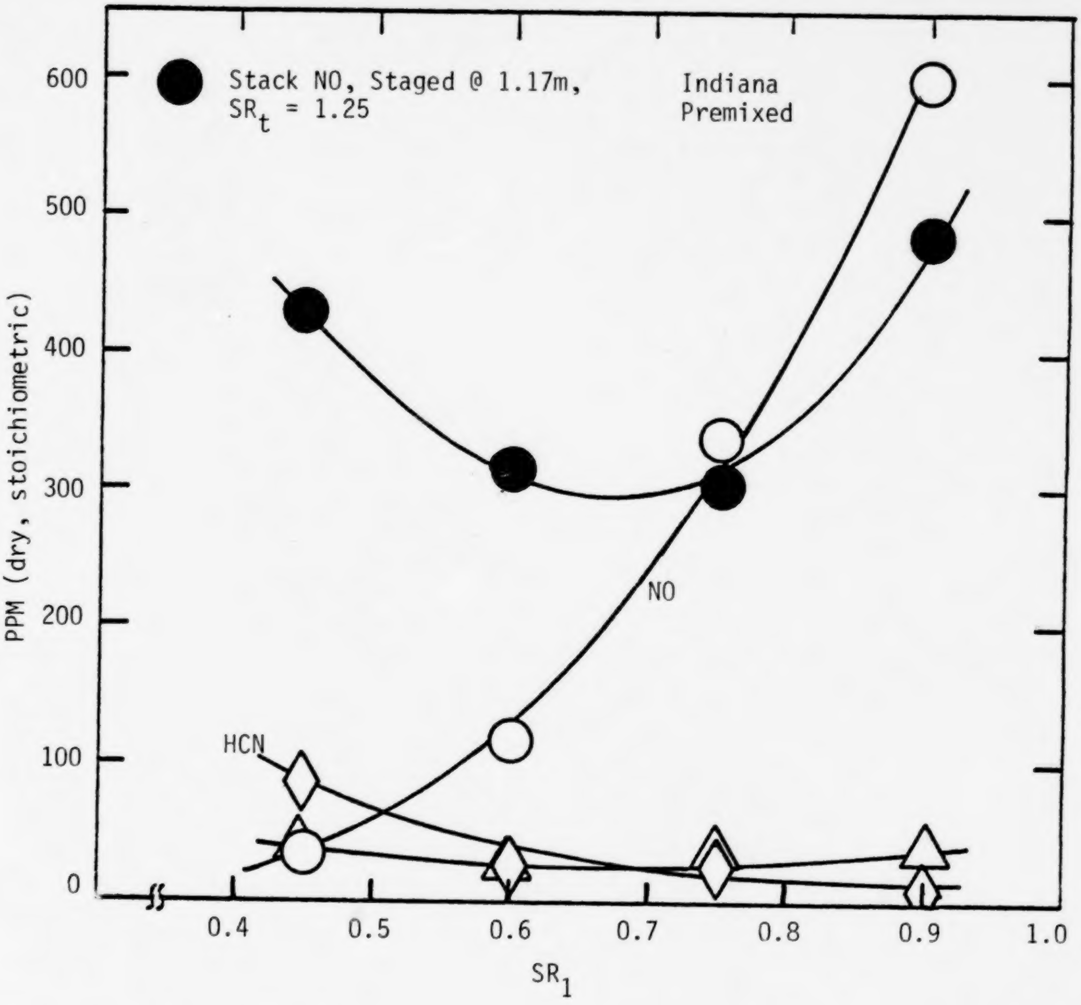

Stack NO, Staged @ 1.17m, SR_t = 1.25
Indiana
Premixed
PPM (dry, stoichiometric)
600
500
400
300
200
100
0
NO
HCN
0.4
0.5
0.6
0.7
0.8
0.9
1.0
SR_1

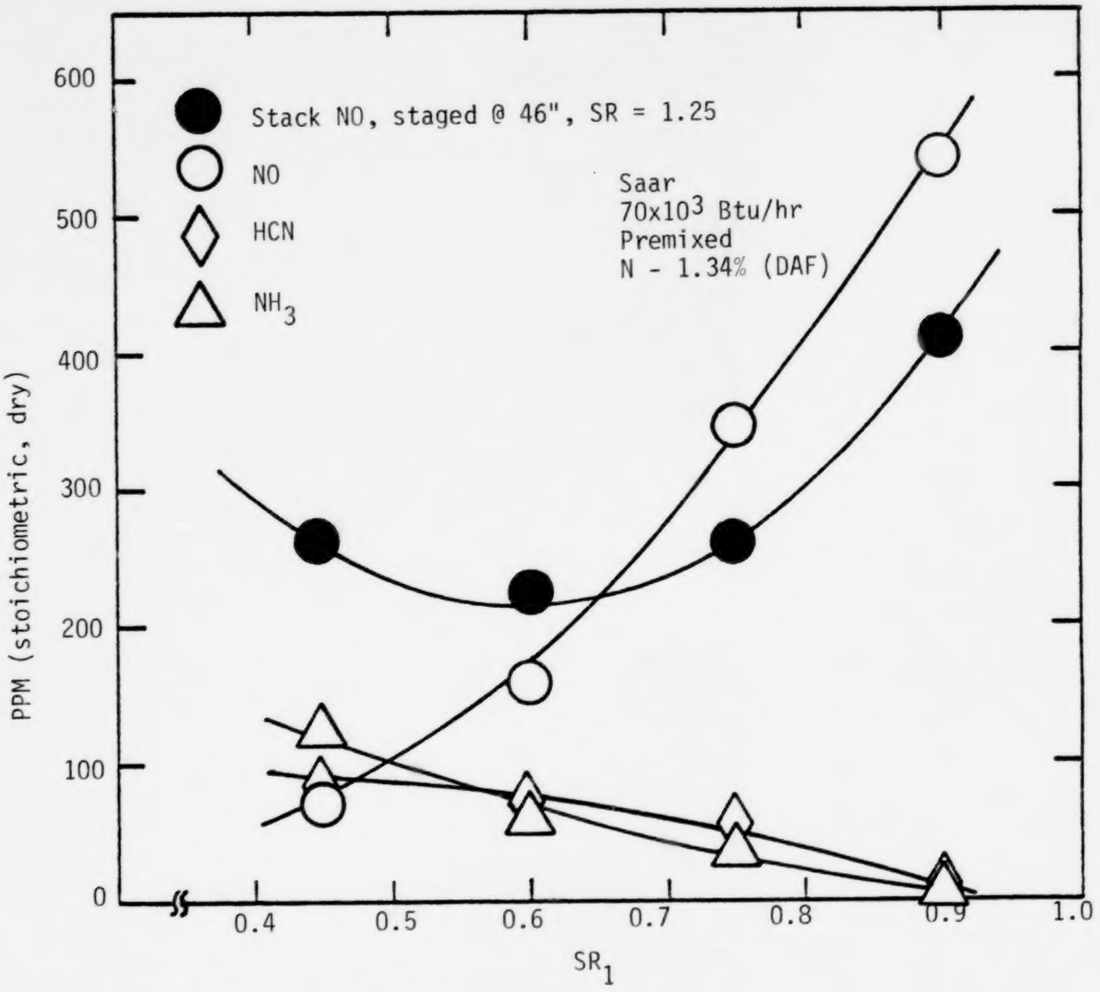
Stack NO, staged @ 46", SR = 1.25
NO
HCN
NH_3
Saar
$70x10^3$ Btu/hr
Premixed
N - 1.34% (DAF)
PPM (stoichiometric, dry)
600
500
400
300
200
100
0
0.4
0.5
0.6
0.7
0.8
0.9
1.0
SR_1